# Buckling of trusses with eccentric joints

Ntonalnt Korakas

Msc. Thesis

2022

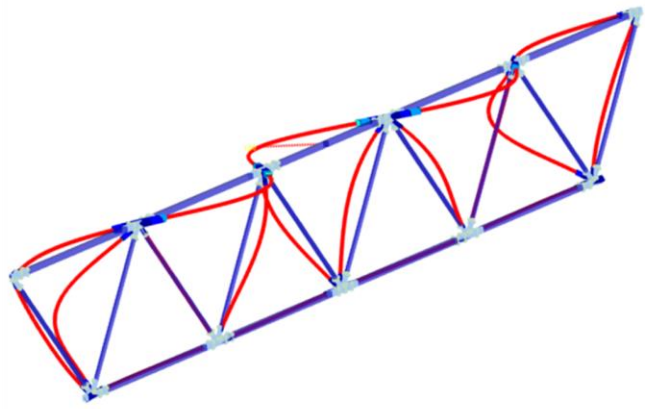

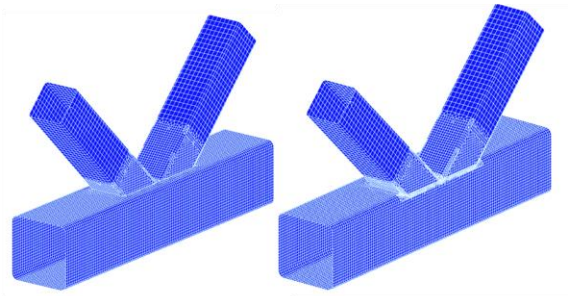

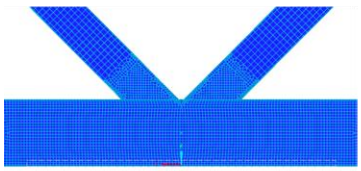

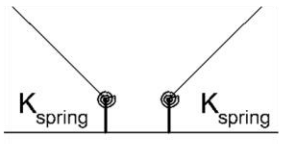


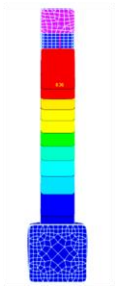

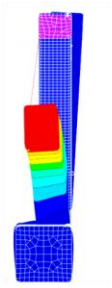

TU Delft

AMPELMANN

# Buckling of trusses with eccentric joints

by

Ntonalnt Korakas

March 2022

in partial fulfilment of the requirements for the degree of

**Master of Science**
in Civil Engineering

at the Delft University of Technology,
to be defended publicly on 13/04/2022

Student number: 5024676

| | | | |
|---|---|---|---|
| Thesis committee: | Prof.Dr. | M. Veljkovic (Chair) | TU Delft |
| | Dr. | F. Kavoura | TU Delft |
| | Dr.ir. | M.A.N. Hendriks | TU Delft |
| | Ir. | L. van Veen | Ampelmann |
| | Dr. | E. Saloumi | Ampelmann |


TU Delft

AMPELMANN

## Abstract

In this thesis an investigation into the buckling behaviour of steel trusses with eccentric joints is performed.

In recent years, Ampelmann motion compensated gangway systems have been pivotal to the advancement of offshore personnel transfers. These systems for functionality reasons require the use of eccentric joints. The behaviour of such joints is not a well-studied topic, and little is known of their effect on the buckling behaviour of structures. Buckling of trusses using conventional centric (non-eccentric) joints has been examined extensively in the literature. This work aims to answer what the effects of using eccentric joints compared to centric are, on the stability of steel truss structures. Additionally, a reduction of the computational and design time is attempted, by extending a simplified approach developed for centric joints, to eccentric joints.

The main investigation is performed on a simply supported truss comprised from eccentric K-joints and square hollow sections (SHS). Detailed models are used, with the joints being modelled by shell elements. The results are compared to equivalent trusses with centric joints. The main conclusions are that due to the eccentric joints, a better buckling behaviour can be realised for the truss members in the case of in-plane buckling. This improvement is more evident for the buckling of the braces and for combinations of chords and braces with $\gamma>8$ and $0.30<\beta<0.70$ respectively. In those cases, a decrease of the buckling length of at least 5% is observed and reaching nearly 20% for $\gamma=15.9$ and $\beta=0.4$. In the case of out of plane buckling, the observed behaviour is slightly worse. The difference is considered negligible in practice, with all configurations checked giving a difference of less than 2% between the buckling lengths.

The simplified design approach, which uses beam elements and rotational springs, is validated, by comparing literature results with detailed shell element models. It is, also, further improved by performing new research on individual centric K-joint models. Having validated the approach for centric joints, three different modifications are proposed to extend it to eccentric joints. None of the proposed modifications give the validation required but insight is gained regarding the behaviour of eccentric K-joint trusses. It is concluded that eccentric joints require non-symmetric stiffness matrices for their behaviour to be captured.

# Acknowledgements

These past two years have been difficult for everyone, and as someone challenged by the circumstances, I would like to thank all the people that supported me through the highs and lows.

Firstly, I would like to thank my committee. I would like to thank Prof. Dr. M. Velkjovic for his guidance during my research, especially in the beginning, as well as for giving me the opportunity to work as a student assistant for Steel Structures II. A very special thanks to Florentia for her help and support throughout my work. I enjoyed working closely with her and will always hold her in the highest regard. I would also like to thank Dr. Ir. Max Hendriks, for being willing to join the committee, even with his already busy schedule, and providing his insights when the time called for them.

I would like to thank Ampelmann for giving me the opportunity to conduct my research through their company. A thank you to the whole structural engineering team for making the weekly meetings interesting and a special thanks to Elsy and Lisanne for putting up with me (especially with the unstructured information overload in the beginning) and always being available to help with any issue that arose.

On a more personal note, I would like to thank the people of 33F for becoming my family away from home, as well as all my Greek friends for all the havale. Adding to that, thanks to all my fellow students that made my daily life in the faculty building enjoyable and special.

I owe a big thanks to my parents for making my move to the Netherlands possible and providing always more than they could bare. Most of the time it goes without saying, but an even bigger thank you for raising me and making me the person I am today.

Again, my deepest gratitude to all that helped me through these difficult two and a half years. Without you, the end of the journey would have been much more challenging and (would feel) longer!

*To all those who helped me throughout this journey.*

# CONTENTS


1 Introduction ..... 1
1.1 Motivation ..... 1
1.2 Problem statement ..... 2
1.3 Research questions ..... 2
1.4 Research methodology ..... 3
1.5 Thesis outline ..... 4
2 Literature study ..... 7
2.1 Buckling of structures ..... 7
2.2 Hollow sectioned truss structures ..... 9
2.3 Buckling length in hollow sectioned truss structures ..... 11
2.4 State of the art ..... 14
2.5 Research work on eccentric joints ..... 26
2.6 Topics that require further investigation ..... 29
3 Investigation of centric joints ..... 33
3.1 Introduction ..... 33
3.2 Effects of corner radius on stiffness ..... 36
3.3 Truss models ..... 45
3.4 Approach ..... 48
3.5 Results ..... 50
3.6 Conclusions ..... 57
4 Investigation of eccentric joints ..... 59
4.1 Introduction ..... 59
4.2 Truss models ..... 59
4.3 Approach ..... 60
4.4 Results ..... 62
4.5 Additional investigations ..... 68
4.6 Conclusions ..... 73
5 Formulating rotational springs for eccentric joints ..... 75
5.1 Introduction ..... 75
5.2 In-plane Rotational stiffness ..... 75
5.3 Out of plane rotational stiffness ..... 79
5.4 Formulation of eccentric springs ..... 83
5.5 Conclusions ..... 91
6 Discussions, conclusions & recommendations ..... 93
6.1 Discussion ..... 93
6.2 Conclusions ..... 94
6.3 Recommendations for future research ..... 96

7 References ..... 99
APPENDIX A Mesh investigation ..... 103
A.1 Centric joints ..... 103
A.2 Mesh investigation Eccentric joints ..... 106
APPENDIX B Effect of brace thickness on stiffness ..... 111
APPENDIX C New method for buckling load calculation of continuous columns ..... 119
C.1 Stiffness of members loaded with an axial load ..... 119
C.2 Calculation of the equivalent spring in the case of a continuous column ..... 120
C.3 Solution process ..... 121
C.4 Numerical application ..... 122
C.5 Conclusions ..... 128
APPENDIX D Proposal of buckling length calculation approach for truss girders ..... 129
D.1 Approach ..... 129
D.2 In-plane buckling ..... 131
D.3 Out of plane buckling ..... 134
D.4 Conclusions ..... 136
APPENDIX E Numerical results ..... 137
E.1 Stiffness calculations ..... 137
E.2 Buckling lengths ..... 138

# 1 INTRODUCTION

## 1.1 Motivation

Due to the high strength of steel available as a building material, very slender members can be realised. This slenderness, however, makes the structures and the members made from steel susceptible to the buckling phenomena. As such, one of the most important verifications performed on steel structures is checking the loss of stability of part or the whole structure. This is especially true for light weight systems designed for minimization of their weight and by extension the cross-sectional area of their members. Such is the case for the newly developed motion compensated gangway systems by Ampelmann (Figure 1).

*Figure 1. 3D representation of the E-5000 system by Ampelmann.*

These structures need to be verified and certified by codes and guidelines which, due to the general nature and the wide range of applications necessary to be covered by them, do not cover every design case encountered. Specifically, owing to the unconventional designs that functionality reasons impose, some cases are not covered by the codes. This is particularly the case when it relates to the buckling verification of truss structured elements of the systems. The added complexity is introduced from the use of non-conventional eccentric joints (Figure 2). As such, it is imperative to understand better the buckling behaviour of structures that make use of such joints. In this thesis, the buckling mechanics and behaviour of trusses whose connections are realized using eccentric joints are going to be investigated.

*Figure 2. Eccentric joints used in Ampelmann's gangway systems.*

## 1.2 Problem statement

Due to not being applied widely, little research has been performed on hollow section trusses with eccentric joints. There is little known on how these joints behave in-plane and out of plane. Additionally, as it relates to their effect on the buckling behaviour of truss members, no research is to be found. When referring to eccentric joints, the eccentricity may be applied in different amounts, giving rise to different types of joints, depending on how the braces are connected to the chords (Figure 2). Additionally, there are different types of joints that can be used (T-joints, K-joints etc). In this work, eccentric K-joints are going to be investigated. The eccentricity introduced will allow for the braces to be welded on the chord face (Figure 3). From some preliminary work it is obvious that eccentric joints behave differently to centric joints. The investigation will aim to give insight to the buckling of truss members connected with eccentric K-joints. The behaviour is to be assessed qualitatively as well as quantitively and the conclusions are to guide future practice.

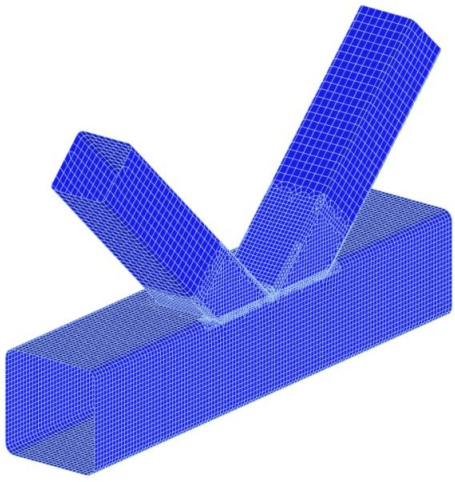

*Figure 3. Eccentric K-joint with brace welded on the chord face.*

## 1.3 Research questions

The main question to be answered through this study is, what the effects of eccentric joints on the buckling behaviour the truss members are. The effects that the eccentric joints will be measured qualitatively and quantitively, by comparing the results to results obtained for centric joints, for which more research is available. As part of this research, the following sub-questions are to be answered:

- *What are the effects of modelling the corner radius of profiles to the connection stiffness of centric joints and are these substantial?*
- *Does Eurocode 3 prescribed buckling lengths provide a safe estimate? And under what assumptions?*

- *Does the buckling behaviour change qualitatively and is this change substantial?*
- *Do trusses with eccentric joints present better or worse buckling behaviour compared to the corresponding trusses with centric joints? Does the conclusion change depending on the buckling direction (in-plane, out of plane)? What effect does the change of joint parameters (β, γ) have on the observed trends?*

Additionally, the use of complex models for all phases of design is time consuming. As such, the simplification of the analysis methods is desired. A method has already been developed for centric joints, by approximating the joint behaviour with rotational springs accounting for the stiffness of the connections. From the approach described in the literature, three different stiffness values can be calculated and it is not yet clear which is definitively correct. This gives rise to the following sub-questions:

- *Do simplified models (beam element models with rotational springs) adequately capture the behaviour of more complex models (shell element models)?*
- *What do the different stiffness values that can be calculated for the same connection represent? Which is the most appropriate stiffness value to be used for trusses with K-joints?*
- *Is it possible for this approach to be extended to eccentric joints? If so, what modifications are necessary for its application?*

## 1.4 Research methodology

### 1.4.1 Literature study

First, a literature study is performed to gain insight into the buckling of truss structures using hollow sections. A state-of-the-art investigation is performed to examine the buckling of truss with centric joints and find what simplified approaches have been developed to analyse the buckling of such truss structures. Additionally, how researchers have approached eccentric hollow section joints in the past is examined.

### 1.4.2 Numerical investigations-Centric joints

Next the numerical investigation of the eccentric joints is performed. First centric joints are investigated, to provide baseline results. The effects of modelling the corner radius on the connection stiffness is assessed by using finite element models and following an approach found from the literature study for the stiffness calculations. Finite element models of a simply supported truss girder are developed for investigating centric joints. The developed models make use of shell elements to capture the complex behaviour of the joints. Buckling analysis is performed for truss used and for different values of β and γ, for the braces and chords respectively. The buckling lengths of chords and braces, for in and out of plane modes are assessed. The results are cross validated by literature results obtained for simplified models (beam element models and rotational springs). Additional supports are introduced to isolate the behaviour of the truss member and compare the results with the buckling lengths prescribed by EC3.

### 1.4.3 Numerical investigations-Eccentric joints

Finite element models using shell elements are developed for investigating eccentric joints. Similar approach to the investigation of centric joints is followed, by calculating the buckling lengths for the braces and chords, for in and out of plane modes. The results are compared to the results obtained for centric joints and conclusions are drawn for the effects that the eccentricity has on the buckling behaviour of the truss members. A parametric study with the shell element models is performed using additional cross sections to investigate for which values of β and γ the differences between centric and eccentric joints are more pronounced. An additional investigation with beam element models and rigid connections is performed to check if assuming rigid connections could provide a safe estimate of the buckling length.

### 1.4.4 Numerical investigations-Formulation of rotational springs

As a final numerical investigation, the development of an approach to simplify the eccentric joint modelling, is attempted. First the centric joints are investigated, to conclude which approach is more appropriate to calculate the rotational stiffness, so it may be introduced in a simplified model (beam element). This is done by comparing the brace buckling loads of K-joint sub-models using shell elements, to beam element models

with an equivalent rotational spring. Having validated the approach and the calculation method of the rotational springs for centric joints, an attempt is made to extended the approach to eccentric joints. Due to the coupled behaviour presented by the eccentric joints, the already developed approaches are not immediately applicable for them. Three different approaches are proposed for the calculation of the stiffness and formulating the rotational springs for eccentric joints. Similar to the centric joints, the buckling loads of shell element models are compared to the buckling loads of beam elements models that use the rotational springs calculated for different approaches.

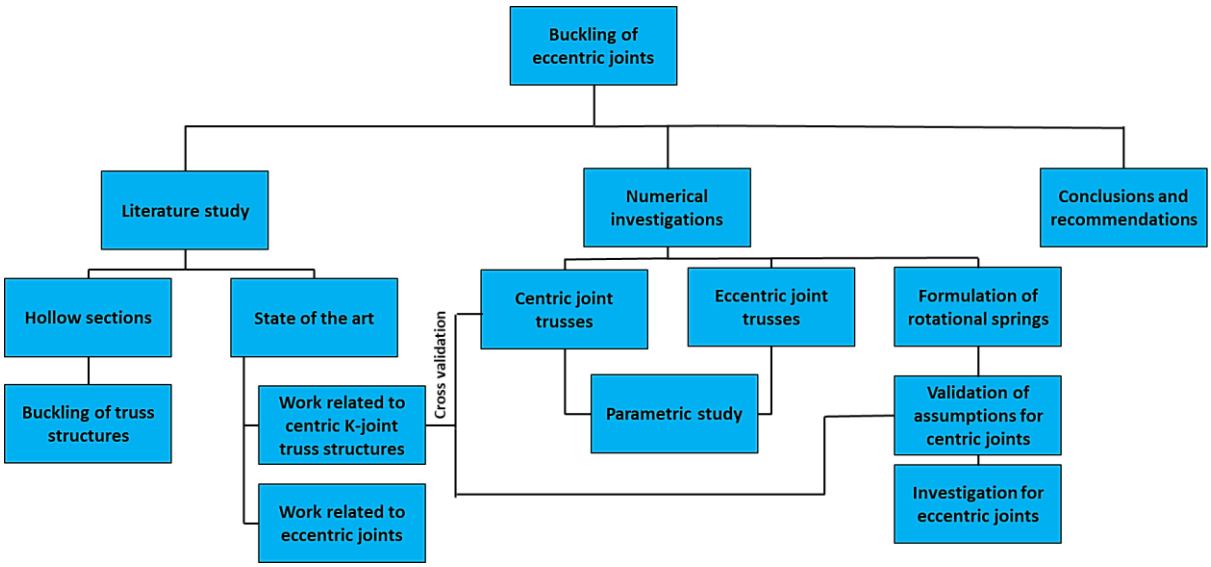


*Figure 4. Schematization of methodology followed.*

## 1.5 Thesis outline

The structure and outline of the thesis is presented below.

In the first chapter, an extensive literature study was performed. Initially, details relating to the things that affect buckling (geometrical non-linearity and imperfections) are presented and how these can be accounted for in codes and in practice. The literature study is followed by general information about hollow sections and then specifically by the buckling of truss structures using hollow sections. Lastly, the state-of-the-art for centric joints is given. As limited research is performed on eccentric joints only a specific work was found relevant and presented.

In the second chapter, the investigation into the buckling of trusses with centric joints is presented. A comparison of the effects the corner radius of the cross sections has on the stiffness of centric joints is performed. The example truss used in the rest of the work is presented and the approach followed is given. Buckling results are created for the example truss and compared to results found in literature. These highlight the differences between different modelling techniques. Additionally, an investigation is performed by changing the support conditions of the example truss, to isolate the buckling behaviour of individual members.

In the third chapter, the investigation into the truss member buckling for eccentric joints is presented. Firstly, how the models and geometry are defined is described. The same approach as with the centric joints is followed. The results are then compared to the buckling lengths obtained from the centric joints. Additional cross sections are investigated and a model using rigid connections is used to help support and form the recommendations and conclusions.

In the fourth chapter, the last investigation into simplifying the joint modelling is shown. In this, an attempt to model the eccentric joints with conventional rotational springs is attempted (for in-plane and out of plane). Initially, a study into the calculation of the rotational stiffness of the springs for centric joints is performed. Then the study on the eccentric joints is presented.

In the last chapter discussion on the results and the approach used is performed. The conclusions of the study are summarized and lastly recommendations for future research are provided.

In the appendices further research, as well as results that helped guide the investigation of the main research questions are provided. These include an investigation into the effect the brace thickness has on the connection stiffness, as well as the mesh investigations performed prior to the creation of the final models. A method developed to calculate the buckling load of continuous columns is presented, along with a description of a new approach that could be used to predict truss structures' buckling lengths. Lastly, all the buckling length results produced for the example truss are gathered and presented together.

# 2 LITERATURE STUDY

## 2.1 Buckling of structures

Buckling refers to a phenomenon in which a member or a structure loses its stability. This means that for loads above a certain level the member or the structure experience disproportionally large displacements, putting the integrity of the system at risk. When it comes to verifying systems against the loss of stability due to buckling the checks are done at the level of the member, as the partial or total collapse of the system will occur at those points. Buckling is a complex phenomenon, in which many aspects of construction play a role in determining the ultimate resistance of the members. These can be grouped in the following two categories: P-Δ/P-δ effects and imperfection.

### 2.1.1 P-δ and P-Δ effects

P-δ and P-Δ refer to the increase of internal forces that a member experiences to stay in equilibrium, due to large deformations. When a member deflects laterally from its undeformed state, relative to its end points, it will develop additional moments to remain in equilibrium. These additional moments are part of the P-δ effects a member under compression may experience. Additionally, if a structure is relatively flexible and its loading conditions produce significant deflections from its undeformed state, additional cross-sectional forces will develop to keep the structure's equilibrium. These forces comprise the P-Δ effects on the structure (Figure 5). The P-δ and P-Δ forces that will develop relate to the stability of the member and the overall stability of the structure, respectively.

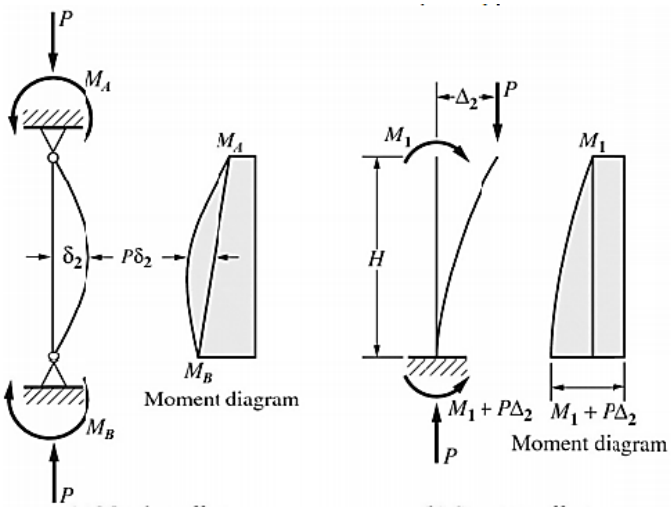


*Figure 5. P-δ and P-Δ effects on structural systems* (Geschwindner et al., 2017)

The main aspect that affects the P-δ and P-Δ effects are the boundary conditions of the system. Both dynamic and kinematic boundary conditions play a role in this. Therefore, apart from the geometry and mechanical characteristics of the system, the loading of the system is equally important. As it relates to individual members, the amount of restrain that can be developed by adjacent members is affected by the axial loading on those. This makes the determination and exact solution of buckling difficult.

### 2.1.2 Imperfections

The other important aspect in the actual behaviour of buckling members is the effects of imperfections. These can take two forms. The first, and more straight forward, are the geometric imperfections. These account for deviations of the actual structure from the idealized form assumed during design. The other important imperfections that need to be accounted for are the structural imperfections (Vayas et al., 2019). These include the influences arising from the manufacturing process of the members. In both cases, the effect of imperfections is the reduction of stiffness of a member. In the case of geometric, it happens at the level of a member (or structure), with the reduction being a result of continuous equilibrium during its deformation (Figure 6). For structural imperfections, the loss of stiffness is done at the cross-sectional level (Figure 7,Figure 8), with the premature yielding of the member. These effects of imperfections may alter the behaviour of a member significantly compared to its idealized response, resulting to a lower resistance than the one theoretically possible.

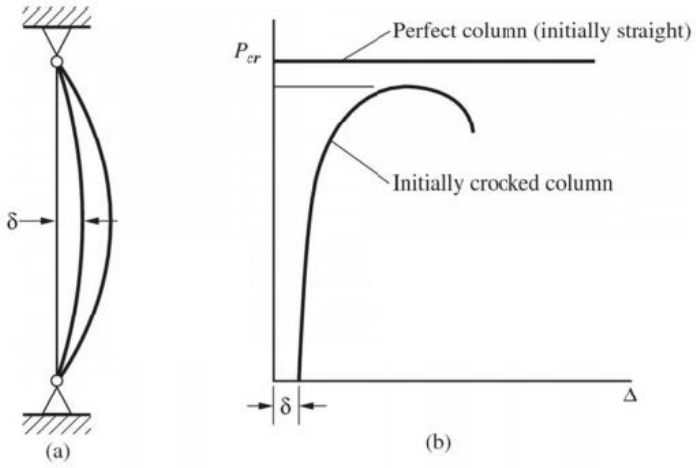


*Figure 6. Effects of geometric imperfections to member's behaviour* (Geschwindner et al., 2017)

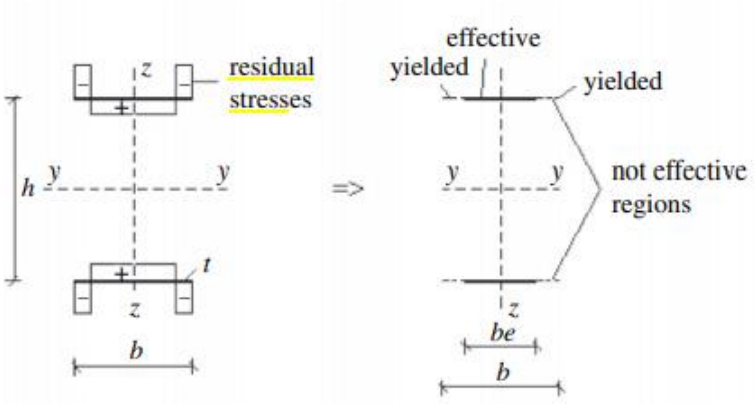


*Figure 7. Effects of residual stresses from production process. Due to early yielding certain areas of the cross section are ineffective* (Vayas et al., 2019)

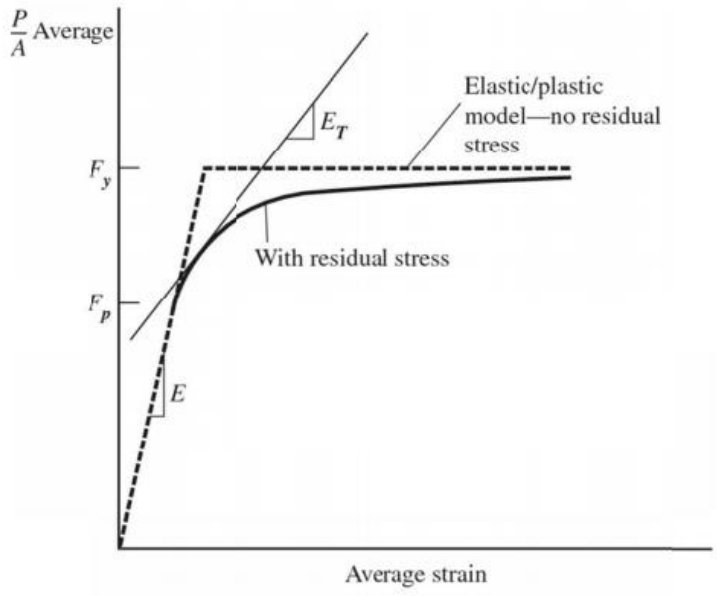


*Figure 8. Effects of structural imperfections to the cross-sectional stiffness of members* (Geschwindner et al., 2017)

## 2.2 Hollow sectioned truss structures

### 2.2.1 Types of hollow section trusses

Trusses can come in many various different geometries, applications and combinations. They can be in 3D space 2D plane and have many different joint types that can be used to connect the different members. This work will be focused on plane trusses so only these are considered. Plane trusses can make use of different joints and different chord variations to produce a multitude of results. A few different designs are presented in Figure 9. For common truss girders, with straight chords, standard naming conventions exist, depending on the configuration and joint type used. The most common types are presented in Figure 10.

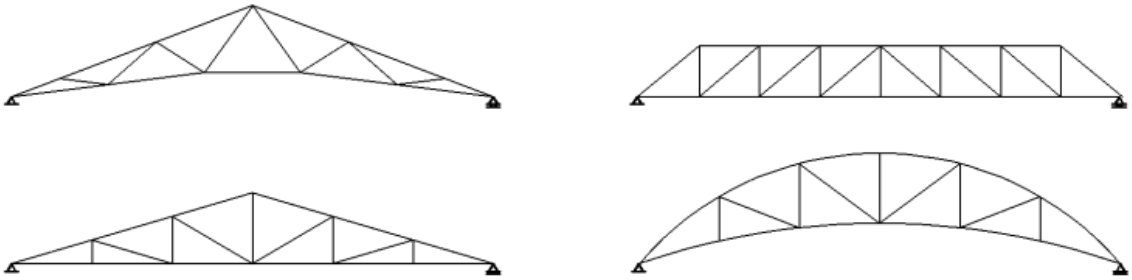

*Figure 9. Examples of plane trusses* (Boel, 2010)

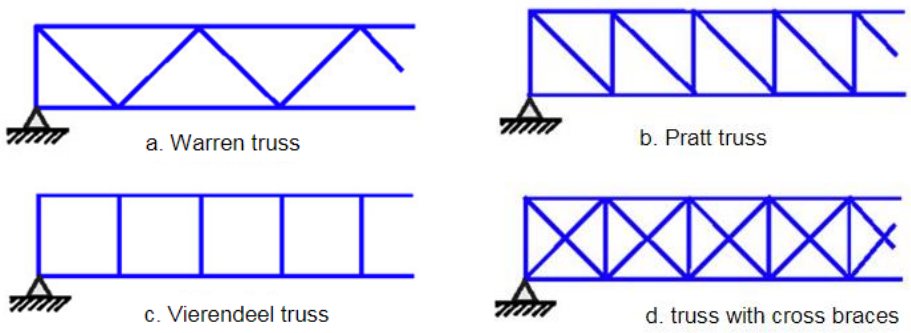


*Figure 10. Names of commonly used plane trusses* (Wardenier et al., 2010)

### 2.2.2 Welded hollow section joints

For plane trusses, typical connections consist of K KT N T and Y joints, depending on geometry of the connected members. Lastly, in Figure 11(a) the most common welded joint types for plane trusses are shown. Connections can be also overlapped (Figure 11(b)) but this work will not be dealing with these types of joints.

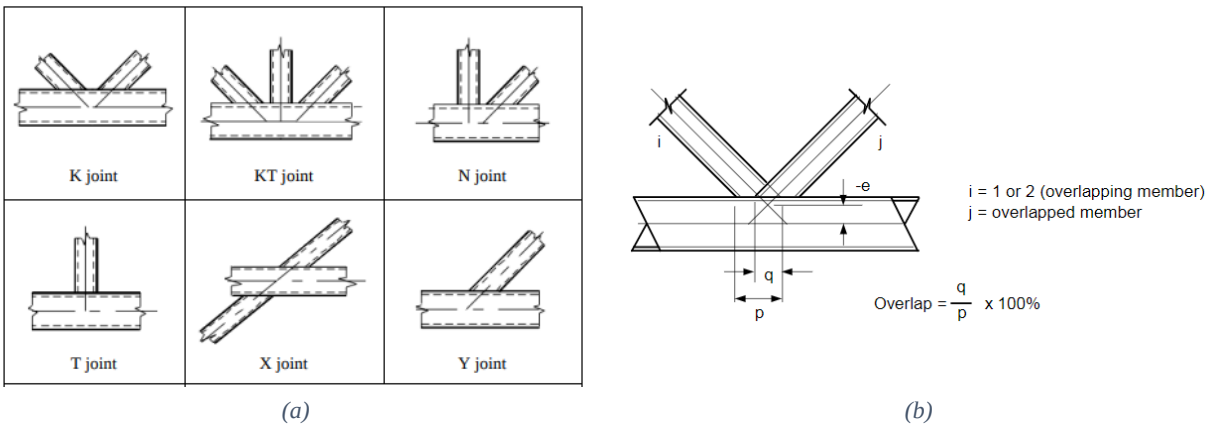


*(a)* *(b)*

*Figure 11. (a) Commonly used joints for plane trusses and (b) definitions of overlapped joints*

In order to describe and categorise the joints, some design parameters have been defined and are used. For K joints, which will be the focus of this thesis, they are equations 1. till 4.. These conventions are going to be used throughout this work.

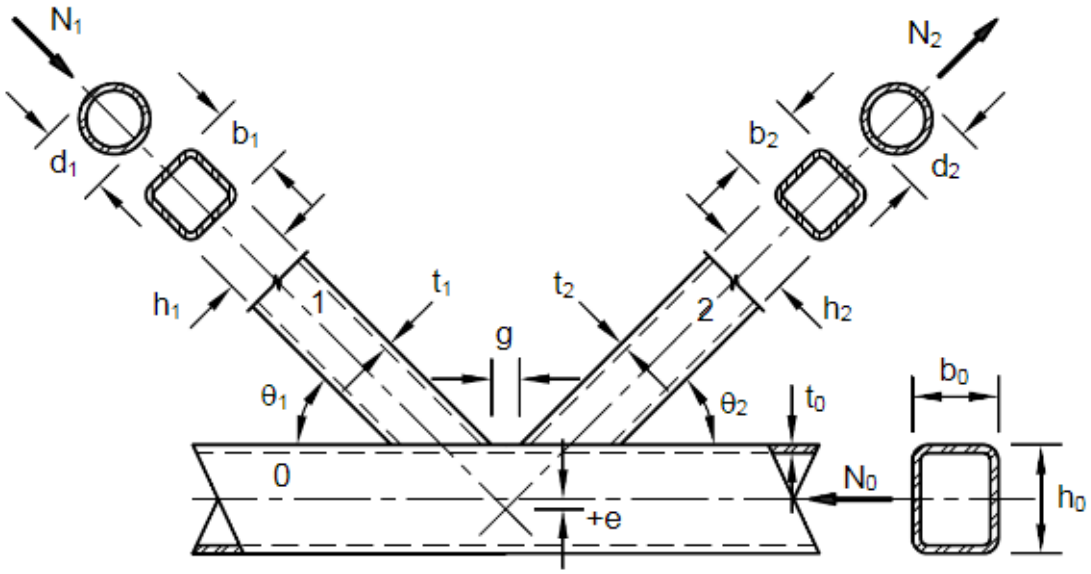


*Figure 12. Definitions of K-joint geometry* (Wardenier et al., 2010)

$$\beta = \frac{d_1 + d_2}{2d_0} \; or \; \frac{b_1 + b_2}{2b_0} \qquad 1.$$

$$\gamma = \frac{d_0}{2t_0} \; or \; \frac{b_0}{2t_0} \qquad 2.$$

$$\tau = \frac{t_i}{t_0} \qquad 3.$$

$$g' = \frac{g}{t_0} \quad 4.$$

## 2.3 Buckling length in hollow sectioned truss structures

### 2.3.1 Buckling length of truss members

It has already been discussed how the effects of global and member buckling can be separated and how different approaches can be used for the analysis of structures depending on the available tools, experience and required detail level. As global buckling can be quite project specific and because various codes and research propose buckling lengths primarily for individual members, the current work will focus on buckling of members.

In calculating the critical buckling load of members, the concept of a buckling factor is usually used. This coefficient encompasses the effects of the boundary conditions on the critical buckling load of individual members. The buckling factor multiplied by the system or reference length gives the buckling length of the problem (Equation 5.). Depending on the boundary conditions, some characteristic examples are presented in Figure 13. In the case of trusses it can be hard to asses the boundary conditions that a member experiences, in order to estimate its buckling length.

$$N_{cr} = \frac{\pi^2 EI}{(KL)^2} \quad 5.$$

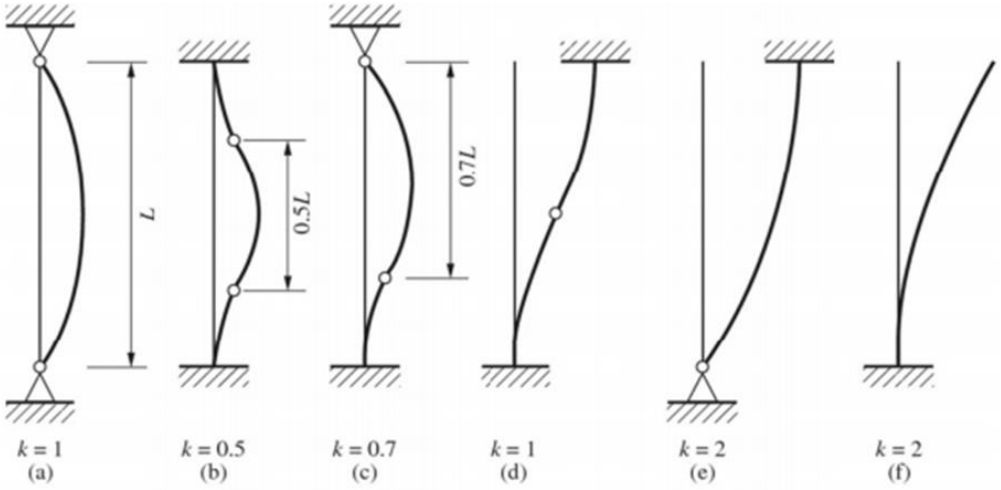


*Figure 13. Characteristic examples of buckling factors for various boundary conditions* (Geschwindner et al., 2017)

For the member's buckling length, the maximum value considered is 1. Since both ends are considered translationally fixed, it accounts only for deformation occurring in the axis between its two ends. Buckling lengths above 1 require that one of the ends is either partially restrained or completely unrestrained. Depending, now, on the rotational restraint that can develop at its ends, the buckling length can be as low as 0.5, in the extreme case that both member's ends are rotationally constrained (Figure 13). The level of rotational restraint that may be developed is influenced by several factors such as the joint and connection types used to connect the members, the geometry of the structure, the relative stiffness between the different members and the loading conditions.

A reasonable assumption for design that could be used in practice would be to take the ends of an individual truss member as hinged. This is what is proposed by the American building codes (AISC, 2016b). Specifically, it states that "… the effective length for flexural buckling of all members shall be taken as the unbraced length unless a smaller value is justified by rational analysis". This would give buckling length equal to the system length, meaning a buckling factor of 1. In reality, this would only be the case if all members of the truss fail simultaneously (Poels, 2017; Ziemian, 2010) where no member can further restrain another. This of course is usually not the case as rarely all members are designed to have close to unity check. There is also the case of very flexible connections compared to the stiffness of the member. In this situation, the restraint that adjacent

members can provide is limited by the connection's stiffness. As such, no meaningful restraint can develop. This is not the case for welded hollow section joints with no overlap though, as they can create quite a rigid connection. For joints with high β the stiffness may be large enough for them to be considered rigid (B. Zhao et al., 2020; X.-L. Zhao et al., 2001). Owing to the beneficial boundary conditions that the relatively high stiffness of welded hollow sectioned joints provide, different approaches and buckling lengths formulas have been developed, to reflect reality more accurately, but also improve design.

### 2.3.2 Significance of connections stiffness on truss structures

The stiffness of the connections plays several significant roles in trusses. Firstly, they may affect the distribution of axial forces, such in the case of shallow Vierendeel girders (Garifullin et al., 2019; W. Wang & Chen, 2005). This, though, is not the case for trusses with diagonal members, which assuming either fully fixed member's ends or pinned member's ends has little effect on the distribution of the axial forces of the members. What is affected by the assumption of the member's boundary conditions is the development and distribution of secondary moments. However, these do not affect the ultimate resistance of the members, because in the ultimate limit state (ULS), due to yielding of the extreme fibres of the members, they dissipate (Ziemian, 2010). Where connections also have a significant role though, is in the buckling behaviour of trusses.

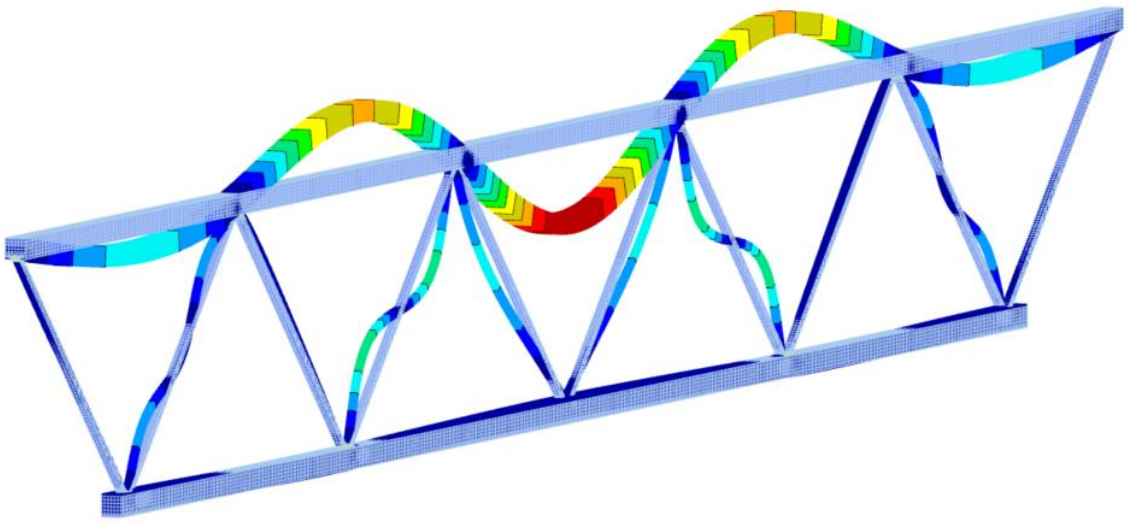

*Figure 14. Chord member buckling mode of a truss girder*

As was mentioned in an earlier section, due to the relatively high stiffness developed between welded hollow members, the buckling behaviour can be improved through higher rigidity throughout the truss. This can affect the global behaviour, such as the case of lateral torsional buckling of a girder (Biegus & Wojczyszyn, 2011; Czepizak & Biegus, 2016; Jankowska-Sandberg & Kołodziej, 2013; Krajewski & Iwicki, 2015), or the buckling behaviour of the individual members (Boel, 2010; Haakana, 2014; Hornung & Saal, 2001; Poels, 2017) (Figure 5). In the current thesis the focus will be on the buckling length of individual members and the effects at a global level are not going to be investigated further. The approaches and research done on the buckling length of individual members are going to be discussed in the upcoming sections.

Lastly, not accounting for the local behaviour of the joints can incur significant errors in other areas, such as estimating deflections, natural frequencies, and dynamic mode shapes (Asgarian et al., 2014, 2015). These do not compose part of the scope of this thesis, but it is good for the reader to be aware of the general importance of accounting for the joints behaviour in practice.

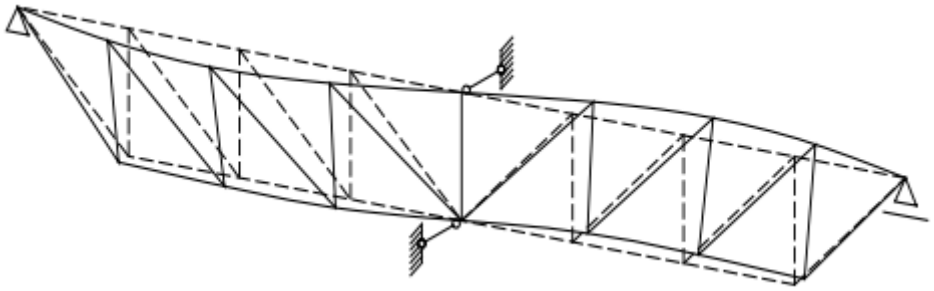

*Figure 15. Example of truss's global buckling mode (Biegus & Wojczyszyn, 2011)*

### 2.3.3 Truss buckling lengths in codes

Taking into consideration the benefits arising from the increased connection stiffness of welded hollow section joints, EN1993.1.1 prescribes buckling factors lower than 1.0. Specifically, in section BB.1.3, it states for hollow section chord members the buckling factor for in and out of plane buckling may be taken as 0.9. For hollow section brace members without cropping or flattening and welded around their perimeter it may be taken as 0.75 irrespective of in or out of plane buckling. Lower values may be used based on testing or calculations. In the case of using the lower buckling lengths given for the braces, the buckling factors of the chords should not be decreased to 0.9. The organization CIDECT (Comité International pour le Développement et l´Etude de la Construction Tubulaire) provides the same values given by EN1993.1.1 but additionally provides formulas for the buckling length of braces that have a limited β factor ($\beta \leq 0.6$). These can be seen in Table 1, taken from CIDECT's design guide 2 (Rondal et al., 1992). The design guide additionally provides buckling length predictions for unrestrained chords, but as this thesis focuses on member buckling and not the global buckling effects, they are not analysed further.

Table 1. Truss buckling lengths for braces according to CIDECT's Design guide 2 (Rondal et al., 1992)

| | |
|---|---|
| $d_o$: outer diameter of a circular chord member<br>$d_1$: outer diameter of a circular bracing member<br>$b_o$: external width of a square chord member<br>$b_1$: external width of square bracing member | 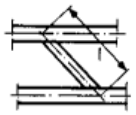 $\beta = \frac{d_1}{d_o}$ or $\frac{d_1}{b_o}$ or $\frac{b_1}{b_o}$ |
| for all $\beta$: $l_b/l \leq 0.75$ | |
| when $\beta < 0.6$, in general $0.5 \leq \frac{l_b}{l} \leq 0.75$<br>calculate with: | |
| chord: CHS<br>bracing: CHS | $l_b/l = 2.20 \left( \frac{d_1^2}{l \cdot d_o} \right)^{0.25}$ (7.1) |
| chord: SHS<br>bracing: CHS | $l_b/l = 2.35 \left( \frac{d_1^2}{l \cdot b_o} \right)^{0.25}$ (7.2) |
| chord: SHS<br>bracing: SHS | $l_b/l = 2.30 \left( \frac{b_1^2}{l \cdot b_o} \right)^{0.25}$ (7.3) |

Table 2. Design values for buckling factors, depending on the boundary conditions (*Code for Lifting Appliances in a Marine Environment*, 2020)

| Diagrammatic representation | Restraint conditions | K |
|---|---|---|
| 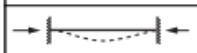 | Constrained against rotation and translation at both ends | 0,7 |
|  | Constrained against rotation and translation at one end and translation only at other end | 0,85 |
| 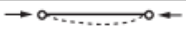 | Constrained against translation only at each end | 1,0 |
| 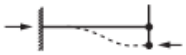 | Constrained against rotation and translation at one end and against rotation only at other end | 1,5 |
|  | Constrained against rotation and translation at one end and free to rotate and translate at other end | 2,0 |

The American codes, as was mentioned earlier, prescribe a standard buckling factor of 1.0 except if a lower value can be justified by rational analysis (AISC, 2016b). What the American codes additionally provide is an increase of the buckling factor for the classic boundary conditions of members to account for deviations that are observed in practice, from the theoretical values. This, though, is not especially useful as the boundary conditions of truss members cannot be approximated by one of these standard cases (except maybe of the case of Pinned-Pinned boundary conditions). A similar table is also given by the Code for Lifting Appliances in a Marine Environment (CLAME) by Lloyd's Register (Table 2). Lastly, the Japanese standard for Steel and Composite structures adopts buckling factor values of 0.9 for chord members and 0.8 in the case of web (brace) members (Commentary (1) in section 12.2.2.2). What is also interesting is that it provides some outdated values from different codes. These can be compared to the values that are currently in use and demonstrate how the buckling factors have changed (Table 4).

Table 3. Outdated buckling factors from various codes (*Standard Specifications for Steel and Composite Structures*, 2009)

| Country/code | Chord member | Web member |
|---|---|---|
| USA AISC (1969) | 1.0 | 1.0 |
| Germany DIN4114 (1978) | 1.0 | 0.9 |
| Eurocodes 3 (1983) | 1.0 | 0.9 |
| Japan JSHB (1994) | 1.0 | 0.8∼1.0 |
| Netherlands NEN3851 (1974) | 1.0 | 0.7∼1.0 |
| Tchecoslovakia CSN (1976) | 1.0 | 0.5∼1.0 |
| Belgium NBN B51-001 (1980) | 0.9 | 0.9 |
| France CM (1966) | 0.9 | 0.8 |
| Switzerland SIA161 (1979) | 0.9 | 0.8 |
| Great Britain BS5400 (1980) | 0.85 | 0.7 |

Table 4. Buckling factors currently prescribed

| Country/code | Chord member | Brace member |
|---|---|---|
| AISC (2016) | 1.0 | 1.0 |
| Eurocodes 3 (2005) | 0.9 | 0.75 |
| Japanese standard (2007) | 0.9 | 0.8 |

## 2.4 State of the art

Since the current thesis will revolve around member buckling of hollow sectioned trusses with eccentrically welded joints, a good starting point is reviewing research done on centrically welded joints. The most relevant literature is presented and analysed in this chapter.

In recent years, researchers Hornung and Saal introduced the concept of replacing shell element models for joint modelling (Figure 16) with rotational springs (Hornung & Saal, 1998). In their work they investigated the out of plane buckling behaviour of braces comprising a truss scaffolding system. The investigation revolved around CHS chords and SHS braces, whilst the joints used were K-joints (Figure 17).

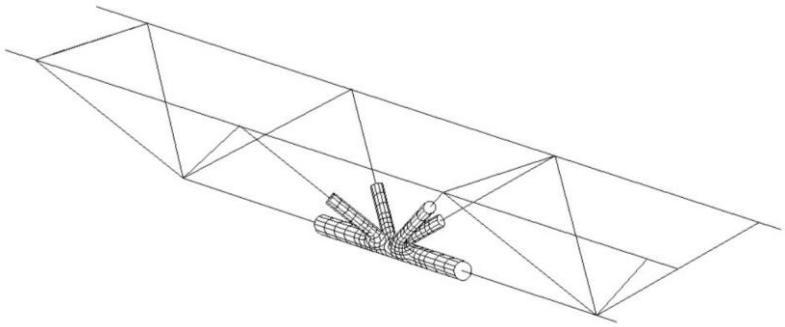

*Figure 16. Conventional modelling of joints for global analysis, using shell element. (ESDEP WG 12, "Lecture 12.4.1: Fatigue Behaviour of Hollow Section Joints (I)")*

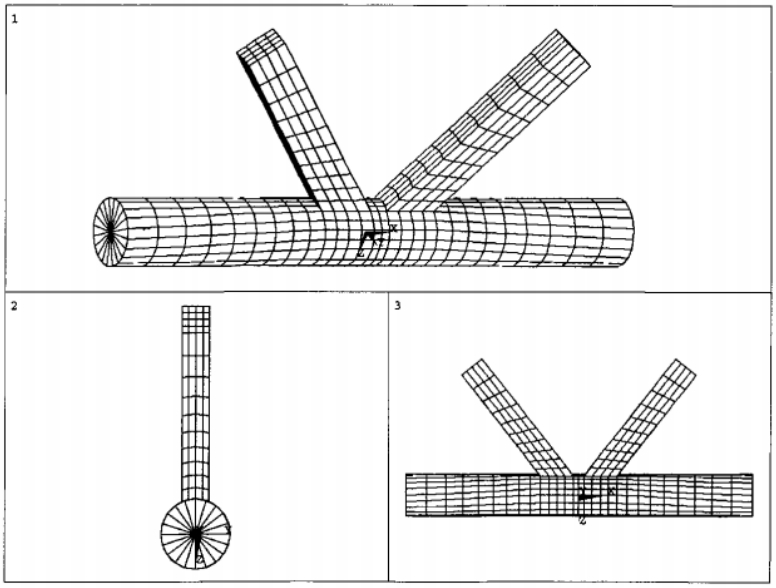


*Figure 17. Shell element model used in Hornung's and Saal's work (Hornung & Saal, 2001)*

The calculation of the stiffness for their joints was done using three different models and load cases (Figure 18). It is not explained what the rationale is behind picking the specific configurations, or what exactly they represent. From the following configurations the rotational springs for each case were calculated by extracting the rotations developed by the assumed spring that represented the connection. This was done by taking the total displacements developed in their sub-model and subtracting the displacements that were not due to the connection (eg. Brace bending), by using the corresponding equations (Figure 18(b)). From this, the smallest value of calculated springs was used for the analysis.

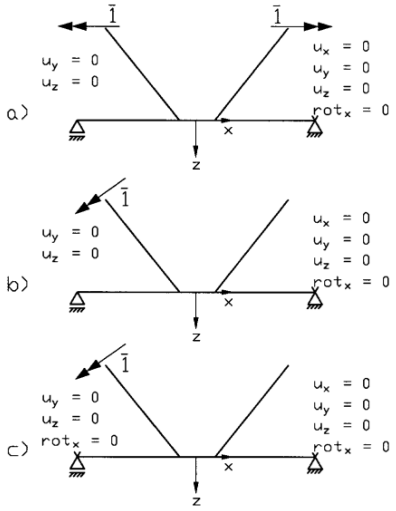


(a)

case a)

$$\bar{\varphi} = \frac{s}{GI_{T,chord}} + \left(\frac{\sin^2\alpha}{EI_{y,diag}} + \frac{\cos^2\alpha}{GI_{T,diag}}\right)\cdot b \qquad C_\varphi = \frac{\bar{1}}{\bar{\varphi} - \varphi}$$

case b)

$$\bar{\varphi} = \frac{(a+s)\cdot\sin\alpha}{GI_{T,chord}} + \frac{b\cdot\cos\alpha}{EI_{y,diag}} \qquad C_\varphi = \frac{\bar{1}\cdot\sin}{\bar{\varphi} - \varphi}$$

case c)

$$\bar{\varphi} = \frac{a\cdot(a+s)\cdot\sin\alpha}{(2\cdot a+s)\cdot GI_{T,chord}} + \frac{b\cdot\cos\alpha}{EI_{y,diag}} \qquad C_\varphi = \frac{\bar{1}\cdot\sin}{\bar{\varphi} - \varphi}$$

(b)

*Figure 18. (a) Model describing the geometry of the joint and (b) equations used to calculate the rotations attributable to the welded connections (Hornung & Saal, 2001)*

Eleven trusses were investigated (Table 5), and three different load cases were used for each truss (Figure 19). For each truss the highest buckling factor arising from the three load cases was set as the decisive factor. The decisive factors were then compared to the buckling factor of 0.75 given by the Eurocodes for out of plane buckling of braces. From the results only two factors were above Eurocode's prescribed value. This led them to the conclusion that Eurocode may be conservative in many cases.

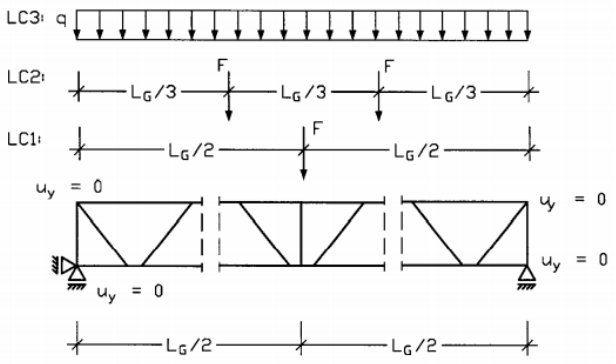


*Figure 19. Truss load cases used in investigation*

Table 5. Parameters for the different truss configurations used (Hornung & Saal, 2001)

| no. comp. | Material | length | height | Ø chord | $t_{chord}$ | Ø diag | $t_{diag}$ | α | g |
|---|---|---|---|---|---|---|---|---|---|
| 1 c1 | S 235 | 3.0 m | 400 mm | 48.3 mm | 3.2 mm | 30*20 mm | 2.0 mm | 51.5° | 18 mm |
| 2 c1 | S 235 | 4.0 m | 400 mm | 48.3 mm | 3.2 mm | 30*20 mm | 2.0 mm | 51.5° | 45 mm |
| 3 c1 | S 235 | 5.0 m | 400 mm | 48.3 mm | 3.2 mm | 30*20 mm | 2.0 mm | 51.5° | 12 mm |
| 4 c1 | S 235 | 6.0 m | 400 mm | 48.3 mm | 3.2 mm | 30*20 mm | 2.0 mm | 51.5° | 33 mm |
| 5 c2 | S 235 | 5.2 m | 400 mm | 48.3 mm | 3.2 mm | 30*20 mm | 2.0 mm | 49.1° | 50 mm |
| 6 c3 | S 235 | 5.0 m | 400 mm | 48.3 mm | 3.2 mm | 30*20 mm | 2.0 mm | 47.0° | 10 mm |
| 7 c4 | S 235 | 3.1 m | 400 mm | 48.3 mm | 3.2 mm | 33.7 mm | 2.6 mm | 41.5° | 60 mm |
| 8 c4 | S 235 | 4.1 m | 400 mm | 48.3 mm | 3.2 mm | 33.7 mm | 2.6 mm | 41.5° | 60 mm |
| 9 c4 | S 235 | 5.1 m | 400 mm | 48.3 mm | 3.2 mm | 33.7 mm | 2.6 mm | 41.5° | 60 mm |
| 10 c4 | S 235 | 6.1 m | 400 mm | 48.3 mm | 3.2 mm | 33.7 mm | 2.6 mm | 41.5° | 60 mm |
| 11 c4 | S 235 | 7.6 m | 400 mm | 48.3 mm | 3.2 mm | 33.7 mm | 2.6 mm | 41.5° | 60 mm |

Regarding the validation of their results, in their originally published paper (Hornung & Saal, 1998), Hornung and Saal did not compare their results with a full shell element model or something more substantial. The only comparison that was done, was with buckling length predicted from an individual member supported by springs at its ends (Figure 20). The springs used were the values of the rotational springs calculated (this is assumed, as they do not explicitly state what springs were used). Of course, the results, for the various formulas used, as well as the exact solution did not match the result obtained from their simplified beam element model.

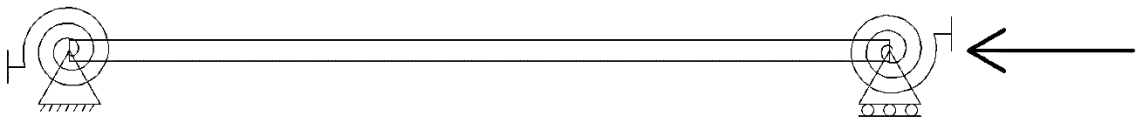

*Figure 20. Individual member with rotational restraints*

They acknowledge that this would be a wrong comparison as the real boundary conditions of the member were not accounted for correctly and the determination of those are quite difficult. It should be noted that the use of the joint's rotational springs as the only boundary conditions only provides the lower bound solution of the buckling factor. This is the case if the member's connections were attached to rigid supports. The adjacent members do not act as rigid supports in most cases, which means that this assumption is often wrong and not on the safe side. In their follow-up paper (Hornung & Saal, 2001) they compared their method with experimental results obtained by Rondal in 1988 and 1992. They concluded that the prescribed buckling length of 0.75 of the ENV1993 is often conservative and that the results from their method and the finite element analysis were satisfactory and safe.

Boel built upon the work of Hornung and Saal in his Master thesis at Eindhoven's TU. In his work he focused on the buckling of lattice girders and in his conclusions proposed buckling length formulas. To achieve his results, he used the approach introduced by Hornung and Saal and used springs to capture the behaviour of the connections (Figure 21).

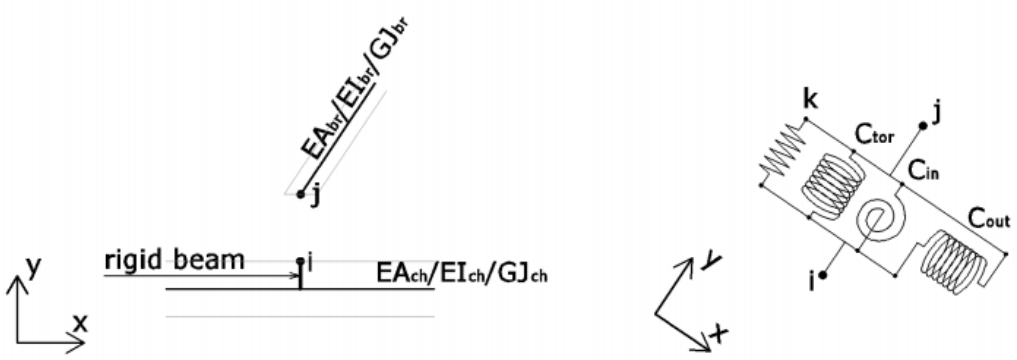


*Figure 21. Concept of describing the connection behaviour with springs in 4 different degrees of freedom* (Boel, 2010)

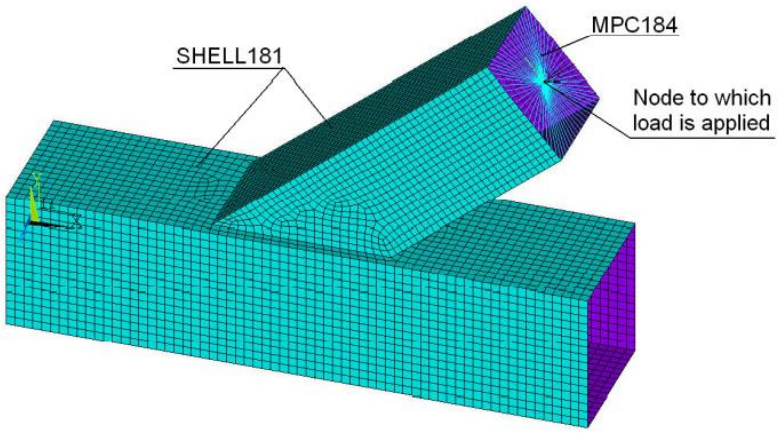


*Figure 22. Example of shell element model of the joint* (Boel, 2010)

In his work he first studied the formulation of the connection stiffness that needed to be calculated and used for a buckling analysis. For the cases of in plane and out of plane stiffness of the connections he proposed three different load cases that could be used for their calculation. Similarly to Hornung and Saal, he calculated the displacement of the spring representing the connection by subtracting from the total displacement the displacements of the other components of the modelled K-joint (Figure 23). From the three load cases, load case 3 computes the lowest stiffness, load case 2 computes the highest and load case 1 gives a stiffness value in between the other two. From his investigation he concluded that the rotational stiffness calculated by load case 1 can be used for the in-plane buckling calculation, whilst the averaged stiffness calculated from the three load cases can be used for the out of plane calculations.

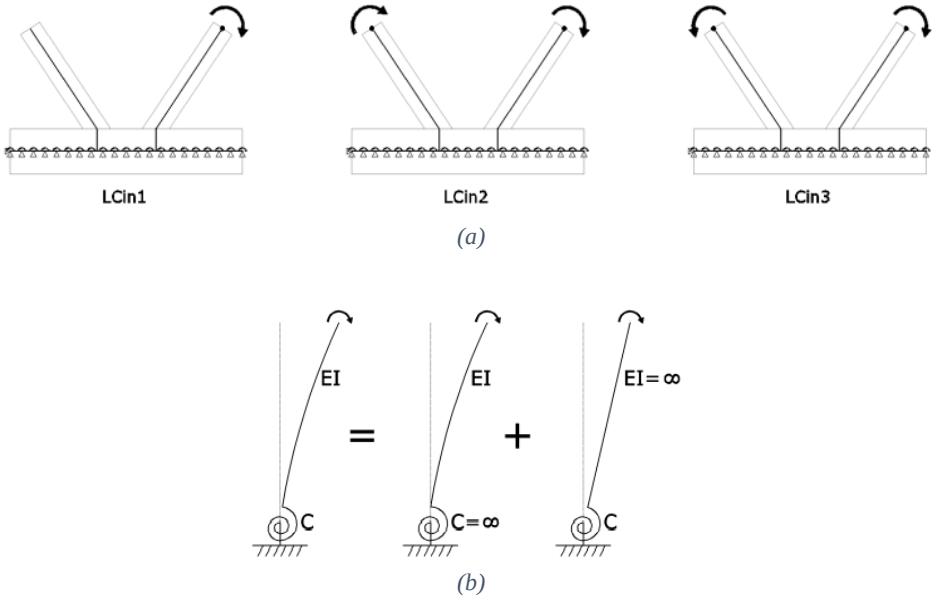


*Figure 23. Components to calculate in plane stiffness of connection. (a) Three load cases used for the calculations and (b) deflections of cantilever beam with rotational spring describing the brace's behaviour*

For the axial and torsional stiffness, he concluded that their value was not important for the results and assuming rigid connections for those degrees of freedom was adequate. He additionally investigated the optimum position for the rotational springs and in general the formulation of the joint geometry for the simplified spring/beam element model (Figure 25). His investigation resulted in proposing that his initial configuration, Variant 1, was the best to describe the truss's buckling behaviour. Lastly, it is pointed out that his conclusions were drawn from comparing his proposed method to the results obtained for a whole truss modelled with shell elements.

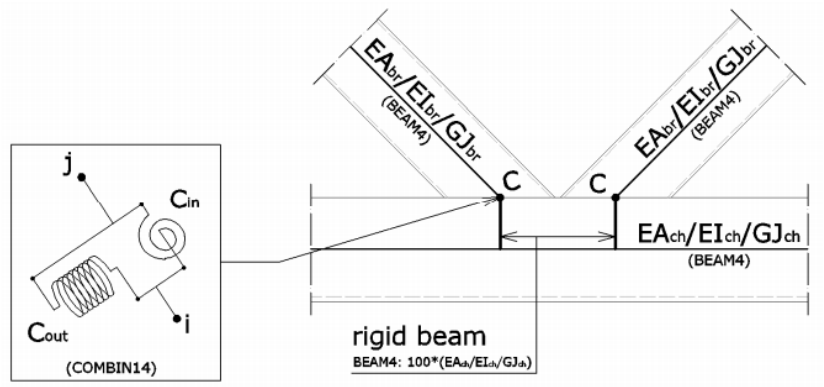


*Figure 24. Final model to simulate the behaviour of the joint* (Boel, 2010)

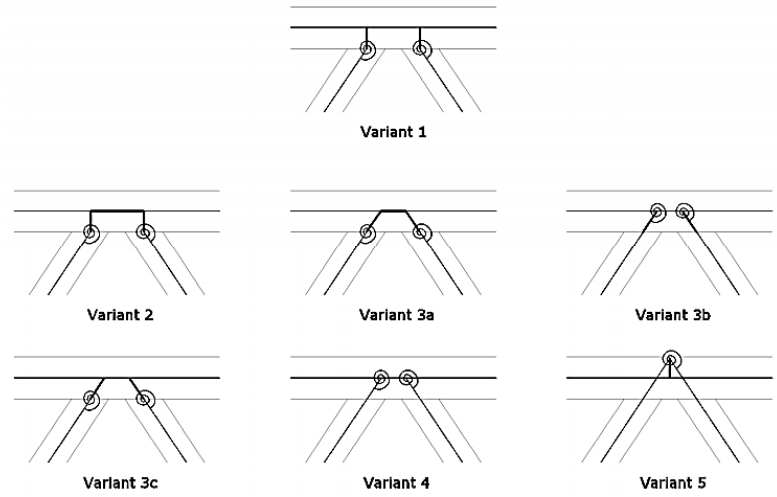


*Figure 25. Different variants that were compared to find the one best describing the joint behaviour* (Boel, 2010)

His investigation continued by calculating the buckling length of a truss girder. The truss had a specific geometry and loading (Figure 26) and it was investigated against different combinations of chord and brace profiles (Chord-Braces: SHS-SHS, SHS-CHS, CHS-CHS). For each combination of cross sections, the top and bottom chords were the same and all the brace members made use of the same profile. In total 21 different configurations were used. From these, the buckling lengths of the end brace and the middle chord were determined for in plane and out of plane. This was done by attributing structure buckling modes to modes of members. Due to the complex buckling modes, in case that there was doubt, he always used the lowest attributable buckling mode to the corresponding member (Brace and chord) and mode (in-plane and out of plane).

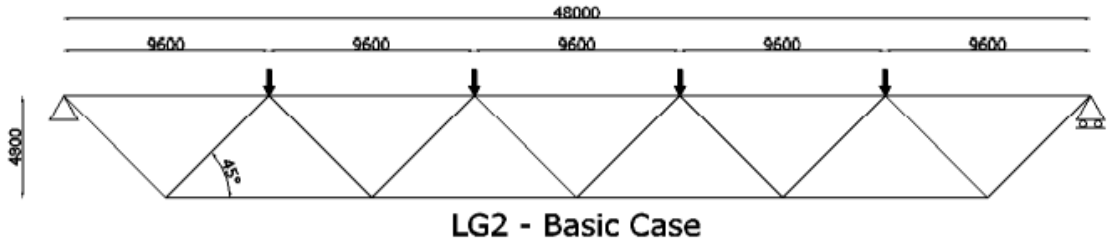


*Figure 26. Truss geometry and support/loading conditions used* (Boel, 2010)

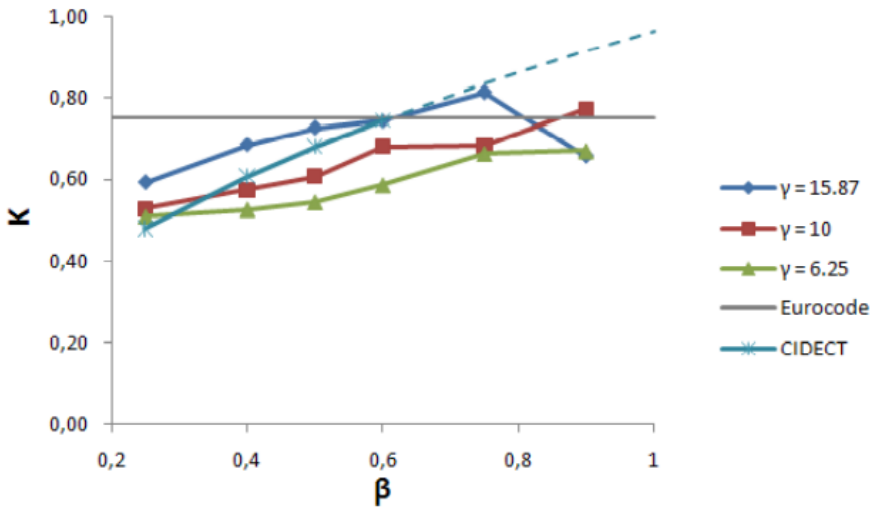


*Figure 27. In-plane buckling lengths of brace members for SHS-200 chords SHS braces* (Boel, 2010)

From his results he concluded that Eurocode buckling lengths are mostly conservative but in some cases, unconservative. The Eurocode is expected to be conservative as it attempts to capture a wide range of applications, so it includes a certain safety margin. This of course is at odds with the fact that Boel concluded that it may be unconservative in some cases. One reason for this could be that the prescribed buckling lengths of the Eurocode are meant for member buckling, meaning the non-sway buckling length. As Boel in his investigation only restrained his top chord and his results were for an unrestrained tension chord, these include sway effects of the whole structure (Figure 28). Another reason, could be misattributed buckling modes. As was mentioned earlier, in cases where the actual mode was in doubt, and a few modes could be attributed to the same member and buckling direction, the smallest was always used in the results. This could lead to an underestimation of the buckling load of a member, which would lead to the conclusion that Eurocode is not conservative. Lastly, Boel uses a length defined differently than what is proposed in practice (Figure 29). Shorter lengths give rise to larger buckling lengths for the same critical buckling load, so comparing with Eurocode is not that straightforward.

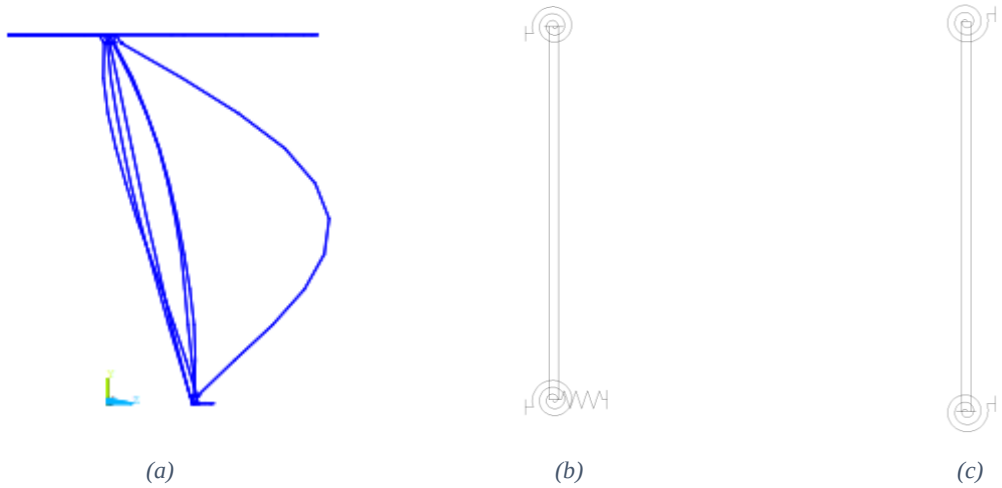

*(a)* *(b)* *(c)*

*Figure 28. (a) Out of plane buckling mode of brace, as was calculated by Boel* (Boel, 2010). *(b) Boundary conditions of braces for accounting for global behaviour and (c) boundary conditions for accounting only for member buckling*

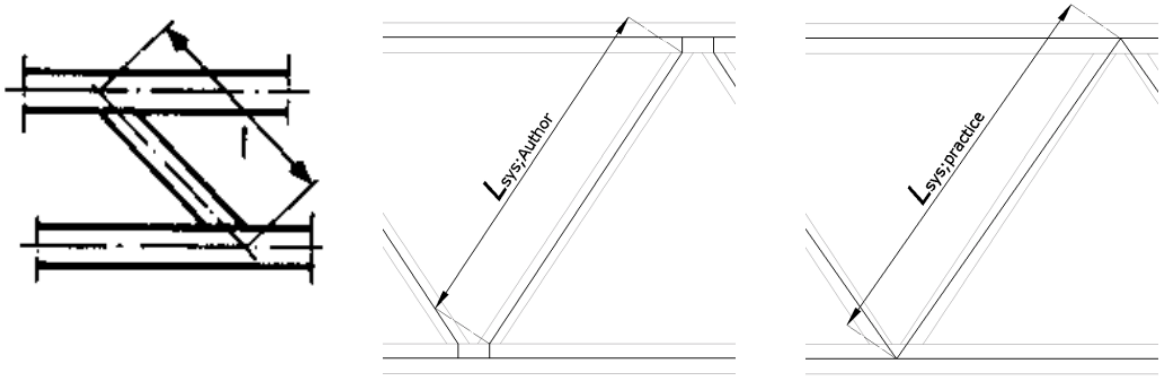


*(a)* *(b)*

*Figure 29. (a) Length of member as given by CIDECT guidelines* (Rondal et al., 1992) *and (b) length of member as defined by Boel* (Boel, 2010)

The last step of his work was to attempt to fit a formula, which could be used in design, from the results obtained from his models. Since no formula existed for the buckling length of chords, he introduced a bilinear design curve which fit his data (Figure 30). For his formula for braces, he altered the ones provided by CIDECT (Figure 28Table 6-Table 8), in which width of the chord and brace, as well as the length of the braces are used

(Figure 31). He specifically changed the exponent, as well as introducing the γ factor as a parameter in the formula. A summary of his proposed buckling lengths can be found from Table 6 till Table 8.

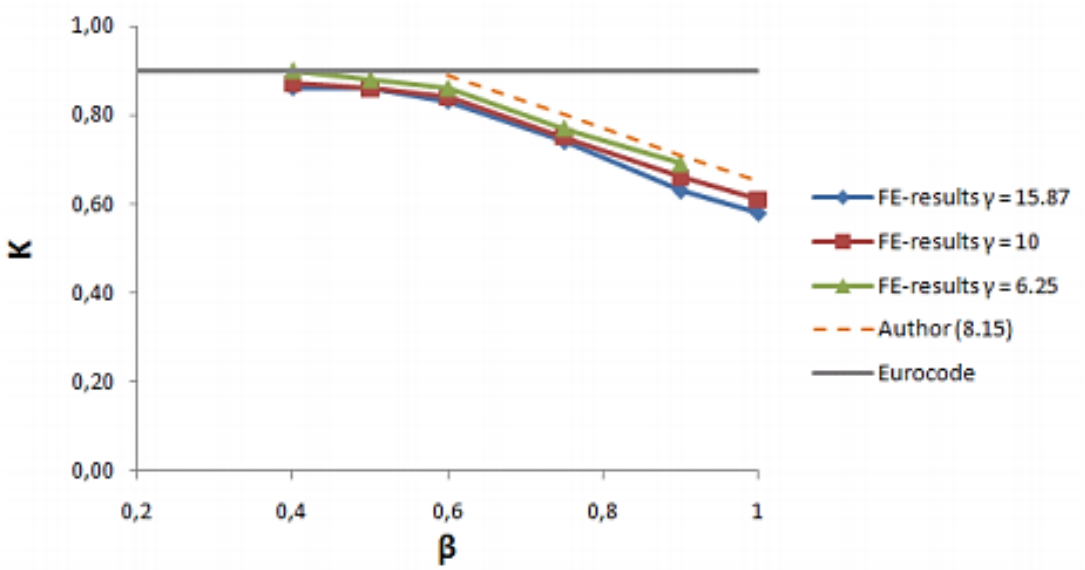


*Figure 30. In-plane buckling lengths of chord members for SHS-200 chords and SHS braces* (Boel, 2010)

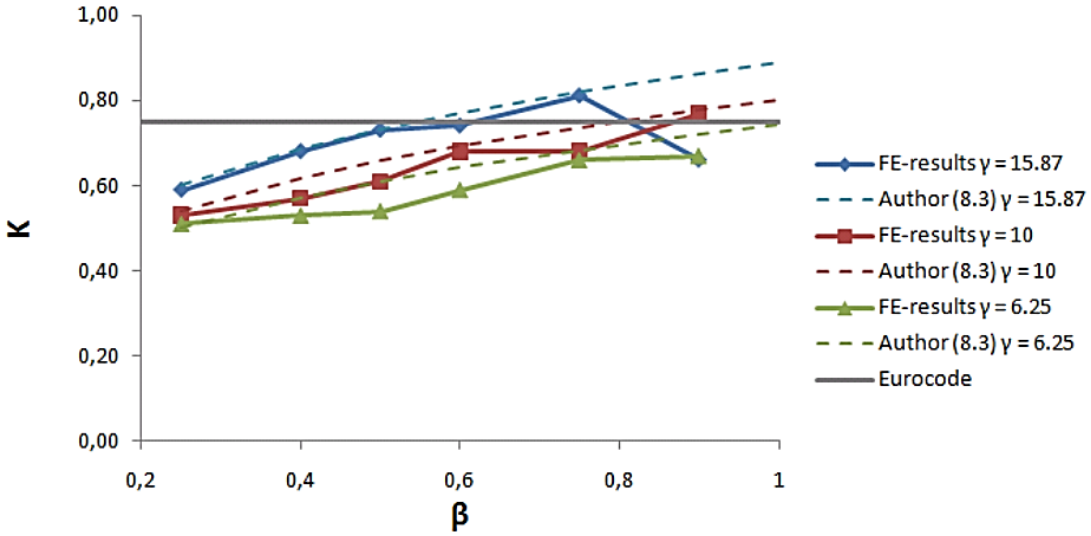


*Figure 31. In-plane buckling lengths of brace members for SHS-200 chords and SHS braces* (Boel, 2010)

Table 6. Proposed buckling length factors for a truss with SHS chords and SHS braces

*Chord and brace combination: SHS-SHS*

| | Eurocode | CIDECT | Boel (2010) |
|---|---|---|---|
| **Chord in-plane:** | 0.9 | 0.9 | $1.25 - 0.6\beta \leq 0.9$ |
| **Chord out of plane:** | 0.9 | 0.9 | $1.17 - 0.45\beta \leq 0.9$ |
| **Brace in- plane:** | 0.75 | $2.30\left(\beta\frac{b_1}{l}\right)^{0.25}, \beta < 0.6 \leq 0.75, for\ all\ \beta$ | $(1.05 + 0.025\gamma\left(\beta\frac{b_1}{l}\right)^{0.14}$ |
| **Brace out of plane:** | 0.75 | $2.30\left(\beta\frac{b_1}{l}\right)^{0.25}$ | $(3 + 1.2\,\gamma\left(\beta\frac{b_1}{l}\right) + 0.55 \leq 1.0$ |

Table 7. Proposed buckling length factors for a truss with SHS chords and CHS braces

*Chord and brace combination: SHS-CHS*

| | Eurocode | CIDECT | Boel (2010) |
|---|---|---|---|
| **Chord in-plane:** | 0.9 | 0.9 | $1.17 - 0.45\beta \leq 0.9$ |
| **Chord out of plane:** | 0.9 | 0.9 | $1.05 - 0.25\beta \leq 0.9$ |
| **Brace in- plane:** | 0.75 | $2.35\left(\beta\frac{d_1}{l}\right)^{0.25}, \beta < 0.6 \leq 0.75, for\ all\ \beta$ | $(0.95 + 0.03\gamma)\left(\beta\frac{d_1}{l}\right)^{0.14} \geq 0.5$ |
| **Brace out of plane:** | 0.75 | $2.35\left(\beta\frac{d_1}{l}\right)^{0.25}$ | $1.2\,\gamma\left(\beta\frac{d_1}{l}\right) + 0.55 \leq 1.0$ |

Table 8. Proposed buckling length factors for a truss with CHS chords and CHS braces

*Chord and brace combination: CHS-CHS*

| | Eurocode | CIDECT | Boel (2010) |
|---|---|---|---|
| **Chord in-plane:** | 0.9 | 0.9 | $1.25 - 0.6\beta \leq 0.9$ |
| **Chord out of plane:** | 0.9 | 0.9 | $1.17 - 0.45\beta \leq 0.9$ |
| **Brace in- plane:** | 0.75 | $2.20\left(\beta\frac{d_1}{l}\right)^{0.25}, \beta < 0.6 \leq 0.75, for\ all\ \beta$ | $(2.5 + \gamma)\left(\beta\frac{d_1}{l}\right) + 0.5 \leq 1.0$ |
| **Brace out of plane:** | 0.75 | $2.20\left(\beta\frac{d_1}{l}\right)^{0.25}$ | $(5 + 1.2\,\gamma\left(\beta\frac{d_1}{l}\right) + 0.55 \leq 1.0$ |

It should be noted that for the case of out of plane buckling of the brace, even though an upper limit of the buckling factor is prescribed (Table 6-Table 8), this is erroneous. As the trusses that were investigated were not restrained at the tension chord, the sway effects are included in the results. This means that the upper limit of 1.0 which applies to non-sway members cannot be used in Boel's formula. This note is quite important as towards the higher end of β values, the buckling factors for the braces attached to an unrestrained tension chord reach unity (Figure 32).

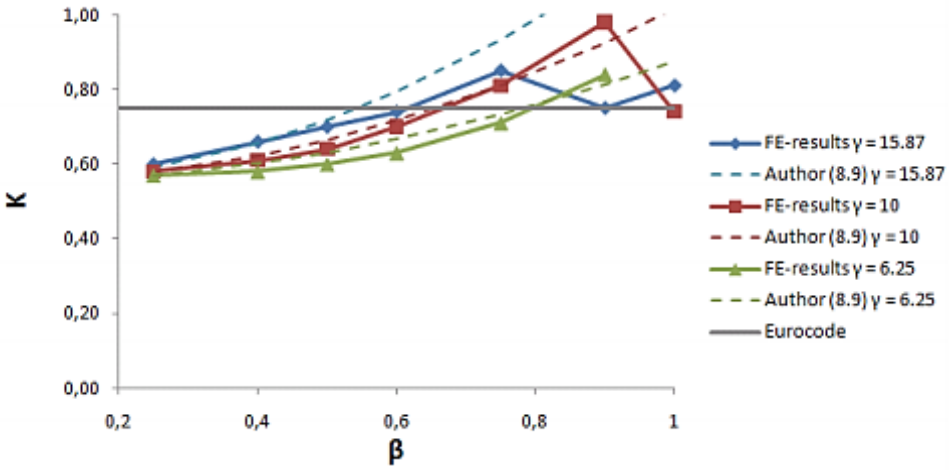


*Figure 32. Out of plane buckling lengths of brace members for SHS-200 chords and SHS braces* (Boel, 2010)

In section 2.3.1 it was mentioned that one of the ways that members of a truss could experience a buckling factor of 1.0 is in the case that all members fail simultaneously, and thus adjacent members provide no restraint to a specific member. This topic was investigated by Poels in 2017 in his master thesis from the University of Eindhoven. In his work, he aimed to study the buckling behaviour of trusses optimized for buckling. By using a truss of specific geometry (Figure 33), he progressively optimized the cross sections used for the chord and braces. His aim was to reach a case for which buckling occurs for most members simultaneously. He studied hollow sections with the specific combinations being SHS-SHS, SHS-CHS and CHS-CHS. The actual profiles varied quite a bit in order to achieve his optimization.

For his investigation he adopted the approach developed by Boel in his master thesis. He initiated his study with a simplified model, where he replaced the joints with rotational springs. The stiffness calculations and joint formulations all conformed with Boel's proposals. With this model he proceeded to progressively optimize the truss structure by reducing the cross-sectional dimensions.

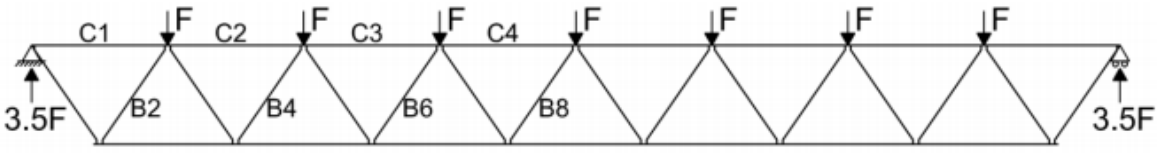


*Figure 33. Geometry and support/loading conditions of truss under investigation* (Poels, 2017)

The optimization was performed by running successive linear buckling analysis and retrieving the buckling lengths. During the process each buckling mode was categorized depending on which member had buckled or was bent and whether it was in or out of plane (Table 9). By using the calculated buckling lengths, he performed the Eurocode 3 verification and aimed to get cross sections near unity. The goal of his initial optimization was to get the different members to buckle for the same buckling load. By performing a few iterations, he managed to get satisfactory results visible in Table 10 and Table 11.

Table 9. Table of results from initial investigation for first iteration (Poels, 2017)

| Configuration 1 SHS-SHS | | | | | | | |
|---|---|---|---|---|---|---|---|
| Eigenvalue | C2 | C3 | C4 | B2 | B4 | B6 | B8 |
| 128873 | | | | | | in | |
| 129223 | | | | | | in | |
| 130511 | | | | | | out | |
| 141052 | | | | | | out | |
| 145084 | | | | in | | | |
| 145129 | | | | in | | | |
| 150253 | | | | | in | | |
| 150415 | | | | | in | | |
| 152741 | | | | | | out | |
| 153485 | | | | | | out | |
| 171287 | | | | | out | | |
| 171725 | | | | | out | | |
| 194578 | | | in | | | | bent |
| 194848 | | | out | | bent | | |

Table 10. Buckling length factors after first optimization

| Configuration 2.4 SHS-SHS | | | | | | | | |
|---|---|---|---|---|---|---|---|---|
| Eigenvalue | C2 | C3 | C4 | B2 | B4 | B6 | B8 | Dir. |
| 136115 | | | 0.93 | | | 0.81 | 0.80 | in |
| 136817 | | | | bent | bent | 0.80 | 0.80 | out |
| 138041 | | | 0.92 | | | bent | | out |
| 146186 | | | | 0.79 | 0.80 | | | out |
| 154682 | | | | | | 0.76 | | in |

Table 11. Chosen cross sections after first optimization

| Configuration 2.4 SHS-SHS | |
|---|---|
| Chords | SHS180/6.3 |
| B1 & B2 | SHS110/6.3 |
| B3 & B4 | SHS100/6.3 |
| B5 & B6 | SHS84/6.3 |
| B7 & B8 | SHS60/6.3 |

He verified his results by using a geometric non-linear analysis with imperfection (GNIA). He stated that the results go asymptotically to the LBA value. This is debatable and the buckling load appears to converge to a lower value than the one predicted by the linear buckling analysis (Figure 34). This is not unexpected though, as introducing imperfections can lower the buckling value of the system (Gantes, 2016). For the out of plane buckling, it appears that it is actually reaching asymptotically to the linear buckling analysis value (Figure 35). Similar observations can be made for the SHS-CHS and CHS-CHS configurations. The results do indeed indicate that the buckling modes selected from the LBA are correct, as they are close to the linear buckling factor and always below it.

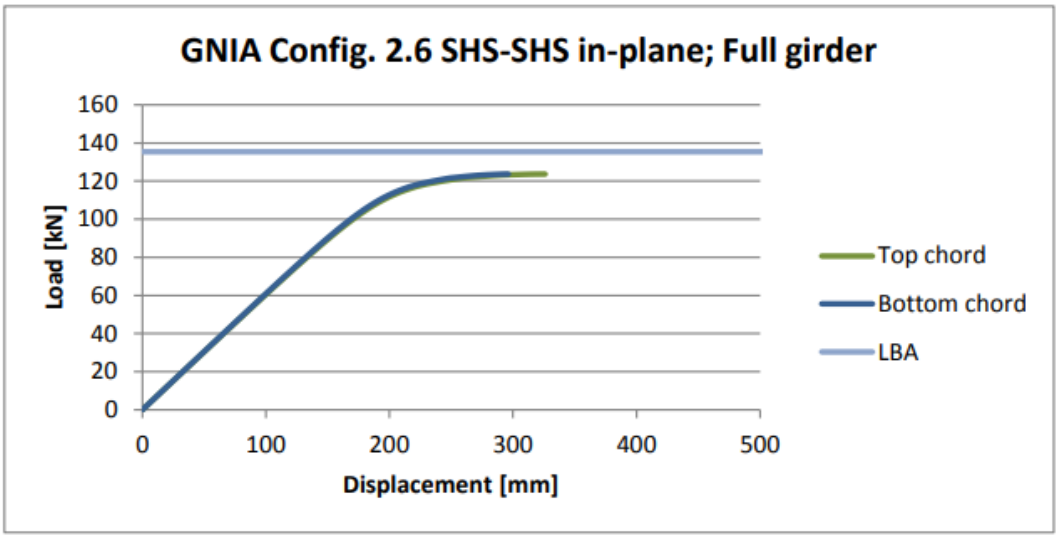


*Figure 34. Load displacement diagram for in plane buckling mode, using a GNIA* (Poels, 2017)

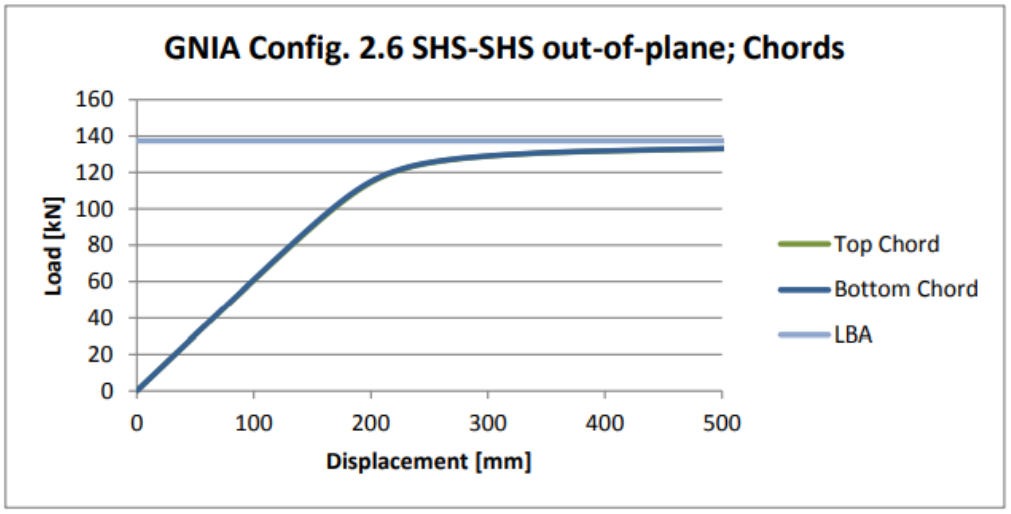


*Figure 35. Load displacement diagram for out of plane buckling mode, using a GNIA* (Poels, 2017)

He followed his GNIA results by adding material non-linearity in his analysis (GMNIA). He did not use the simplified beam element and spring model. The process and investigation include the behaviour of the connection under plasticity was deemed way too complex for the scope of his thesis. Very coarse mesh was used for the shell element modelling. Too cross validate his previous results and the new models, he compared his LBA results between shell element and beam element. His results matched quite well. The only notable example was the case of CHS-CHS configuration. The buckling length of the chord was calculated equal to 1.0 and concluded that Eurocode 3 was not conservative in this case, with its prescribed factor of 0.9. Eurocode 3 though also states that if the reduced buckling length is used for the braces, then no reduction is allowed for the chord. This is exactly in line with his findings (Table 12). In general, the difference appeared only for the circular hollow sections. This, according to Poels, could be due to axial and rotational stiffness interacting. In Boel's investigations he checked the two stiffnesses separately, so no interaction would be accounted for.

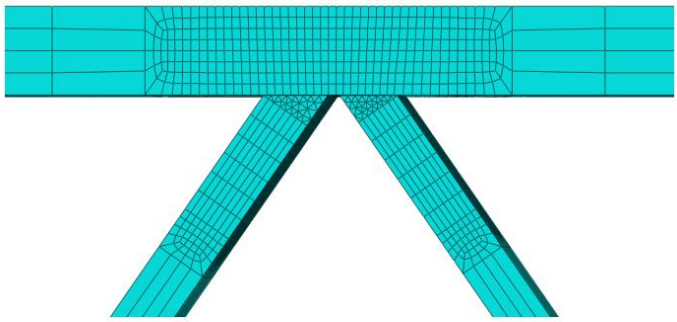

*Figure 36. Shell element model used in the GMNIA investigation* (Poels, 2017)

Table 12. Linear buckling analysis results for shell element model (Poels, 2017)

| Configuration 2.6 CHS-CHS; SE model | | | | | | | | |
|---|---|---|---|---|---|---|---|---|
| **Eigenvalue** | **C2** | **C3** | **C4** | **B2** | **B4** | **B6** | **B8** | **Dir.** |
| 125659 | | | 1.01 | | | bent | bent | out |
| 129505 | | | 1.00 | | | | bent | in |
| 129905 | | | 1.00 | | | | | out |
| 135822 | | | | 0.78 | | | | in |
| 150827 | | | | 0.74 | 0.76 | 0.76 | 0.75 | out |
| 159651 | | | | | | 0.74 | | out |

In his investigation which included the material non-linearity, it became apparent that the failure and buckling of the structure were initiated from the yielding of the connection (Figure 37). From this, an initiation of stiffness loss for the connection could be assumed. Due to this, different members appeared to have much lower buckling loads than the ones predicted by the LBA. His main conclusion was that joints should be designed with adequate overstrength to avoid premature failure. This would guarantee that the buckling lengths are not affected by the yielding of the joints.

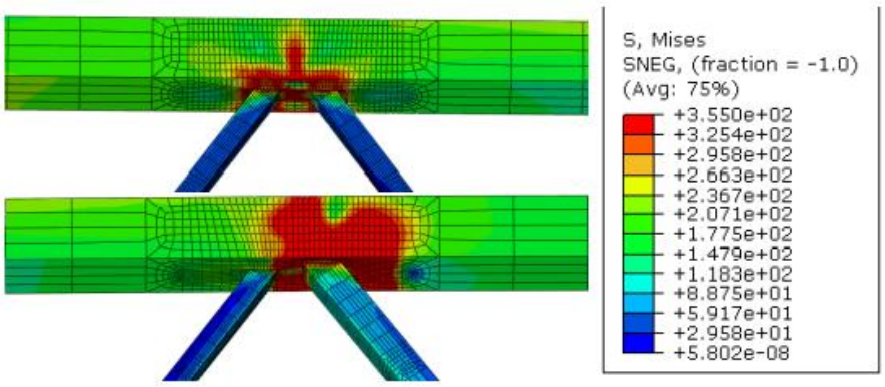


*Figure 37. Yielding of the connections prior to the appearance of buckling of members* (Poels, 2017)

## 2.5 Research work on eccentric joints.

In general, little work has been done on eccentric joints that are comprised of hollow sections, probably due to their rarity and use of them only on specific applications. The most recent work done on eccentric hollow section joints is from a paper in 2020 (B. Zhao et al., 2020). In their work, the researchers studied the out of plane behaviour of an eccentric joint comprised of rectangular hollow sections. They investigated the moment-rotation behaviour for out of plane moments and chord stress. In their investigation they used finite element model (FEM) and performed experiments to support their findings.

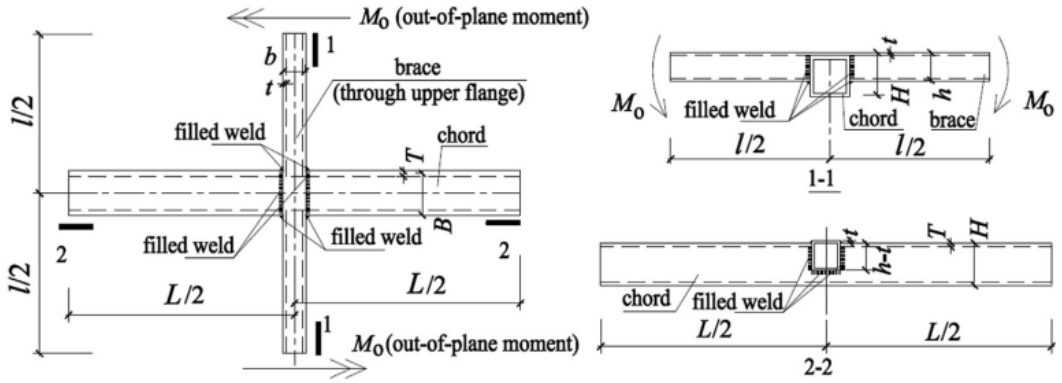


*Figure 38. Drawing of eccentric joint under investigation*

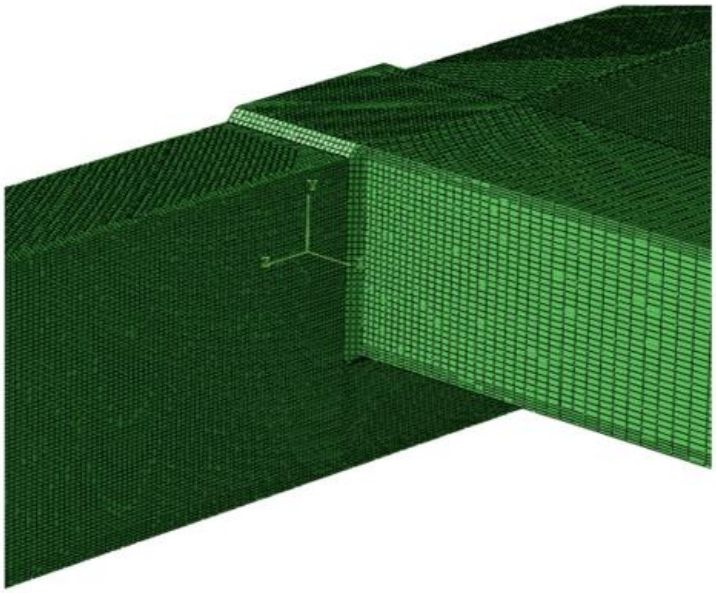

*Figure 39. Solid element model used in the investigation. Symmetry conditions were used.*

For the generation of their finite element models, they used the commercial software ABAQUS. The type of element used for their analysis was solid elements (Figure 39). The length of the chord and braces were taken adequately large for the connection behaviour not to be affected by the boundary conditions applied at their ends. They simulated the contact of the top plate with the chord with contact elements, although changing the active friction coefficient of the surfaces did not change the results substantially.

To retrieve the rotations attributable to the connection, the same method that has been mentioned in previous literature was used. In this, the displacements due to the connection are separated from the displacements due to the rest of the components of the set up (Figure 40).

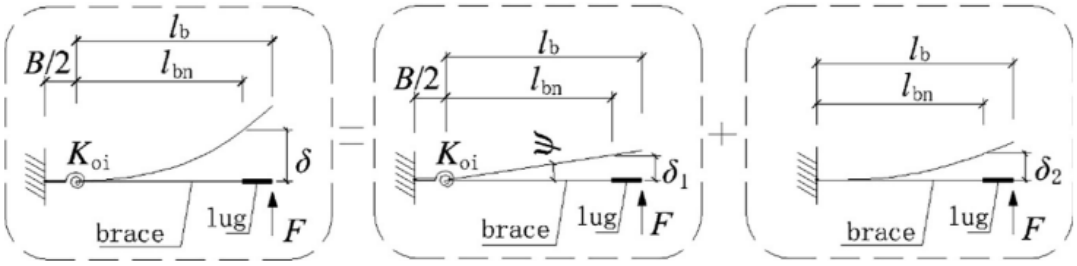


*Figure 40. Deflections of cantilever beam with rotational spring describing the brace's behaviour*

They additionally used an experiment to study the static behaviour of the connection and used the results to validate their finite element models. From their comparison they concluded that the FEM could predict well

the failure mode of the actual joint, as well as the Moment-Rotation behaviour until the end of the experiment (Figure 41).

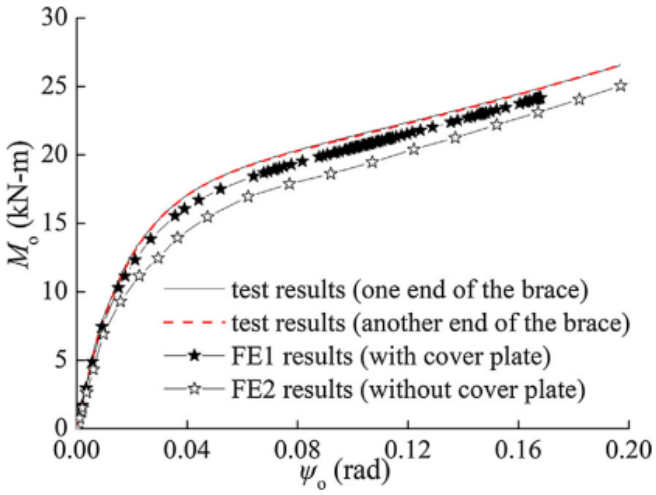


*Figure 41. Comparison of FEA results to experimental results of the eccentric joint*

A major part of their work was developing a semi-rigid model to describe the behaviour of the joint under out of plane moment and chord stress. Their model is based on the semi-rigid exponential model used to describe bolted end-plate connections. The model can be described by equation 6. and typical diagrams of the model are presented in Figure 42.

$$M_o = M_{op}\left\{1 - \exp\left[\frac{-(k_{oi} - k_{op} + C\psi_o)\psi_o}{M_{op}}\right]\right\} + k_{op}\psi_o \qquad 6.$$

Where:

| | |
|---|---|
| $C$ | Constant coefficient associated with the slope and shape of the curve |
| $M_{op}$ | The intercept moment |
| $k_{oi}$ | Initial stiffness |
| $k_{op}$ | Tangent stiffness |

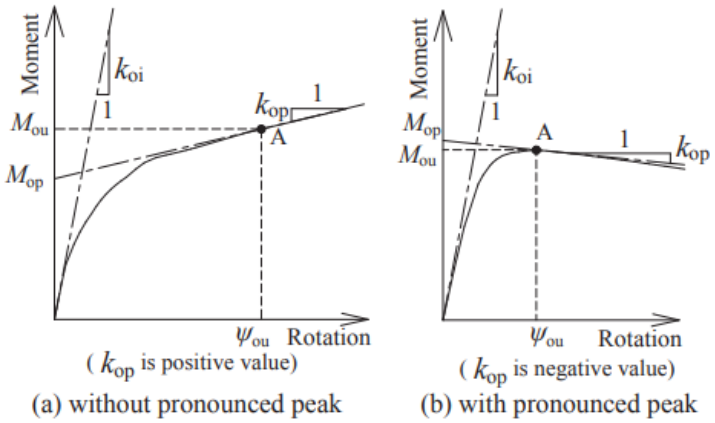


*Figure 42. Moment-rotation diagrams for the eccentric joints, including characteristic parameters of the semi-rigid model* (B. Zhao et al., 2020)

To verify their semi-rigid model, they compared 16 additional configurations and compared the results between their developed model and the results of an FEA of their validated model. From the results they concluded that the semi-rigid model predicted the behaviour of the connection well and that it could also capture the strength

degradation (Figure 43Figure 43. (a) The developed semi-rigid model compared to FE results and experimental results and (b) the developed semi-rigid model compared to 1 of the additional configurations used for validation)

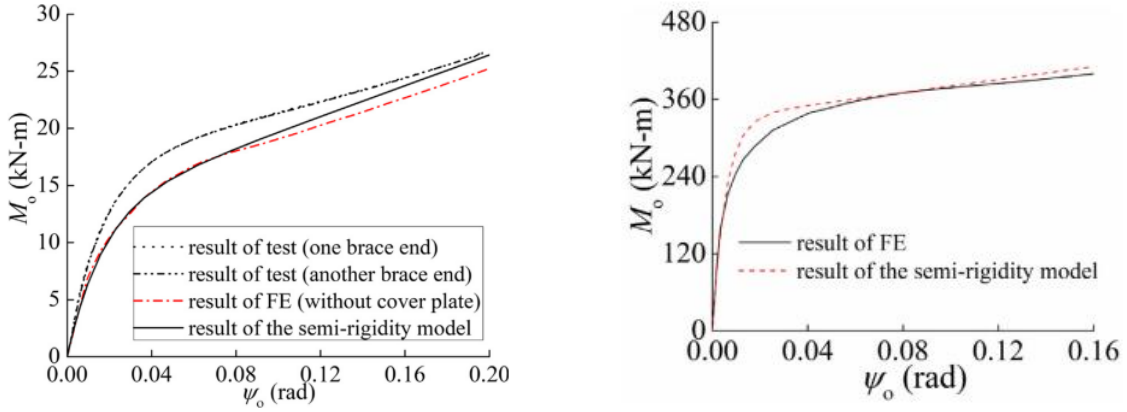


*(a)* *(b)*

*Figure 43. (a) The developed semi-rigid model compared to FE results and experimental results and (b) the developed semi-rigid model compared to 1 of the additional configurations used for validation*

Lastly, they investigated the effects of chord stress loading. For this investigation they used a total of 184 FE with varying characteristics and under various chord stress combinations. The modification of the stiffness due to the presence of chord strength is given by a factor with which you multiply the original stiffness, that is not under chord stress. This is a standard way of dealing with the presence of chord stress and is used in codes (*EN 1993-1-8: Eurocode 3: Design of Steel Structures - Part 1-8: Design of Joints*, 2005) as well as other researchers (Garifullin, Pajunen, et al., 2017). To conclude they verified their improved semi-rigid model, which included the effects of the chord stress, by using eight more joint configurations. It was concluded that their improved model predicted well the joint behaviour subjected to both chord stress and out of plane bending moment.

From their investigations they managed to extract a few useful conclusions. Firstly, they produced a semi-rigid model for the moment-rotation behaviour of the connection. This can be used for the analysis and design of the truss structure. This is especially important for the global buckling of single-layered reticulated structures, by which this study was inspired by. The results also help with the design of the members in buckling, so that the boundary conditions out of plane are better accounted for. What was not investigated though was the in-plane behaviour, which would help with the design of the members against buckling. What is more, the eccentric joint out of plane is symmetric, but the in-plane behaviour is not symmetric. This can give rise to a more complicated response which would warrant an investigation.

## 2.6 Topics that require further investigation

### 2.6.1 Topics to be investigated

When it comes to eccentric hollowed sectioned joints much work is needed. Especially in the case of the non-symmetric plane of the joint. No literature was found describing the behaviour in the specific plane, which indicates that a lot is yet to be known about the behaviour of such joints. Through this work, an attempt will be made to answer what effects the introduced eccentricity has on the buckling behaviour qualitatively and quantitatively. The main comparison will be against the centric joints that are used widely in practice.

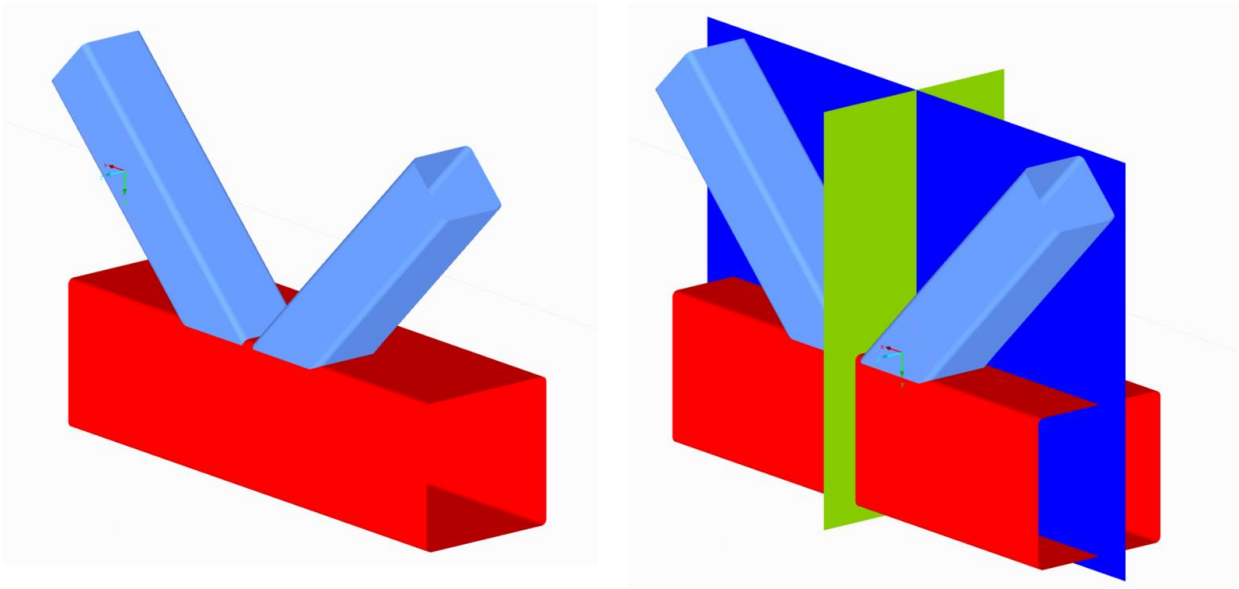

*(a)* *(b)*

*Figure 44. Example of eccentric joint. With green the symmetric plane is indicated, whilst with blue the non-symmetric plane*

The main focus of the thesis will be the investigation of plane trusses using K-joints that have an included eccentricity. This configuration is currently being used in Ampelmann's gangway systems and the results will be directly relevant in practice. From this literature study it has been concluded that the effects from member buckling and global buckling can be separated in design and verification of structures. As global buckling modes may be quite project specific it is regarded that investigating member buckling more important as it will produce results and conclusions useful for a wider array of applications.

From the literature it can be determined that the aspects that can affect buckling of a planar truss are the cross sections used, the actual geometry of the structure, the loading and support conditions and the stiffness of the connections. The latter is again affected by quite a few parameters. These include the β and γ factors of the joint, the gap between the braces and connection angle.

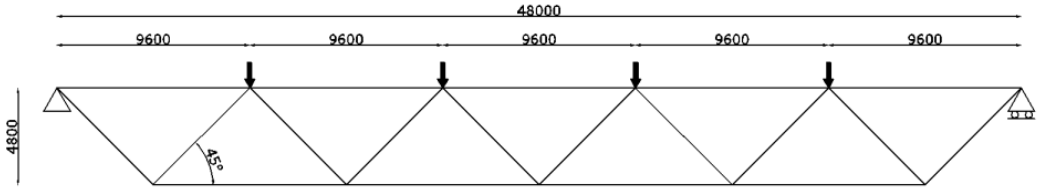


*Figure 45. Basic geometry and load case used in Boel's research* (Boel, 2010)

To limit the scope of this research, it was decided that structures similar to Boel's research (Boel, 2010) are going to be used for the investigations in following chapters. This would help give a benchmark for the results of this thesis, but also further verify Boel's findings. From having a standard geometry, loading and support conditions, the main parameters that can be used to describe the buckling behaviour of the truss members are β and γ. These two factors more directly include information regarding the stiffness of the joint, i.e. these are the main parameters that have been identified as affecting the stiffness of K-joints. Additionally, they include information regarding the cross sections used for the chords and braces. It is of interest to investigate if the relationships between β, γ and buckling length factors remain the same when comparing the buckling results of trusses with centric joints and eccentric joints.

Another aspect of design that can be addressed is the detailed modelling of joints. This can be quite time consuming and complicated to implement in global design models, especially with complicated geometries that arise from eccentric joints. This makes interesting the investigation of simplified modelling processes,

such as the introduction of rotational springs, which was done in the research presented in the state of the art (Chapter 2.4). The first question that is of interest is, why are there three load cases defined and what exactly they represent (Figure 46). Having three distinct stiffness values for the same joint seems counter intuitive. An additional study into their meaning and use would increase confidence in the method.

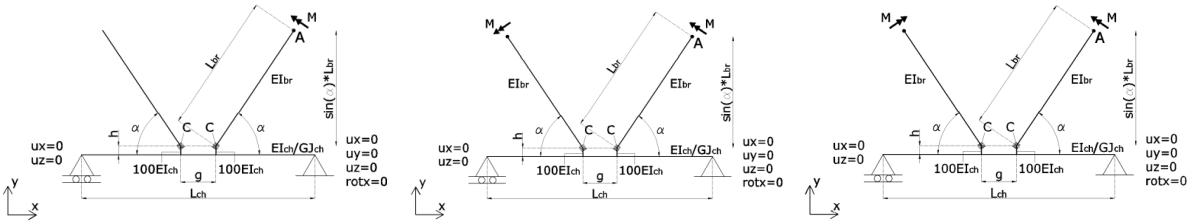


*Figure 46. The three load cases used to calculate the out of plane stiffness of connections* (Boel, 2010)

Another question that arises for the implementation of rotational springs for eccentric joints is how to calculate the stiffness. Due to the existing non-symmetry, the behaviour may be highly irregular and different to what is expected with normal centric K-joints that have been used up till now (Figure 47). This means that the definition and calculation of the rotational spring may be more complex than what has been presented in the literature this far.

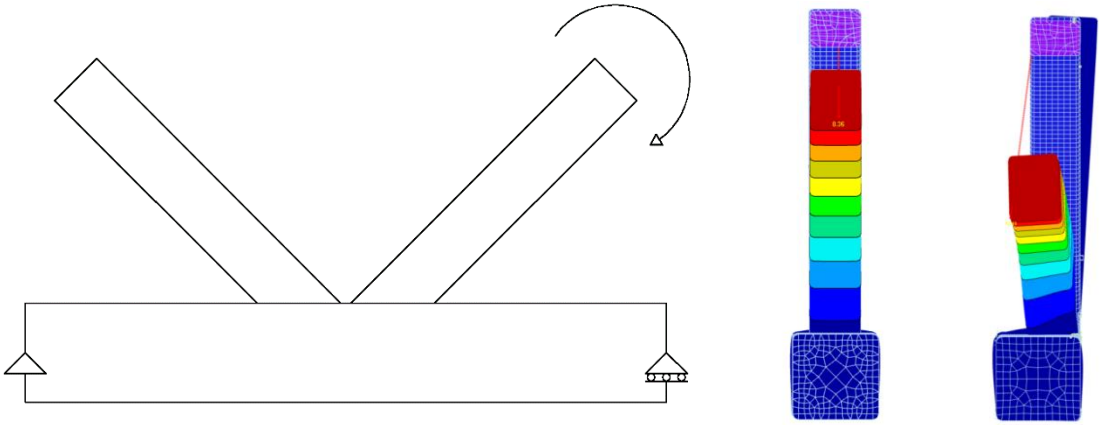


*Figure 47. Out of plane behaviour of (b) centric and (c) eccentric K-joint under in plane bending moment (a)*

The last point that can be investigated is if the brace thickness influences the stiffness of the connections. In the literature study, it is considered that the brace thickness plays a minor role in the stiffness of the joints, so it is not accounted for. The main effect of the brace thickness on the connection stiffness is on the deformation distribution on the chord face (Figure 48). The thicker the brace the less deformation is allowed to the chord. In the extreme case of a rigid brace, all contact positions between brace and chord will displace purely rotationally.

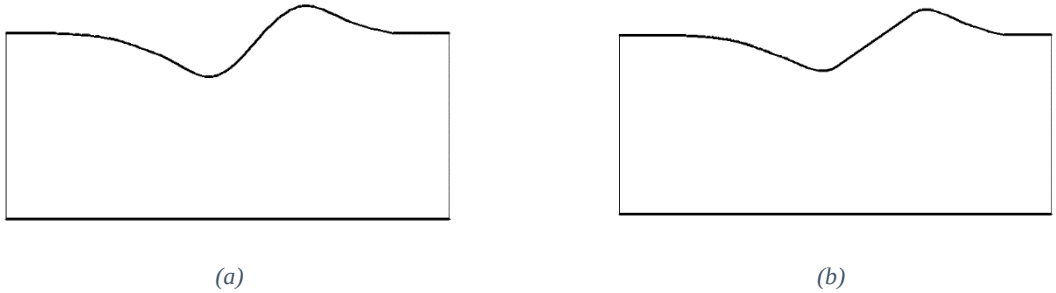


*Figure 48. Chord face deformations for (a) normal thickness brace and (b) rigid brace*

### 2.6.2 Topics outside the scope

From the literature study, a few interesting questions arose regarding parameters that affect the resistance of truss structures but that are outside the scope of this investigation due to time constraints. Firstly, as was stated before, global stability issues are not going to be dealt with. These may play a significant role in the final resistance of the truss and its members, depending on the support and loading conditions. The interaction between the different components of the truss (joints, members and supports) and how they relate to the global modes of trusses are not going to be part of this study.

Another issue that is not yet well determined is how much the buckling behaviour is affected by non-linear effects of the truss components. When calculating the linear buckling loads, the stiffness used is that of the undeformed structure. In reality though, non-linear effects may arise that affect the boundary conditions of the members. An example of this are joints under chord stress. In the presence of an axial load on the chord the stiffening or softening of the brace connections can be observed (Figure 49). This phenomenon has been investigated in works presented in the state of the art, as well as by other researchers (Garifullin, Pajunen, et al., 2017), but its effects and how it relates to the final resistance of hollow section trusses is still unclear. These can only be accounted for through a detailed non-linear analysis. This means that a linear buckling analysis may overestimate the actual critical buckling load. Further validation may be needed into the direct use of buckling eigenvalues for the buckling resistance calculations.

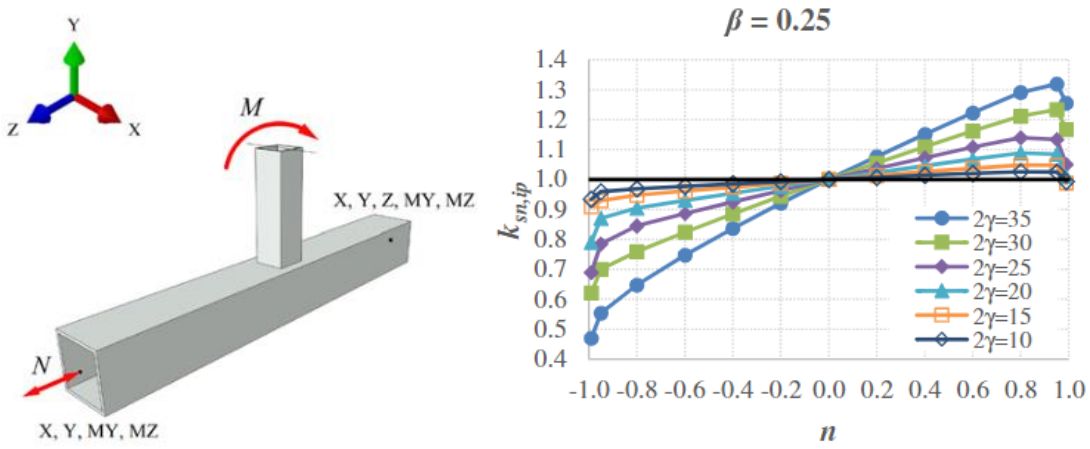


*Figure 49. Change of in plane stiffness of T-joint connection as a function of chord stress factor n* (Garifullin, Pajunen, et al., 2017)

The non-linear effects mentioned already relate to geometric non-linearities. Another set of non-linearities that need further investigation, as they relate to the buckling resistance of truss members, is that of the material. Specifically, as it relates to the joints, it was seen in the literature study that their yielding can substantially affect the buckling length of a member. What is not fully known is the interaction between the predicted buckling resistance and the resistance of the joint. In the case where the resistance of the joint is much lower than the calculated buckling resistance, then the joint would already be governing for the design. If the joint resistance is higher than the calculated buckling resistance, then early yielding of the joint is not to be expected and the calculated buckling resistance will develop fully. There is still the question of whether there is a situation in between, for which the yielding of the joint may affect the final resistance of the members and would make the governing failure mode lower that the predicted.

Another interesting topic that is not yet fully investigated is the effects of welds. Welds theoretically should increase the resistance of a connection and additionally increase the stiffness. Thus, the buckling resistance of the members would be expected to increase. However, welding can also introduce residual stresses and deformations. These may not be implicitly considered in the design codes with the prescribed imperfections, so further investigations are needed to verify that their effects in the final resistance are minor or provide proposals for accounting for them.

# 3 INVESTIGATION OF CENTRIC JOINTS

## 3.1 Introduction

The first step to investigating eccentric connections is to investigate the behaviour of trusses comprised of centric joints. This allows obtaining results that permit the comparison between the centric joint and the eccentric joint behaviour (Figure 50). Boel in his master thesis has already investigated centric joints in 2010, as was presented in the literature study. One of the assumptions adopted was that the cross sections were modelled without accounting for the corner radius of the profiles (Figure 51 (b)). Also, the models used for his final results were simplified using beam elements and rotational springs to account for the joints stiffnesses. For the eccentric connections, a more detailed model is needed for the investigation, in order to get reliable initial results.

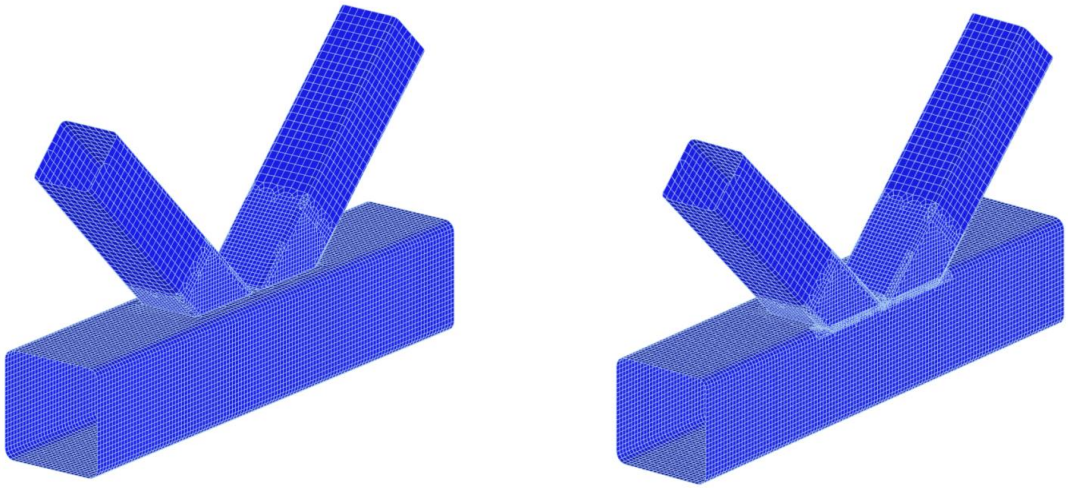

*(a)* *(a)*

*Figure 50. Finite element models for (a) centric and (b) eccentric K-joint*

In this chapter an investigation of centric joints is going to be performed, by working with detailed models, using shell element. This will make the comparison between the detailed eccentric joints and the centric results straightforward.

To facilitate comparisons to Boel's work, similar cross sections to the ones used in this work will be chosen. This will allow to cross validate the results obtained from the shell element models of this work and the approach that Boel developed. Additionally, the structural system and load case used in his investigation will also be adopted in this work. This limits the scope of the investigations, which is outlined below:

- Profiles to be used are hot rolled, of steel grade S355 and Square Hollow Sections (SHS). Cross sectional data taken according to EN 10210-2:2006.
- The total chord and brace combinations to be used for the centric investigation are 15. These can be seen in Table 13. The β factor is limited to 0.75 as for larger brace to chord width ratios, the effects of eccentricity should diminish. In the extreme case of β=1.0 no eccentricity can actually be defined (Figure 52).
- The structural system consists of a simply supported truss loaded with vertical loads on its compressive chord nodes (Figure 54).
- The compression chord is supported out of plane at its nodes.
- The gaps used for the joints were the minimum permissible by the EN 1993-1-8 (2005). So, for the K-joint of this study, which both braces have the same thickness, the minimum gap introduced was 2t. Noticeable exceptions are for the joints with β=0.25 and β=0.40, where the minimum gap of the brace with β=0.50 was used, i.e. 12.6 mm. This was done to be able to model the specific joints with mid-surface modelling. Otherwise, the models arising from such geometries would be nonsensical (Figure 53).
- Welding of the brace on the chord face is not accounted for in this work and no welds are modelled during the investigations performed.

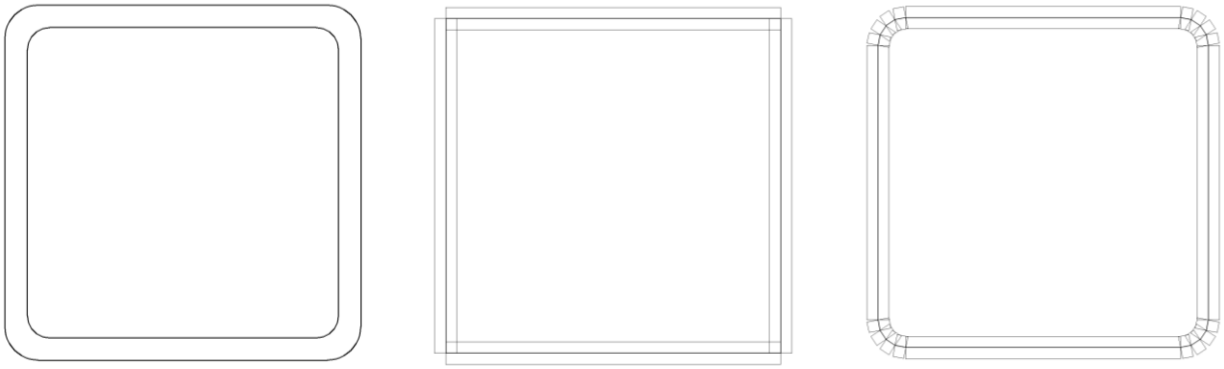

*(a)* *(b)* *(c)*

*Figure 51. Different modelling assumptions for representing the actual geometry of a SHS (a), by assuming no rounding at its corners (b) or by accounting for the corner radius (c)*

Table 13. Cross sections used in the centric joint investigation

| | | Chords | | |
|---|---|---|---|---|
| **γ=** | 15.9 | 10 | 6.25 | |
| | SHS 200/6.3 | SHS 200/10 | SHS 200/16 | |
| | | **Braces** | | |
| **β=** | 0.25 | 0.4 | 0.5 | 0.6 | 0.75 |
| | SHS 50/4 | SHS 80/5 | SHS 100/6.3 | SHS 120/7.1 | SHS 150/8 |

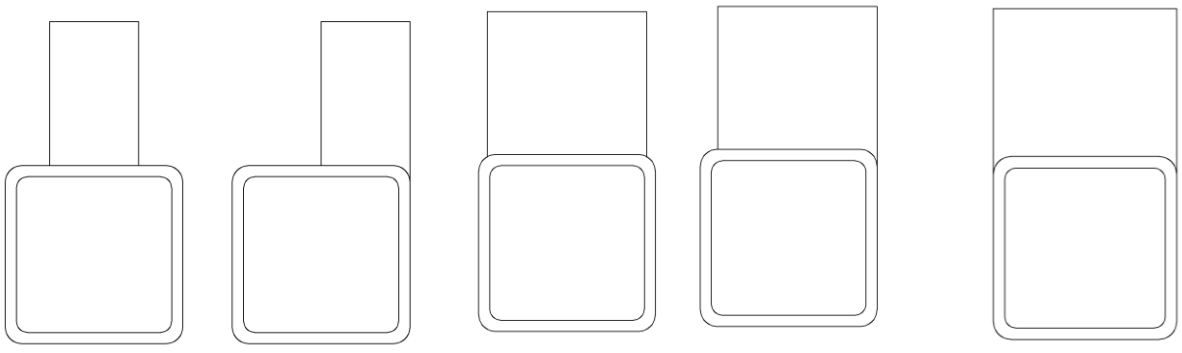


*Figure 52. Front views of centric K-joints and the equivalent eccentric joints for (a) β=0.5, (b) β=0.9 and (c) β=1.0 (no eccentricity definable)*

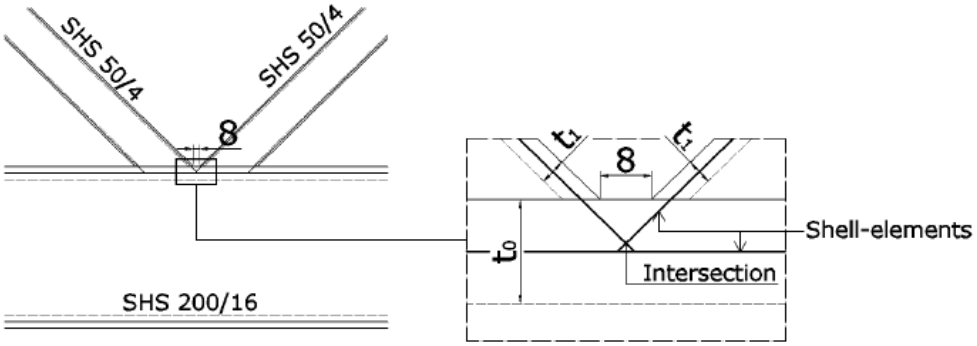


*Figure 53. Intersection of shell elements in model, when using the minimum gap for the joint with γ=6.25 and β=0.25* (Boel, 2010).

One of the parameters not to be investigated is the effects of the brace thickness. Due to the geometry of the connections changing with different brace thicknesses, the stiffness results obtained from the changes do not match the expected changes in stiffness. This was investigated and is presented in APPENDIX B. Because of this, only the cross sections used by Boel are going to be employed in the investigations. These will provide representative results for the joint behaviour and primarily have intermediate thicknesses for the width of the cross sections chosen, which is also expected in practice. For all the investigations mid-surface modelling was used. This is a simplification, but substantially reduced the computational demand and time so it was necessary to adopt.

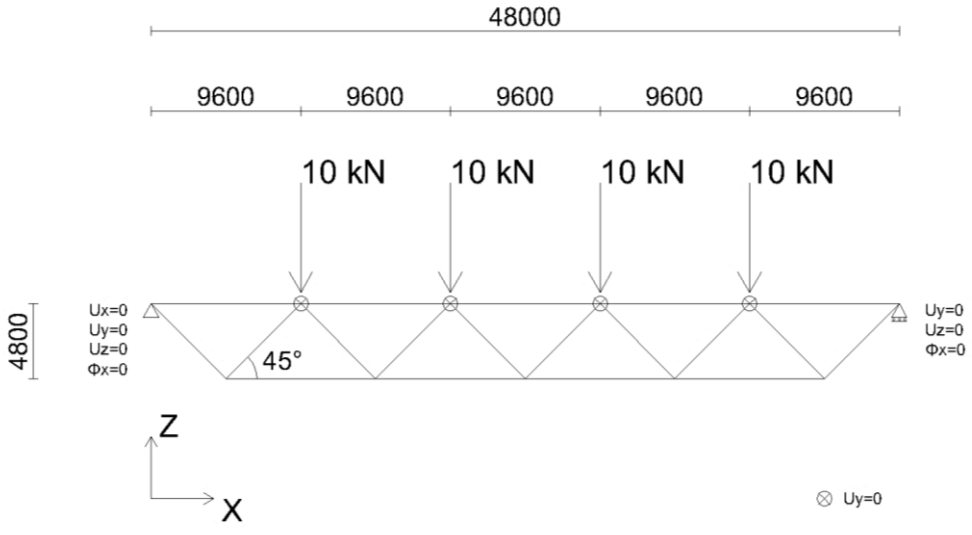


*Figure 54. Structural system of the simply supported truss used in the investigation*

## 3.2 Effects of corner radius on stiffness

As Boel did not account for the corner radius in the profiles used (Snijder et al., 2011), a simplification that is commonly used in practice, it is of interest to investigate how this assumption affects the in plane and out of plane stiffness of the connections. For the comparison, the basic load cases introduced by Boel and described in the literature study were used. For in plane stiffness Load case 1 is going to be used to calculate the in-plane stiffness, whilst for the out of plane stiffness the average of the three load cases is to be used. In Chapter 5 (Formulating rotational springs for eccentric joints) it is shown that taking the average stiffness of the three load cases for the out of plane stiffness may be inaccurate, but it still gives a good indication of the stiffness and gives results comparable to Boel.

### 3.2.1 In plane stiffness calculation

The process used for calculating the stiffness was the same as the one described in Boel's master thesis (Boel, 2010), except for two main differences. The first modification was in regard to the support introduced along the chord. In order to exclude the effects of the chord bending and introducing additional displacements at the end of the brace, Boel introduced line supports at the middle of the chord wall. These constrained the vertical displacements as well as the in-plane rotations. As the main goal of these supports is to eliminate the chord bending in-plane, the constraint of the vertical displacement is required. The constraint of the rotations along the chord wall mid-line, though, is questionable. There is no requirement for such a constraint and it introduces the possibility of over-stiffening the connection response. As such, for the in-plane stiffness calculations in this work only the vertical constraint component was introduced in the line supports of the chord walls.

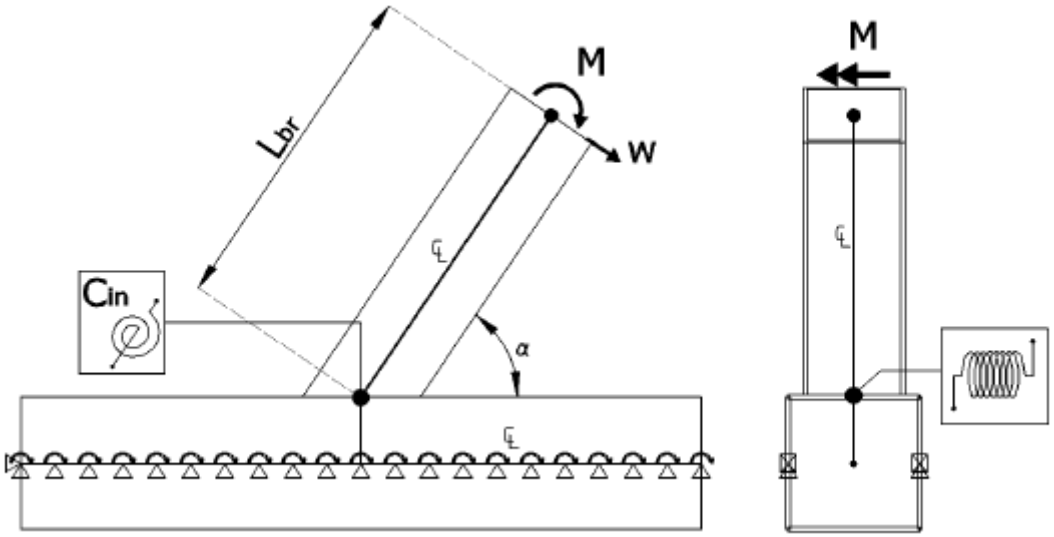


*Figure 55. Schematazation of the finite element model used by Boel for the in-plane stiffness calculations* (Boel, 2010)

Having excluded the effects of the chord bending on the brace end displacements, the only additional component increasing these displacements is the bending of the brace. In order to calculate the displacements attributable to the connection, the displacements due to the brace bending need to be calculated. Assuming the brace as a cantilever beam (Figure 56), Boel used Equation 7. to calculate the deflections. In this work the brace deflections are also calculated assuming the brace as a cantilever, but the shell element model is used to calculate the values (Figure 57). This decision was taken, as calculating the deflections with Equation 7. gave inconsistent results. This was mainly due to some configurations for which the deflections due to the connection were very small, so the calculation was sensitive to the deflection value calculated for the brace.

$$w_{brace} = \frac{ML_{br}}{2EI} \qquad 7.$$

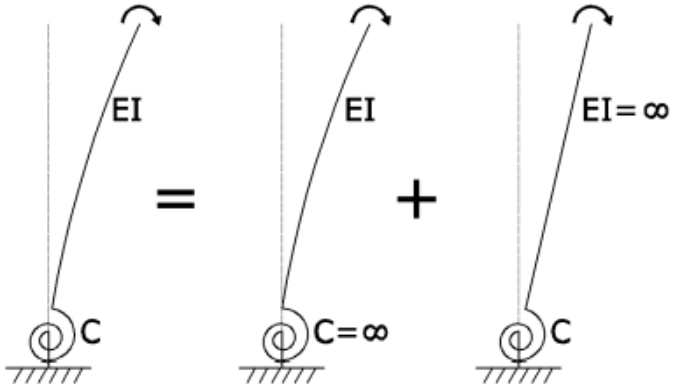


*Figure 56. Schematization of super positioning of stiffnesses of system (Boel, 2010)*

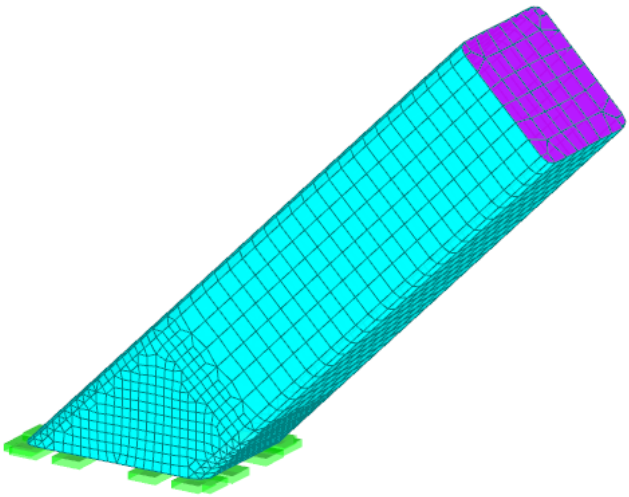

*Figure 57. Model used for the calculation of the brace deflections. Constraints for all degrees of freedom were introduced on the base lines.*

In general, it is noted that both assumptions, of supporting the chord against vertical displacements and treating the brace as a cantilever, are generally accepted conventions and are used by other researchers (Garifullin et al., 2018; Havula et al., 2018; B. Zhao et al., 2020). To conclude, the in-plane stiffness calculation was performed by subtracting the in-plane deflection due to the bending of the brace, from the total in-plane deflections at the end of the brace, calculated for the whole K-joint under loading prescribed by each Load case (Figure 23 (a)). This is given by Equation 8., from which the rotations arising from the connection can be calculated (Equation 9.). From this, the stiffness of the connection is calculated by dividing the applied moment with the calculated rotations (Equation 10.).

$$w_{connection} = w_{K-joint,FEM} - w_{brace,FEM} \quad 8.$$

$$\varphi_{connection} = \frac{w_{connection}}{L_{br}} \quad 9.$$

$$C_{in-plane} = \frac{M}{\varphi_{connection}} \quad 10.$$

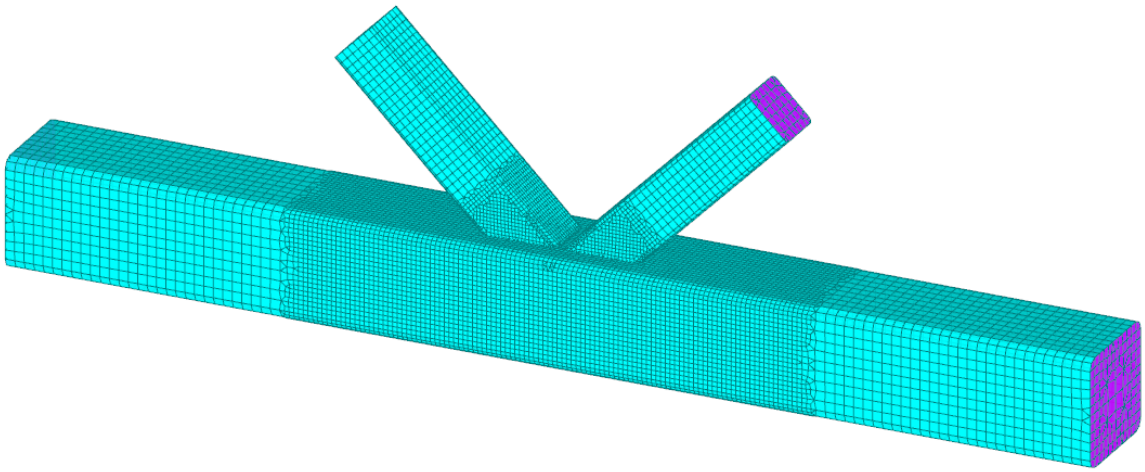

*Figure 58. K-joint modelled using shell elements, used for the calculation of stiffnesses*

### 3.2.2 Out of plane stiffness calculation

In the case of the out of plane stiffness calculations, things are more complicated. This is primarily due to not needing to support the chord walls. Since out of plane displacements and torsion of the chord are expected from the out of plane loading, supporting the chord side walls would over constrain and lead to higher stiffness than expected. This means that bending and torsion of the chord needs to be accounted for and subtracted from the total displacements in order to acquire the displacements due to the connections. The displacement due to the bending and torsion of the chord are dependent on the Load case as the moments applied on the ends of the braces interact. For this reason, the equations used to calculate the connection displacements change for every Load case. As with the in-plane stiffness calculation, the deflection of the brace is calculated using a finite element model of the K-joint brace section. The figures schematizing the joints for the stiffness calculation are taken from Boel's work, as the same set ups were used for the calculations in this work.

#### *3.2.2.1 Out of plane Load case 1*

For the case of Load case 1, Equation 11. is used to calculate the displacements at the end of the brace owing to the connection. In this equation the first term is taken from an analysis of a fixed brace, the second describes the displacements due to torsion, the third the displacements due to rotation of the chord around the vertical axis and the last term describes the displacement due to the vertical deflection of the chord. By calculating the displacement due to the connection, Equations 9. and 10. can be used to calculate the out of plane stiffness for Load case 1.

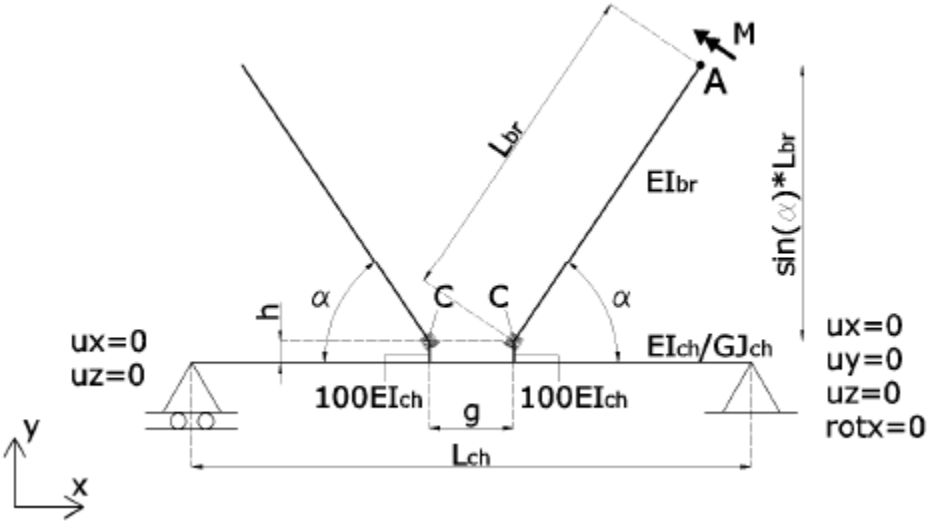


*Figure 59. Schematization of joint for the stiffness calculation of Load case 1* (Boel, 2010)

$$w_{connection} = w_{K-joint,FEM} - \left( \begin{array}{l} w_{brace,FEM} + \frac{\sin(\alpha)\, M(L_{ch} - g)}{2GJ_{ch}} (\sin(\alpha)\, L_{br} + h) + \\ + \frac{M(3g^2 + L_{ch}^2)}{12EI_{ch}L_{ch}} \cos^2(\alpha)\, L_{br} + \frac{Mg(g^2 - L_{ch}^2)}{12EI_{ch}L_{ch}} \cos(\alpha) \end{array} \right) \quad 11.$$

### 3.2.2.2 Out of plane Load case 2

For the case of Load case 2 Equation 12. is used to calculate the displacements at the end of the brace owing to the connection. In this equation the first term is taken from an analysis of a fixed brace, the second describes the displacements due to torsion, the third the displacements due to rotation of the chord around the vertical axis and the last term describes the displacement due to the vertical deflection of the chord. By calculating the displacement due to the connection, Equations 9. and 10. can be used to calculate the out of plane stiffness for Load case 2.

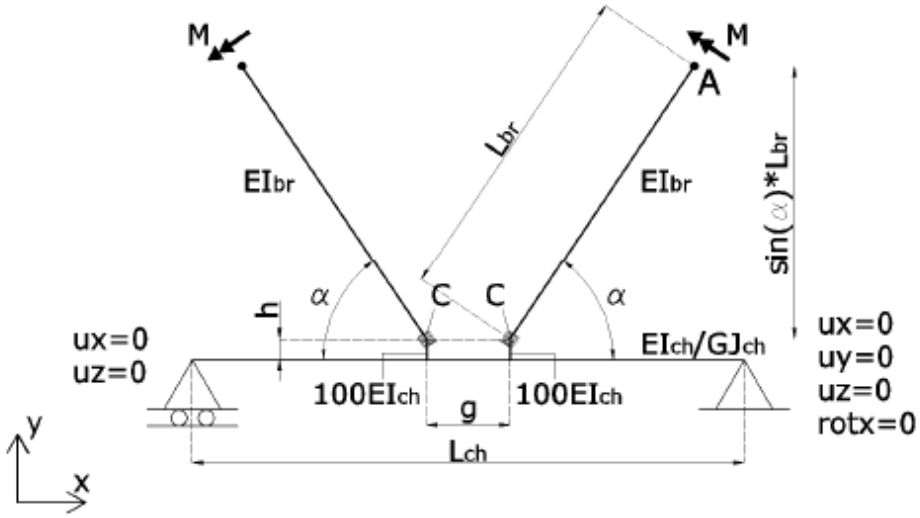


*Figure 60. Schematization of joint for the stiffness calculation of Load case 2* (Boel, 2010)

$$w_{connection} = w_{K-joint,FEM} - \left( \begin{array}{c} w_{brace,FEM} + \frac{\sin(\alpha)\, M(L_{ch} - g)}{2GJ_{ch}} (\sin(\alpha)\, L_{br} + h) + \\ + \frac{Mg}{2EI_{ch}} \cos^2(\alpha)\, L_{br} + \frac{Mg(g - L_{ch})}{4EI_{ch}} \cos(\alpha) \end{array} \right) \quad 12.$$

### 3.2.2.3 Out of plane Load case 3

For the case of Load case 3, Equation 13. is used to calculate the displacements at the end of the brace owing to the connection. In this equation the first term is taken from an analysis of a fixed brace, the second describes the displacements due to rotation of the chord around the vertical axis and the last term describes the displacement due to the vertical deflection of the chord. From calculating the displacement due to the connection, Equations 9. and 10. can be used to calculate the out of plane stiffness for Load case 3.

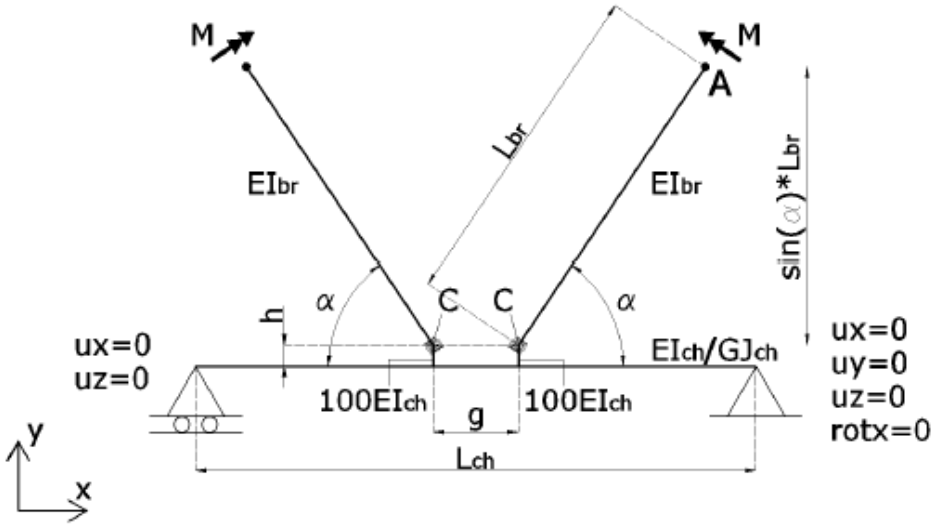


*Figure 61. Schematization of joint for the stiffness calculation of Load case 3*(Boel, 2010)

$$w_{connection} = w_{K-joint,FEM} - \left( \begin{array}{c} w_{brace,FEM} + \frac{M\left(3g^2 - 3gL_{ch} + L_{ch}^2\right)}{6EI_{ch}L_{ch}} \cos^2(\alpha)\, L_{br} + \\ + \frac{Mg(2g^2 - 3gL_{ch} + L_{ch}^2)}{12EI_{ch}L_{ch}} \cos(\alpha) \end{array} \right) \quad 13.$$

## 3.2.3 Results

Using the approach described in the previous sections, the stiffness of the various configurations was calculated. The first set of results are for the case of cross sections with no rounding in their corners. This was done to compare the results with the results of Boel, in order to validate the tools and the method used in this work. The results would be expected to match closely to the results obtained by Boel. This, though, is not the case. The results are presented below.

Table 14. In-plane stiffness of SHS K-joints, without accounting the corner radius of the cross sections

In-plane stiffness (kNm/rad)

| | | γ = 15.9 | | | γ = 10 | | | γ = 6.25 | | |
|---|---|---|---|---|---|---|---|---|---|---|
| | | Present work | Boel (2010) | Diff. | Present work | Boel (2010) | Diff. | Present work | Boel (2010) | Diff. |
| | 0.25 | 81.0 | 82.4 | -1.6% | 283.1 | 292.1 | -3.1% | 1015.2 | 953.5 | 6.5% |
| | 0.40 | 183.8 | 188.4 | -2.5% | 615.1 | 627.8 | -2.0% | 2146.8 | 2144.8 | 0.1% |
| β | 0.50 | 342.7 | 355.5 | -3.6% | 1097.2 | 1133.3 | -3.2% | 3672.6 | 3680.7 | -0.2% |
| | 0.60 | 678.0 | 711.7 | -4.7% | 2060.2 | 2141.5 | -3.8% | 6547.9 | 6547.2 | 0.0% |
| | 0.75 | 2303.2 | 2766.2 | -16.7% | 6165.8 | 6888.3 | -10.5% | 16623.2 | 17717.9 | -6.2% |

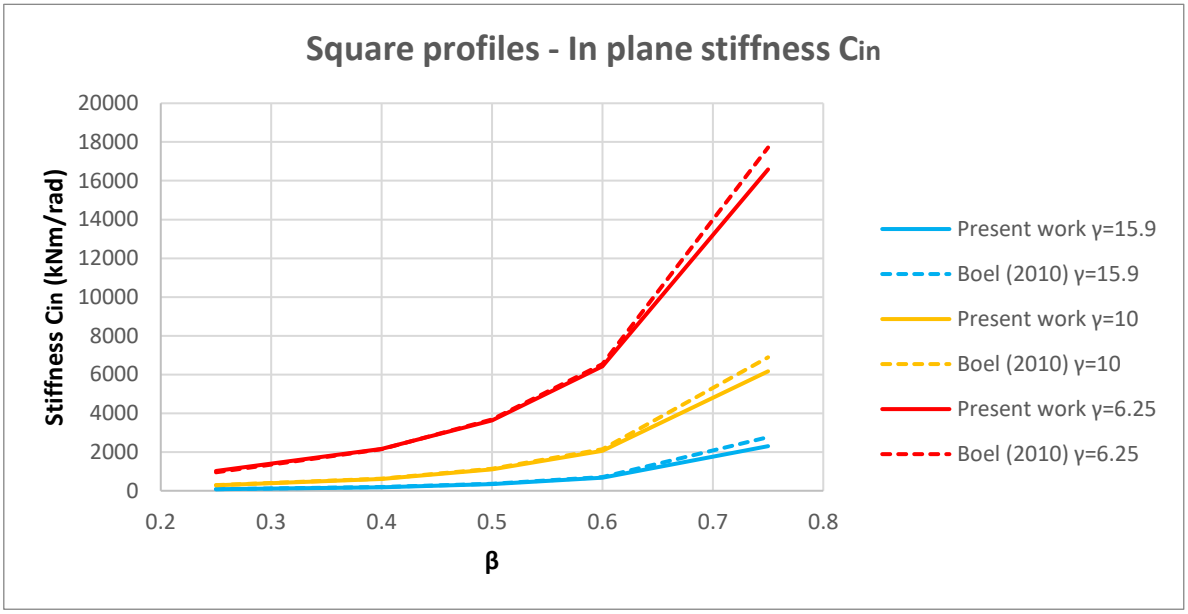


*Figure 62. In-plane stiffness of SHS K-joints, without accounting the corner radius of the cross sections*

Table 15. Out of plane stiffness of SHS K-joints, without accounting the corner radius of the cross sections

Out of plane stiffness (kNm/rad)

| | | γ = 15.9 | | | γ = 10 | | | γ = 6.25 | | |
|---|---|---|---|---|---|---|---|---|---|---|
| | | Present work | Boel (2010) | Diff. | Present work | Boel (2010) | Diff. | Present work | Boel (2010) | Diff. |
| | 0.25 | 216.6 | 225.3 | -3.9% | 630.8 | 673.2 | -6.3% | 2031.5 | 1726.4 | 17.7% |
| | 0.40 | 469.1 | 481.9 | -2.6% | 1349.9 | 1376.2 | -1.9% | 4229.4 | 4046.5 | 4.5% |
| β | 0.50 | 806.6 | 831.2 | -3.0% | 2148.5 | 2247.1 | -4.4% | 6598.2 | 6643.9 | -0.7% |
| | 0.60 | 1256.9 | 1376.8 | -8.7% | 3384.9 | 3605.9 | -6.1% | 10047.7 | 10657.5 | -5.7% |
| | 0.75 | 3242.6 | 3489.3 | -7.1% | 7883.1 | 8584.8 | -8.2% | 21474.8 | 23322.5 | -7.9% |

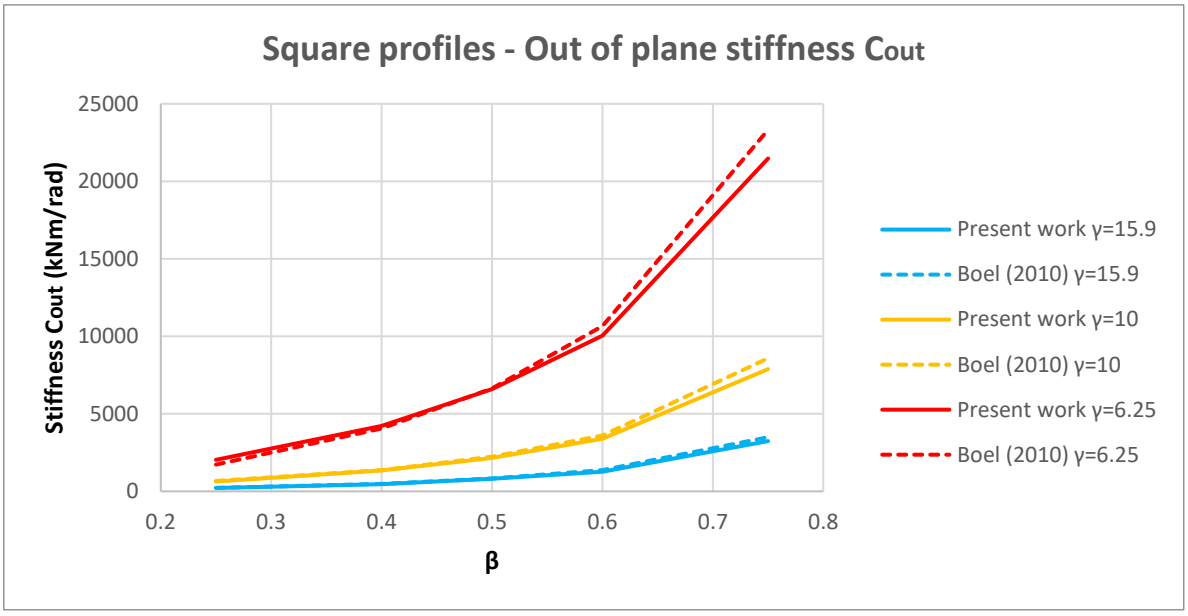


*Figure 63. Out of plane stiffness of SHS K-joints, without accounting the corner radius of the cross sections*

As can be seen in Table 14 and Table 15, for most cases the results do not agree with the results presented by Boel and in some cases the difference reaches around 18%. This could be due to several reasons. One potential reason could be that in this work, the deflection of the brace was calculated from a FE analysis, whist Boel used analytical formulas. This can have a substantial effect on the calculated stiffness, especially in cases that the displacements attributable to the braces and the connections have similar values. This would mean that a slight change in the displacement attributed to the brace creates a relatively substantial increase in the stiffness value. It is also mentioned that for the in-plane stiffness, Boel additionally constrained the rotations. This may have a over constraining effect leading to a stiffer calculation of the stiffness.

Additionally, a general increase in the difference can be observed for an increase in the brace to chord width ratio (β). One possible answer is the differences in mesh sizing. From Boel's ANSYS script presented in his thesis Appendix it is evident that for all his investigations he used the same number of elements for the brace and chord, irrespective of the cross section used in each case. In the current investigation the element size is chosen as a function of the surface thickness. This can potentially explain the increasing differences with increase in brace widths. Lastly, Poels also compared some stiffness calculations to Boel's results. He also found that Boel's stiffness values were in general higher than the ones Poels calculated (Table 16). Without access to Boel's models it is impossible to attribute the difference to something more specific.

Table 16. Relative differences between Poel's and Boel's in-plane stiffness calculations (Poels, 2017)

| | Load case | | | |
|---|---|---|---|---|
| Brace dimensions | LCin0 | LCin1 | LCin2 | LCin3 |
| SHS50/6.3 | -2.8% | -4.1% | -4.9% | -4.3% |
| SHS100/6.3 | -1.9% | -5.2% | -5.0% | -5.3% |
| SHS150/6.3 | -3.6% | -17.7% | -17.8% | -17.6% |
| SHS200/6.3 | -1.7% | -2.5% | -6.8% | 0.8% |

For the next investigation, the effects of the corner radius on the stiffness are going to be checked. In order to make a suitable comparison, the results obtained from the previous investigation for cross sections with no radius is going to be used to compare to the cross sections with rounded corners. The results are compared and presented in Table 17 and Table 18.

Table 17. In-plane stiffness of SHS K-joints, with and without accounting for the corner radius of the cross sections

In-plane stiffness (kNm/rad)

| | | γ = 15.9 | | | γ = 10 | | | γ = 6.25 | | |
|---|---|---|---|---|---|---|---|---|---|---|
| | | Rounded corners | No radius | Diff. | Rounded corners | No radius | Diff. | Rounded corners | No radius | Diff. |
| | 0.25 | 78.8 | 81.0 | -2.7% | 279.0 | 283.1 | -1.4% | 1025.4 | 1021.9 | 0.3% |
| | 0.40 | 179.5 | 183.8 | -2.3% | 615.7 | 615.1 | 0.1% | 2189.6 | 2156.6 | 1.5% |
| β | 0.50 | 326.8 | 342.7 | -4.6% | 1076.0 | 1097.2 | -1.9% | 3734.5 | 3637.9 | 2.7% |
| | 0.60 | 639.9 | 678.0 | -5.6% | 2021.1 | 2060.2 | -1.9% | 6643.8 | 6423.8 | 3.4% |
| | 0.75 | 2160.1 | 2303.2 | -6.2% | 6005.2 | 6165.8 | -2.6% | 16826.1 | 16585.7 | 1.4% |

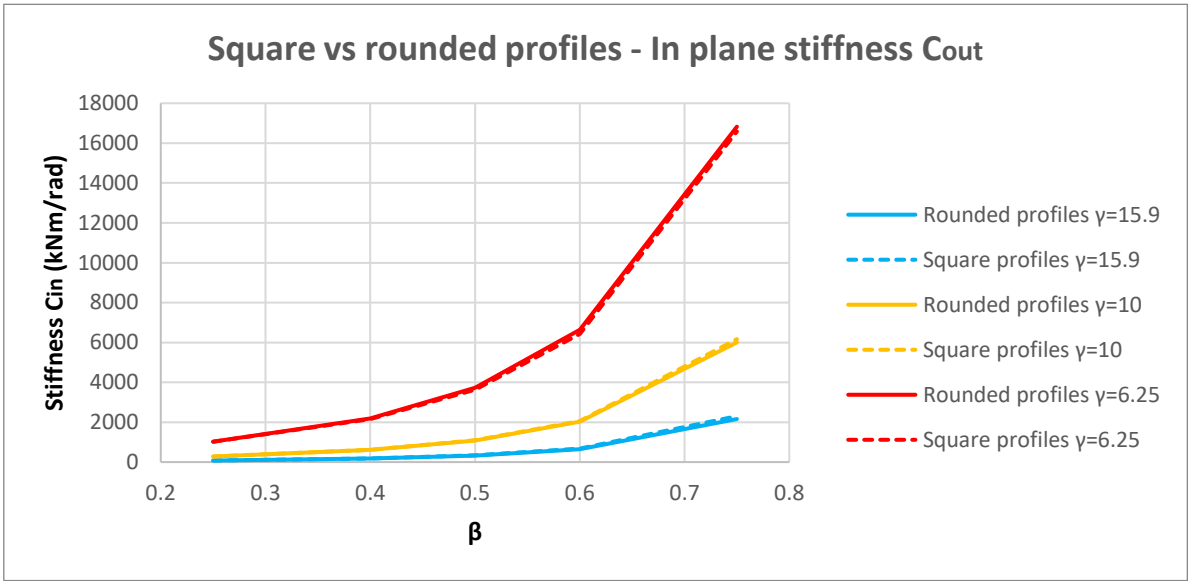


*Figure 64. In-plane stiffness of SHS K-joints, with and without accounting for the corner radius of the cross sections*

Table 18. Out of plane stiffness of SHS K-joints, with and without accounting for the corner radius of the cross sections

Out of plane stiffness (kNm/rad)

| | | γ = 15.9 | | | γ = 10 | | | γ = 6.25 | | |
|---|---|---|---|---|---|---|---|---|---|---|
| | | Rounded corners | No radius | Diff. | Rounded corners | No radius | Diff. | Rounded corners | No radius | Diff. |
| | 0.25 | 203.8 | 216.6 | -5.9% | 606.1 | 630.8 | -3.9% | 1948.4 | 2031.5 | -4.1% |
| | 0.40 | 442.1 | 469.1 | -5.8% | 1296.1 | 1349.9 | -4.0% | 4159.2 | 4229.4 | -1.7% |
| β | 0.50 | 758.3 | 806.6 | -6.0% | 2074.0 | 2148.5 | -3.5% | 6463.9 | 6598.2 | -2.0% |
| | 0.60 | 1231.8 | 1256.9 | -2.0% | 3362.2 | 3384.9 | -0.7% | 10538.9 | 10047.7 | 4.9% |
| | 0.75 | 2930.7 | 3242.6 | -9.6% | 7685.7 | 7883.1 | -2.5% | 22063.7 | 21474.8 | 2.7% |

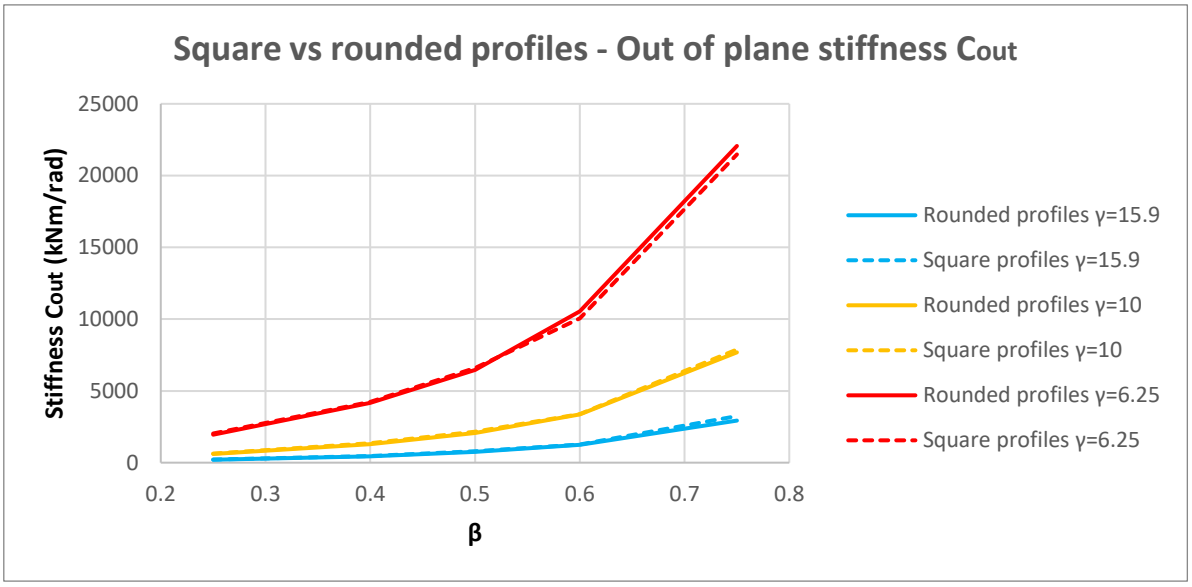


*Figure 65. Out of plane stiffness of SHS K-joints, with and without accounting for the corner radius of the cross sections*

For the in-plane stiffness there are small differences that increase with the increase of the brace to chord width ratio (β). The trends appear to show that rounding of the corners decrease the stiffness of the connection. But for the case of γ=6.25 the trend appears to show that the rounding of the corners increases the stiffness. For the out of plane stiffness even higher differences can be observed.

Due to the rounding of the corners an increase in flexibility is expected, as the corners of the braces become less stiff (Haakana, 2014). This would indicate a decrease in stiffness compared to the square cross sections with the increase of the β factor. But there is also a second effect, which explains the stiffening of the connection for thicker chords. Due to the increase in thickness of the chord, the radius modelled is also larger. This means that as the support conditions provided by the chord wall moves towards the brace's edge, the radius becomes larger.

The change of boundary conditions from non-rounded to rounded cross sections depends only on the chord thickness used. Depending on the width of the brace used though, the relative difference is affected. For smaller braces, the decrease in the unsupported length becomes a much smaller percentage of the total unsupported length. This means that the stiffening effect of the chord radius becomes greater with higher values of β. These two effects compete between them and provide the explanation of the differences observed. It is noted that these conclusions hold only for mid-surface modelling because with solid elements, the different effects mentioned, may be more or less pronounced. In Figure 66, a representation and an example of the described effect is provided.

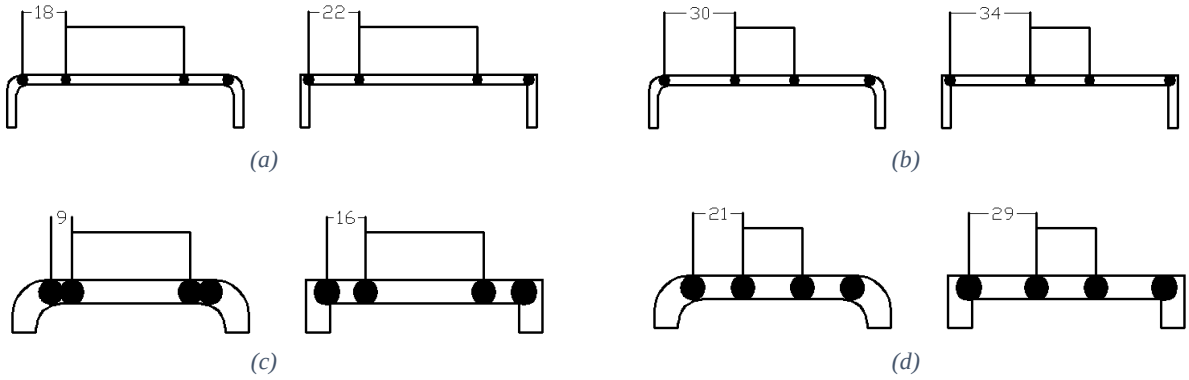


*Figure 66. Chord face section for different K-joint configurations. Indication of the boundary conditions for the chord face in bending component is given by the black circles. Extreme cases of chord thickness and brace width are presented to aid with the comparison between rounded vs unrounded corners.*

From Figure 66 the mechanism that leads to stiffer response for thicker chords and wider braces becomes more apparent. The dark circles indicate the chord face in bending boundary conditions. These unsupported lengths contribute the most to the stiffness. In each subfigure the difference between rounded and unrounded cross sections is demonstrated. To show the effects for different brace widths the same chords are used for pairs Figure 66 (a)-(b) and Figure 66 (c)-(d). The difference between rounded and unrounded remains the same for the same chord cross sections and independent from the brace used. But the total unsupported length is affected by the brace used. So, for larger braces, the decrease in length from unrounded to rounded, is a larger percentage of the total unsupported length. It is also seen that for a small radius the differences between rounded and unrounded for the chord are small. Therefore, for the thinnest chord ($\gamma$=15.9) all the stiffnesses for the rounded cross sections are smaller than the corresponding unrounded ones. The decrease of stiffness due to the rounding corners of the brace is the dominating effect. The opposite is true for the thickest chord ($\gamma$=6.25) and the larger braces, where the rounded cross sections appear to be stiffer.

To conclude, in general, the differences between the results appear not to be substantially large and are not expected to affect the buckling behaviour substantially. This means that a comparison between results obtained in the present work and Boel's work should be possible. This would also indicate that if a stiffness calculation is required, square profiles may be used. For the remainder of the investigations this work will continue using rounded cross sections as a more accurate representation of reality.

## 3.3 Truss models

To limit computational time and aid the investigation, it was decided that the models used would be comprised by a combination of shell and beam elements. The joints were to be modelled with shell elements, to capture the detailed behaviour of the structure. The remaining parts of the members were to be modelled using beam elements connected via rigid elements to the joints. This will be referred to as a hybrid model.

To investigate if this would affect the results, compared to using a complete shell element model, an investigation was performed using a smaller truss structure (Figure 67). The cross sections used were SHS 100-6.3 and SHS 50-4 for the chords and braces respectively. The first four eigenmodes were used for the comparison.

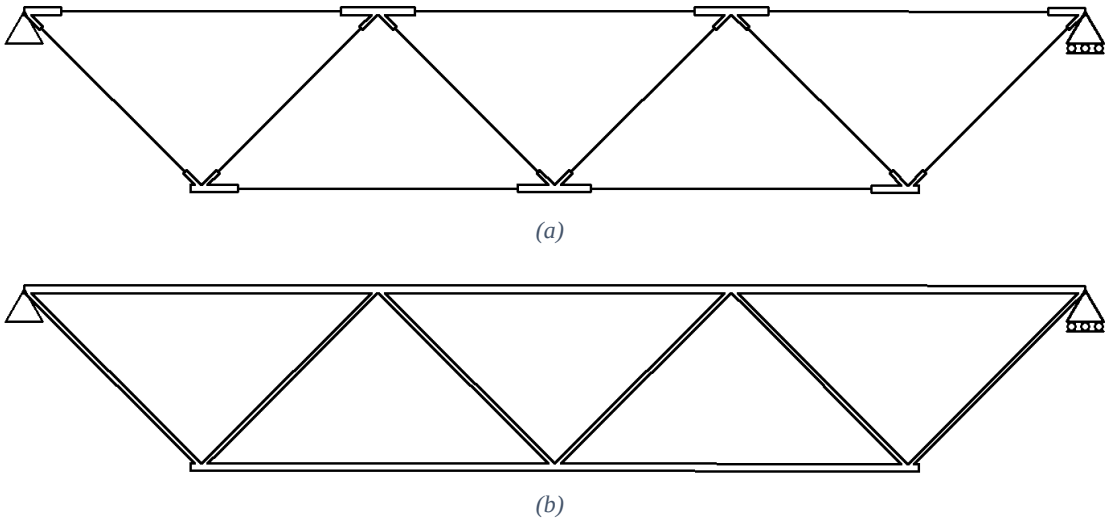

*(a)*

*(b)*

*Figure 67. Models used to arrive to the final model used in the investigations. For the hybrid mode (a) the joints are modelled using shell elements and beam elements for the rest of the members, whist for the shell element model (b) only shell elements were used.*

The results are presented in Table 19. A difference of around 5% exists between the results of the hybrid model and the shell element model, for the first four eigenmodes. This difference is primarily attributed to the difference existing in the cross sections modelled. Depending on the mesh density and the number of elements created on the corner radius of the rounded cross sections, the actual perimeter can be quite smaller than reality. In this case, the mesh density used created two shell elements on the corner (Figure 68).

Table 19. Eigenvalue results for shell element and hybrid truss models

| | Load factors | | |
|---|---|---|---|
| | Shell element model | Hybrid model | Difference (%) |
| Eigenmode 1 | 15.57 | 16.35 | 4.8 |
| Eigenmode 2 | 18.69 | 19.66 | 4.9 |
| Eigenmode 3 | 19.15 | 20.21 | 5.2 |
| Eigenmode 4 | 20.22 | 21.27 | 4.9 |

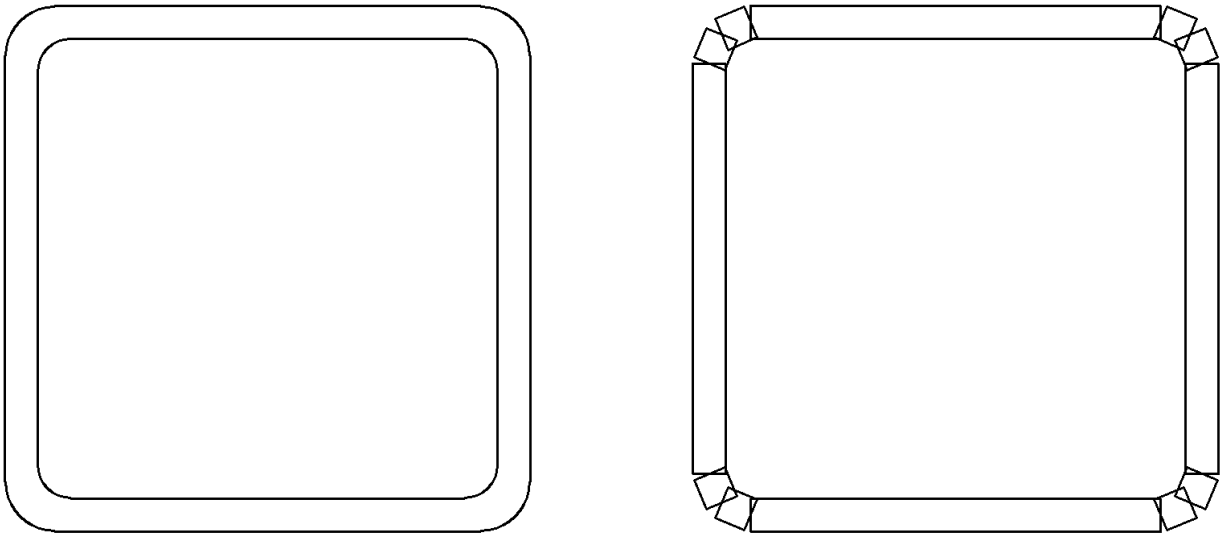

*Figure 68. Differences between reality and models using shell elements. On the left the actual cross sections of members, whilst on the right the modelled cross sections due to the use of shell elements*

To calculate these effects, a single member with the same cross section as the brace, was supported as a cantilever and put under axial compressive load. The shell element mesh was kept the same as with the previous investigation, to be able to compare results. Then the results from a shell element model and beam element model were compared. As can be seen from the results the differences are around 4-5%. This indicates that the differences expected from using a hybrid model compared to a fully shell element model is below 1%. As such, using hybrid modelling to calculate the eigenvalues is considered adequate and the following investigations will make use of it.

Table 20. Eigenvalue results for shell element and beam element cantilever model

| | Load factors | | |
|---|---|---|---|
| | Shell element model | Hybrid model | Difference (%) |
| Eigenmode 1 | 1.38 | 1.44 | 4.2 |
| Eigenmode 2 | 1.38 | 1.44 | 4.2 |
| Eigenmode 3 | 12.35 | 12.94 | 4.6 |
| Eigenmode 4 | 12.37 | 12.94 | 4.4 |

Having demonstrated that the hybrid model can be and will be used in all the following investigations a few other details about the models used are presented. First it is pointed out that the lateral supports were introduced in the middle of the joints, at the mid-height of the chord wall (Figure 69). The effects of this assumptions are minor and are checked in section 4.5. Secondly, the introduction of the loads on the top nodes was done through

line loads on the middle of the joints (Figure 69). Although care was taken to introduce the prescribed load of 10 kN, the actual values are not important for the final conclusions. The reason is because the results are described in terms of buckling lengths which is a normalized quantity. What is important is to introduce the correct proportion per load i.e. the same load per node, which was done. At the places where the shell elements interacted with beam elements or the boundary conditions, rigid surfaces were introduced, to facilitate with the interaction (Figure 70). Rigid surfaces were also introduced at the ends of the tension chord where the ends are free. To not over stiffen the connection a reasonable length of the joint was modelled (Figure 70).

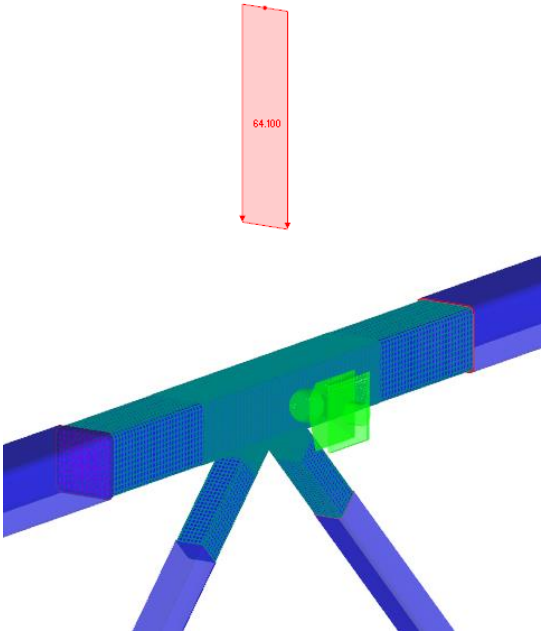


*Figure 69. Detail of a joint from the top (compressive) chord, from the hybrid model used.*

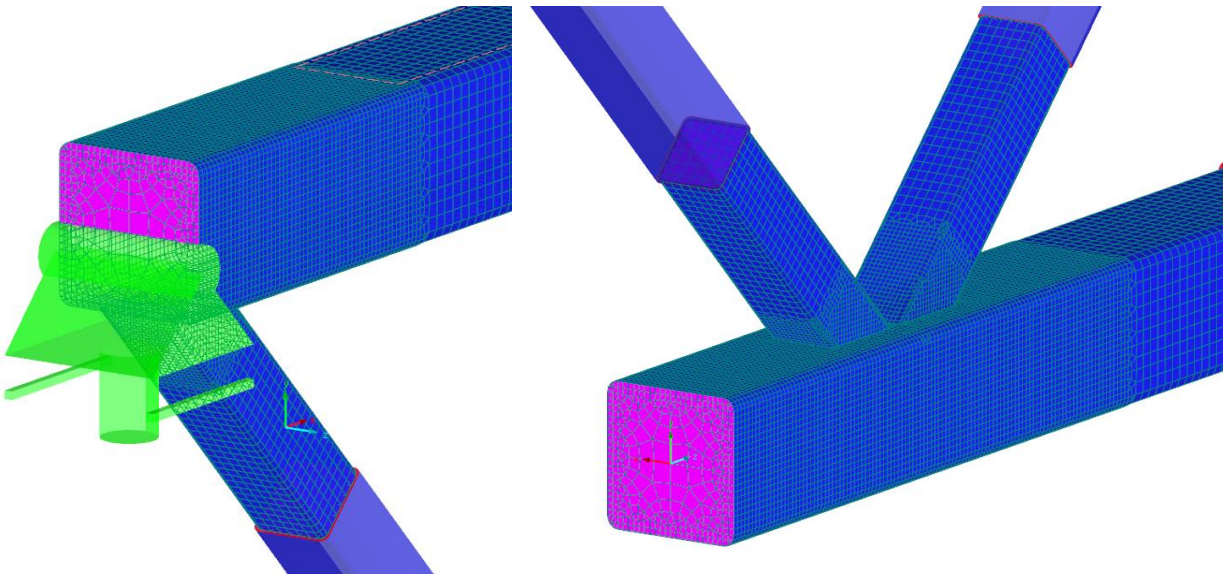

*(a)* *(b)*

*Figure 70. Details from the chord end conditions of the truss structure. In (a) the rolling support conditions applied on the top (compressive) chord and in (b) the free end of the bottom (tension) chord. With purple the rigid surfaces are displayed.*

## 3.4 Approach

To process the results, different calculated eigenmodes will be attributed to the buckling of different members and directions. In regard to direction in-plane modes and out of plane modes will be distinguished depending on which plane the deformations occur. In regard to the members, the most critical chord member is the one in the middle which is maximally loaded and will buckle first between the rest of the chord members. For the buckling of the braces, the most critical is the compressive braces closer to the end supports (Figure 71). From each model four eigenmodes will be attributed to one of each specific mode: chord buckling in-plane, chord buckling out of plane, brace buckling in-plane and brace buckling out of plane (Figure 72Figure 1).

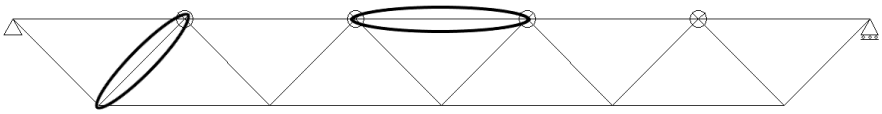

*Figure 71. Members of the truss, most critical to buckling; middle chord and end brace*

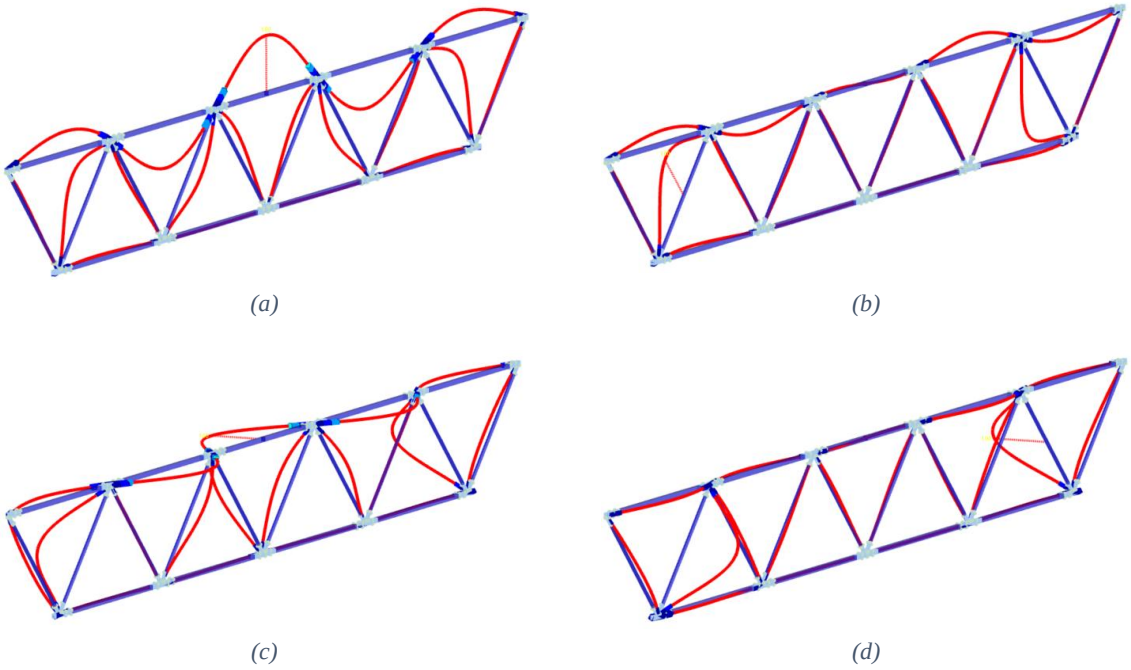


*Figure 72. Truss buckling modes categorized per member and direction. In-plane buckling of (a) chord and (b) brace and out of plane buckling of (c) chord and (d) brace.*

When it comes to the results, it is important to attribute the correct eigenmode to the appropriate member (chord and brace) and mode (in and out of plane). In many cases this can be unambiguous, but in some cases, it can be impossible to attribute since the members may buckle together. Boel addressed this issue by always attributing the lowest possible eigenmode to the corresponding member and mode. This is a safe estimate and appropriate since Boel's work revolved around trying to produce predictive formulas for buckling lengths. In the present work, in cases of doubt, the lowest eigenmode will also be used. This though may produce results that do not follow the intuitive trend followed by all results. To demonstrate one such case, the alternative results for the out of plane buckling of the chord are presented with the tension chord is restrained. In this case the buckling modes of chords $\gamma$=10 and $\gamma$=6.25 for the brace width ratio of $\beta$=0.6 are presented (Figure 73).

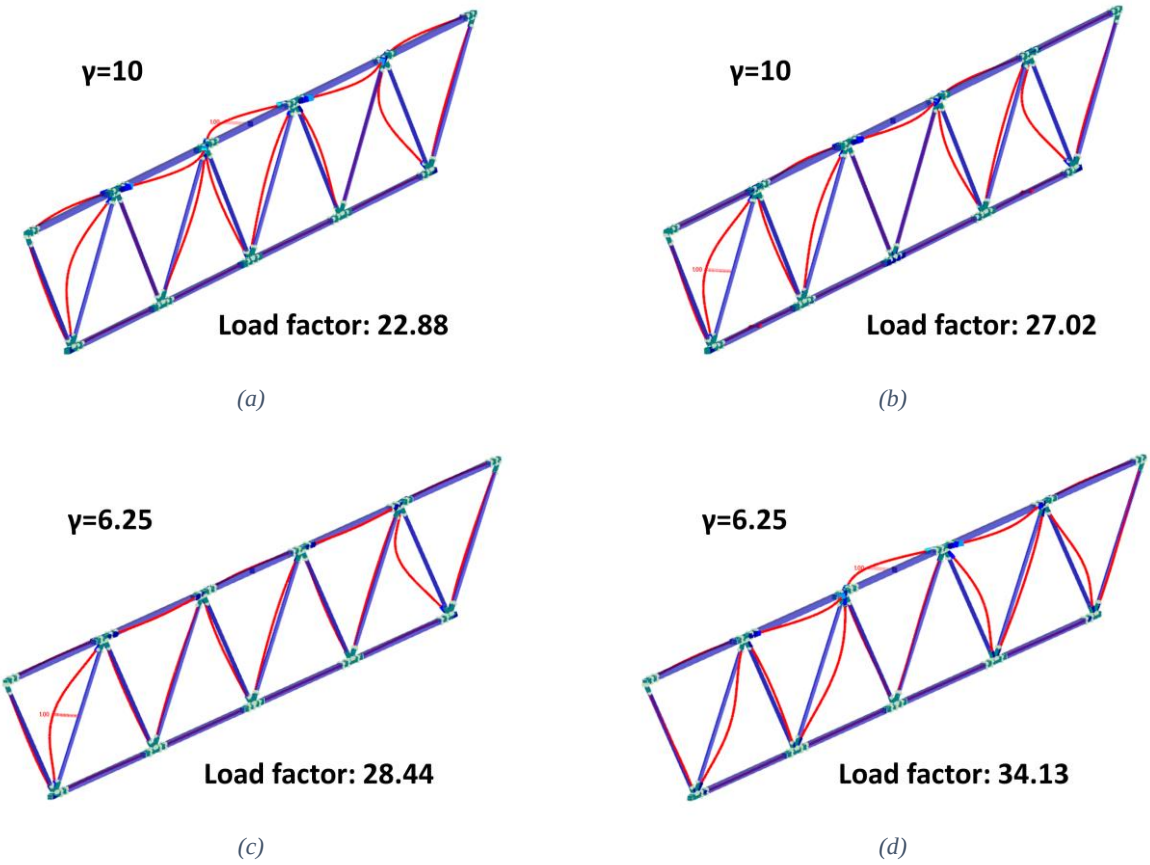


*Figure 73. Possible modes attributable to the chord buckling out of plane for the configurations with γ=10 ((a) and (b)), and γ=6.25 ((c) and (d)) and β=0.6.*

It is obvious that for the chord out of plane for the configuration with γ=10, Figure 73 (a) as it has the lower eigenvalue of the two presented and the chord presents the maximum deformation. For the case of the configuration with γ=6.25, it is obvious that the corresponding mode is from Figure 73 (d), as for Figure 73 (c) the chord presents minimal deformations. These are the values used to plot the final results for the chord buckling out of plane. It can be seen, though, that the graph for γ=6.25 does not follow the same trend as the graphs for γ=10 and γ=15.9 (Figure 74). It is of interest to note that the lowest eigenvalues (Figure 73 (a) and (c)) present the same characteristics, meaning that braces and chord deform towards the same directions indicating the same "eigen-shape". The same can be said for the higher eigenvalues (Figure 73 (b) and (d)) where the braces deform in the opposite direction of the chord. It is interesting to see the results that can be produced by using the same "eigen-shape" for γ=6.25, as the one used for γ=10. The alternative graph of γ=6.25 is now plotted, by using the eigenmode from Figure 73 (c) instead of (d). It can be seen from the results that the graph is now more in line with the trend presented from γ=10 and γ=15.9 (Figure 74). This is an example that the buckling analysis is quite a complex phenomenon and may not always follow the expected trend.

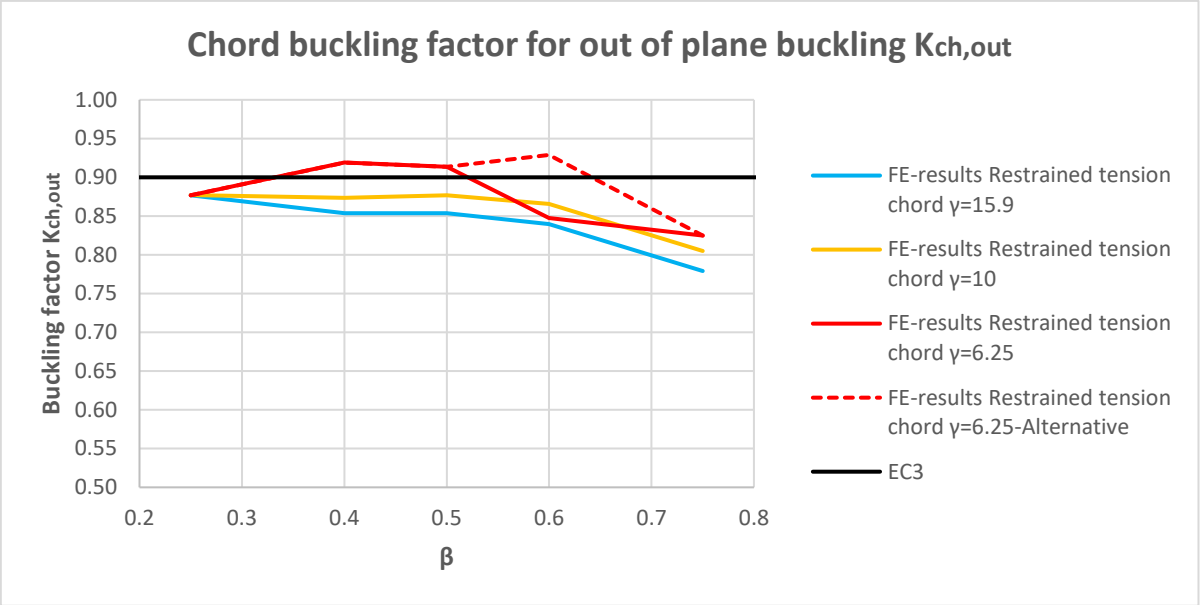


*Figure 74. Chord buckling factors for out of plane in the case of a restrained tension chord, along with an alternative assumption for γ=6.25 and β=0.6*

Having attributed a certain eigenmode to a member and mode, the critical buckling load of the member can be calculated. This is done by multiplying its axial load from a linear elastic analysis with the load factor (LF) of the attributed eigenmode (Equation 14.). Then the buckling factor is calculated by using Equation 15.. The only unambiguous parameter left is which length is to be used. In the present work, Boel's definition is used (Figure 75), which would allow for immediate comparison with his results.

$$N_{cr} = LF * N_{ed} \quad 14.$$

$$K = \sqrt{\frac{\pi^2 EI}{N_{cr} L^2}} \quad 15.$$

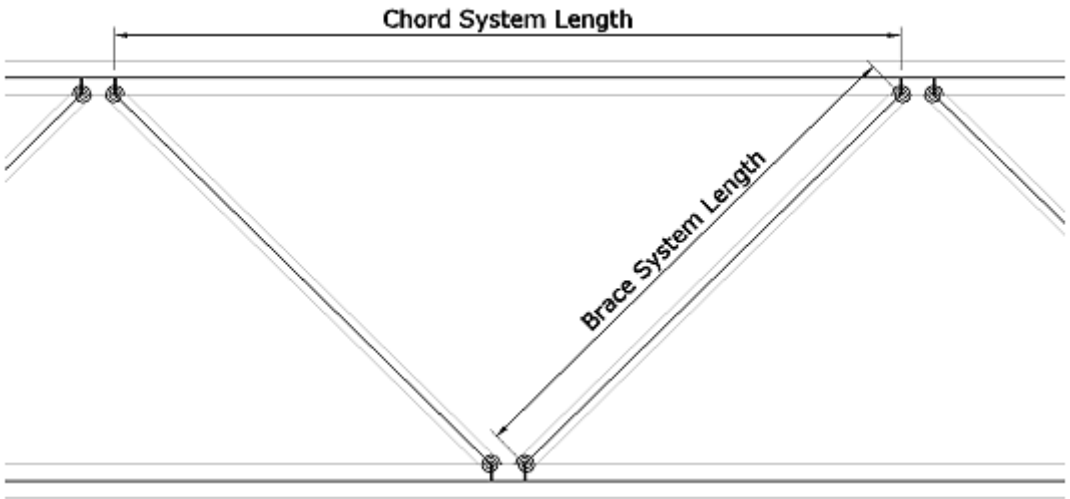


*Figure 75. System length as defined by Boel* (Boel, 2010)

## 3.5 Results

In this section the results are presented. Firstly, a table with the results and the comparison to Boel's is given, followed by the visual representation with graphs. The results will be first presented for the in-plane direction for chord and brace buckling and then for the out of plane direction for the chord and brace buckling. It should

be noted that the results taken from Boel (2010) were already rounded so the differences may be smaller or larger. Additionally, the percentile difference is given for the unrounded number of the present work. Thus, even if the rounded numbers are the same, a difference amount might be present.

Table 21. Chord buckling factors for in plane buckling

| | | γ = 15.9 | | | γ = 10 | | | γ = 6.25 | | |
|---|---|---|---|---|---|---|---|---|---|---|
| | | Present work | Boel (2010) | Diff. | Present work | Boel (2010) | Diff. | Present work | Boel (2010) | Diff. |
| | 0.25 | 0.88 | - | - | 0.88 | - | - | 0.89 | - | - |
| | 0.40 | 0.85 | 0.86 | -0.7% | 0.86 | 0.87 | -0.6% | 0.90 | 0.90 | -0.1% |
| β | 0.50 | 0.85 | 0.86 | -1.1% | 0.86 | 0.86 | 0.1% | 0.88 | 0.88 | 0.4% |
| | 0.60 | 0.82 | 0.83 | -0.8% | 0.84 | 0.84 | -0.4% | 0.86 | 0.86 | 0.4% |
| | 0.75 | 0.73 | 0.74 | -1.0% | 0.75 | 0.75 | -0.4% | 0.77 | 0.77 | 0.0% |

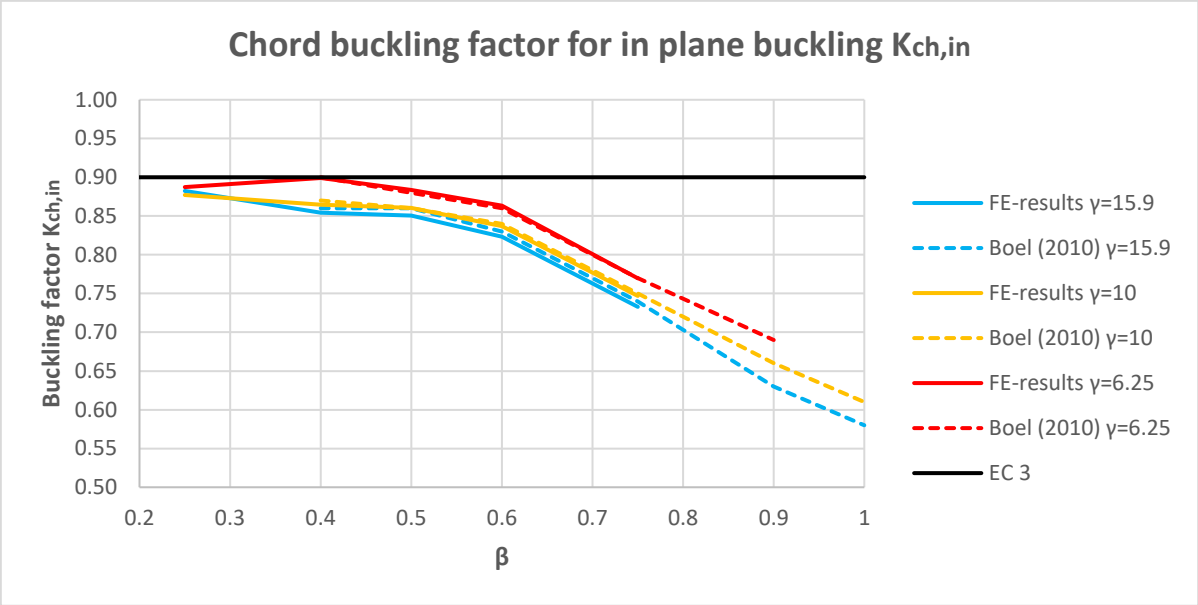


*Figure 76. Chord buckling factor for in plane buckling $K_{ch,in}$*

Table 22. Brace buckling factors for in plane buckling

| | | γ = 15.9 | | | γ = 10 | | | γ = 6.25 | | |
|---|---|---|---|---|---|---|---|---|---|---|
| | | Present work | Boel (2010) | Diff. | Present work | Boel (2010) | Diff. | Present work | Boel (2010) | Diff. |
| | 0.25 | 0.59 | 0.59 | -0.3% | 0.53 | 0.53 | -0.7% | 0.51 | 0.51 | -0.7% |
| | 0.40 | 0.68 | 0.68 | -0.6% | 0.57 | 0.57 | 0.1% | 0.52 | 0.53 | -1.2% |
| β | 0.50 | 0.72 | 0.73 | -1.3% | 0.61 | 0.61 | -0.6% | 0.56 | 0.54 | 2.8% |
| | 0.60 | 0.74 | 0.74 | 0.5% | 0.63 | 0.68 | -7.1% | 0.58 | 0.59 | -2.5% |
| | 0.75 | 0.81 | 0.81 | 0.1% | 0.68 | 0.68 | 0.2% | 0.61 | 0.66 | -7.2% |

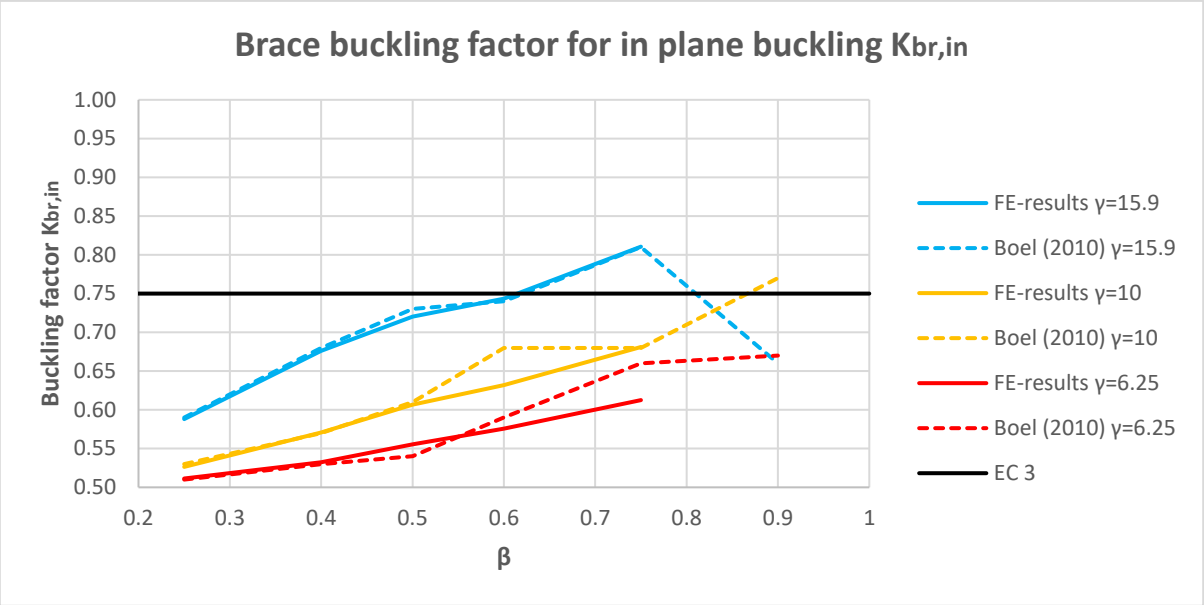


*Figure 77. Brace buckling factor for in plane buckling $K_{br,in}$*

It can be seen that the buckling lengths of the chords decrease with the increase of the chord width ration. This is because the stiffness of the connections increase, as well as the stiffness of the braces. This has as a result that the braces provide increasing restrain to the chords, decreasing the buckling length. For the buckling length of the braces the opposite effect is observed. This is due to the increasing stiffness of the brace members. As the stiffness of the braces increase the relative restraint experienced, for the same number of absolute values of rotational stiffness, decreases. This results in the buckling length of the braces decreasing, even though an increase in connection stiffness is observed.

From the presented graphs it can be seen that the results for the chord buckling in plane match pretty well the results given by Boel in his work. In regard to the brace buckling in plane, most of the results match the values given by Boel, but there are some specific points that present quite a large deviation. As one of the goals for investigating the centric joints is to validate Boel's results and his proposed approach, the reasons behind the discrepancy was investigated in detail.

As the points in question usually had buckling lengths higher than the ones attributed in the present work, some of the possible eigenmodes with lower eigenvalues were checked. From this investigation it was found that by changing the eigenvalues chosen the results extracted from the hybrid model could match well with the results presented by Boel. This evident in Table 23 and Figure 78. The reasons for these differences may be due to Boel misattributing eigenmodes by being conservative in his judgement. Without access to his models, it is difficult to make safe conclusions. The positive conclusion is that his approach is able to predict the same eigenmodes and eigenvalues calculated by the hybrid model used in the present work.

Table 23. Brace buckling factor for in plane buckling using eigenmodes that best fit Boel's results

| | | γ | | | | | | | | |
|---|---|---|---|---|---|---|---|---|---|---|
| | | 15.9 | | | 10 | | | 6.25 | | |
| | | Present work | Boel (2010) | Diff. | Present work | Boel (2010) | Diff. | Present work | Boel (2010) | Diff. |
| β | 0.25 | 0.59 | 0.59 | -0.3% | 0.53 | 0.53 | -0.7% | 0.51 | 0.51 | -0.7% |
| | 0.40 | 0.68 | 0.68 | -0.6% | 0.57 | 0.57 | 0.1% | 0.52 | 0.53 | -1.2% |
| | 0.50 | 0.72 | 0.73 | -1.3% | 0.61 | 0.61 | -0.6% | 0.54 | 0.54 | 0.4% |
| | 0.60 | 0.74 | 0.74 | 0.5% | 0.67 | 0.68 | -0.9% | 0.58 | 0.59 | -1.4% |
| | 0.75 | 0.81 | 0.81 | 0.1% | 0.68 | 0.68 | 0.2% | 0.66 | 0.66 | -0.3% |

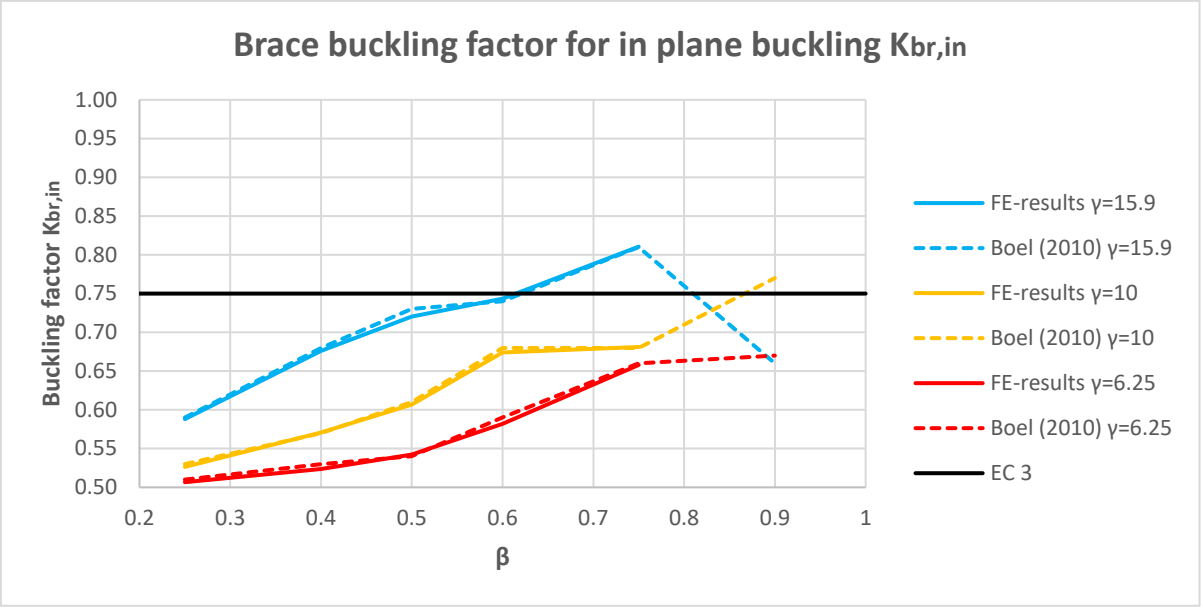


*Figure 78. Brace buckling factor for in plane buckling $K_{br,in}$, using eigenmodes that best fit Boel's results*

Another interesting observation is that for the thinnest chord and a larger value of the brace width ratio the buckling length trends above the prescribed buckling length of 0.75 from the Eurocode. This cannot be fully attributed to the different system length definition (Figure 29) as even with changing the system length, the buckling length becomes 0.79, above the Eurocode value. This could indicate that the buckling length factor of 0.8 given by the Japanese steel codes (*Standard Specifications for Steel and Composite Structures*, 2009) may be a safer assumption for the design of steel trusses.

The results for the out of plane buckling of the members are presented next.

Table 24. Brace buckling factor for in plane buckling

| | | γ | | | | | | | | |
|---|---|---|---|---|---|---|---|---|---|---|
| | | 15.9 | | | 10 | | | 6.25 | | |
| | | Present work | Boel (2010) | Diff. | Present work | Boel (2010) | Diff. | Present work | Boel (2010) | Diff. |
| | 0.25 | 0.88 | - | - | 0.88 | - | - | 0.88 | - | - |
| | 0.40 | 0.85 | 0.86 | -0.7% | 0.87 | 0.88 | -0.7% | 0.93 | 0.92 | 0.5% |
| β | 0.50 | 0.86 | 0.86 | -0.2% | 0.88 | 0.88 | 0.0% | 0.92 | 0.91 | 0.9% |
| | 0.60 | 0.84 | 0.84 | 0.1% | 0.87 | 0.86 | 1.1% | 0.85 | 0.86 | -0.6% |
| | 0.75 | 0.78 | 0.79 | -0.9% | 0.80 | 0.81 | -0.6% | 0.83 | 0.83 | -0.5% |

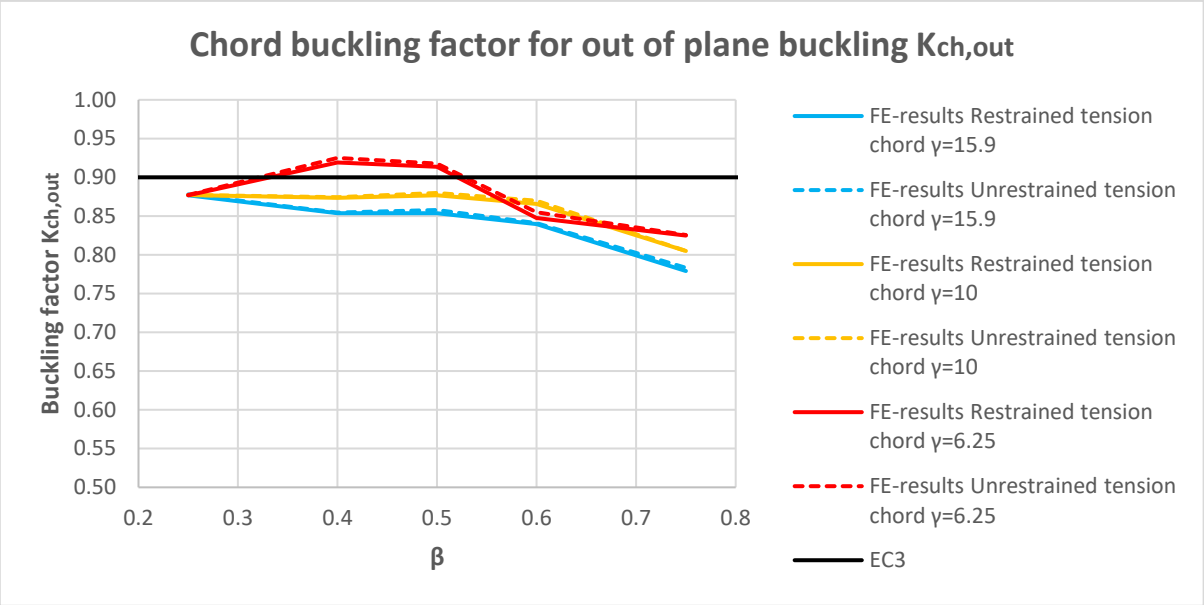


*Figure 79. Chord buckling factor for out of plane buckling $K_{ch,out}$*

Table 25. Brace buckling factor for out of plane buckling

| | | γ | | | | | | | | |
|---|---|---|---|---|---|---|---|---|---|---|
| | | 15.9 | | | 10 | | | 6.25 | | |
| | | Present work | Boel (2010) | Diff. | Present work | Boel (2010) | Diff. | Present work | Boel (2010) | Diff. |
| β | 0.25 | 0.60 | 0.60 | -0.8% | 0.58 | 0.58 | -0.6% | 0.57 | 0.57 | -0.1% |
| | 0.40 | 0.65 | 0.66 | -1.8% | 0.61 | 0.61 | 0.8% | 0.59 | 0.58 | 1.4% |
| | 0.50 | 0.69 | 0.70 | -1.2% | 0.64 | 0.64 | 0.5% | 0.61 | 0.60 | 2.0% |
| | 0.60 | 0.74 | 0.74 | 0.2% | 0.70 | 0.70 | 0.1% | 0.64 | 0.63 | 1.8% |
| | 0.75 | 0.85 | 0.85 | 0.1% | 0.82 | 0.81 | 0.7% | 0.69 | 0.71 | -3.2% |

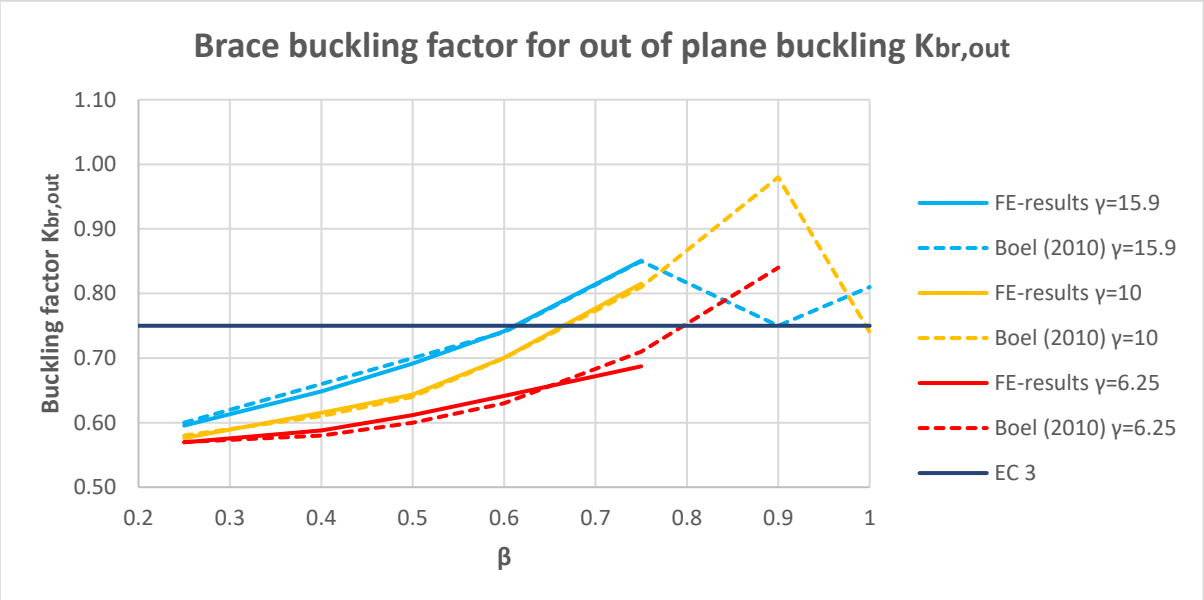


*Figure 80. Brace buckling factor for out of plane buckling $K_{br,out}$*

The results for the out of plane buckling it is determined that most results are within 1% of the results presented by Boel (2010). The only noticeable difference is the trend that can be observed for the out of plane buckling of the truss with the chord of γ=6.25. This is potentially because, from what will be presented in Chapter 5, Boel's approach of calculating the out of plane stiffness using the average of the three load cases may provide a slightly inaccurate approximation. Another explanation could be again the misattributing eigenmodes. As was mentioned earlier without the models it is difficult to judge the exact cause of the discrepancy. In any case the differences are quite small, so we can say that Boel's approach captures the behaviour of the hybrid model adequately.

It is interesting to note that the buckling length calculated for the brace out of plane are quite above the given buckling length of the Eurocode, with the additional tendency to increase even more, as it is evident from Boel's results for larger values of brace width ratio. This does not mean that Eurocode is unconservative, but that it is not applicable in the case of trusses with unrestrained chords. Due to the tension chord being unrestrained the braces act as if they have a translational spring on one of their ends. This accounts for the partial restraint to out of plane movements the tension chord provides to the braces. This can be schematized in Figure 81, where the deformations of characteristic buckling modes of the braces for restrained and unrestrained are compared to their mechanical representation. Due to the unrestrained tension chord, the buckling lengths of the braces can theoretically have buckling lengths even above 1.00.

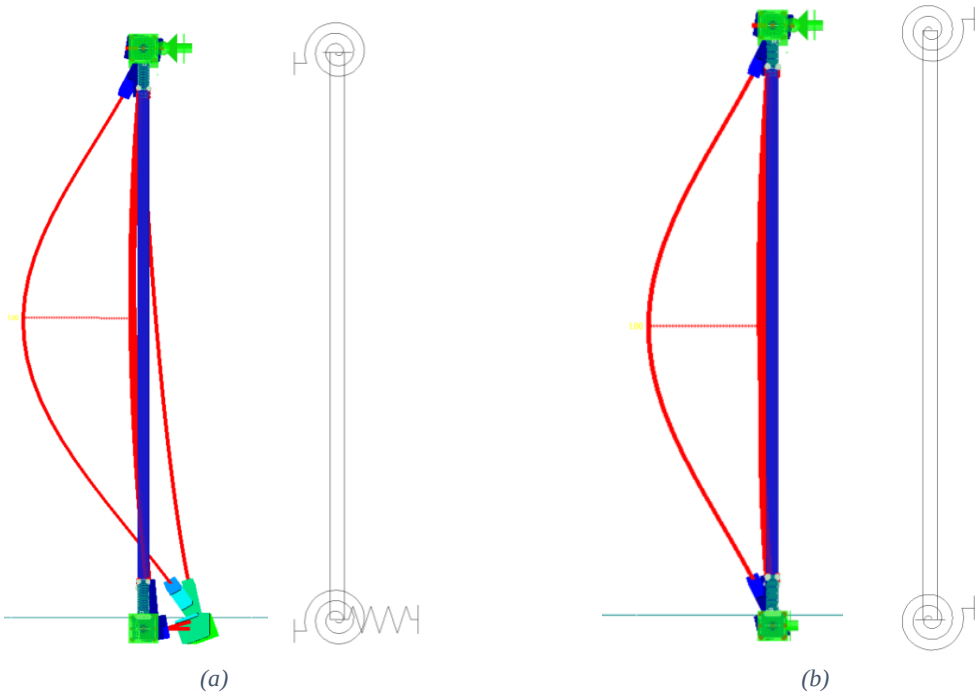

*(a)* *(b)*

*Figure 81. Mechanical schematization of the boundary conditions of the braces for (a) unrestrained tension chord and (b) restrained tension chord*

The last investigation performed was getting results for the truss with restrained tension chord. The tension chord was support in a similar manner as the compressive chord. The results of the in plane buckling did not change as the in plane buckling is unaffected by the out of plane boundary conditions of the truss, in the case of the centric joints.

Table 26. Chord buckling factor for out of plane buckling.

| | | γ = 15.9 | | | γ = 10 | | | γ = 6.25 | | |
|---|---|---|---|---|---|---|---|---|---|---|
| | | Supp. tension chord | Unsupp. tension chord | Diff. | Supp. tension chord | Unsupp. tension chord | Diff. | Supp. tension chord | Unsupp. tension chord | Diff. |
| β | 0.25 | 0.88 | 0.88 | -0.1% | 0.88 | 0.88 | 0.0% | 0.88 | 0.88 | 0.0% |
| | 0.40 | 0.85 | 0.85 | -0.1% | 0.87 | 0.87 | -0.1% | 0.92 | 0.93 | -0.6% |
| | 0.50 | 0.85 | 0.86 | -0.5% | 0.88 | 0.88 | -0.3% | 0.91 | 0.92 | -0.4% |
| | 0.60 | 0.84 | 0.84 | -0.2% | 0.87 | 0.87 | -0.4% | 0.85 | 0.85 | -0.9% |
| | 0.75 | 0.78 | 0.78 | -0.5% | 0.80 | 0.80 | 0.0% | 0.82 | 0.83 | -0.1% |

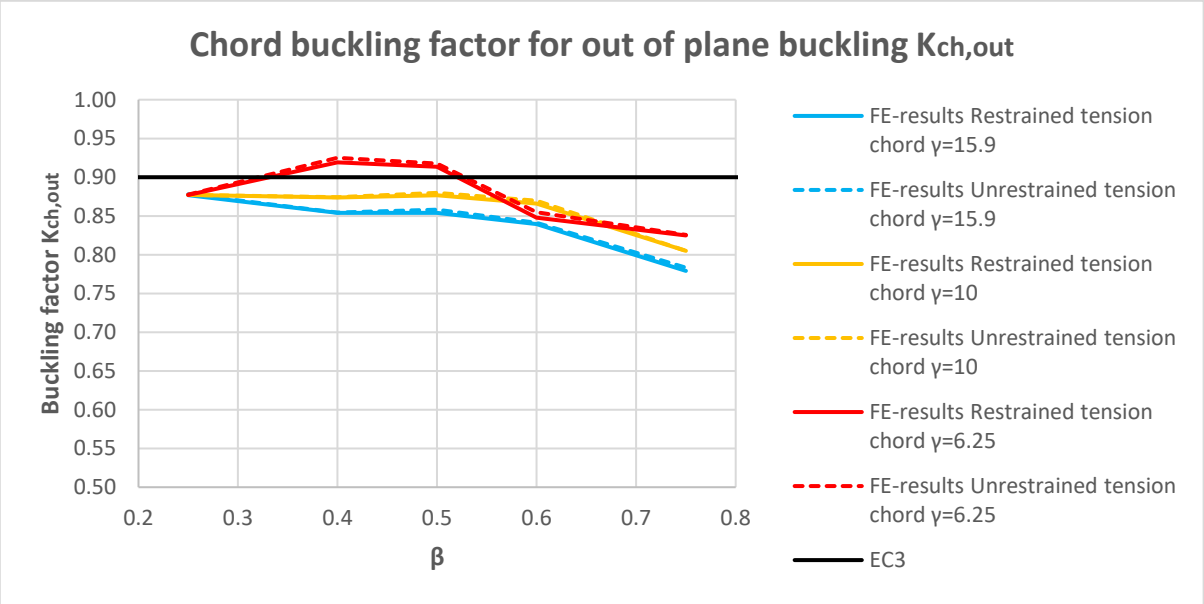


*Figure 82. Chord buckling factor for out of plane buckling $K_{ch,out}$*

Table 27. Brace buckling factor for out of plane buckling.

| | | γ = 15.9 | | | γ = 10 | | | γ = 6.25 | | |
|---|---|---|---|---|---|---|---|---|---|---|
| | | Supp. tension chord | Unsupp. tension chord | Diff. | Supp. tension chord | Unsupp. tension chord | Diff. | Supp. tension chord | Unsupp. tension chord | Diff. |
| β | 0.25 | 0.57 | 0.60 | -4.4% | 0.54 | 0.58 | -5.5% | 0.53 | 0.57 | -6.6% |
| | 0.40 | 0.63 | 0.65 | -2.6% | 0.59 | 0.61 | -4.5% | 0.56 | 0.59 | -4.6% |
| | 0.50 | 0.68 | 0.69 | -1.7% | 0.63 | 0.64 | -2.7% | 0.59 | 0.61 | -3.5% |
| | 0.60 | 0.71 | 0.74 | -4.8% | 0.66 | 0.70 | -5.7% | 0.63 | 0.64 | -2.4% |
| | 0.75 | 0.75 | 0.85 | -11.5% | 0.74 | 0.82 | -9.6% | 0.67 | 0.69 | -2.2% |

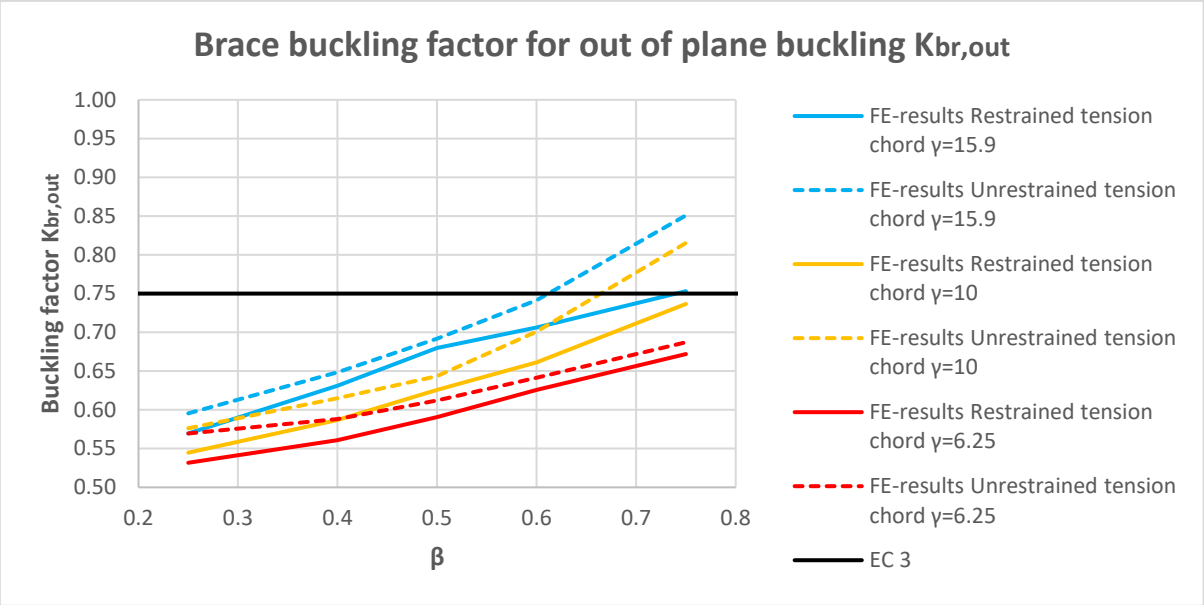


*Figure 83. Brace buckling factor for out of plane buckling $K_{br,out}$*

From the results it is evident that the additional restraint of the tension chord plays little role in the buckling values of the chord buckling out of plane. In the case of the brace buckling, larger deviations are observed. This makes sense as the change in supporting conditions have a more immediate effect on the boundary conditions of the braces. A general decrease in buckling length is observed as it would be expected. Additionally, the largest of buckling lengths are around the prescribed length from the Eurocode which is an indication that the lengths prescribed by the Eurocode refer only to member buckling lengths, without accounting for effects from the global behaviour of the structure.

## 3.6 Conclusions

In this chapter an investigation into the buckling behaviour of trusses with centric joints was performed. From the investigations, several conclusions were drawn.

Firstly, the effects of the corner radius on the stiffness of K-joints connections were examined. The expected result is that the inclusion of the corner radius will decrease the stiffness, as the rounding softens the response at the corners of the braces. This is also supported by the current results. The larger the profile used for the brace, and thus the radius of the corner, the lower the stiffness compared to the non-rounded profiles that was observed. Another observation was that for thicker chords the difference in stiffness between rounded and unrounded became smaller. Surprisingly, for the case of the thickest chord examined, the in-plane stiffness of the rounded corner profiles was larger. This is due to the gap between brace and support conditions becoming smaller, due to the radius. Additionally, any differences were more pronounced for the out of plane stiffness, which is to be expected. In general, though, the effects were not very large and assuming rounded or unrounded profiles should not affect the analysis substantially.

When it comes to investigating the buckling lengths of trusses, some difficulties exist when attributing buckling modes to specific members and directions. This issue has been noted in the literature (Boel, 2010; Poels, 2017) and was also encountered in this work. In general, it would be beneficial to develop a method to ascertain the buckling modes of each member unambiguously. Until such a method is created, the buckling load attributable to specific members and directions, from a linear buckling analysis, is prone to human error. This was attempted by developing a new method, to calculate the buckling loads of individual members. It accomplished to calculate the buckling loads for a continuous column but was not further developed due to time restrictions. This new method is presented in APPENDIX C.

In regard to the buckling length factor investigation, the results from the truss girder used were split into restrained tension chord and unrestrained tension chord. The results for the unrestrained tension chord were compared to the results from literature (Boel, 2010), whilst the results for the restrained tension chord were

compared with the unrestrained. From the comparison with Boel's results it was concluded that the results from the shell element model (hybrid model) match the results he produced with his approach. This validates further the approach he developed, with which the stiffness of the connections is accounted for with rotational springs in a beam element model.

What was further observed was that for the unrestrained tension chord the buckling lengths factors for out of plane buckling were above the prescribed buckling length factor of the Eurocode of 0.75. This it to be expected as the unrestrained structure includes sway effects. For the restrained tension chord all values were around or below the prescribe buckling length factor. This indicates that the provided buckling length factor of the Eurocode refers to the buckling lengths of individual members and that global effects need to be considered separately. The last remark regarding the buckling length factor of the Eurocode is that of the in plane buckling of the braces, there was as singular value above 0.75. This may indicate that Eurocode may need to revise the provided buckling lengths to 0.8 as are given by the Japanese structural steel codes (*Standard Specifications for Steel and Composite Structures*, 2009).

During this investigation a new approach was proposed for calculating the buckling length factors of trusses. The approach relies on using the stiffness of the members and the connections, as opposed to only relying on the brace width ratio β and chord thickness ratio γ, as proposed by Boel. This approach may be promising as the thickness of the braces can be more immediately be accounted for and would also be applicable to any kind of cross sections, not only square hollow ones that were used in this investigation. The development and investigation regarding this are presented in APPENDIX D.

Lastly, regarding the general behaviour of the buckling length factor depending on the brace width ratio β. The buckling length factor of chords plateau for smaller values of β and decrease by increasing the β. This is because the smaller the β is the less stiff the braces are, and the smaller the stiffness the connections have. This means that the chords are primarily supported by the adjacent chord members. With the increase of β, the braces become capable of providing larger amounts of restraint for the chords, which decrease the buckling length factor. For the buckling of the braces, with an increasing β there is an increase of the buckling lengths factors. This is because with the increase of β the stiffness of the braces increases. It follows that they then require larger amounts of rotational restraints in absolute numbers to "feel" the same restraint as the smaller cross sections.

# 4 INVESTIGATION OF ECCENTRIC JOINTS

## 4.1 Introduction

In this section the investigation of the buckling behaviour of trusses with eccentric joint was performed. When it comes to eccentric joints, one additional characteristic is required to be defined. This is the amount of eccentricity introduced compared to a centric joint. Depending on the displacement a percentage eccentricity or an absolute value can be defined. In this investigation introducing the maximum feasible eccentricity is of interest. This also provides more information on the differences between centric and eccentric joints as it is the extreme between the two cases.

As in the case of centric joints, some geometries cannot be reasonably defined with mid-surface modelling. Such is the case of when a maximum eccentricity is introduced for a brace that has a thinner thickness than the chord (Figure 84). From the figure it is obvious that trying to model the specific configuration by the mid-surface definition, would prove quite difficult. For this reason, in all joints, the braces were put at the edge of the chord such that the brace's side wall was in line with the chords side wall (Figure 85).

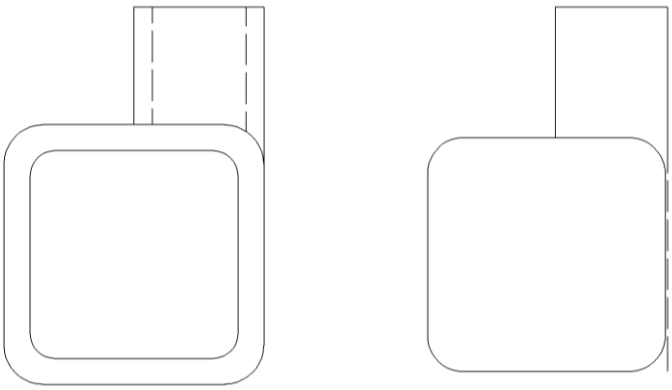

*Figure 84. Actual geometry vs theoretical geometry of model using mid-surface modelling for the case of brace having thinner walls than the chord.*

Additionally, to describe the brace width ratio, a new factor would be needed, as the β factor has a very specific meaning and should be used for centric joints. For simplicity reasons the $\beta_e$ factor will simply be referred to as β factor. In all graphs, when comparisons between centric and eccentric joints is performed, simply β is going to be used to describe both centric and eccentric brace width ratio.

## 4.2 Truss models

As with the centric joint investigation, a hybrid model was used to perform the analysis. The joints were formed using shell elements and the rest of the truss was done using beam elements.

In the case of the centric joints the symmetry in the trusses plane provided the simplification that the lateral supports did not matter which side they were placed on. In the case of eccentric joints this symmetry does not exist. In this case, the positioning may actually affect the results, so it was decided to place the supports on a specific side. For all the investigations, the supports were placed on the opposite side in which the eccentricity was introduced (Figure 85). Additionally, to investigate the effect the support placements have on the buckling, two additional positions were investigated, by changing the height placement of the supports.

*(a)* *(b)*

*Figure 85. Lateral support positions for (a) centric joints and (b) eccentric joints*

In order to get additional data points to support the conclusions, both restrained and unrestrained tension chords were used in the investigations. Lastly, an additional meshing investigation was performed. The change in geometry gives additional requirements for the mesh refinement, especially in areas between the two braces' meeting point and the chord edge. This investigation is presented in APPENDIX A.

## 4.3 Approach

As with the centric joint trusses, the eigenmodes were characterized depending on the member that has buckled (chord or brace) and the direction (in plane or out of plane). The calculation of the buckling load and the buckling length were done in same manner as the centric joint investigation. The system length definition was kept the same because in most cases the majority of the cross section lay on the chord face and not on the corner radius. If in some cases the brace cross section laid primarily on the corner radius a change of definition may be appropriate, but the differences in length were marginal so not worth addressing it.

One point that is worth noting is the fact that the eccentric joint trusses give rise to couple behaviour between in plane and out of plane. Already, from the linear static analysis, it can be seen that the behaviour of the eccentric joint differs from the centric joint behaviour (Figure 86).

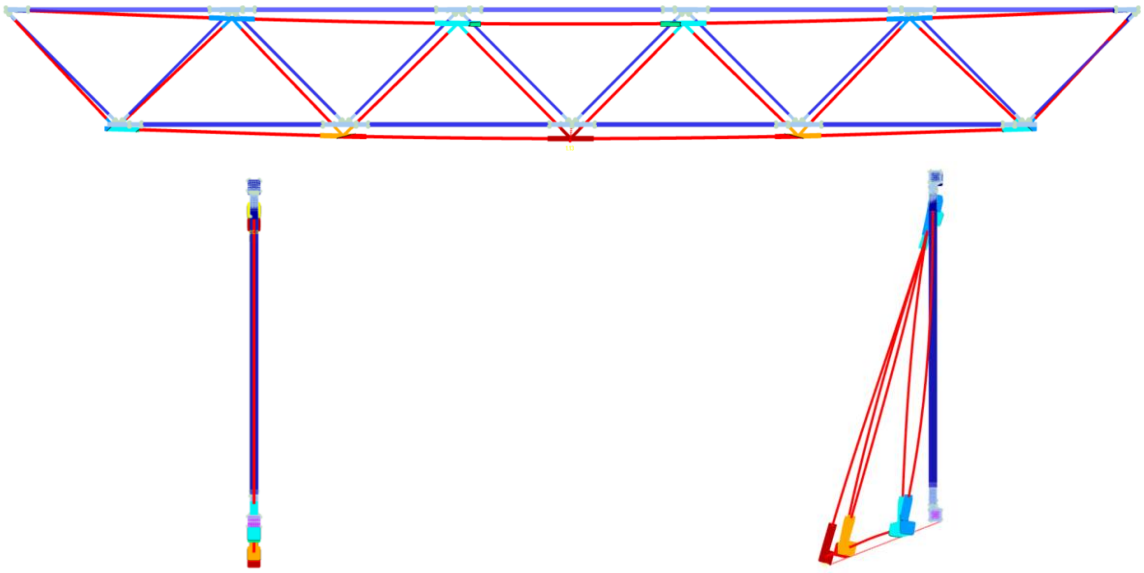

*(a)* *(b)*

*Figure 86. Displacements of linear static analysis of models with (b) centric and (c) eccentric joints. The displacements have been enlarged by a factor of 150.*

The same coupling is observed in the buckling behaviour. This means that for the in plane buckling modes, out of plane eigen-displacements were observed and vice versa. Nonetheless, in all configurations tested, the members continued to buckle predominantly in one or the other direction. This allowed for the classification of the buckling modes for in and out of plane depending on the predominate direction of buckling. Classifying the buckling modes in the same manner as the centric joints allows the comparison of the results with the previous results. The results and comparisons are presented in the next section.

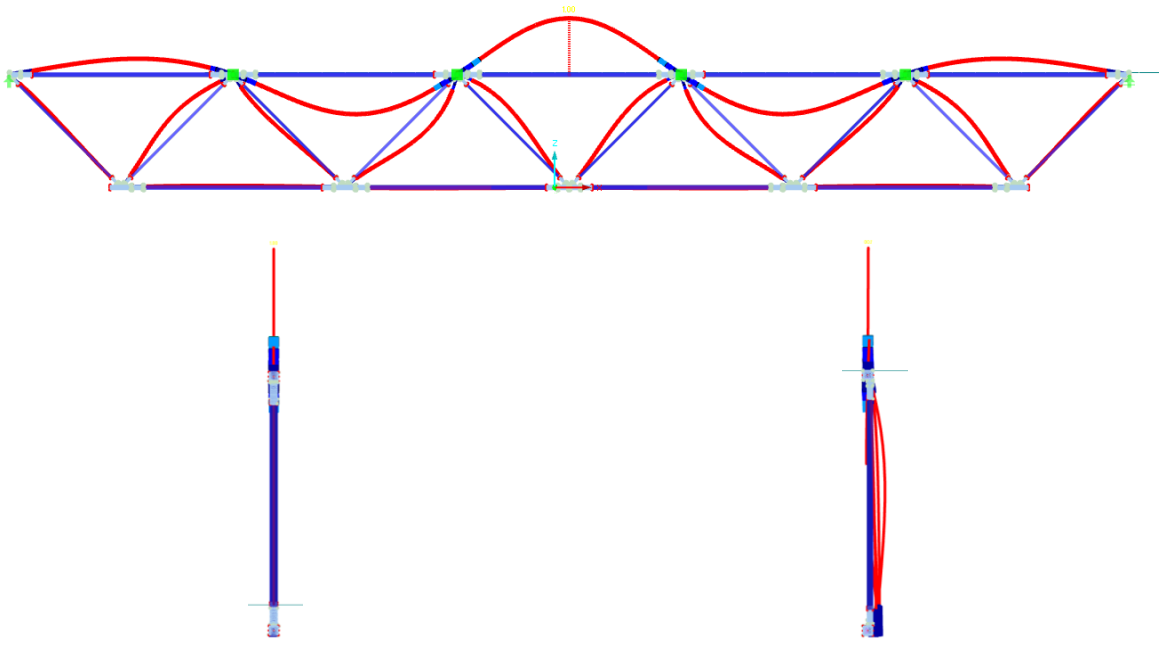

*(a)* *(b)*

*Figure 87. Example of coupled buckling. In plane buckling of the chord for (a) centric and (b) eccentric joint*

## 4.4 Results

As with the centric joint investigation, first the results for in plane are going to be presented, followed by the result for the out of plane buckling. Additionally, the results for the unrestrained tension chord are going to be presented, followed by the results for the restrained tension chord.

### 4.4.1 Results for unrestrained tension chord

From the first set of results a general decrease in the buckling length for the in-plane buckling can be observed (Figure 88). This would indicate that there is a better buckling behaviour in plane from the use of eccentric joints compared to centric joints. This effect appears to diminish with the increase of β. This makes sense as the closer to unity the β is, the eccentric joint approaches the geometry of a centric joint. In the extreme case of β=1 an eccentric joint cannot be defined anymore. The results also support that the cut-off limit of 0.75 chosen was a reasonable assumption for the investigations performed.

Table 28. Brace buckling factor for out of plane buckling

| | | γ | | | | | | | |
|---|---|---|---|---|---|---|---|---|---|
| | | 15.9 | | | 10 | | | 6.25 | |
| | | Eccentric | Centric | Diff. | Eccentric | Centric | Diff. | Eccentric | Centric | Diff. |
| β | 0.25 | 0.87 | 0.88 | -1.4% | 0.87 | 0.88 | -0.4% | 0.89 | 0.89 | 0.0% |
| | 0.40 | 0.80 | 0.85 | -6.2% | 0.86 | 0.86 | -1.0% | 0.89 | 0.90 | -0.7% |
| | 0.50 | 0.79 | 0.85 | -7.1% | 0.84 | 0.86 | -1.9% | 0.88 | 0.88 | 0.1% |
| | 0.60 | 0.79 | 0.82 | -4.3% | 0.82 | 0.84 | -2.1% | 0.86 | 0.86 | -0.9% |
| | 0.75 | 0.71 | 0.73 | -3.0% | 0.74 | 0.75 | -0.8% | 0.75 | 0.77 | -1.9% |

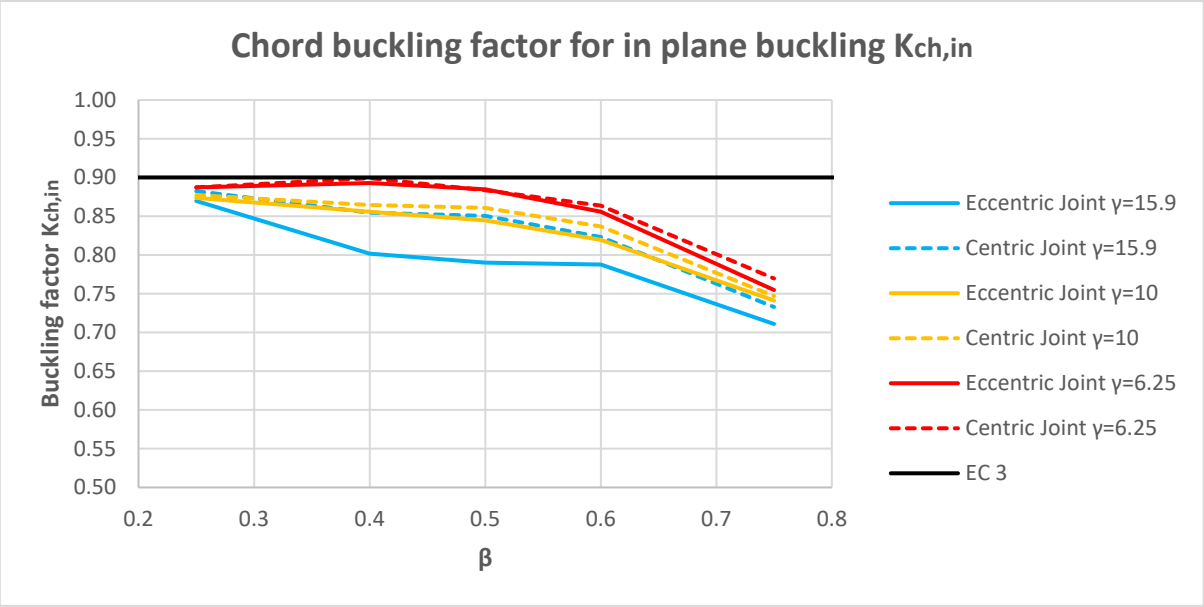


*Figure 88. Chord buckling factor for in plane buckling $K_{ch,in}$*

Table 29. Brace buckling factor for out of plane buckling

| | | γ | | | | | | | |
|---|---|---|---|---|---|---|---|---|---|
| | | 15.9 | | | 10 | | | 6.25 | |
| | | Eccentric | Centric | Diff. | Eccentric | Centric | Diff. | Eccentric | Centric | Diff. |
| | 0.25 | 0.51 | 0.59 | -12.5% | 0.51 | 0.53 | -3.8% | 0.50 | 0.51 | -1.2% |
| | 0.40 | 0.54 | 0.68 | -19.5% | 0.53 | 0.57 | -7.7% | 0.51 | 0.52 | -2.0% |
| β | 0.50 | 0.60 | 0.72 | -16.6% | 0.55 | 0.61 | -8.6% | 0.53 | 0.54 | -2.5% |
| | 0.60 | 0.66 | 0.74 | -11.5% | 0.59 | 0.63 | -6.7% | 0.55 | 0.56 | -1.6% |
| | 0.75 | 0.79 | 0.81 | -2.3% | 0.67 | 0.68 | -1.3% | 0.59 | 0.59 | -0.3% |

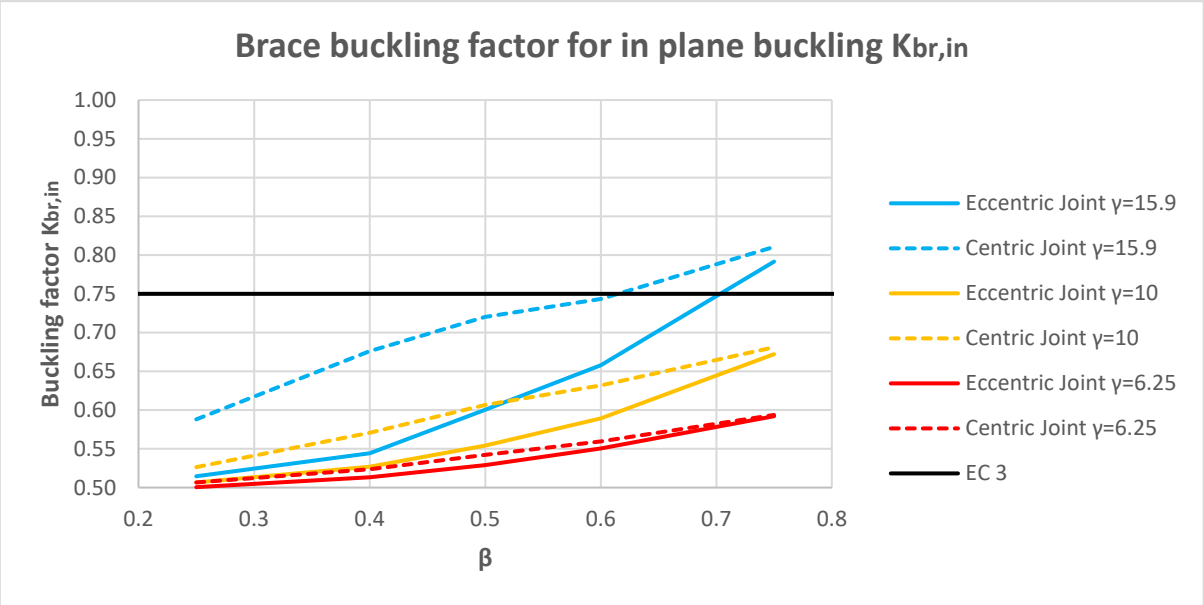


*Figure 89. Brace buckling factor for in plane buckling $K_{br,in}$*

Additionally, the effect is much less pronounced for the thicker chords used. This indicates that the thickness of the chord affects the decrease in buckling length from centric to eccentric joints.

This could be explained by attributing the improvement in behaviour to the increase of stiffness from the introduction of the eccentricity. In a centric joint, of $\beta<0.85$ (X.-L. Zhao et al., 2001), the forces are transferred primarily with the mechanism of the chord face in bending. From the introduction of the eccentricity, due to the brace being connected immediately with the chord wall, the transfer of forces can be done through the much stiffer mechanism of the chord wall. Since for thick chords, the mechanism of the chord face is already quite stiff, the increase in stiffness due to the introduction of the eccentricity is expected to be less. Due to this, the reduced improvement observed from thinner to thicker chords makes sense.

Table 30. Brace buckling factor for out of plane buckling

| | | γ | | | | | | | | |
|---|---|---|---|---|---|---|---|---|---|---|
| | | 15.9 | | | 10 | | | 6.25 | | |
| | | Eccentric | Centric | Diff. | Eccentric | Centric | Diff. | Eccentric | Centric | Diff. |
| | 0.25 | 0.88 | 0.88 | 0.0% | 0.88 | 0.88 | 0.0% | 0.88 | 0.88 | 0.5% |
| | 0.40 | 0.85 | 0.85 | 0.1% | 0.87 | 0.87 | 0.1% | 0.93 | 0.93 | 0.6% |
| β | 0.50 | 0.86 | 0.86 | 0.0% | 0.88 | 0.88 | 0.3% | 0.93 | 0.92 | 1.2% |
| | 0.60 | 0.84 | 0.84 | 0.3% | 0.88 | 0.87 | 0.8% | 0.86 | 0.85 | 0.3% |
| | 0.75 | 0.79 | 0.78 | 0.5% | 0.81 | 0.80 | 0.4% | 0.83 | 0.83 | 0.3% |

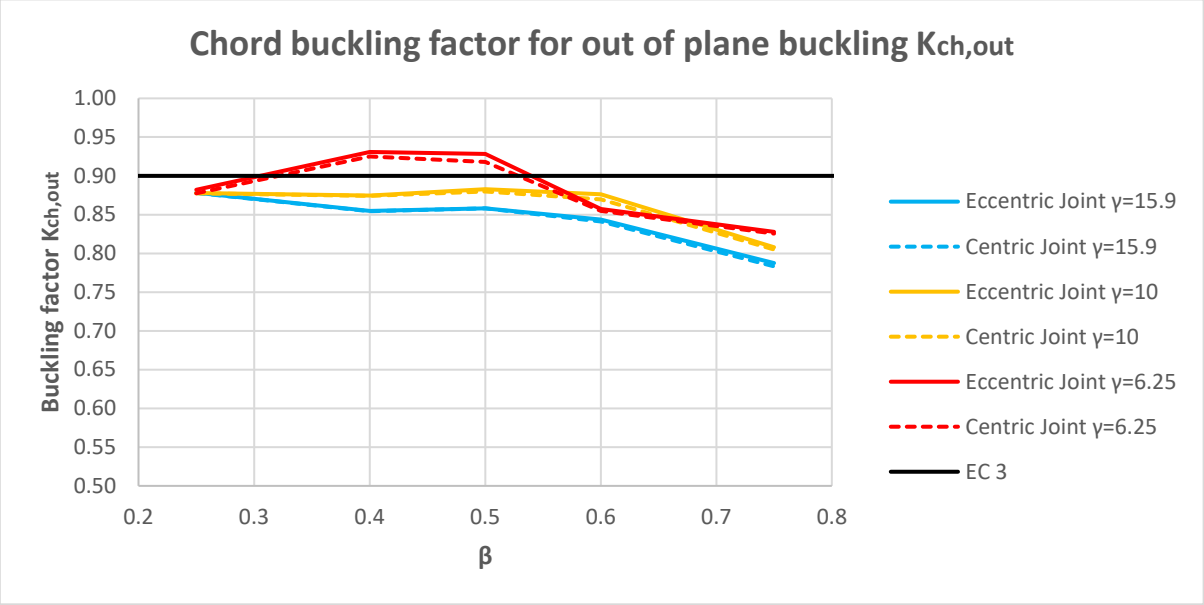


*Figure 90. Chord buckling factor for out of plane buckling $K_{ch,out}$*

Table 31. Brace buckling factor for out of plane buckling

| | | γ | | | | | | | | |
|---|---|---|---|---|---|---|---|---|---|---|
| | | 15.9 | | | 10 | | | 6.25 | | |
| | | Eccentric | Centric | Diff. | Eccentric | Centric | Diff. | Eccentric | Centric | Diff. |
| | 0.25 | 0.60 | 0.60 | 1.3% | 0.58 | 0.58 | 0.8% | 0.57 | 0.57 | -0.7% |
| | 0.40 | 0.66 | 0.65 | 1.4% | 0.62 | 0.61 | 0.5% | 0.59 | 0.59 | 1.1% |
| β | 0.50 | 0.70 | 0.69 | 1.3% | 0.65 | 0.64 | 1.5% | 0.62 | 0.61 | 1.7% |
| | 0.60 | 0.74 | 0.74 | 0.4% | 0.71 | 0.70 | 0.8% | 0.65 | 0.64 | 1.6% |
| | 0.75 | 0.85 | 0.85 | 0.3% | 0.82 | 0.82 | 0.4% | 0.69 | 0.69 | 1.0% |

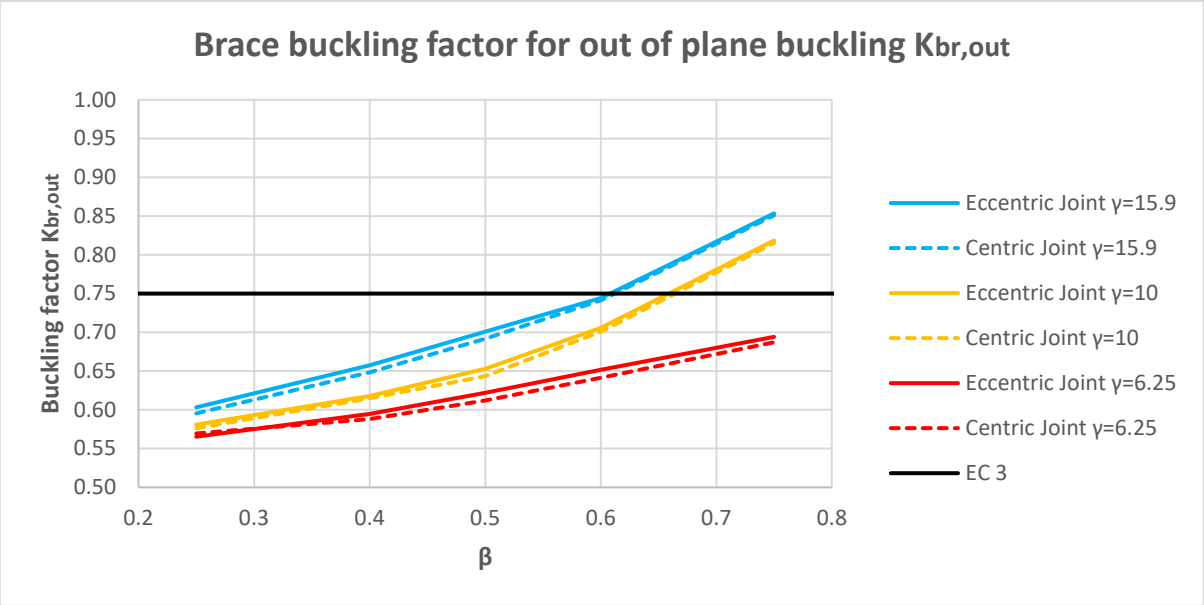


*Figure 91. Brace buckling factor for out of plane buckling $K_{br,out}$*

From the results of the out of plane buckling the eccentric joints perform slightly worse than the centric. This would indicate a potential decrease in stiffness. From the literature study there is an example of calculated stiffness of an eccentric joint but has a stiffening plate. Thus, there cannot be a straight comparison between centric and eccentric with the results being extrapolated to this investigation. Additionally, there is not a conclusive method to calculate the out of plane stiffness of eccentric joints (Garifullin, Mela, et al., 2017).

To check if decreased stiffness provides an adequate explanation, a simple T-joint model is used. Part of the connection is modelled and is simply supported at the chord ends. By applying an out of plane moment, the out of plane displacements are compared for a centric and two eccentric joints, with increasing eccentricity. The displacement for all the components except for the displacements due to the connection should remain the same. It can be seen from the results (Figure 92) that by increasing the eccentricity there is a progressive increase in the displacements.

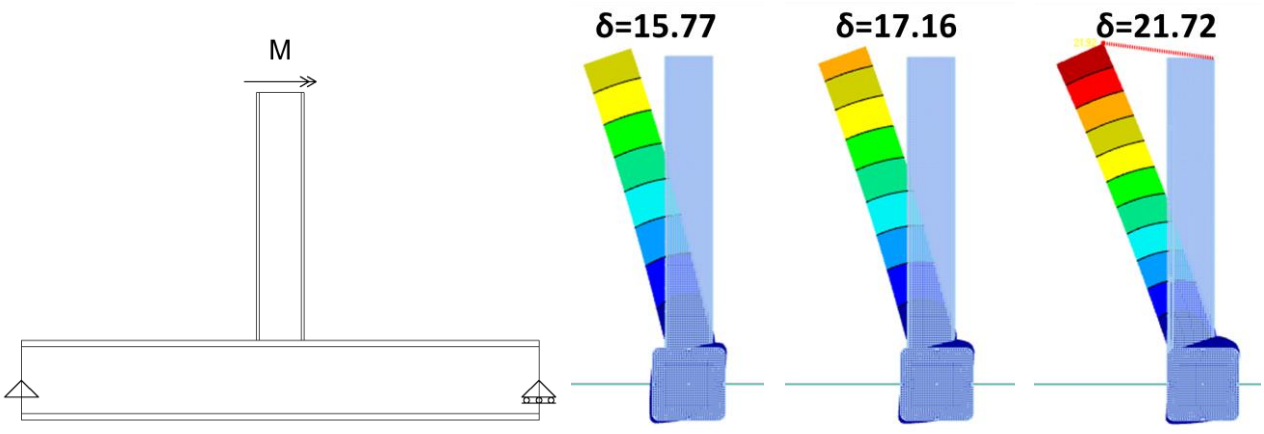


*Figure 92. Out of plane displacements for T-joints loaded with an out of plane moment (a), with increasing levels of eccentricity from left to right. Joint (b) is centric whilst joint (d) an eccentric joint with the full eccentricity possible applied.*

### 4.4.2 Results for restrained tension chord

As was done with the centric joints, to investigate the member buckling lengths for the out of plane buckling of braces, the tension chord is restrained. Additionally, the buckling length of the chord is presented as they

were slightly affected by the change in boundary conditions. The results for in plane are not presented as they were virtually the same. This means that the out of plane boundary conditions do significantly affect the buckling in plane, even though coupled behaviour is present.

Table 32. Chord buckling factor for out of plane buckling

| | | γ | | | | | | | | |
|---|---|---|---|---|---|---|---|---|---|---|
| | | 15.9 | | | 10 | | | 6.25 | | |
| | | Eccentric | Centric | Diff. | Eccentric | Centric | Diff. | Eccentric | Centric | Diff. |
| | 0.25 | 0.88 | 0.88 | 0.1% | 0.88 | 0.88 | 0.1% | 0.88 | 0.88 | 0.6% |
| | 0.40 | 0.85 | 0.85 | 0.1% | 0.87 | 0.87 | 0.1% | 0.93 | 0.92 | 0.6% |
| β | 0.50 | 0.85 | 0.85 | 0.1% | 0.88 | 0.88 | 0.4% | 0.92 | 0.91 | 1.2% |
| | 0.60 | 0.84 | 0.84 | 0.4% | 0.87 | 0.87 | 0.6% | 0.85 | 0.85 | 0.4% |
| | 0.75 | 0.78 | 0.78 | 0.6% | 0.80 | 0.80 | 0.0% | 0.83 | 0.82 | 0.1% |

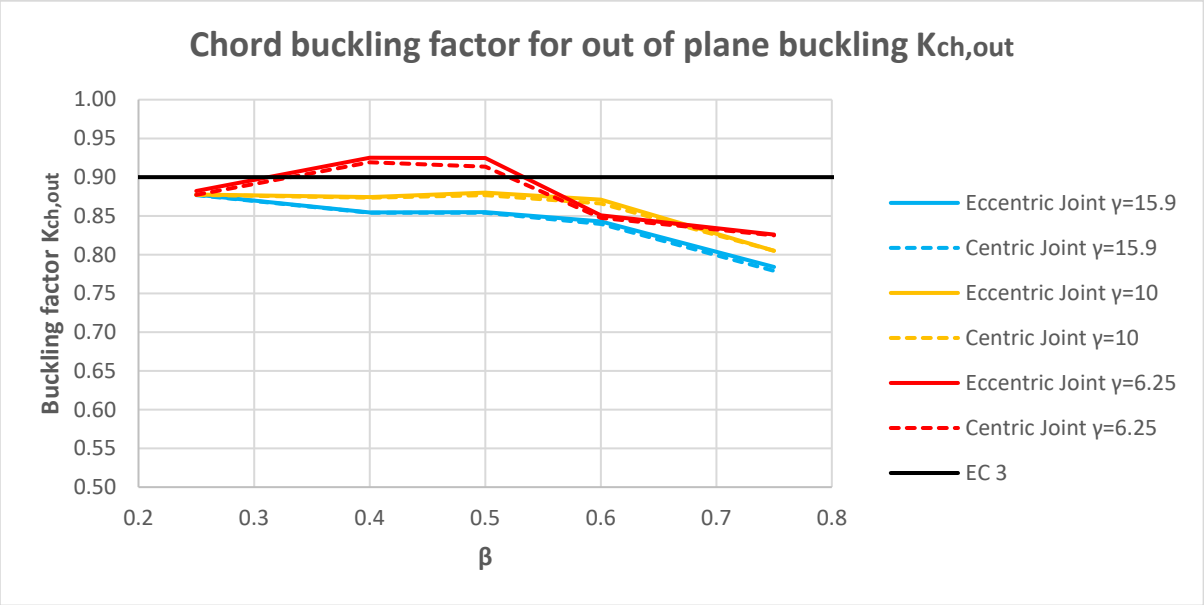


*Figure 93. Chord buckling factor for out of plane buckling $K_{ch,out}$*

Table 33. Brace buckling factor for out of plane buckling

| | | γ | | | | | | | | |
|---|---|---|---|---|---|---|---|---|---|---|
| | | 15.9 | | | 10 | | | 6.25 | | |
| | | Eccentric | Centric | Diff. | Eccentric | Centric | Diff. | Eccentric | Centric | Diff. |
| | 0.25 | 0.58 | 0.57 | 1.6% | 0.55 | 0.54 | 0.7% | 0.53 | 0.53 | 0.3% |
| | 0.40 | 0.64 | 0.63 | 1.6% | 0.60 | 0.59 | 1.7% | 0.57 | 0.56 | 1.6% |
| β | 0.50 | 0.69 | 0.68 | 1.3% | 0.64 | 0.63 | 1.7% | 0.60 | 0.59 | 1.5% |
| | 0.60 | 0.71 | 0.71 | 0.9% | 0.67 | 0.66 | 1.4% | 0.64 | 0.63 | 1.8% |
| | 0.75 | 0.76 | 0.75 | 0.8% | 0.74 | 0.74 | 0.7% | 0.68 | 0.67 | 0.9% |

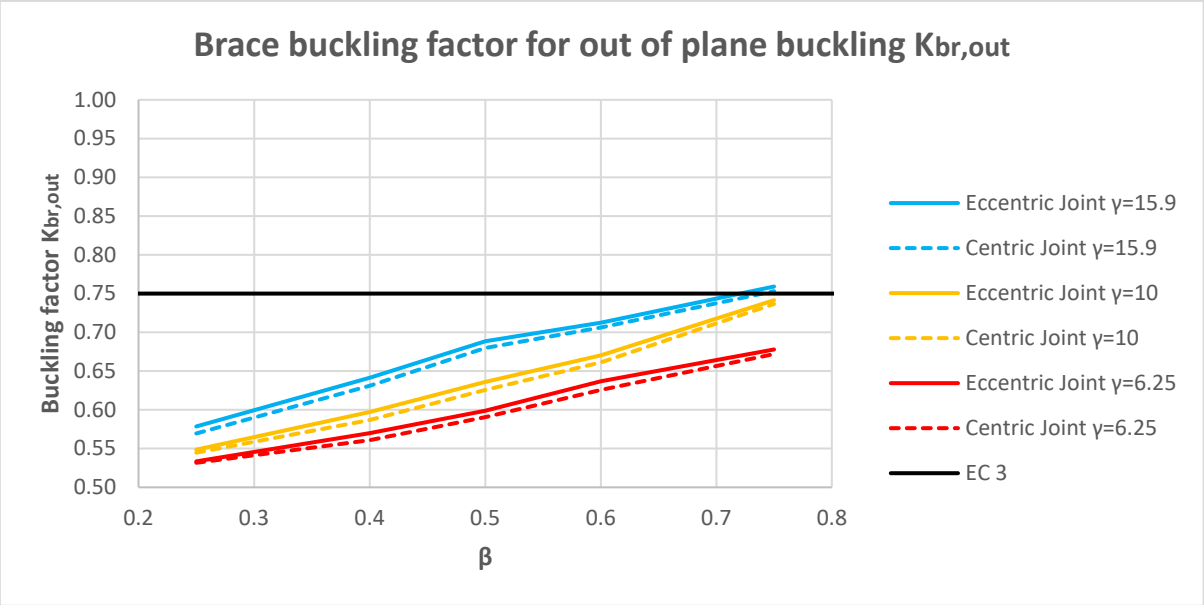


*Figure 94. Brace buckling factor for out of plane buckling $K_{br,out}$*

As was observed from the previous out of plane results (unrestrained tension chord), the buckling lengths appear slightly higher for the eccentric joints, indicating a worst buckling behaviour. As was mentioned before this is due to a slightly less stiff response by the connection.

### 4.4.3 Results for different support positions

The buckling lengths for the restrained tension chord are assumed to be the buckling lengths of the members. To confirm this assumption, it is necessary to investigate if the position of the lateral supports affect the calculated buckling lengths greatly. By confirming that the lateral support position plays an insignificant role in the value of the buckling load, it would unambiguously mean that the calculated buckling length does indeed correspond to the member's buckling length.

The investigation was done by changing the height position of the supports on the chord wall. To limit the investigation time, results for only one of the chord thicknesses was produced. In case a big difference was observed, additional chord cross sections would be used to investigate the changes that the chord thickness incurs on the effects. Additionally, only three different positions were investigated with the prospect of investigating additional configurations if the effects appeared major.

For the preliminary investigation the middle chord, with the γ factor of 10, was used. The three positions chosen were taken as follows (Figure 95):

- On the middle of the chord wall (middle),
- by placing the supports as further away as possible (external) and
- lastly, by placing the supports as close as possible (internal).

From the results a few conclusions were drawn. Firstly, the changes in support position did not affect the buckling in plane at all. This makes sense as the lateral restraint should primarily affect the out of plane behaviour. However, due to the coupling effect observed in the modes there was potential for interaction between in plane and out of plane. Apparently, this was not the case, or it was so slight that it is outside the accuracy of the analysis results obtained.

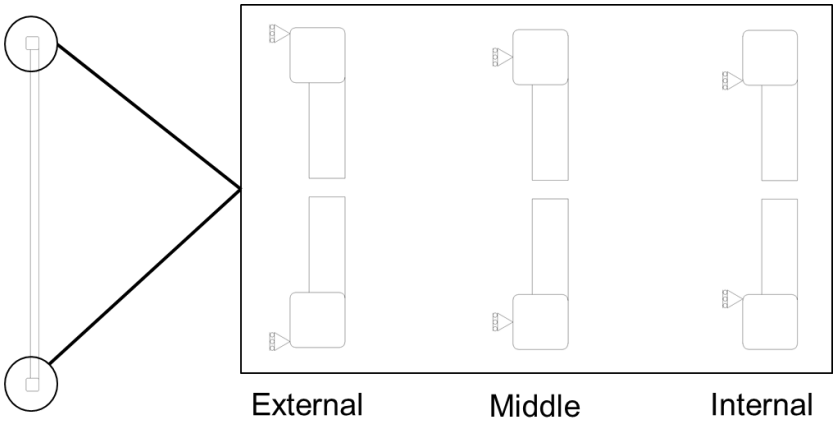


*Figure 95. Lateral constraint positions for the three alternatives investigated*

Another observation is that the results for the out of plane buckling are practically unaffected. The results differ slightly but the effects are so slight that they are not even visible in graphs. The effects are more pronounced for the brace out of plane buckling and it is presented for demonstration purposes (Figure 96). The rest of the results can be found in APPENDIX E.

Table 34. Brace buckling factor for out of plane buckling

| | | γ = 10 | | |
|---|---|---|---|---|
| | | External support | Middle support | Internal support |
| β | 0.25 | 0.570 | 0.549 | 0.551 |
| | 0.40 | 0.631 | 0.597 | 0.598 |
| | 0.50 | 0.680 | 0.636 | 0.637 |
| | 0.60 | 0.706 | 0.670 | 0.672 |
| | 0.75 | 0.753 | 0.741 | 0.742 |

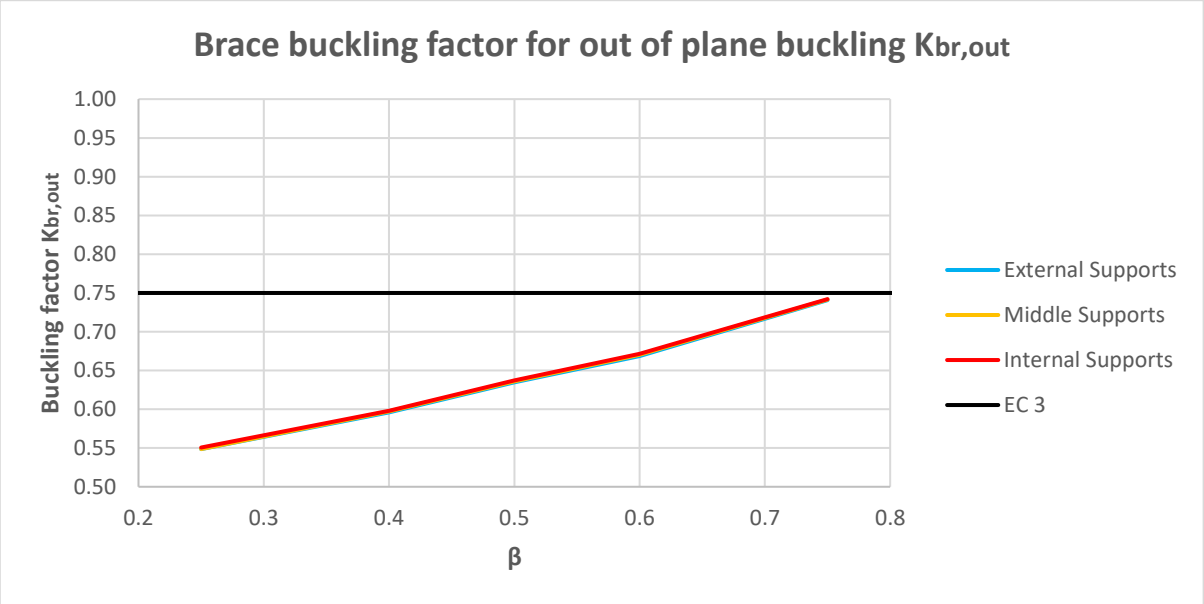


*Figure 96. Brace buckling factor for out of plane buckling $K_{br,out}$*

## 4.5 Additional investigations

From previous results it was observed that with an increase in the chord thickness, the observed decrease of buckling lengths (eccentric vs centric) was reduced. In order to investigate the rate at which the beneficial effects of eccentric joints diminish, two cross sections were additionally investigated. The profiles were chosen

so that the cross-sectional thickness was between the profiles already used, with γ=10 and γ=6.25. According to the EN 10210-2:2006 two profiles existed and so those were picked. As to have results to compare to, except for the eccentric joint trusses, the centric joint trusses were also created and used in the investigation.

The results follow the trends observed in all previous results regarding the comparison between centric and eccentric. For this reason, only the graph of the brace in plane is going to presented below. The analytical results, as well as the results for the rest of the cases (chord/brace, in-plane/out of plane) can be found in APPENDIX E. In the graph presented, the data points for the thinnest chord used has been excluded in order for the graph to be clearer.

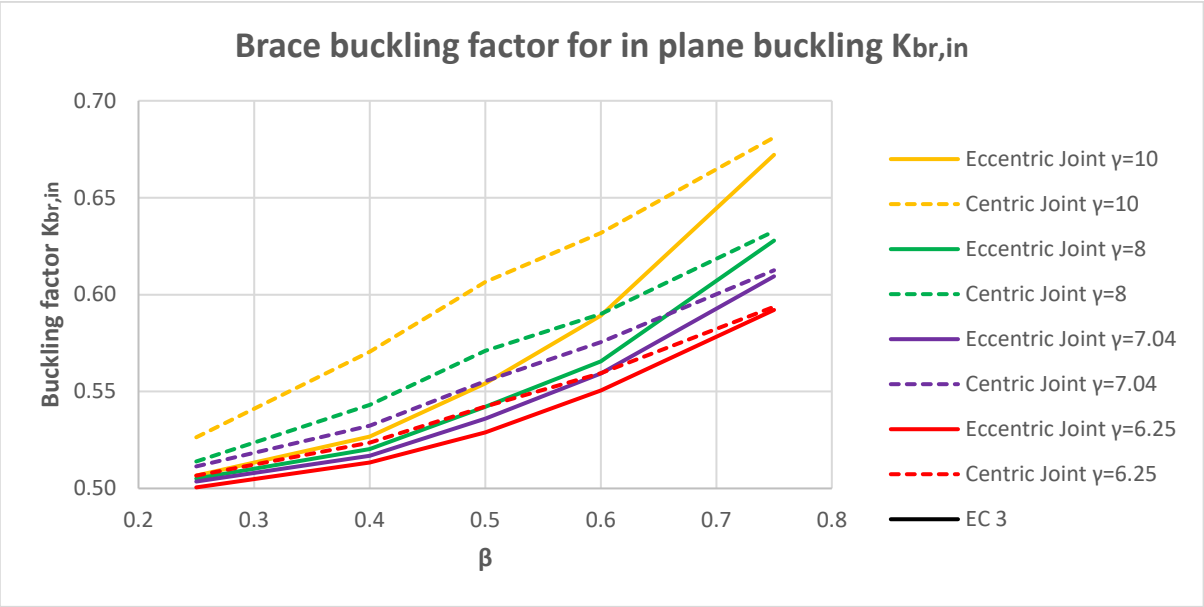


*Figure 97. Brace buckling factor for in plane buckling Kbr,in*

In order to visualise the results better and to be able to draw useful conclusions, the buckling lengths of the eccentric joints are normalized against the corresponding buckling length from the centric joint.

From the results already presented it can be stated that in the case of in plane buckling (chord and brace) the eccentricity does not necessarily need to be modelled. As the effects of eccentricity have a positive effect on the buckling length it would be on the safe side to deal with the design in regard to buckling, as if it were centric. It is of interest to conclude if and when it would be beneficial to actually account for the eccentric joint and obtain the decreased buckling length expected due to the better behaviour. In this work the limit is chosen as 5%. It is assumed that if the normalized buckling length value for an eccentric joint is below 0.95, it would be beneficial to account for the eccentricity.

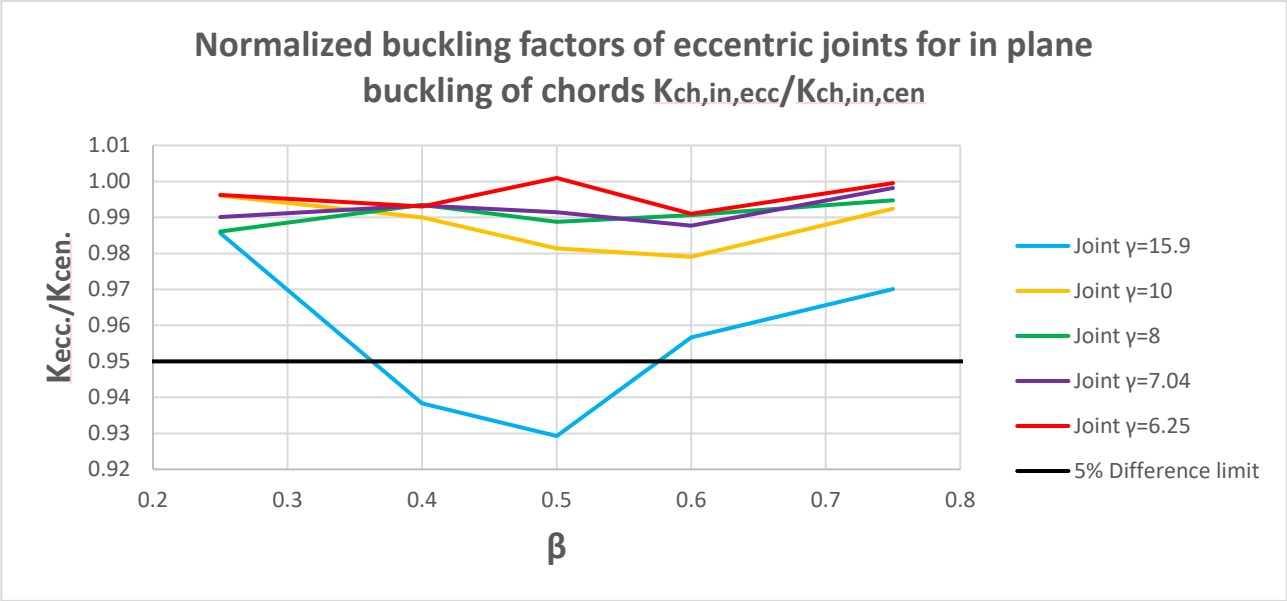


*Figure 98. Normalized buckling factors of eccentric joints for in plane buckling of chords $K_{ch,in,ecc}/K_{ch,in,cen}$.*

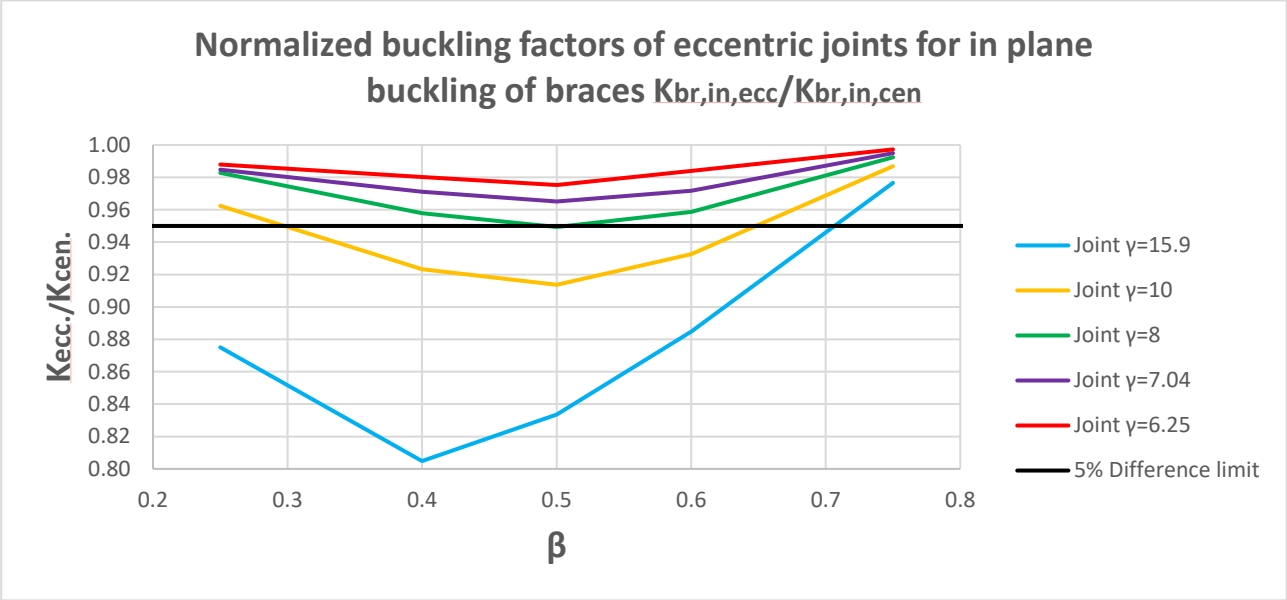


*Figure 99. Normalized buckling factors of eccentric joints for in plane buckling of braces $K_{br,in,ecc}/K_{br,in,cen}$.*

From Figure 98 it can be observed that the differences between eccentric joints and centric joints are not that big for the chord buckling in plane. This means that it would not be especially beneficial to go into the detail of accounting for the eccentricity, except for the thinnest chord used and medium range braces (β≈0.35-0.55). As it relates to buckling of the braces in plane, for chords that have γ higher than 8 it would appear to be beneficial to account for the eccentricity. As it relates to the β factor for the higher end of the range (above 0.7) and the lower end of the range (below 0.3), it would appear that it would not be beneficial. Interestingly, for the case of γ=15.9 and β=0.4 the reduction in buckling length can reach around 20% for eccentric joints compared to centric.

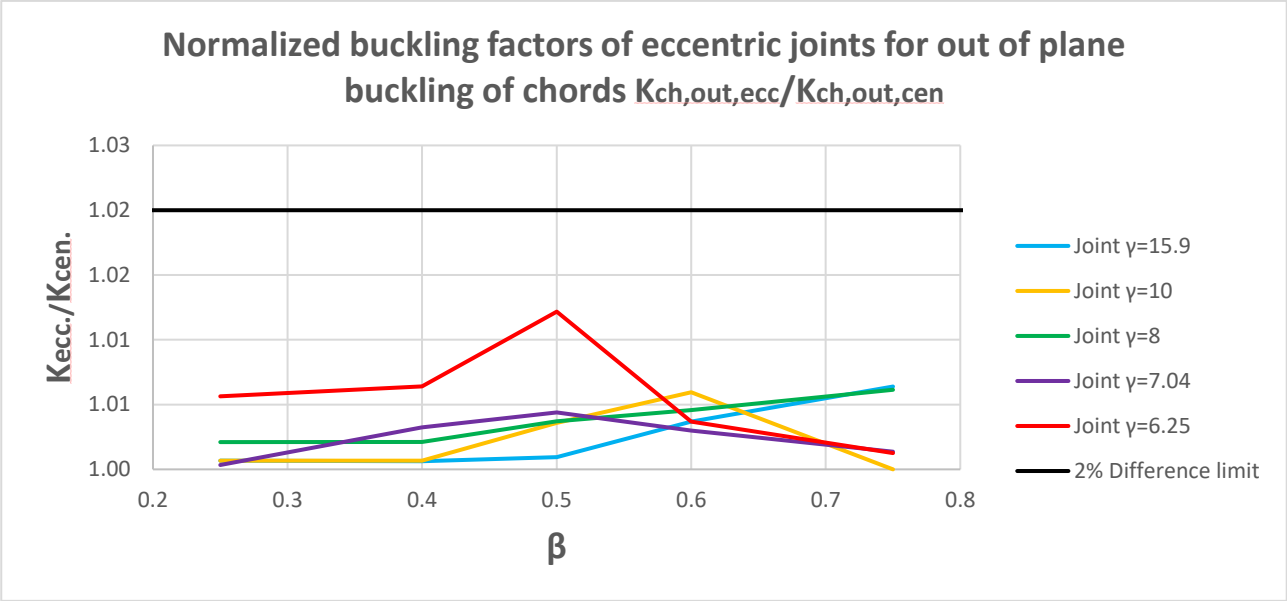


*Figure 100. Normalized buckling factors of eccentric joints for out of plane buckling of chords $K_{ch,out,ecc}/K_{ch,out,cen}$*

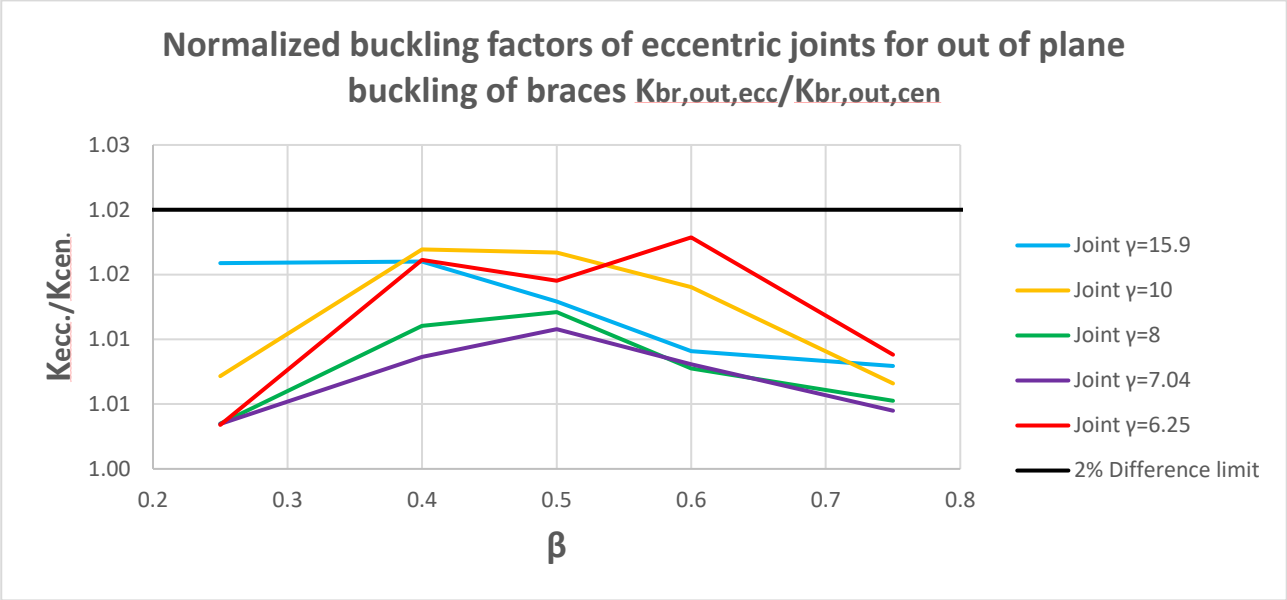


*Figure 101. Normalized buckling factors of eccentric joints for out of plane buckling of braces $K_{br,out,ecc}/K_{br,out,cen}$.*

As it relates to the out of plane buckling, it was concluded that introduction of the eccentricity produces results slightly worse than the ones expected from centric joints. In this case, as the comparison between centric and eccentric is a matter of safety, a cut-off limit of 2% is adopted. This means that for normalized buckling length values of the eccentric joint truss of above 1.02, the eccentricity needs to be accounted for, otherwise the design may not be on the safe side. From the results presented above, it is evident that all the results are below the assumed limit of 2% set. This would indicate that the eccentricity can be ignored when it comes to calculating the buckling load of the truss.

It is noted that for the case of the chords with $\gamma$=6.25, there is a relatively pronounced change in trend for the braces with $\beta$=0.5. This was investigated thoroughly and no specific issue was found in the results or the models (centric and eccentric). Even without this potential error, if the results followed the expected trend the difference would be marginal to the conclusions already made.

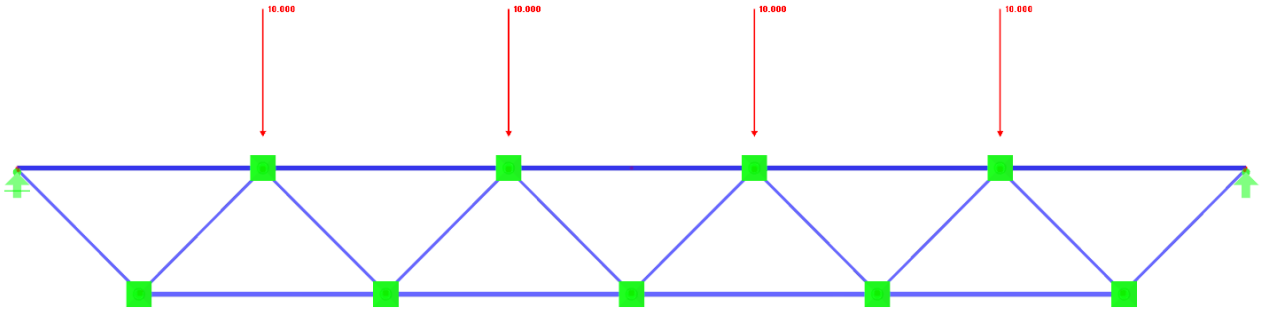


*Figure 102. Beam element model of the truss used in this work.*

From the results up till now, it has been indicated that the difference between centric and eccentric for thick cords is small. It has been argued that this is due to thick chords providing significantly stiff connections and thus a substantial increase in stiffness from the introduction of eccentricity should not be expected. Since accounting for any flexibility requires additional work and calculations, it is of interest to investigate if the connections of thicker chords can be approximated as rigid.

For this investigation beam element models were used. The geometry near the connections was modelled similarly to the one proposed by Boel (Figure 103). The only difference was that the connections between the braces and the rigid elements was taken as rigid. From a preliminary investigation, it was found that modelling the eccentricity by offsetting the node connecting the braces and rigid elements had marginal effects (0.01% difference). As such, the geometry of the centric joint truss was used for this investigation.

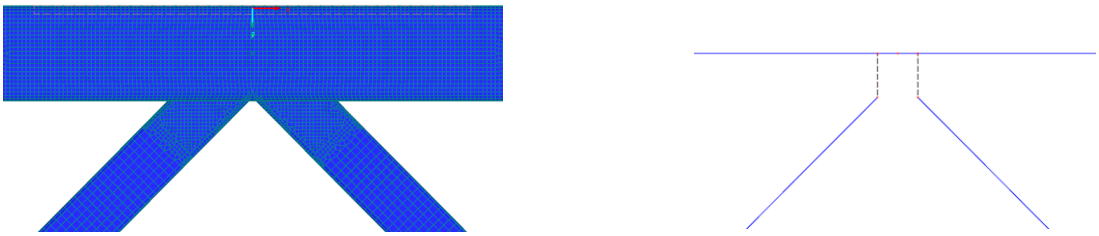

*(a)* *(b)*

*Figure 103. Representation of K-joints using (a) shell elements and (b) beam elements, assuming a rigid connection.*

The results presented are the buckling lengths of the eccentric joint truss, normalized against the beam element model buckling lengths. As the out of plane buckling lengths are quite affected by the connection stiffness they are not presented here as the differences are quite large. The results are given only in table form as many values are close and a graph would be hard to read (Table 35 and Table 36). A colour scale is used to indicate configurations that may be safe to assume rigid connections between the braces and the chords. As a cut-off limit a 2-percentile difference is set. For values above 1.02 assuming rigid connections for the model is considered unsafe.

Table 35. Normalized buckling lengths $K_{ch,in,hybrid}/K_{ch,in,beam}$

| γ \ β | 0.25 | 0.40 | 0.50 | 0.60 | 0.75 |
|---|---|---|---|---|---|
| 15.90 | 1.01 | 1.03 | 1.06 | 1.03 | 1.05 |
| 10.00 | 1.00 | 1.01 | 1.01 | 1.02 | 1.03 |
| 8.00 | 1.00 | 1.00 | 1.01 | 1.02 | 1.02 |
| 7.04 | 1.01 | 1.00 | 1.01 | 1.02 | 1.02 |
| 6.25 | 1.00 | 1.00 | 1.01 | 1.01 | 1.01 |

Colour scale: 1.00 1.02 1.05

Table 36. Normalized buckling lengths $K_{br,in,hybrid}/K_{br,in,beam}$

| γ \ β | 0.25 | 0.40 | 0.50 | 0.60 | 0.75 |
|---|---|---|---|---|---|
| 15.90 | 1.03 | 1.06 | 1.12 | 1.16 | 1.04 |
| 10.00 | 1.01 | 1.03 | 1.05 | 1.05 | 1.03 |
| 8.00 | 1.01 | 1.02 | 1.04 | 1.04 | 1.03 |
| 7.04 | 1.01 | 1.02 | 1.03 | 1.04 | 1.03 |
| 6.25 | 1.00 | 1.01 | 1.02 | 1.03 | 1.03 |

Colour scale: 1.00 1.02 1.05

It can be seen that for the case of the chord buckling in plane for smaller braces and for all from the medium chord it is able to be approximated by a rigid connection. This is due to the fact that the braces do not significantly contribute to the chord's restraint, as they are significantly less stiff than the chords. In the case of the brace buckling in plane the stiffness of the connections alters the buckling lengths substantially. This means that the stiffness of the connections needs to be accounted for, when calculating the buckling lengths of the structures. Otherwise, the buckling length will be severely and unsafely miscalculated.

## 4.6 Conclusions

In this chapter, an investigation into the buckling behaviour of trusses making use of eccentric joints was performed. From the investigations several conclusions can be drawn.

Firstly, the implementation of eccentric joints has a positive effect for in plane buckling, compared to the use of centric joints. This is attributed to the stiffening effect that the chord wall provides, opposed to the chord face in bending mechanism primarily used by the centric joints for the force transfer. Depending on the brace and chord dimensions, the effects can be larger or smaller. In the cases of relatively thin chords ($\gamma>8$) and medium sized braces ($0.3<\beta<0.7$), it may be beneficial to account for eccentricity of the joints and the decreased buckling lengths. Accounting for the increase in stiffness a reduction of the buckling length of at least 5% can be realized.

For the case of the out of plane buckling, a slight increase of the buckling lengths is observed compared to the centric joints. This indicates that the eccentricity affects the buckling behaviour negatively. This is attributed, to the change of stiffness in the connection. For the case of out of plane stiffness, it is a bit harder to describe a conclusive mechanism behind the decrease in stiffness, but sub-model analysis and argumentation indicate that this is the case. This slightly negative effect can be ignored as quantitatively gives a difference of less than 2% in all cases investigated. In general, it is safe to treat the eccentric joints as the centric, regarding the buckling of the members.

The trusses used for the investigation had lateral constraints introduced in their models. These were positioned on the chord side wall, at the mid-height of the cross section. What was additionally concluded was that changing the support position height wise, made a negligible difference. This indicates that when calculating the member buckling lengths, the actual implementation of the support is more important compared to the exact position.

Lastly, by additionally investigating the assumption of rigid connection between the brace and the chords, it was concluded that in all cases the stiffness needs to be accounted for. Especially for the buckling of the braces, the effects of ignoring the connection flexibility are substantial. For this reason, modelling using rigid connections between members is not a safe assumption for performing a buckling investigation.

# 5 FORMULATING ROTATIONAL SPRINGS FOR ECCENTRIC JOINTS

## 5.1 Introduction

In the literature study an approach was presented which was first presented in a paper by Hornung and Saal, and further developed by Boel in his master thesis. In this approach the stiffness and effects of the connections of K-joints are captured by assigning a rotational stiffness. This rotational stiffness is then used to define rotational springs in a beam element model and captures the buckling behaviour of the truss. From the results presented in a previous chapter (chapter centric investigation), it was shown that the proposed approach does indeed capture the behaviour of more detailed models satisfactorily. In this chapter it is attempted to extend this approach to its use for eccentric joints.

Before investigating in more detail the behaviour of eccentric joints, a few questions raised in the literature study will be addressed. Specifically, the use of three load cases as proposed by Boel. Each load case calculates a distinct stiffness value, which gives three different values for the same connection. Boel does not address this and simply performs a comparative study to decide with which one he will continue his investigation. This topic will be addressed before investigating further a spring formulation for eccentric joints

## 5.2 In-plane Rotational stiffness

In his work, Boel (2010) proposed that connections experience three different load cases (Figure 104). Each one provides a different stiffness value for the rotational spring approximating the connection. From his investigations, Boel concluded that the most appropriate stiffness value for in plane buckling was calculated from Load case 1 (LCin1). This in turn could be used as the stiffness value of the springs used in his beam element model. What was not elaborated was why three different Load cases existed and what exactly they represent. By assuming different ratios of moments applied on each brace, infinite different values of stiffness can be calculated between the maximum and the minimum values (Load case 2 and Load case 3 respectively).

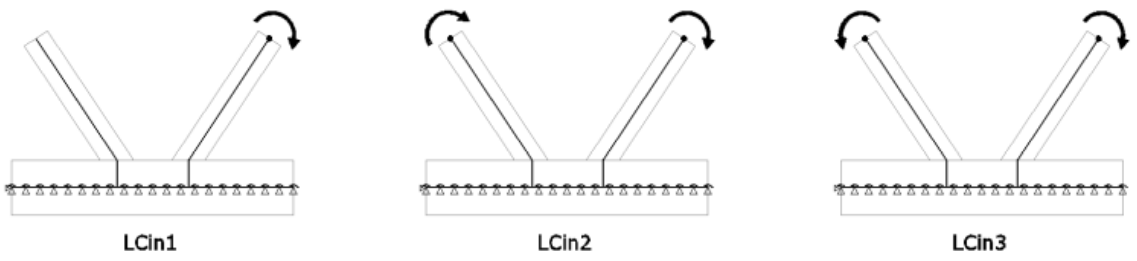


*Figure 104. Three possible load cases that provide three different stiffness estimations, according to Boel (2010)*

To study what these three load cases represent, the buckling loads between a shell element models and beam element models with rotational springs are going to be investigated. To simplify the investigation, the same models used to calculate the in-plane stiffness are going to be used. This means that the contribution of the chord member in restraining the brace is cancelled out by the line supports included on the chord wall (Figure 55). As such, the beam element model that is going to be used for comparison will consist of a cantilevered member supported on a rotational spring (Figure 105). This way, the contribution of only the connections is accounted for and makes the comparison more straightforward. The rotational springs are calculated as presented in Section 3.2.

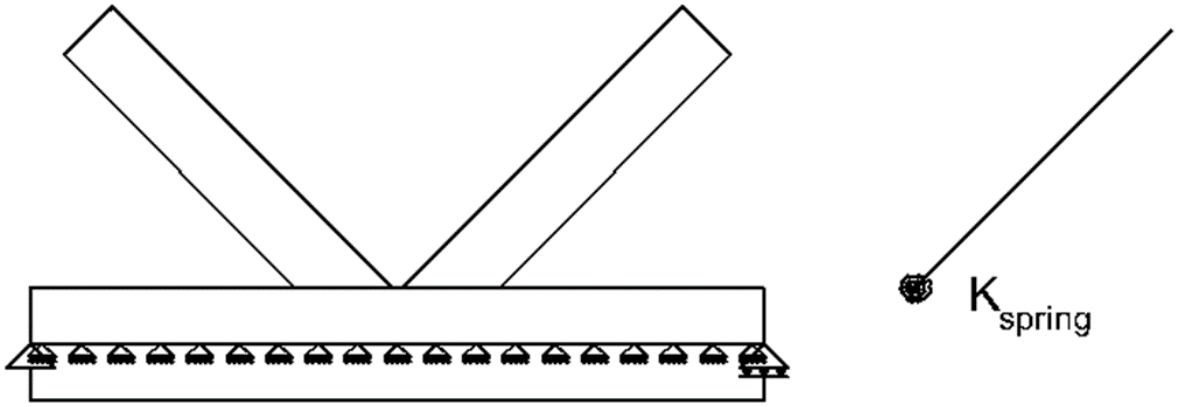


*(a)* *(b)*

*Figure 105. Shell element model (a) and beam element model (b) used in the investigation of the rotational springs for the in-plane direction*

The load cases that are going to be investigated regarding the buckling of the joint sub-models were selected as the actual load analogy to the moment load cases used in the stiffness calculations. Stiffnesses that are logically derived for various buckling cases experienced by a joint were chosen e.g. the lowest stiffness (Load case 3) to be used in the case of both braces are under compression and the highest stiffness (Load case 2) in the case of one brace in compression and the other in tension (Figure 106). The investigation includes the following cases:

a. K-joint with one brace loaded in compression,
b. K-joint with one brace loaded in compression and the second brace loaded in tension by an equal amount,
c. K-joint with both braces loaded in compression and lastly,
d. Y-joint with the brace loaded in compression

For the investigation, the buckling loads of the four different cases were calculated for the shell element models. From the results, the in plane buckling load was used. Then this value was compared to the buckling load of a brace loaded in compression, modelled with beam elements. Its base is supported rotationally by a spring. The rotational stiffness of the springs was calculated using the corresponding load case as described earlier and are presented in Figure 106. For the geometry, no rounding of the corners was considered as it would not affect the conclusions and it would make the investigation easier.

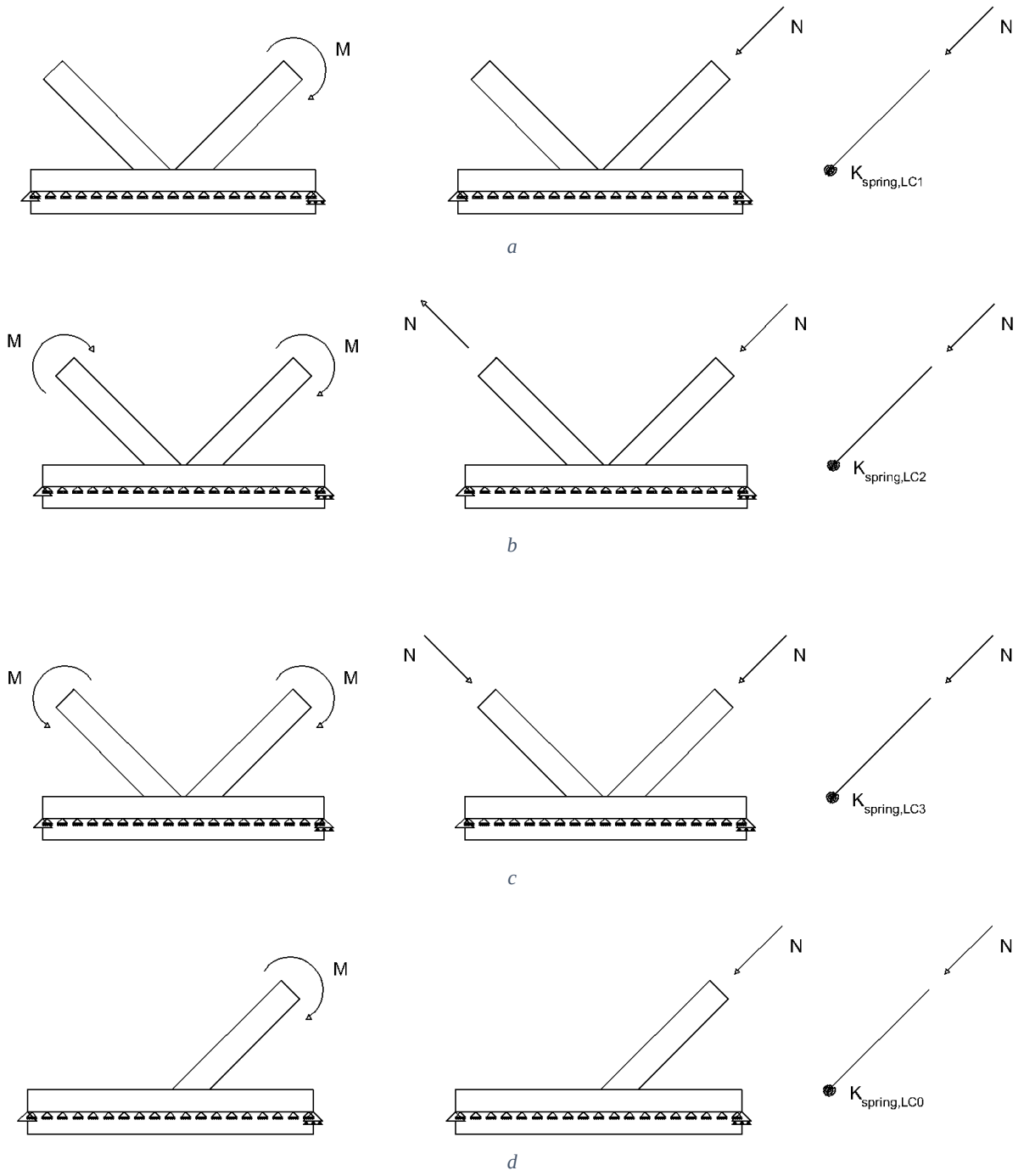


*Figure 106. Equivalent rotational springs that make intuitive sense for the comparison of the four different cases. From left to right; the model used to calculate the rotational stiffness, model used to calculate the buckling load of the shell element model and the model used to calculate the buckling load of the beam element model. Each sub-figure corresponds to the equivalent case, meaning that (a), (b), (c) and (d) correspond to the cases a, b, c and d.*

From a preliminary investigation, it was concluded that the stiffness calculated by Load case 2 significantly overestimated the predicted buckling load of the beam element model compared to the shell element model. From additional results, it was concluded that the stiffness of the connection for case b is better capture by Load case 1, which is also used for case a (Figure 107). For this reason, all the following results and comparisons for case b. are done by using the stiffness calculated by Load case 1.

To ensure the validity of the conclusions, six different configurations were considered. For the chords two different chords were used. For the first chord (SHS 50/2.6) one brace width ratio (β=0.60) but three different

thicknesses (2.6,4 and 5 mm). For the second chord (SHS 120/5) three different brace width ratios were used (β=0.33,0.66 and 0.83), with only one thickness being considered per profile. The complete set of configurations used are presented in Table 37.

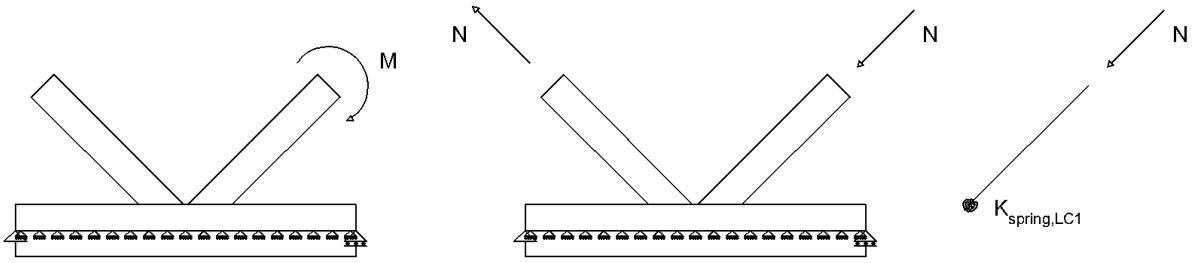


*Figure 107. Models used for the comparisons of case b, guided from preliminary results*

Table 37. Different configurations used in the investigation of the three load cases

| Configuration number | Chord | Brace |
|---|---|---|
| **1** | SHS 50/2.6 | SHS 40/2.6 |
| **2** | SHS 50/2.6 | SHS 40/4 |
| **3** | SHS 50/2.6 | SHS 40/5 |
| **4** | SHS 120/5 | SHS 40/2.6 |
| **5** | SHS 120/5 | SHS 80/6.3 |
| **6** | SHS 120/5 | SHS 100/10 |

In presenting the results, the beam element buckling loads are normalized against the buckling loads of the shell element models. From the results (Figure 108) it becomes evident that for cases a, c and d, the load cases assumed for the rotational stiffness calculation capture the behaviour well. The differences between the shell element model and beam element model's buckling loads are marginal. For the case b, there is an observed and consistent difference. Specifically, the use of Load case 1 appears to underestimate slightly the stiffness that the shell element model experiences whilst buckling.

These results can be explained by the effect the opposite brace has on the brace under compression. In case c, both braces are under compression. As both braces are under compression, they buckle simultaneously and provide a negative effect to the other's buckling behaviour. This translates in a decrease in stiffness and is why the minimum stiffness can be used for the calculation (Load case 3). The same can be said for case b. The tension load has a beneficial effect and helps the brace under compression to resist buckling. This translates to an increase of the rotational stiffness experienced by the compressed brace. It would be expected for the results for case b to be close to the stiffness of Load case 2 (maximum), just like the results of case c are close to the stiffness of Load case 3 (minimum). This does not happen, as the stiffening effect of tension is much smaller than the effect compression has on the loss of stability. As such, case b tends to Load case 2, but the effect is minor. Lastly, for case a, the second brace has no effect on the buckling of the compressed brace, and as such Load case 1 can be used; similarly for case d.

When investigating the buckling of the trusses in Chapter 3, most of the joints were under the load case described by case b. From the braces connected to the joint, one would be under compression and the other under tension. As was shown in this investigation, the stiffness of these joint can be approximated well by Load case 1. Boel also concluded that Load case 1 should be used for his approach and used this in his analysis. These results further support the use of Load case 1 for the stiffness calculation of K-joint trusses and explains why the results obtained by Boel and his beam element model matched well with the results of the hybrid model used in this work.

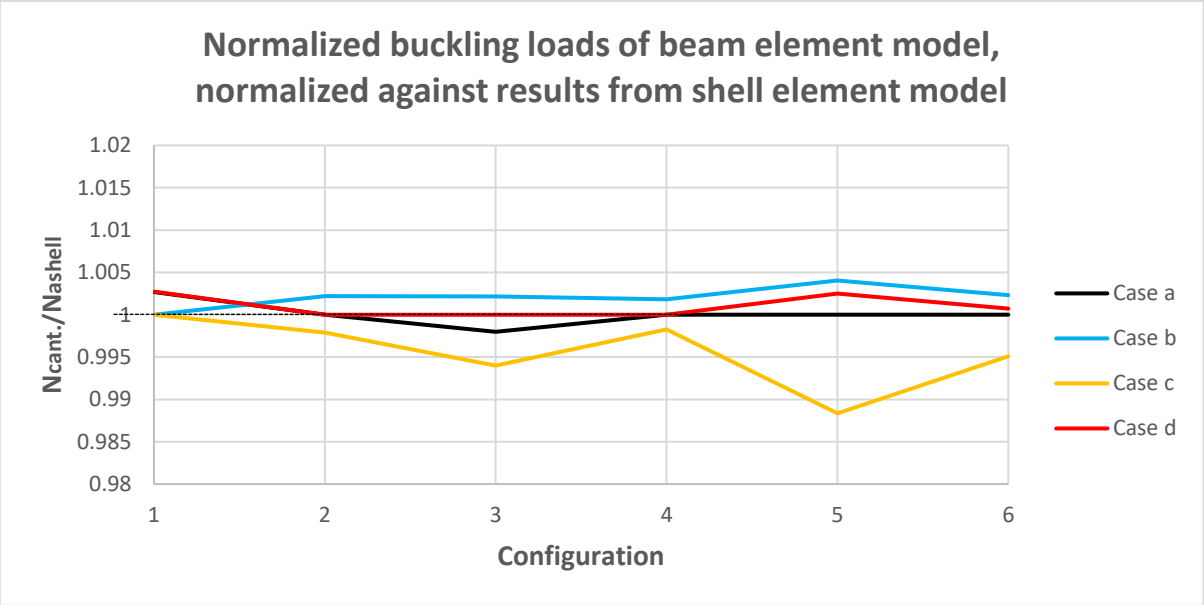


*Figure 108. Comparison of results of shell element models and beam element models, for the in-plane direction.*

## 5.3 Out of plane rotational stiffness

As with the in-plane stiffness calculations, Boel also defines three Load cases for the out of plane stiffness (see Section 3.2). The investigation in this section will be performed similarly to the one performed for the in-plane stiffness. The main change will be in the formulation of the beam element models. For the stiffness calculation of the out of plane spring, the shell element model used is not supported by a line support in the middle of the chord wall. As such, the shell element model behaviour includes the effects of the chord member. These effects will be included in the beam element model, by using the whole joint sub-models (Figure 109) not only the braces, as was done for the in-plane stiffness. Due to this, how the shell element joints are approximated by a beam element model is important.


*Figure 109. Shell element model (a) and beam element model (b) used in the investigation of the rotational springs for the out of plane direction*

In his thesis, Boel checked many different variants for this approximation (Figure 110). From his investigation he concluded that Variant 1 was the most suitable to capture the behaviour of the shell element model. The other variant that presented some promise was 3c. From some preliminary investigation perforemd, it was also concluded that Variant 1 provides the better approximation. Additionally, by considering a joint that has a small angle and/or large gap, it can be argued that the position where the forces are introduced to the chord make little sense. As such, for this investigation the same formulation as Boel's Variant 1 is used.

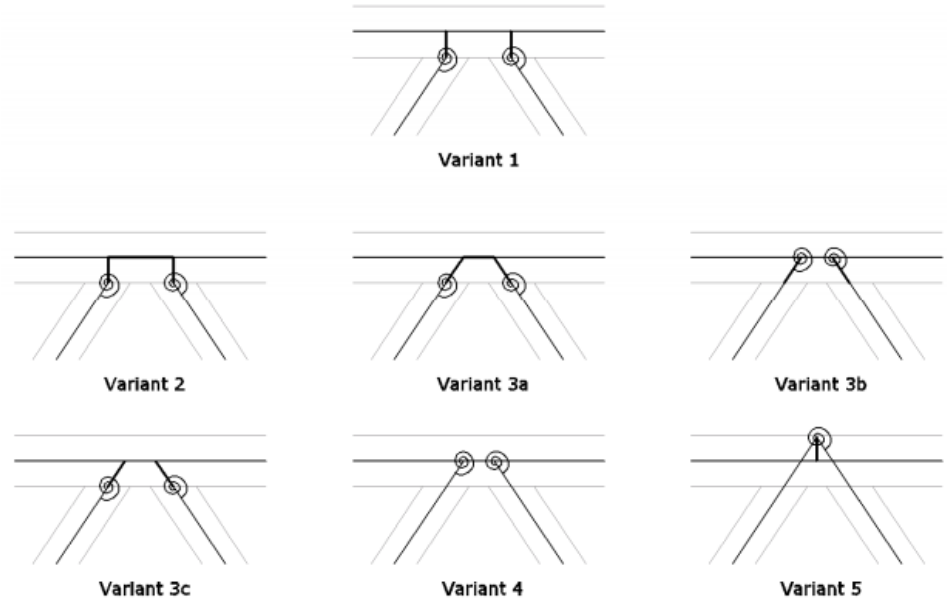


*Figure 110. Different variants tested by Boel (2010) for connection modelling using 1D elements and springs*

As with the in-plane investigation, cases a, b, c and d are going to be used. Case a is going to be compared to the beam element model with a spring stiffness calculated from Load case 1, whilst case d with Load case 0. In the case of out of plane stiffness Load cases, using Load case 2 gives the minimum stiffness whilst Load case 3 the maximum. As such, case c is going to be compared with Load case 2. From preliminary investigations, on the out of plane case b, the stiffness calculation does not appear to have a straightforward comparison. For this reason, it is compared with Load case 1, Load case 3 (maximum) and the average of the three Load cases. The last approximation was checked and adopted by Boel in his work. An overview of the corresponding cases and load cases that were used in the out of plane investigation are presented in Figure 111 for cases a, c, and d and Figure 113 for case b. Since similar results to the previous investigation are expected, only four configurations (chord and brace combinations) are going to be used. These are taken from Table 37 and are going to be configurations 1, 4, 5 and 6.

As with the in-plane results, the beam element buckling loads are normalized against the buckling loads of the shell element models. Two different figures are presented. The first one (Figure 112) includes the results for cases a, c and d. In these cases, the differences between the shell element model and beam element models' buckling loads are small. For all configurations tested, the error of approximation is below 2%. This indicates that the conclusions formed from the in-plane investigation, hold for the out of plane stiffness formulation as well. The slightly larger differences compared to the results obtained from the in-plane investigation can be attributed to the modelling of the whole joint and not just the brace, as was the case in the previous investigation.

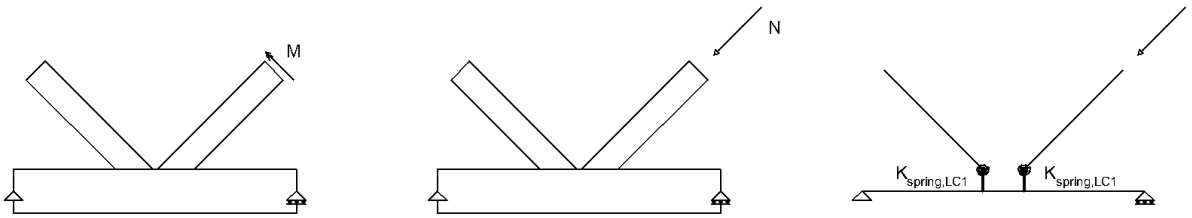


*(a)*

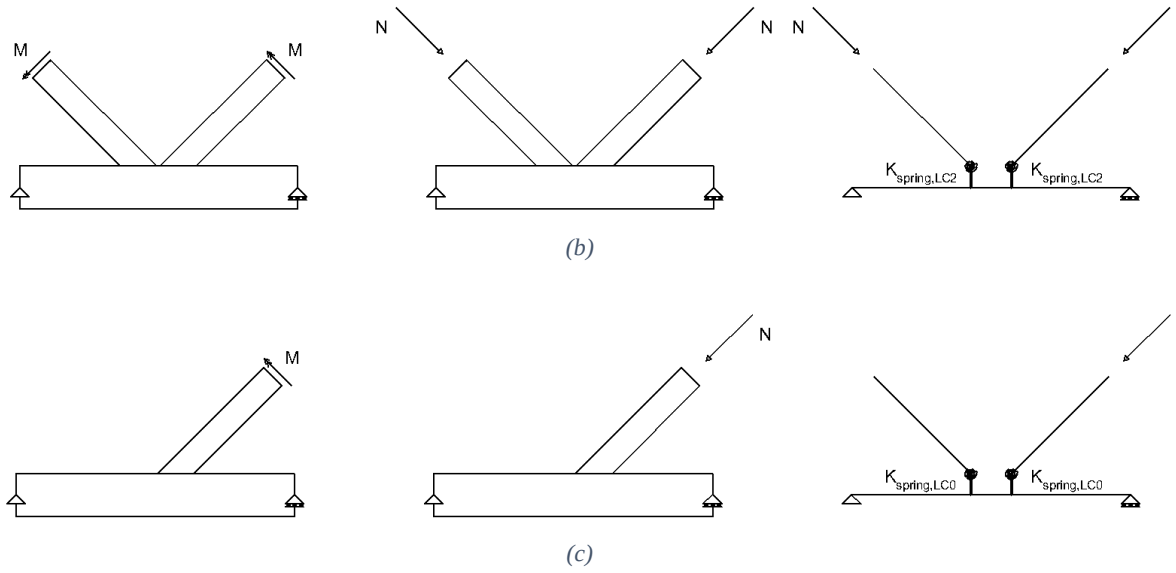


*Figure 111. Shell element models (left) used to calculate the equivalent rotational spring for the beam element models (right). The beam element models are compared to the different cases defined with figures (a), (b), and (c) corresponding to cases a, c and d respectively.*

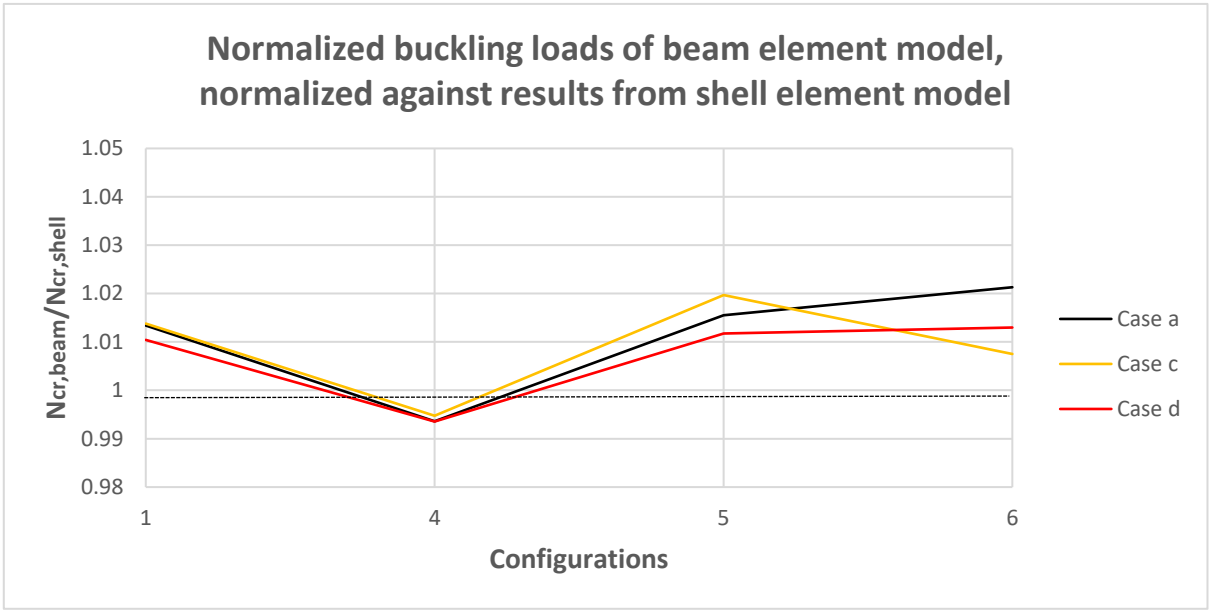


*Figure 112. Comparison of results of shell element models and beam element models, for out of plane direction in cases a,b and d.*

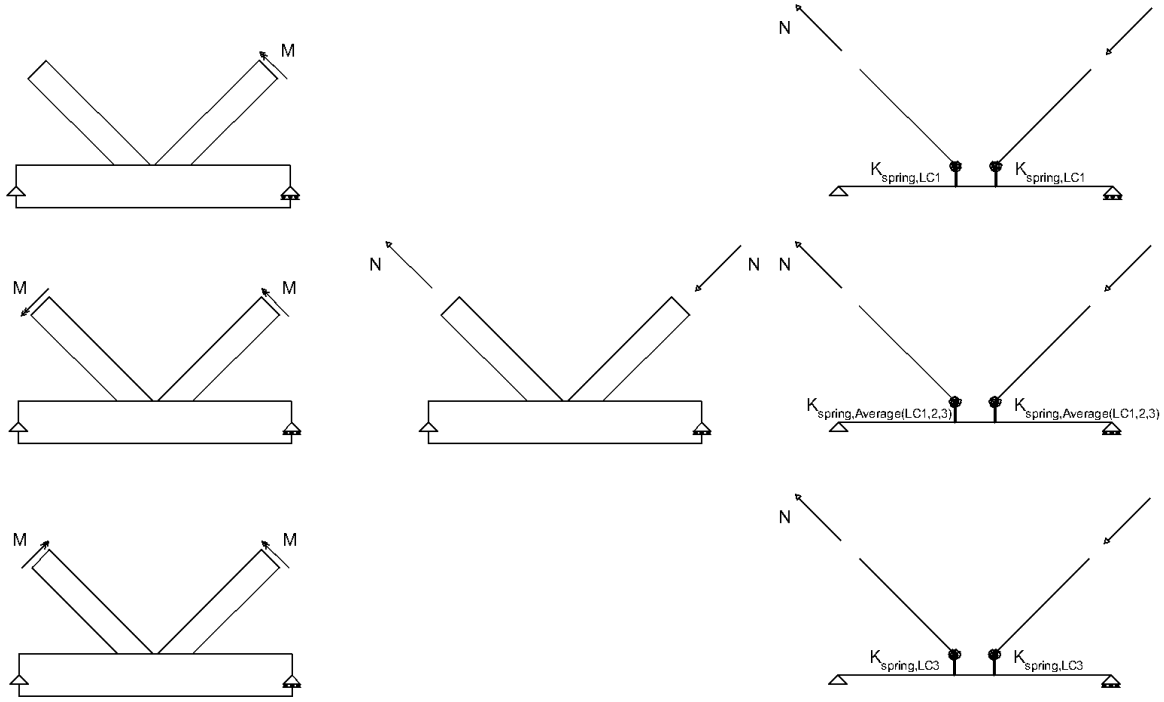


*Figure 113. Different assumptions for the calculation of the equivalent rotational spring for case b.*

The second graph presented (Figure 114) includes the results obtained for the case b, in which one of the braces is loaded in compression and the other in tension. As was mentioned, three different comparisons are made. As is expected, when using Load case 1 to calculate the stiffness, the beam element model underestimates the stiffness experienced by the shell element model. Compared to the in-plane results, though, the difference is much larger. By using Load case 3, it can be observed that the beam element model overestimates the stiffness. Lastly, by taking the average of the three Load cases, the beam element model overestimates the stiffness again but not as much as for Load case 3. As expected, the stiffness for case b lies between Load case 1 and Load case 3, but the effect of the tension load is much larger compared to the in-plane direction.

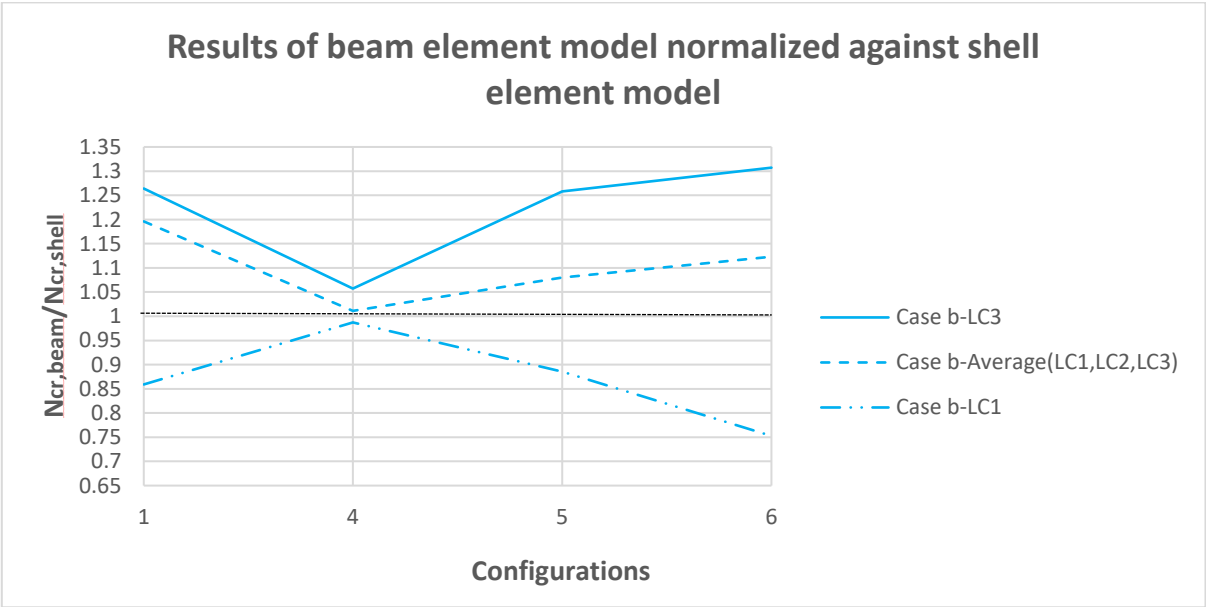


*Figure 114. Comparison of results of shell element models and beam element models, for the out of plane direction in case b.*

To conclude, the initial intuition and analogy presented in Figure 111 appears to hold true for the cases a, c, and d. In case b, the intuition holds regarding the fact that the stiffness of the connection, in the presence of a

tension force tends to the Load case that gives the maximum stiffness. In the case of in plane buckling the effects are small and the stiffness can be approximated by Load case 1. For the out of plane buckling, the effects of the tension force are much larger and there is no clear approximation that produces close results. In his work, Boel used the average of the three Load cases as an approximation. However, this has been demonstrated to not provide representative results. Even though this is the case, from the investigation into the buckling lengths of trusses with centric joints, small differences existed between the hybrid models used and Boel's results. This would indicate that taking the average of the three Load cases for the calculation of the out of plane stiffness may be adequate. This, though, could potentially be only for the specific cases investigated. For other cases, the difference may be larger and taking the average may produce larger than acceptable differences. For this reason, the use of Load case 1 would be recommended for the use on trusses.

## 5.4 Formulation of eccentric springs

It was shown from the investigation into the buckling behaviour of trusses with eccentric joints that the effects of the eccentricity may be ignored. On the other hand, it was demonstrated that accounting for the connection stiffness can be beneficial for the case of in plane buckling. In order to facilitate better design, an investigation is performed, in order to extend the approach described by Boel for eccentric joints. Additionally, it would provide insight in dealing with other kinds of eccentric connections, not only the ones for which the braces are welded on the chord face.

### 5.4.1 Challenges

The main issue to be dealt with is the calculation of the stiffness. Unlike the calculation of the centric joints, the eccentric joints' behaviour is much more complicated. Owing to the complicated geometry and interface conditions between the brace and the chord, the eccentric joints appear to have a coupling of their in-plane and out of plane displacement (Figure 115). This is not the case for the centric joints as solely in plane loading gives rise to only in plane displacements, and similarly for the out of plane degrees of freedom. These differences in joint behaviour were also observed in the buckling behaviour of the trusses utilising the corresponding joint. This means that a simple spring, with stiffnesses defined in the same axis as the centric joints, may not adequately describe the behaviour of the joints.

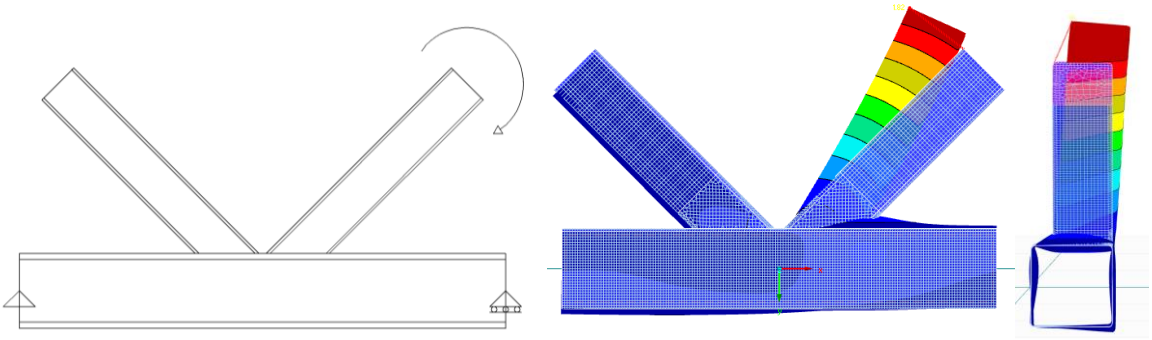

*Figure 115. In-plane and out of plane displacements of a simply supported K-joint under in-plane moment load at one of its brace's end.*

### 5.4.2 Different approaches

Due to the coupling of in and out of plane displacements, the approach used up till now to calculate the stiffness may need modifications. For this reason, three different approaches are proposed, to calculate the stiffness of the eccentric joints.

#### *5.4.2.1 Approach 1*

The first approach proposed, is to use only the displacements developed in the corresponding plane of the applied moment. In the case of the in-plane stiffness, an in-plane moment is to be introduced and only the in-plane displacements will be considered. With this approach, the in-plane displacements attributable to the connection are going to be calculated and used to calculate the stiffness. Any out of plane displacements are ignored and not accounted for.

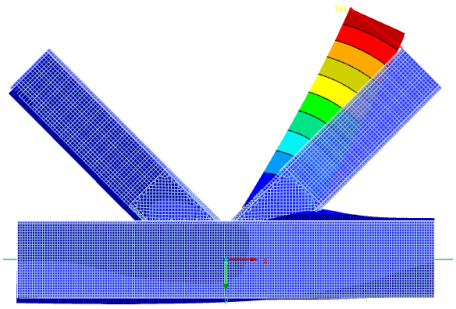

*Figure 116. Calculating the in-plane stiffness by taking only the in-plane deformations and disregarding the out of plane deformations.*

### 5.4.2.2 Approach 2

With the second approach, the introduction of a counter moment is proposed. This counter moment would be applied in the direction not under investigation. The aim of this moment would be to set the coupled displacements to zero (Figure 117). This would mean that for the in-plane stiffness, an out of plane moment would be introduced, in order for the out of plane displacements to be set to zero. Then, similarly to the first approach, the rotation of the spring can be calculated, by calculating the displacements attributable to the connection.

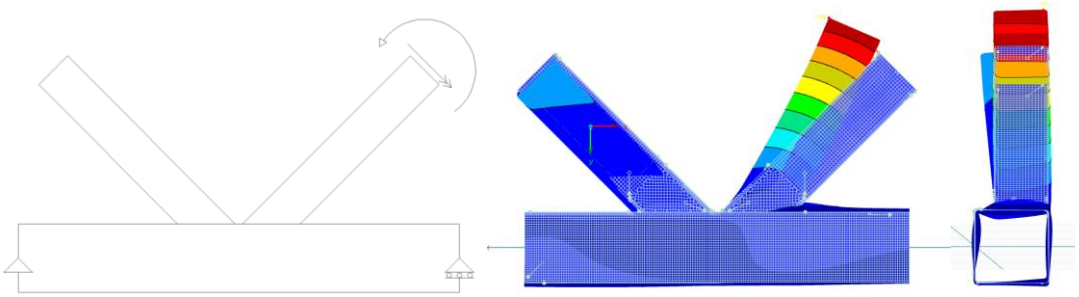

*Figure 117. Setting the out of plane displacements by introducing a counter moment, for the in-plane stiffness calculation.*

### 5.4.2.3 Approach 3

In approach 3, it is proposed that the rotational spring is defined in rotated axis (Figure 118). In these rotated axes, it is assumed that no coupled displacements occur. By assuming rotated axes, the coupling of displacements can be attributed to the expression of the spring stiffness in the original axes. Due to the rotated axes, the spring would have components in both the degrees of freedom defined as in-plane and out of plane. This can be demonstrated by using an arbitrary direction and defining a diagonal stiffness matrix on it that would give no coupling (Figure 118 (b)). If the axes are X' and Y', the assumed stiffness matrix would be given by Equation 16.. If the assumed axes are at angle θ to the global axes X and Y, then a rotation matrix can be defined as per Equation 17.. This rotation matrix can be used to transform the stiffness matrix of Equation 16. to the global axes, by pre-multiplying with the transpose of the rotation matrix and post-multiplying with the rotational matrix (Equation 18.). It is obvious that the result of such manipulations is a non-diagonal stiffness matrix that would be able to account for the coupling of the in plane and out of plane direction.

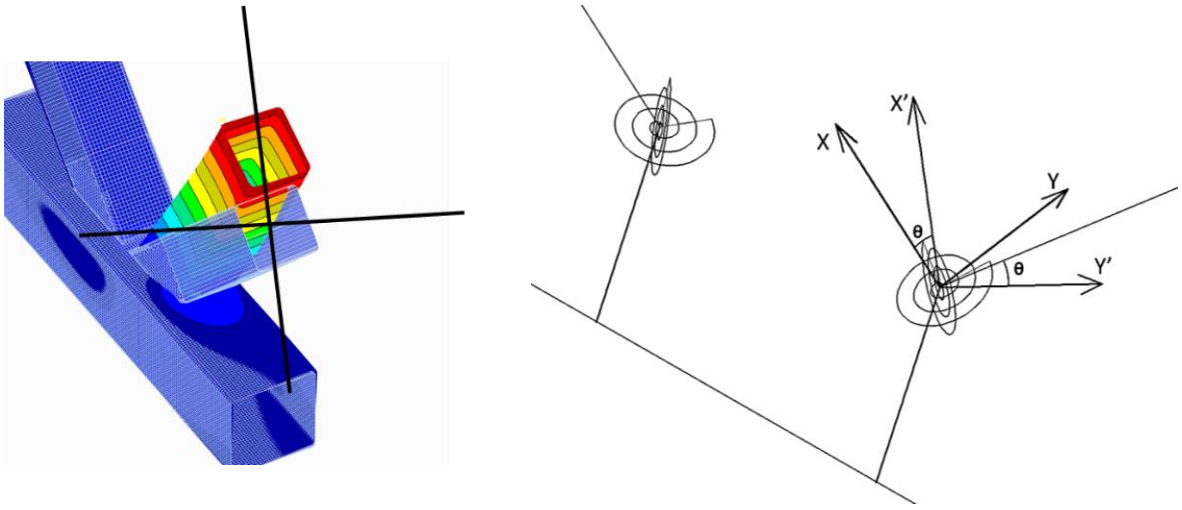


*(a)* *(b)*

*Figure 118. Definition of rotated system of the equivalent rotational springs (b) to capture the coupled behaviour of the eccentric joints (a).*

$$K^{X'Y'} = \begin{bmatrix} K_{X'X'} & 0 \\ 0 & K_{Y'Y'} \end{bmatrix} \quad 16.$$

$$R_\theta = \begin{bmatrix} cos\theta & sin\theta \\ -sin\theta & cos\theta \end{bmatrix} \quad 17.$$

$$K^{XY} = R_\theta^T K^{X'Y'} R_\theta \Rightarrow K^{XY} = \begin{bmatrix} cos\theta & -sin\theta \\ sin\theta & cos\theta \end{bmatrix} \begin{bmatrix} K_{X'X'} & 0 \\ 0 & K_{Y'Y'} \end{bmatrix} \begin{bmatrix} cos\theta & sin\theta \\ -sin\theta & cos\theta \end{bmatrix} \quad 18.$$

### 5.4.3 Investigation

As with the investigation performed for the centric joints, simplified K-joints are going to be used for the calculation of the stiffness and the buckling. By calculating specific rotational spring stiffnesses, they will be replaced in a beam element model and a buckling analysis will be performed. The results of the equivalent beam element model will be compared to the shell element model. The geometry of the beam element model will follow Boel's guidelines, as was presented in the out of plane stiffness investigation in section 5.3. Additionally, an eccentricity will be introduced for the intersection point of the braces with the rigid elements. This point will be at the intersection point of the brace's midline and the chord face (Figure 119).

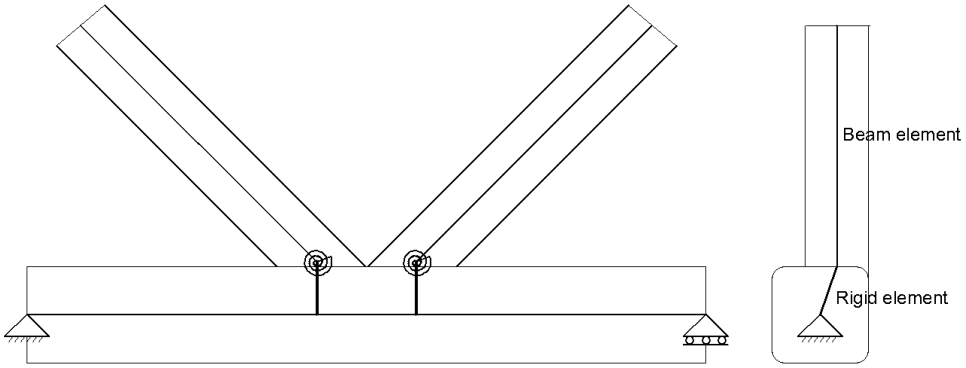


*Figure 119. Eccentricity of interception point of brace's beam elements with the rigid elements connecting to the chord.*

A slight change in the model used will also be introduced. This will be done for the case of the in-plane displacements. As opposed to the models used in all previous sections, in this investigation the chord will not be supported. As out of plane displacements are expected to arise for in-plane loading, it is unknown how these will interact with the whole joint behaviour. For this reason, line supports will not be introduced on the chord

wall (Figure 120). This helps with not over constraining the model and gives the most accurate results. From this assumption, it follows that the chord displacements due to bending need to be subtracted from the total displacements to calculate the displacements due to the connection. This is done by using Equation 19., with the definitions used in Section 3.2. This is then additionally subtracted from Equation 8. to give Equation 20., which is used in this investigation.

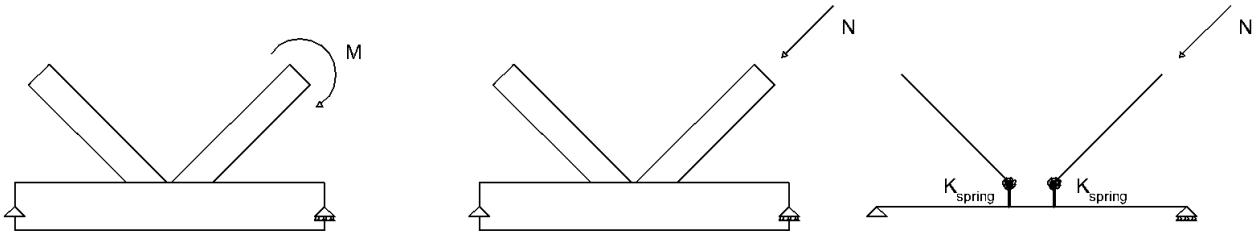


*Figure 120. Configuration used for the in-plane investigation of the equivalent spring for eccentric joints.*

$$w_{chord,bending} = \frac{M\left(3g^2 + L_{ch}^2\right)}{12EI_{ch}L_{ch}} cos(\alpha)\, L_{br} \quad 19.$$

$$w_{connection} = w_{K-joint,FEM} - w_{brace,FEM} - w_{chord,bending} \quad 20.$$

In the case of approach 3, rotated axes are defined at an angle θ from the original in plane and out of plane direction. These will be named principal axes and have no coupling of displacements, meaning the rotational stiffness matrix defined is diagonal. From these, a transformation matrix is defined (Equation 17.). The longitudinal axis (brace's midline) remains the same for both coordinate systems. Totating the system to the original coordinates (Equation 18.) the stiffness in the original coordinates is defined. The stiffness is given as a function of the two stiffnesses in the principal axes and the angle they are rotated by θ (Equation 18.). As the matrix is assumed symmetric, by calculating three quantities from the FE models the three unknowns can be calculated: two stiffnesses in the principal axes and the angle it is rotated by θ. To make the investigation easier, as in-plane and out of plane moments are going to be applied in each case and the degrees of freedom of the equivalent rotational springs will be both free, the compliance matrix will be used. By calculating each column of the compliance matrix by applying the load in each degree of freedom, the stiffness matrix can be found by calculating the inverse of the compliance matrix (Equation 21.).

$$K^{XY} = (C^{XY})^{-1} \quad 21.$$

### 5.4.4 Results

The results of the investigation are going to be presented by normalizing the beam element results against the shell element results. This will give an indication of how well the different approaches approximate the rotational stiffness of the shell element model.

### 5.4.4.1 Approach 1

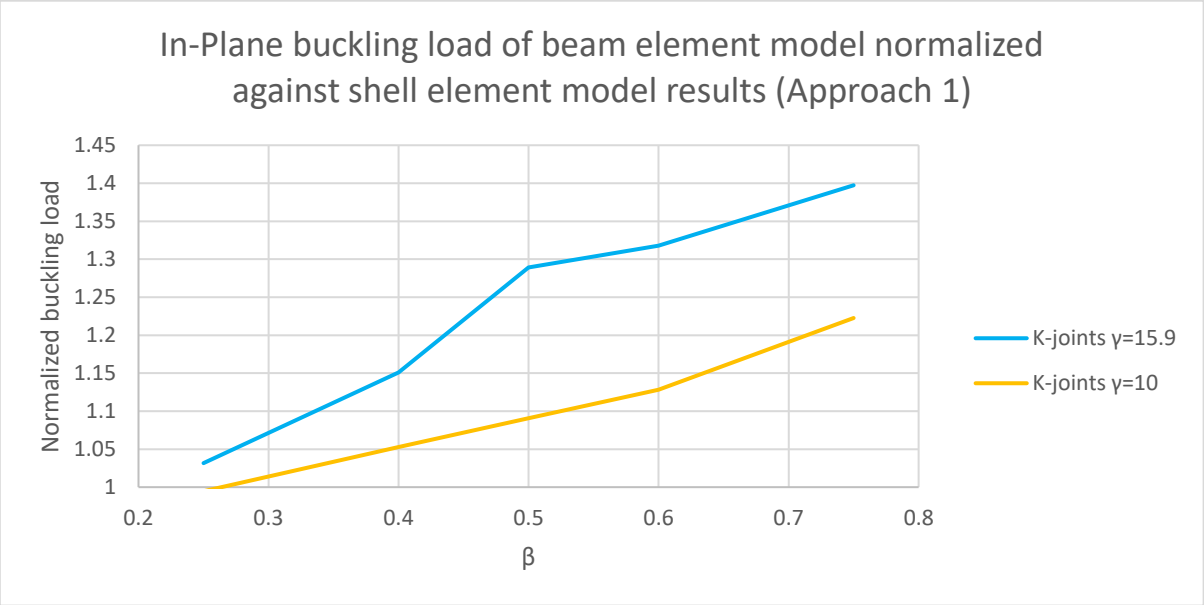


*Figure 121. Normalized results for the in-plane buckling of the beam element model, using Approach 1 for the stiffness calculation.*

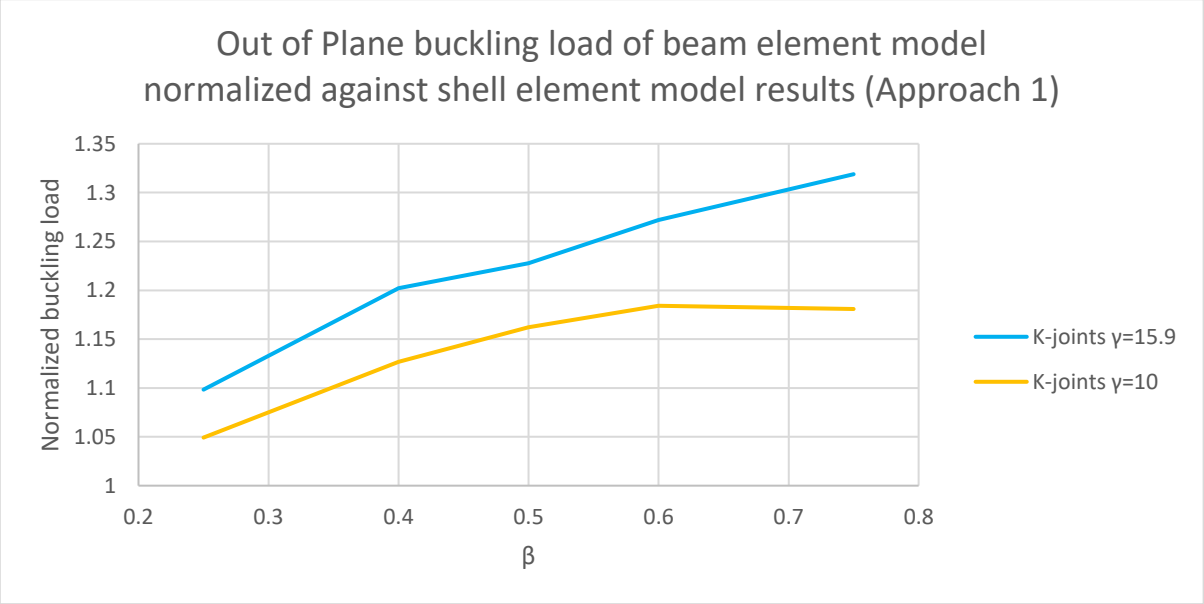


*Figure 122. Normalized results for the out of plane buckling of the beam element model, using Approach 1 for the stiffness calculation.*

The results obtained by the stiffness formulation according to approach 1 indicate that Approach 1 does not approximate the stiffness very well. The results appear to diverge from the shell element model. They also appear to diverge for larger values of β. This is linked to the fact that for larger braces, larger coupled displacements are observed. Additionally, no coupling was observed in the results of the beam element model, which was expected. The results appear to mean that the approach 1 overestimates the stiffness of the connection. Since the issue was one of overestimating stiffness, it could indicate that the displacements used for the stiffness calculated were underestimated. The total displacements were also taken and used as equivalent "in-plane" displacements (Equation 22.) but this approach did not give any substantial differences compared to the original assumptions.

$$u_{"in-plane"} = \sqrt{u_{in-plane}^2 + u_{out\ of\ plane}^2} \qquad 22.$$

### 5.4.4.2 Approach 2

Results from approach 2 appear to be worse. Due to the coupling, by implementing the counter moment, the displacements in the direction analysed decrease. Due to the calculations, this produces a stiffer rotational spring. Since the results from Approach 1 overestimate the connection stiffness, the results from Approach 2 are even further away. Again, no coupling of displacements was observed for the beam element model.

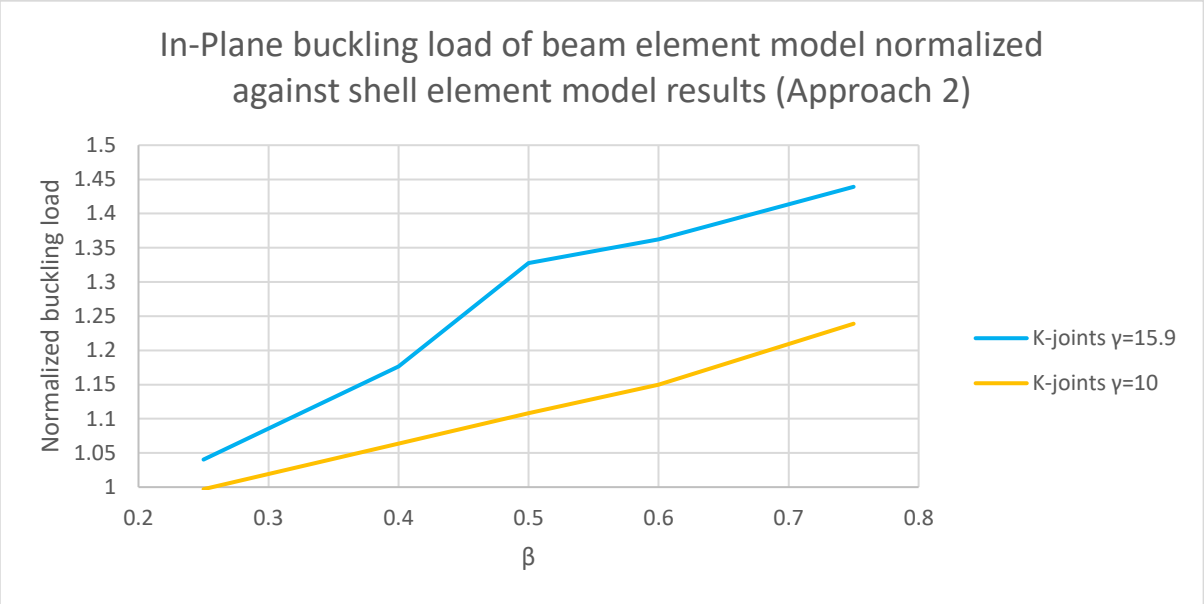


*Figure 123. Normalized results for the in-plane buckling of the beam element model, using Approach 2 for the stiffness calculation.*

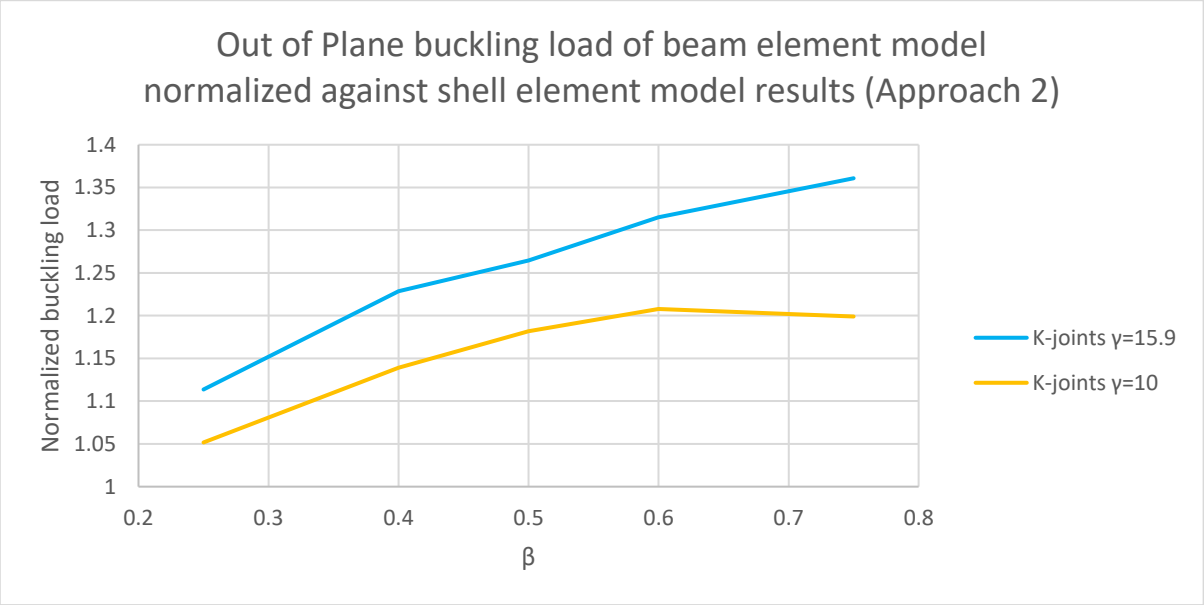


*Figure 124. Normalized results for the out of plane buckling of the beam element model, using Approach 2 for the stiffness calculation.*

### 5.4.4.3 Approach 3

As was mentioned in section 5.4.3, the stiffness matrix of the connection is assumed to be symmetric. From the results obtained a peculiarity emerged. The spring's stiffness matrix behaves in a non-symmetric manner. The in-plane rotations attributable to out of plane moments are not equal to the out of plane rotations attributable to in plane moments. This means that the stiffness matrix arising from an eccentric joint has to be non-symmetric. To understand better how an eccentric joint may have a non-symmetric stiffness matrix, the

example of a T-joint is recruited. From this it becomes more evident how a non-symmetric stiffness matrix is needed to account for the complex behaviour of an eccentric joint.

For the example, an eccentric T-joint simply supported is assumed. It is loaded firstly by an in-plane moment at the end of its brace and then from an out of plane moment. Assuming that the degrees of freedoms of the equivalent spring at the base of the brace are 1 and 2 for in-plane and out of plane respectively, the compliance matrix of the connection is defined by Equations 23. and 24.. In Figure 125 the behaviour of the eccentric T-joint under in-plane moment is demonstrated. Using Equation 24. it follows that the compliance matrix takes the form of Equation 25., with the first column being populated by the respective values of deformation in the in and out of plane direction, and the second column yet to be determined. In Figure 126 the behaviour of the eccentric T-joint under out of plane moment is demonstrated. By populating the second column of Equation 25., Equation 26. is created and the complete compliance matrix is formed

$$C^{12} = \begin{bmatrix} c_{11} & c_{12} \\ c_{21} & c_{22} \end{bmatrix} \quad 23.$$

$$\begin{bmatrix} \varphi_1 \\ \varphi_2 \end{bmatrix} = \begin{bmatrix} c_{11} & c_{12} \\ c_{21} & c_{22} \end{bmatrix} \begin{bmatrix} M_1 \\ M_2 \end{bmatrix} \quad 24.$$

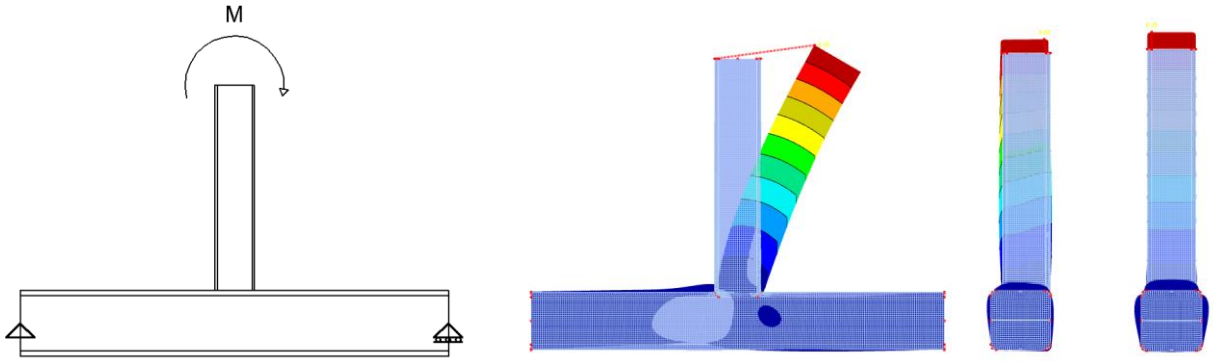


(a) (b) (c) (d)

*Figure 125. Simply supported eccentric T-joint under in-plane moment (a). Except for the expected in-plane deformations (b), additional out of plane deformations are observed (c), compared to the equivalent centric joint (d).*

$$C^{12} = \begin{bmatrix} c_{11} & ? \\ c_{21} & ? \end{bmatrix} \quad 25.$$

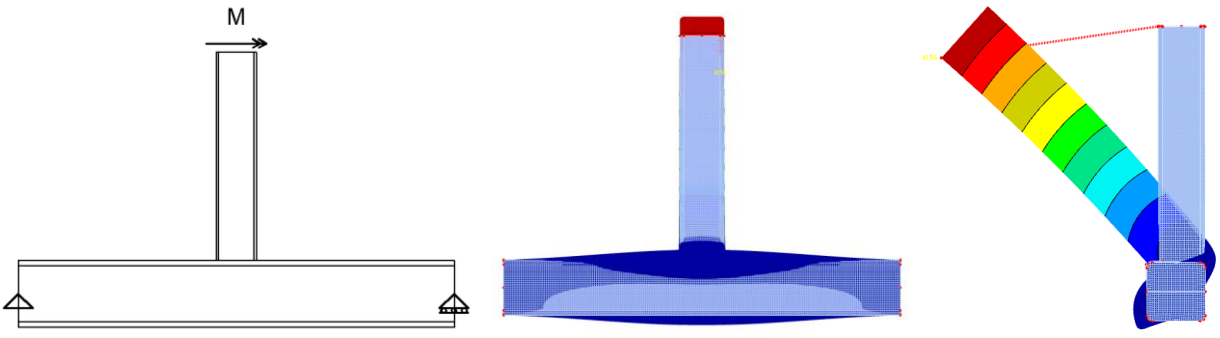


(a) (b) (c)

*Figure 126. Simply supported eccentric T-joint under out of plane moment (a). Due to the symmetry conditions no in-plane deformations (b) accompany the out of plane deformations (c).*

$$C^{12} = \begin{bmatrix} c_{11} & 0 \\ c_{21} & c_{22} \end{bmatrix} \quad 26.$$

From the produced compliance matrix, it becomes evident that from eccentric joints, non-symmetries may arise. Of course, this does not mean that the shell element model has a non-symmetric stiffness matrix. It merely means that the symmetric matrix which the shell element degrees of freedom generate cannot be simplified down to a formulation of 2 degrees of freedom with a symmetric matrix. In general, it would be theoretically possible to formulate a non-symmetric stiffness element, but from a practical standpoint it has little value. Due to this, the formulation of such an element is not investigated further.

To be able to define the rotated axis, a simplification is assumed in order to investigate if Approach 3 is able to produce results close to the shell element results. This is done by taking the average of the formulated compliance matrix and its transpose (Equation 27.). By making this assumption it is possible to define a symmetric matrix and define principal axes for the equivalent rotational spring.

$$C^{XY} = 0.5[(C^{XY})^T + C^{XY}] \qquad 27.$$

By using Equation 27., Equation 21. can be used to calculate the stiffness matrix of the equivalent rotational spring. From there, by using Equation 18. the stiffness of the rotational spring in the principal axes can be calculated, as well as the angle of rotation from the original axes. Having this information, the rotational springs can be introduced in the beam element models and compare the results with shell element models. From the analysis it becomes evident that the springs in rotated axis provide a better approximation for the equivalent rotational springs, at least qualitatively. From the eigenmodes, it can be seen that coupled buckling does indeed occur and it closely matches the results from the shell element model (Figure 127).

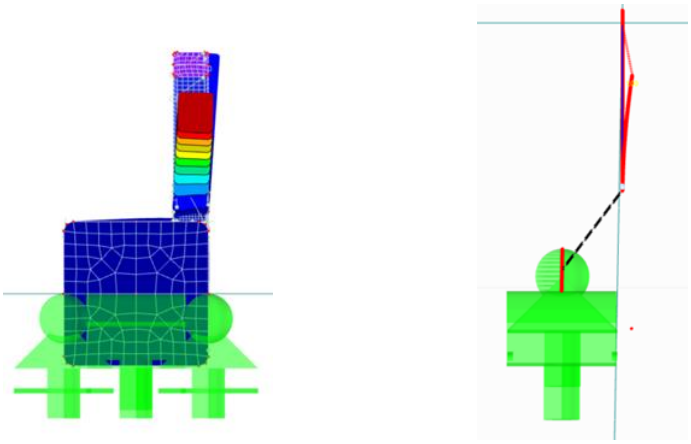

*(a)* *(b)*

*Figure 127. Buckling mode of eccentric joint using (a) shell elements and (b) beam elements with rotational springs formulated according to Approach 3.*

Quantitatively, though, the results are not better than the other proposed approaches and do not match the shell element model. The results are plotted and compared with the ones obtained from Approach 1, as it gave the better results between the first two approaches (Figure 128,Figure 129). It can be observed that for the in plane buckling it provides worst outcomes compared to Approach 1, whilst for the out of plane it provides a better approximation. In any case, the results are quite off from expressing or approximating the results obtained from the shell element model. Due to the initial negative results and the complex behaviour encountered from the eccentric joints, no other simplified formulation was investigated.

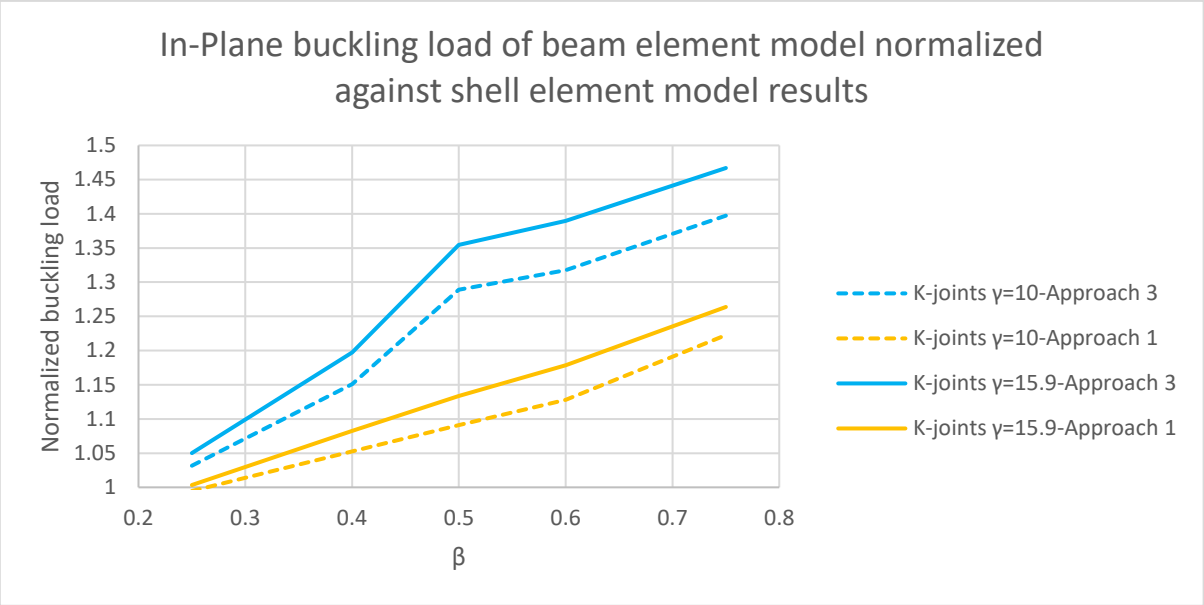


*Figure 128. Normalized results for the in-plane buckling of the beam element model, using Approach 3 and Approach 1 for the stiffness calculation.*

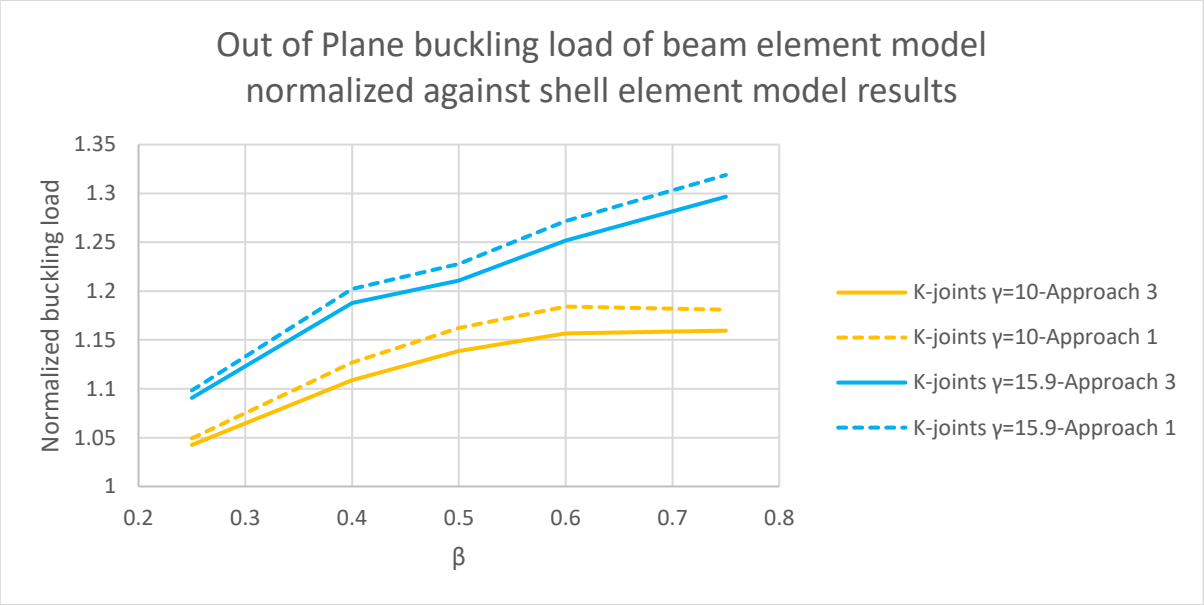


*Figure 129 Normalized results for the out of plane buckling of the beam element model, using Approach 3 and Approach 1 for the stiffness calculation.*

## 5.5 Conclusions

In this chapter, an investigation into the rotational stiffness of centric connections was performed. The stiffness calculation was related to the buckling load of members connected to K-joints and how the stiffness is affected depending on the loading conditions of the connected members. Additionally, an attempt to extend the calculation method to eccentric joints was done. From this, a better understanding of the rotational stiffness of connections on K-joints, as it relates to the buckling of members was gained. Additionally, insight to the general behaviour of the eccentric joints, as well as the details involved in calculating their stiffness was gathered.

From the investigations several conclusions were drawn. In the case of in-plane stiffness, it was concluded that using Load case 1 for its calculation gives the most accurate results. This is related to calculating the buckling loads of a truss that uses centric K-joints. As in trusses, one of the members connected to the K-joint

is expected to be under tension, and tension loading affect the stiffness only slightly, calculating the stiffness by using Load case 1 provides a good approximation. This is also the conclusion that was reached by Boel (Boel, 2010).

In the case of out of plane buckling, Boel proposed the use of the average stiffness produced by the three Load cases. From the investigation into the buckling lengths of centric joint in section 5.3, it is demonstrated that the approximation is quite adequate for capturing the behaviour of shell element models. However, the results produced in this chapter would indicate that the stiffness of the connection is overestimated by this assumption. This would indicate that the effect of changing the stiffness slightly has a small effect on the buckling length. Through this work it was determined that Load case 1 should be used to calculate the out of plane stiffness. Even if the effect is slight, it would be advisable to keep the calculations on the safe side, as the effect may be not as slight for other cases which were not checked.

Regarding the eccentric joints, the behaviour encountered was much more complex than the centric ones. This was due to the coupling of the in-plane and out of plane degrees of freedom. Due to that, three different approaches were proposed to calculate the rotational stiffness. The first approach involved the complete disregard of the coupled displacements, whilst for the second, the introduction of a counter moment to eliminate the coupled displacement was proposed. For the third approach, the introduction of a rotated system was proposed and defining the rotational stiffnesses in those axes. For all approaches proposed, the results produced are far from capturing the actual buckling response of the shell element model. The only one that gave some positive approximation was approach 3, due only to the coupled displacement it was able to capture.

Lastly, the more interesting outcome of this investigation came when attempting to formulate approach 3. It was found that the connection behaved in a non-symmetric manner. This would mean that a non-symmetric stiffness element would have to be defined, to accurately describe the shell element model's behaviour. Such a thing was considered unpractical for engineering practice, so its actual application was not investigated further. In order to obtain some results from Approach 3, a symmetric stiffness matrix was created by taking the average of the calculated non-symmetric matrix and its transpose. As was mentioned earlier, the results of this simplification did not give adequately good results.

# 6 DISCUSSIONS, CONCLUSIONS & RECOMMENDATIONS

## 6.1 Discussion

A few topics that may affect the validity and application of the results are going to be addressed in this section.

As was seen through the investigations presented, in some cases it is difficult to attribute a certain eigenmode to a specific member. This makes the process of using eigenmodes in buckling verification prone to human error. From this, it follows that any results obtained from an eigenvalue analysis for which human judgement was used to categorize the modes could be erroneous. Preferably, a method would be used calculate the buckling load of members and per direction which would not involve human judgement. An attempt was made to develop such a method but was only successful to the point at which a continuous column buckling load could reliably be predicted. This is presented in APPENDIX C.

In APPENDIX B there is also an investigation into the effects of the brace thickness on the stiffness of the connections. It showed that for the same chord and brace widths, thicker chords actually had a decreasing effect on the stiffness of the connection. This is not actually the expected result, and it is attributed to the use of mid-surface modelling. Although, mid-surface modelling doesn't appear to capture the expected behaviour, the results and conclusion drawn from such models should be on the safe side since it should underestimate the connections stiffness. Because mid-surface modelling was assumed throughout this study, the conclusions should still be valid and applicable in practice. Having stated that, better results can be expected from using a different modelling process for the joints, such as using solid elements. By changing the modelling method, it would potentially allow for the inclusion of the welds in the analysis. This would make the investigation more realistic and provide additional insight into the actual behaviour of the joint. Especially in the case of eccentric joints, the welds may have more important effect since they would be adding to the non-symmetry of the joints.

From investigating the position of the lateral supports which were introduced, it was seen that changing their position by height did not have any effect. The lateral supports were introduced to separate global effects from the buckling of the members, and the conclusion indicates that indeed the results obtained can be used as the buckling lengths for member buckling. Although the conclusions were also valid for buckling including global effects (sway buckling of the braces for unrestrained tension chord), care should be taken if they are to be extrapolated to more cases of global buckling. For this reason, limiting the scope primarily to member buckling lengths is suggested.

Lastly, regarding the general behaviour of the buckling length factor as it relates to the stiffness of the brace and chord members a few observations are made. The stiffer the chords are compared to the braces; the lower the buckling length factors are for the braces and the higher they become for the chords and vice versa. In other words, making the braces stiffer leads to the buckling length of the chords to decrease and the buckling length

of the braces to increase. This effect is quite expected and has already been seen in the literature, so it is not included in the conclusions of this work.

## 6.2 Conclusions

In this section the conclusions drawn from the thesis are going to be summarized and presented. First the scope of use is going to be described and then the conclusions of the investigations persented. Lastly, design recommendations are going to be given. The conclusions are based on 60 hybrid (shell element-beam element) truss models and 15 beam element truss models. To aid with the investigations 16 additional shell element sub-models of the K-joints were used.

### 6.2.1 Scope of use

As the conclusions of this study were produced for specific configurations, care must be taken with extrapolating the results to other cases. The main characteristics used throughout the investigations are listed below. To ensure that no serious miscalculation is made, when conclusions and results of this work are applied in practice, the problem in hand needs to match or approximate to the data below:

- Eccentric K-joints used, with the braces welded on the chord face. The maximum allowable eccentricity introduced.
- Trusses with identical upper and lower chords. Warren type trusses (K-joints) and with identical cross section for the brace. Trusses loaded on the nodes of the top chord.
- Hot-rolled, square hollow sections, according to EN 10210-2:2006.
- The compressive chord laterally supported at its nodes. Bottom chord may be supported or unsupported as both cases were checked. The whole truss is simply supported with additional forked supports at its ends.
- The gap introduced needs to be close to the minimum permissible by the Eurocode 3.
- Trusses with height to length ratio of around 1/10 and 5 spans.
- The angle of the braces to be around 45°.

In the case that the characteristics of the truss deviate significantly from the data above, similar methodology used in this work can be followed and conclusions drawn. By creating hybrid models and following the approach described in sections 3.4 and 4.3, any number of cases can be additionally investigated.

### 6.2.2 Investigation conclusions

In this section, the main conclusions of this work are presented by answering the research questions posed in the introduction.

*What are the effects of modelling the corner radius of profiles to the connection stiffness of centric joints and are these substantial?*

- From the investigation into the centric joints a few conclusions were drawn. Specifically, the stiffness for the rounded cases of corner cross sections was found, in general, to be lower. However, in the thicker chords, the response becomes less severe and in some cases the effect was reversed, making the rounded cross sections' connections stiffer.

*Does Eurocode 3 prescribed buckling lengths provide a safe estimate? And under what assumptions?*

- Comparing the buckling lengths of the centric join trusses to the Eurocode prescribed values it was seen that Eurocode buckling lengths were mostly conservative, although some were slightly higher. Due to this, Eurocode may need to slightly adjust the buckling lengths it gives, specifically for very thin chords and for larger braces. However, it is noted that in practice, due to the limitation of the scope (shell element models, no welds modelled), Eurocode is most likely safe to use. Additionally, it was also concluded that Eurocode prescribed buckling lengths are to be used only as buckling length of members, and not when global effects are included in the analysis.

*Does the buckling behaviour change qualitatively and is this change substantial?*

- For trusses with eccentric joints, coupling of their displacements in their eigenmodes is observed. This means that when vertical displacements are present, lateral displacements are also observed and vice

versa. Even though this is the case, the members still buckle predominantly in one or the other direction, making the categorization of the buckling modes into in-plane and out of plane possible. It should be pointed out, though, that this is a simplification used to aid the comparison of the results with centric joint trusses. Since verification methods are usually developed for the principal axis of the cross sections and in the case of eccentric joints the members buckling in a non-principal axis, it is not known how this behaviour affects the ultimate limit state of the members.

*Do trusses with eccentric joints present better or worse buckling behaviour compared to the corresponding trusses with centric joints? Does the conclusion change depending on the buckling direction (in-plane, out of plane)? What effect does the change of joint parameters (β,γ) have on the observed trends?*

- From the investigation into the eccentric joint trusses, a better behaviour for in plane buckling was observed. This is attributable to the stiffening effect that the chord wall has. Due to the eccentricity, the brace is placed closer to the chord wall, leading to the more immediate transfer of forces through that mechanism. For the out of plane buckling behaviour, slightly higher buckling lengths were observed. This again is attributable to the change in the stiffness of the connection.
- In general, as is expected, the effects of the eccentric joints diminish with the increase of β. For the largest brace used in this work (β=0.75), the effects of the eccentric joints were already quite small for all configurations and directions (in-plane and out of plane), with a trend towards further reduction of any effect. Minimal effect is also observed for the smaller braces with low β values. This is attributed to the brace members which have very low stiffness. In the case of the buckling of the chords, the stiffness of the braces is insignificant compared to the chord's members and have little effect on their buckling lengths. In the case of the buckling of the braces, any change in the stiffness of the connection makes little difference because the connections are already stiff enough to act as relatively rigid connections. The last point is also indicated by the buckling lengths of the braces for low β being close to 0.5 which would indicate a completely fixed boundary condition.
- Eccentric joints are also more affected by high γ values (thinner chords). As has been explained, this is due to the connections already being quite stiff from the component "chord face in bending". As such, the increase in stiffness from the chord wall due to the eccentricity makes little difference.
- The values of β and γ that are affected the most by the introduction of the eccentricity are thinner chords and medium braces.
- To conclude, for in-plane buckling, the values of β and γ that are affected the most by the introduction of the eccentricity are thinner chords ($\gamma>8$) and medium sized braces ($0.3<\beta<0.7$). For all these values, a reduction of the buckling lengths by at least 5% can be expected, with the maximum observed being nearly 20% for $\gamma=15.9$ and $\beta=0.40$. For out of plane buckling, the buckling lengths are hardly affected by the eccentricity, with all configurations checked giving a difference of below 2%.
- Lastly, although a substantial increase in stiffness can be expected for the eccentric joints, assuming rigid connections instead of accounting for the connection's flexibility produces quite unsafe results in many cases, especially for the buckling of the braces.

*Do simplified models (beam element models with rotational springs) adequately capture the behaviour of more complex models (shell element models)?*

- Lastly, from the results produced from the hybrid model with the centric joints it is evident that the approach developed by Boel appears to capture the behaviour of the more detailed models. This means that in practice, replacing the stiffness of the connections for centric joints with rotational springs and using beam elements is a viable approach in designing truss structures for buckling.

*What do the different stiffness values that can be calculated for the same connection represent? Which is the most appropriate stiffness value to be used for trusses with K-joints?*

- From the investigation into the rotational stiffness of the connections under buckling it was concluded that using Load case 1 for the in-plane stiffness calculation, as was concluded by Boel, is correct for the use in warren trusses. In the case of the out of plane stiffness calculation, Boel's conclusion was that the average of the three load cases should be used. From the investigation into the centric joints, using this approximation would produce results close to the ones expected from using shell element

models for the joints. However, from a more detailed investigation it was concluded that the average of the three Load cases would overestimate the response. For this reason, Load case 1 is also proposed in these conclusions, in order to provide a safe estimate for any joint combination.

- For the stiffness calculations of the connections, it is recommended that Load case 1 be used for both in-plane and out of plane. This practically disregards any positive effects that tensile forces on opposite braces have on the stiffness of the connections.

*Is it possible for this approach to be extended to eccentric joints? If so, what modifications are necessary for its application?*

- To finish, a much more complicated behaviour is observed from the eccentric joints compared to the one encountered by the centric joints. This is primarily due to the coupling of the in plane and out of plane behaviour, owing to the non-symmetric nature of the geometry. Additionally, it was discovered that eccentric joints require a non-symmetric stiffness element if their behaviour is to be captured. Even though this was the case, three different approaches were proposed in order to be able to define a rotational stiffness and incorporate it in the analysis with a spring. Unfortunately, none of the proposed approaches were able to produce a good enough approximation for joint behaviour.

## 6.3 Recommendations for future research

In this section various topics will be recommended for future research. These aim for a better understanding of trusses with eccentric joints to aid with their application in engineering practice.

As was already mentioned in the discussion section (Section 6.1), more accurate results can be obtained from better modelling approximations of the joints. It is recommended for future investigations that 3D solid elements be used for a more realistic representation of the joints. Additionally, it would be beneficial if the effects of welds were included. More importantly, more work is needed in the out of plane stiffness formulation, to provide more insight about the mechanisms that affect its behaviour.

The investigation of different amounts of eccentricity would also be interesting. By decreasing the amount of eccentricity introduced, the conclusions already produced for the eccentric joints of this study may potentially change. There is also the possibility of introducing eccentricities beyond the range for which the braces are welded on the chord face. This would give rise to different types of eccentric joints and would provide additional insight into their use and design.

Concerning the joints, another important aspect is predicting their ultimate limit state (ULS) resistance. Due to the eccentricity, the behaviour of the eccentric joints in ULS is expected to be quite different from the centric ones. Special attention would be needed for the behaviour of the interception point of the corner of the chord and the brace. It would be very important to investigate the effects of welds on the eccentric joint because they may not be the same as the effects on centric joints.

Also mentioned in the discussion sections, is the problem with attributing the correct eigenmode and eigenvalue to the buckled member. It would be beneficial for a method to be created which could be used to find the buckling loads of members, without being prone to human errors. The method developed in APPENDIX C may provide a starting point for such an investigation.

Another topic out of the research scope was the effect of non-linearities of the connection stiffness. Using the linear buckling load in design, assumes and uses the linear and initial stiffness of the structure. However, it is also known that in the actual connection response, non-linear behaviour is expected (not due to yielding). One such example is the decrease or increase of the connection stiffness when the chord is under compression or tension respectively. Because the critical buckling load does not account for the change in the boundary conditions (non-linearity of stiffness), differences between the load predicted in the ultimate limit state by the critical buckling load and the actual behaviour are expected. Another topic related to the ultimate limit state (ULS) of the members with eccentric joint is the coupled behaviour encountered. As was mentioned in the conclusions section (section 6.2.2), it is unknown what effects this coupling has on the ULS of the members, making it a topic that requires further research.

Lastly, an important topic to be addressed is the effects that eccentric connections have on the global buckling behaviour. As global effects were outside the scope of research, global buckling of the structure was not

investigated thoroughly. Nonetheless, due to the structure used in the investigation, which was taken from prior research, some global effects were found. Specifically, the sway buckling mode of the braces was encountered. Since these differences may not immediately be attributable to the connection stiffness, no conclusive remark can be made regarding the effects of the eccentric joints on global modes. Further research of the interaction between different global modes of buckling and eccentric joints is needed.

# 7 REFERENCES


*ADVANCED PROFESSIONAL TRAINING NON-LINEAR AND STABILITY*. (2018). SCIA Engineer.

AISC. (2016a). *Code of Standard Practice for Steel Buildings and Bridges*. www.aisc.org

AISC. (2016b). *Specification for Structural Steel Buildings*.

Asgarian, B., Alanjari, P., & Aghaeidoost, V. (2015). Three-dimensional joint flexibility element for modeling of tubular offshore connections. *Journal of Marine Science and Technology*, *29*(6), 629–639. https://doi.org/10.1007/s00773-015-0317-2

Asgarian, B., Mokarram, V., & Alanjari, P. (2014). Local joint flexibility equations for Y-T and K-type tubular joints. *Ocean Systems Engineering*, *4*(2), 151–167. https://doi.org/10.12989/ose.2014.4.2.151

Biegus, A., & Wojczyszyn, D. (2011). Studies on buckling lengths of chords for out-of-plane instability. *ARCHIVES OF CIVIL AND MECHANICAL ENGINEERING*, *XI*(3).

Boel, H. D. (2010). *Buckling length factors of hollow section members in lattice girders*.

*Code for Lifting Appliances in a Marine Environment*. (2020). Lloyd's Register Group Limited.

Czepizak, D., & Biegus, A. (2016). Refined calculation of lateral bracing systems due to global geometrical imperfections. *Journal of Constructional Steel Research*, *119*, 30–38. https://doi.org/10.1016/j.jcsr.2015.12.007

*EN 1993-1-1: Eurocode 3: Design of steel structures - Part 1-1: General rules and rules for buildings*. (2005).

*EN 1993-1-8: Eurocode 3: Design of steel structures - Part 1-8: Design of joints*. (2005).

Gantes, C. J. (2016). *Nonlinear Structural Behavior - Emphasis on Metal Structures*. Hellenic Academic EBooks.

Garifullin, M., Bronzova, M., Pajunen, S., Mela, K., & Heinisuo, M. (2019). Initial axial stiffness of welded RHS T joints. *Journal of Constructional Steel Research*, *153*, 459–472. https://doi.org/10.1016/j.jcsr.2018.10.025

Garifullin, M., Mela, K., Heinisuo, M., & Kemi, R. (2017). *Unified approach for structural behavior of RHS T joints*.

Garifullin, M., Pajunen, S., Mela, K., & Heinisuo, M. (2018). Finite element model for rectangular hollow section T joints. *Rakenteiden Mekaniikka*, *51*(3), 15–40. https://doi.org/10.23998/rm.70439

Garifullin, M., Pajunen, S., Mela, K., Heinisuo, M., & Havula, J. (2017). Initial in-plane rotational stiffness of welded RHS T joints with axial force in main member. *Journal of Constructional Steel Research*, *139*, 353–362. https://doi.org/10.1016/j.jcsr.2017.09.033

Geschwindner, L. F., Liu, J., & Carter, C. J. (2017). *Unified design of steel structures* (3rd ed.).

Haakana, A. (2014). *IN-PLANE BUCKLING AND SEMI-RIGID JOINTS OF TUBULAR HIGH STRENGTH STEEL TRUSSES*.

Havula, J., Garifullin, M., Heinisuo, M., Mela, K., & Pajunen, S. (2018). Moment-rotation behavior of welded tubular high strength steel T joint. *Engineering Structures*, *172*, 523–537. https://doi.org/10.1016/j.engstruct.2018.06.029

Hayeck, M. (2016). *DEVELOPMENT OF A NEW DESIGN METHOD FOR STEEL HOLLOW SECTION MEMBERS RESISTANCE*.

Hornung, U., & Saal, ; H. (1998). A method for calculating the out-of-plane buckling length of diagonals of truss girders with hollow sections and K-joints. In *Journal of Constructional Steel Research* (Vol. 46, Issue 3).

Hornung, U., & Saal, H. (2001). A method of calculating the out of plane buckling length of diagonals of truss girders with hollow sections and K or N Joints. *Tubular Structures IX : Proceedings of the Ninth International Symposium and EuroConference on Tubular Structures*, 323–329.

Jankowska-Sandberg, J., & Kołodziej, J. (2013). Experimental study of steel truss lateral-torsional buckling. *Engineering Structures*, *46*, 165–172. https://doi.org/10.1016/j.engstruct.2012.07.033

Jaspart, J.-P., & Weynand, K. (2016). *Design of joints in steel and composite structures*.

Krajewski, M., & Iwicki, P. (2015). Analysis of brace stiffness influence on stability of the truss. *International Journal of Applied Mechanics and Engineering*, *20*(1), 97–108. https://doi.org/10.1515/ijame-2015-0007

Newmark, N. M., Hall, W. J., & Chajes, A. (1974). *CIVIL ENGINEERING AND ENGINEERING MECHANICS SERIES PRI NCI PLES OF STRUCTURAL STABILITY THEORY*.

Poels, A. R. J. E. (2017). *Coupled buckling of hollow section braces and chords in optimized welded lattice griders*. www.tue.nl

Rondal, J., Wurker, K. G., Dutta, D., Wardenier, J., & Yeomans, N. (1992). *STRUCTURAL STABILITY OF HOLLOW SECTIONS*. CIDECT.

Simitses, G. J., & Hodges, D. H. (2006). *Fundamentals of structural stability*. Elsevier/Butterworth-Heinemann.

Snijder, H. H., Boel, H. D., Hoendekamp, J. C. D., & Spoorenberg, R. C. (2011). Buckling length factors for welded lattice girders with hollow section braces and chords. *Proceedings of the 6th European Conference on Steel and Composite Structures (Eurosteel2011)*, 1881–1886. www.tue.nl/taverne

*Standard Specifications for Steel and Composite Structures* (First Edition). (2009). Japan Society of Civil Engineers.

Vayas, I., Ermopoulos, J., & Ioannidis, G. (2019). *Springer Tracts in Civil Engineering Design of Steel Structures to Eurocodes*. http://www.springer.com/series/15088

Wang, C. M., Wang, C. Y., & Reddy, J. N. (2004). *EXACT SOLUTIONS FOR BUCKLING OF STRUCTURAL MEMBERS*. CRC PRESS.

Wang, W., & Chen, Y. (2005). Modelling and classification of tubular joint rigidity and its effect on the global response of CHS lattice girders. *Structural Engineering and Mechanics*, *21*(6).

Wardenier, J. (Jacob), Packer, J. A., Zhao, X.-L., & Vegte, G. J. (2010). *Hollow sections in structural applications*. CIDECT.

Zhao, B., Sun, C., & Li, H. (2020). Study on the moment-rotation behavior of eccentric rectangular hollow section cross-type connections under out-of-plane bending moment and chord stress. *Engineering Structures*, *207*. https://doi.org/10.1016/j.engstruct.2020.110211

Zhao, X.-L., Herionm, S., Packer, J. A., Puthli, R. S., Sedlacek, G., Wardenier, J., Weynand, K., Wingerde, A. M., & Yeomans, N. F. (2001). *Design Guide for Circular and Rectangular Hollow Section Welded Joints Under Fatigue Loading*. TÜV-Verlag GmbH.

Ziemian, D. R. (Ed.). (2010). *Guide to Stability Design Criteria for Metal Structures* (Sixth). John Wiley & Sons, Inc. www.EngineeringBooksPdf.com

# APPENDIX A MESH INVESTIGATION

## A.1 Centric joints

Before calculating the stiffness of the connections in section 3.2, it is important to define and use a suitable mesh density of elements. In this investigation an element size will be determined, with which the results of the models used are expected to converge to an accurate value. To do this, similar models as the ones used in the main investigation are going to be used. This means that simply supported K-joints are going to be used of which the chord wall is supported against vertical displacements, at the mid-height of the chord. The models were loaded by an axial load at the end of the braces (Figure 130).

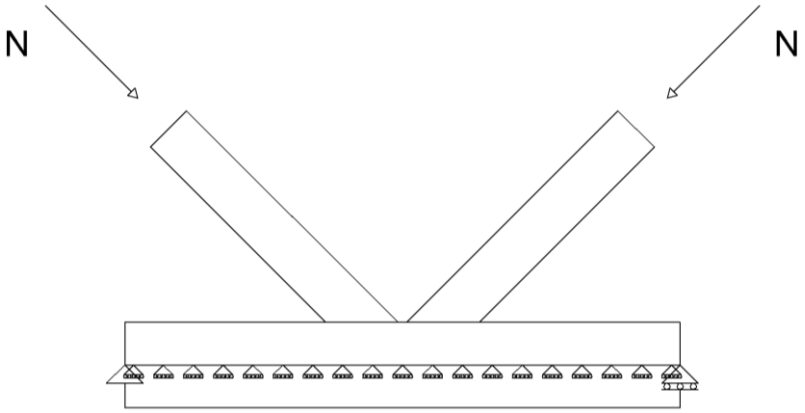


*Figure 130. Model used for the mesh density investigation.*

The cross sections used will not account for the rounding of the corners. The convergence criteria will be the buckling load of a brace, for the previously described model. By making the mesh denser convergence to a specific value of buckling load is expected and a suitable element size to be determined. The element size will be defined as fraction of the chord thickness, as chord face in bending is expected to affect the stiffness of the connections, and thus the convergence, the most. The application of the mesh densifying is applied around the intersection of the brace with the chord, at the connection (Figure 131).

For the investigation two different chords were used: SHS 50/2.6 and SHS 200/5. For the first chord two different braces were checked: SHS 40/2.6 and SHS 40/5. For the second chord four different braces were used: SHS 40/2.6, SHS 80/4, SHS 80/8 and SHS 160/5. The profiles were chosen such that a variety of β values and thicknesses were checked. Various element sizes were checked, with rations of shell element size over chord thickness ranging from 2.0 down to 0.5. The results are presented by plotting the relative error of each fraction used compared to the densest mesh used. This means that for Element length/Chord thickness

ratios of 0.5 the relative error in results is going to be zero. The relative error is calculated by Equation 28. and is used for the results of this investigation.

$$Error = \frac{N_{cr,densest} - N_{cr,i}}{N_{cr,densest}}\% \quad 28.$$

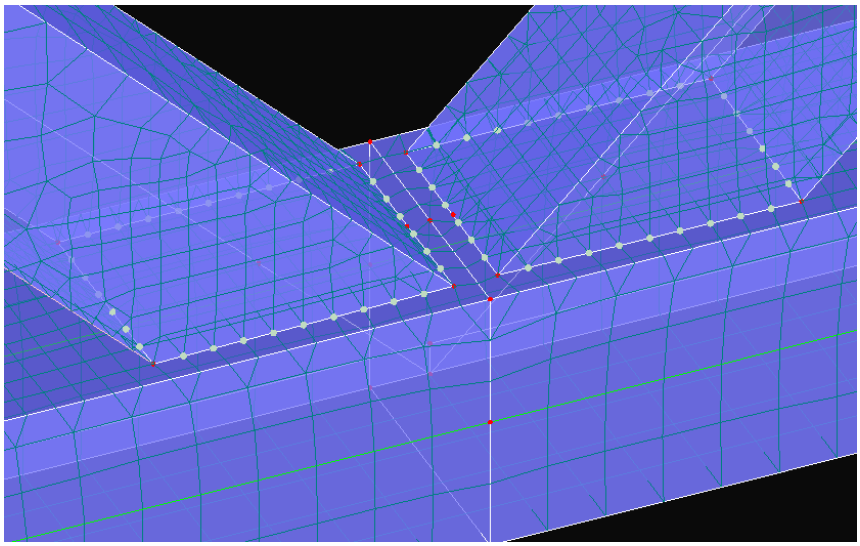

*Figure 131. Detail from the K-joint models used in the investigation. The yellow points around the connection indicate the positions where the density of the mesh is increased.*

## A.1.1 Chord of SHS 50-2.6

The results of the analysis are presented in Figure 132. For ratios of 1.0 the results appear to converge adequately. Also, more importantly, it appears that from ratios of 2.0 to 1.5 there is no improvement in the results. This is due to the number of elements that are generated from the meshing, between the side of the brace and the chord corner (Figure 133). The error can be minimized if at least 2 elements between chord corner and brace side are generated.

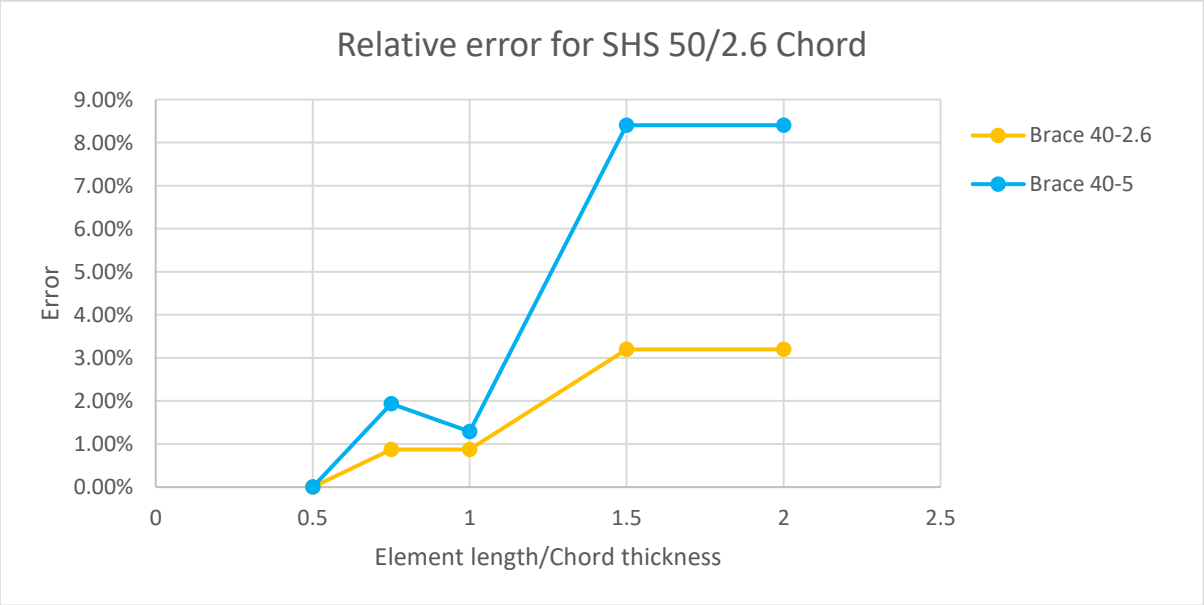


*Figure 132. Results compared to the finest mesh used for braces connected to SHS 50/2.6 chords*

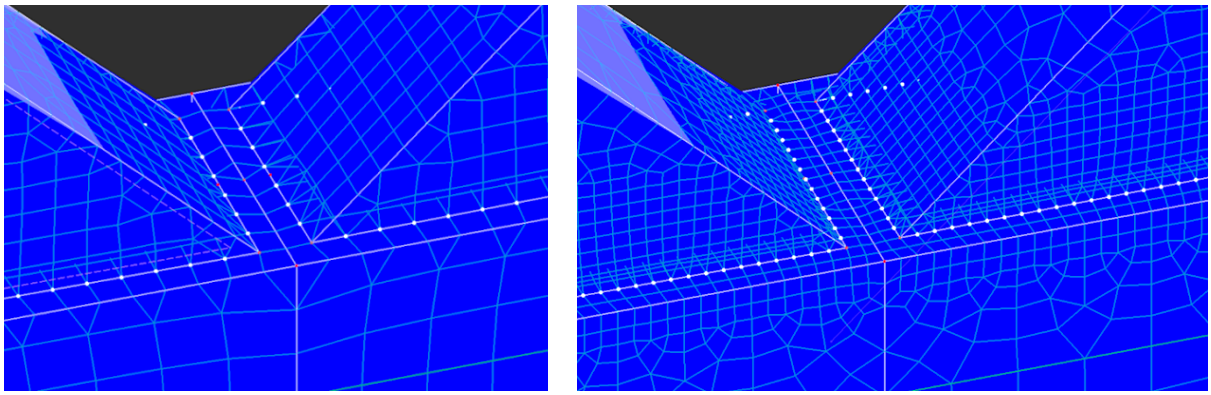

(a) (b)

*Figure 133. Example of different meshing on connection. (a) Example with 1 element between chord wall and brace's side and (b) at least 2 elements between chord wall and brace's side*

## A.1.2 Chord of SHS 200-5

To generate another pool of results a cross section of SHS 200-5 was used for the chord. From the results (Figure 134) it can be observed that using a ratio of 1.0 is adequate for the investigation that needs to be done.

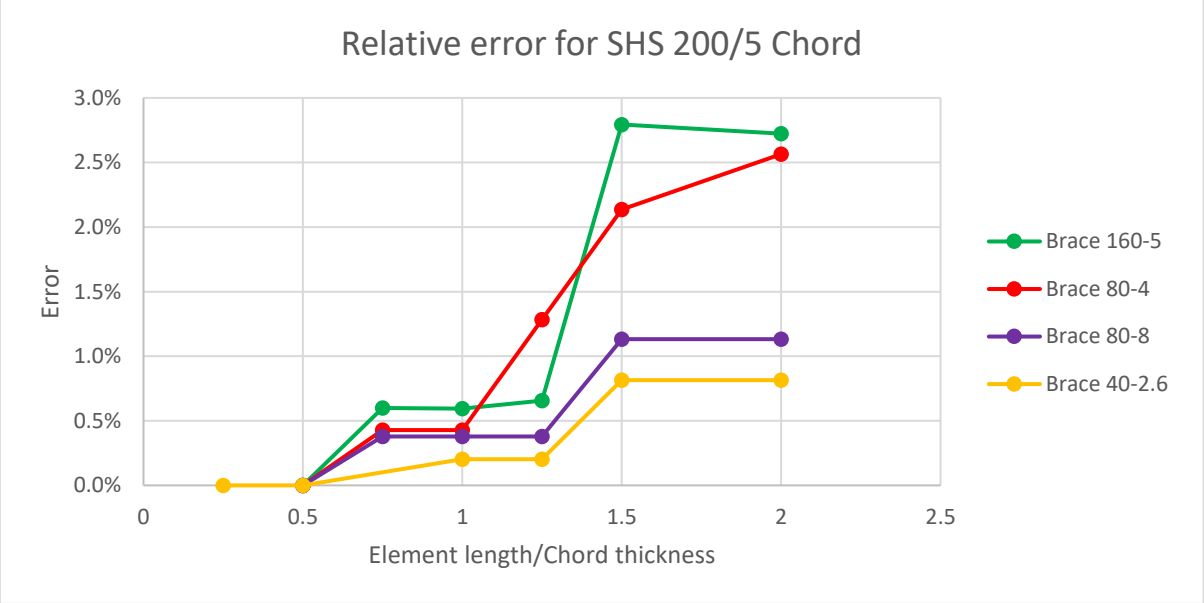


*Figure 134. Results compared to the finest mesh used for braces connected to SHS 200/5 chords*

Lastly, as the chord is supported along its length, the conditions far from the connections is not expected to affect the behaviour much. As such a reasonable element size is chosen. From an investigation performed, it was determined that at least 5 elements are needed to model each side of the chord wall (Figure 135). To conclude, a length to thickness ratio of 1.0 is adequate and at least two elements should be generated between the brace side and the chord's corner to ensure reliable results. The mentioned were used for the investigations into the stiffness of the connections of section 3.2.

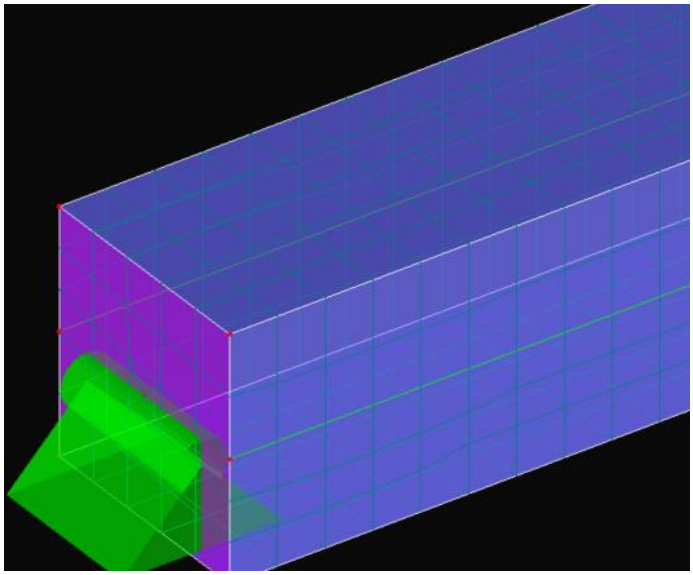

*Figure 135. Chord that is modelled using at least 5 elements per chord wall.*

## A.2 Mesh investigation Eccentric joints

As was mentioned in the main text, due to the additional geometry requirements of the eccentric joints, to get accurate results, but also limit the computational time, an additional mesh investigation is performed. The main aspects that are of interest is the stiffness of the connection and the behaviour in a linear buckling analysis. As such, a simple model with only the joint is investigated. The models used are similar to the ones used in the previous investigation (see section A.2) with some minor differences. Firstly, the chord wall is not supported along its length and additionally the loading introduced on the braces is tensile on one brace and compressive on the other (Figure 136).

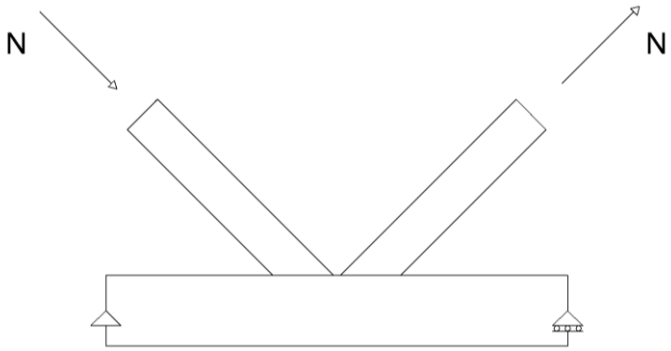


*Figure 136. Model used for the mesh density investigation.*

From the models used, a linear buckling analysis is performed, and the load factors of the first two eigenmodes are used to gauge the convergence of results. The thinnest and thickest chords are used in this investigation (SHS 200/6.3 and SHS 200/16 respectively), as well as the smallest and largest braces (SHS 50/4 and SHS 150/8 respectively). By producing an adequate mesh for the extreme cases used, the guidelines would be adequate for the rest of the combinations used.

Each surface was meshed with a preferred element size given as a ratio of its thickness. This means that the surfaces comprising the braces and chords, were assigned an element target length a factor of the corresponding surface. These ratios were 2, 1.5, 1, 0.75 and 0.5. Additionally, for the chord SHS 200/16, due to its large thickness, an additional refinement was used with which only the chord surfaces used a ratio of 0.25, whilst the braces remained at an element ratio of 0.5. This is named “0.5t+”.

As was done in the previous investigation (see section A.2), to aid comparison, the results are normalized against the densest mesh used, according to Equation 29.. The results are then plotted against the No. of elements used in each model, to indicate the computational time.

$$N_{normalized} = \frac{N_{cr,i}}{N_{cr,densest}} \quad 29.$$

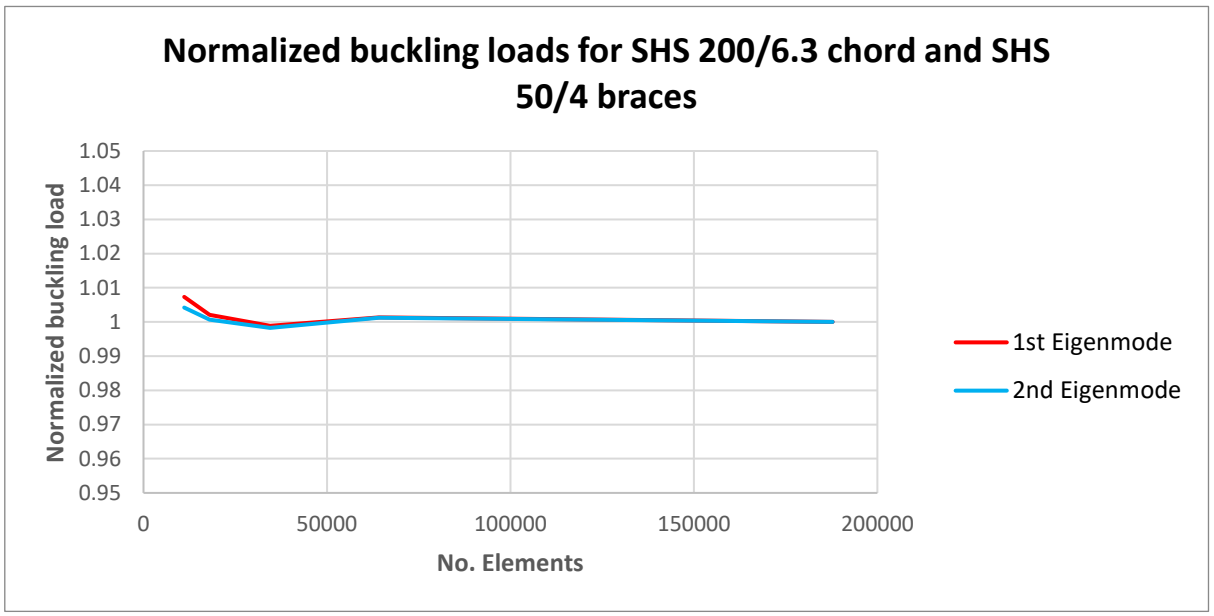


*Figure 137. Normalized buckling loads for SHS 200/6.3 chord and SHS 50/4 braces*

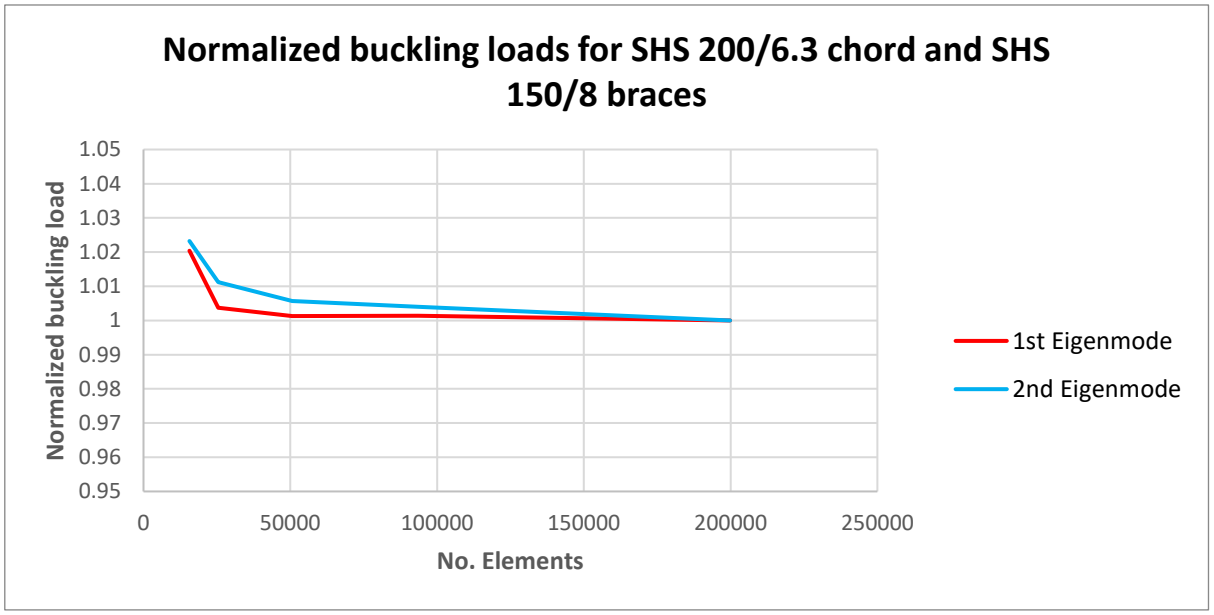


*Figure 138. Normalized buckling loads for SHS 200/6.3 chord and SHS 150/8 braces*

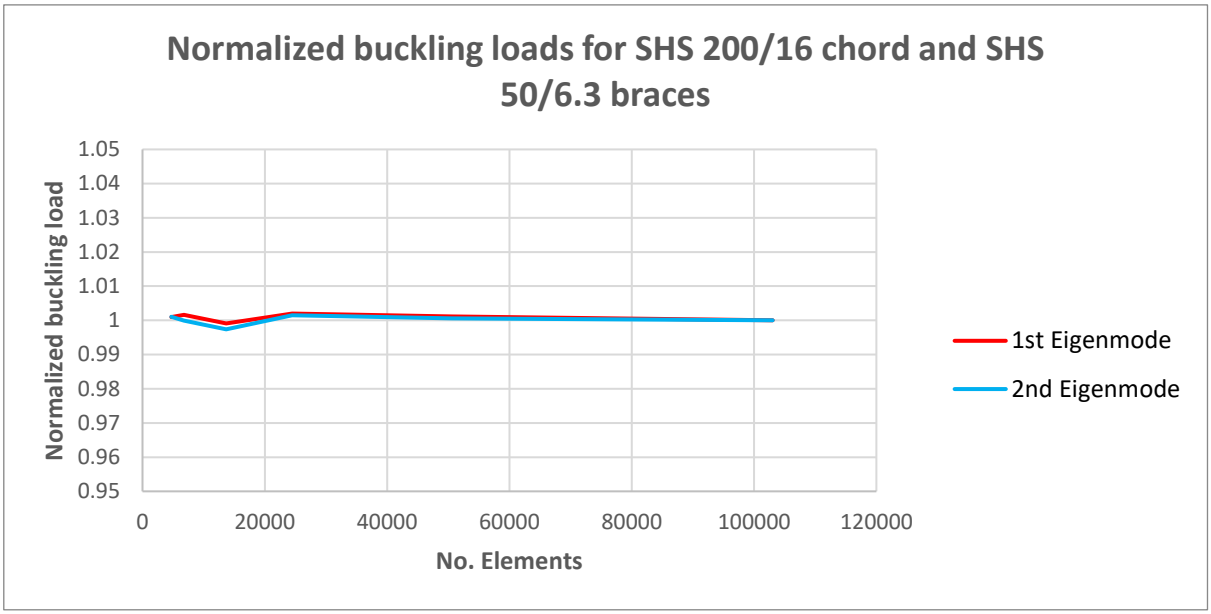


*Figure 139. Normalized buckling loads for SHS 200/16 chord and SHS 50/6.3 braces*

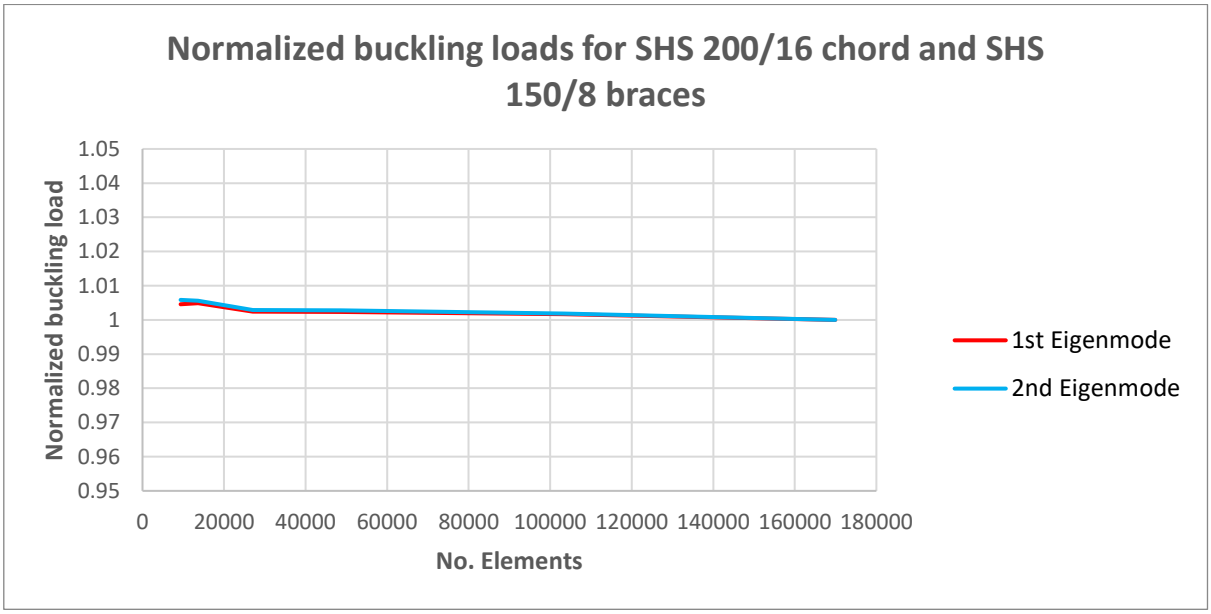


*Figure 140. Normalized buckling loads for SHS 200/16 chord and SHS 150/8 braces*

The results can be seen in Figure 137, Figure 138, Figure 139, and Figure 140. and two observations can be made. Firstly, the results do not appear to be very sensitive to the mesh density. This means a quite coarse mesh may be utilized, but this effect may be due to the next observation. In many cases instead of the normalized buckling load appear to have reversing of its trend, by decreasing and then increasing in value, with the refinement of the mesh it increases. Also, in the cases with the braces being SHS 50/4, the values drop below 1.0, which is counter intuitive as by refining the mesh an increase in flexibility would be expected by the model. These results can be explained by accounting for the cross-sectional area modelled for the corresponding meshing. For coarser meshes the cross-sectional area modelled may be substantially smaller than the one created by a finer mesh. This can have the result that coarser meshing can produce lower buckling loads than a refined one (Figure 68). This effect was also encountered in section 3.3 when comparing shell element models and beam element models.

To represent reality more accurately, but also limit the computational time, a more specific discretization is proposed (Figure 141 (d)). More specifically, for all the chords, far from the connection a target length of 16 mm was prescribed, while near the connection 8 mm. In the immediate proximity to the connection a target

length equal to the thickness of the brace was prescribed. For all the braces, for the area near the connection a target length equal to the brace's thickness was chosen, whilst for far from the connections a target length of two times the brace's thickness was used.

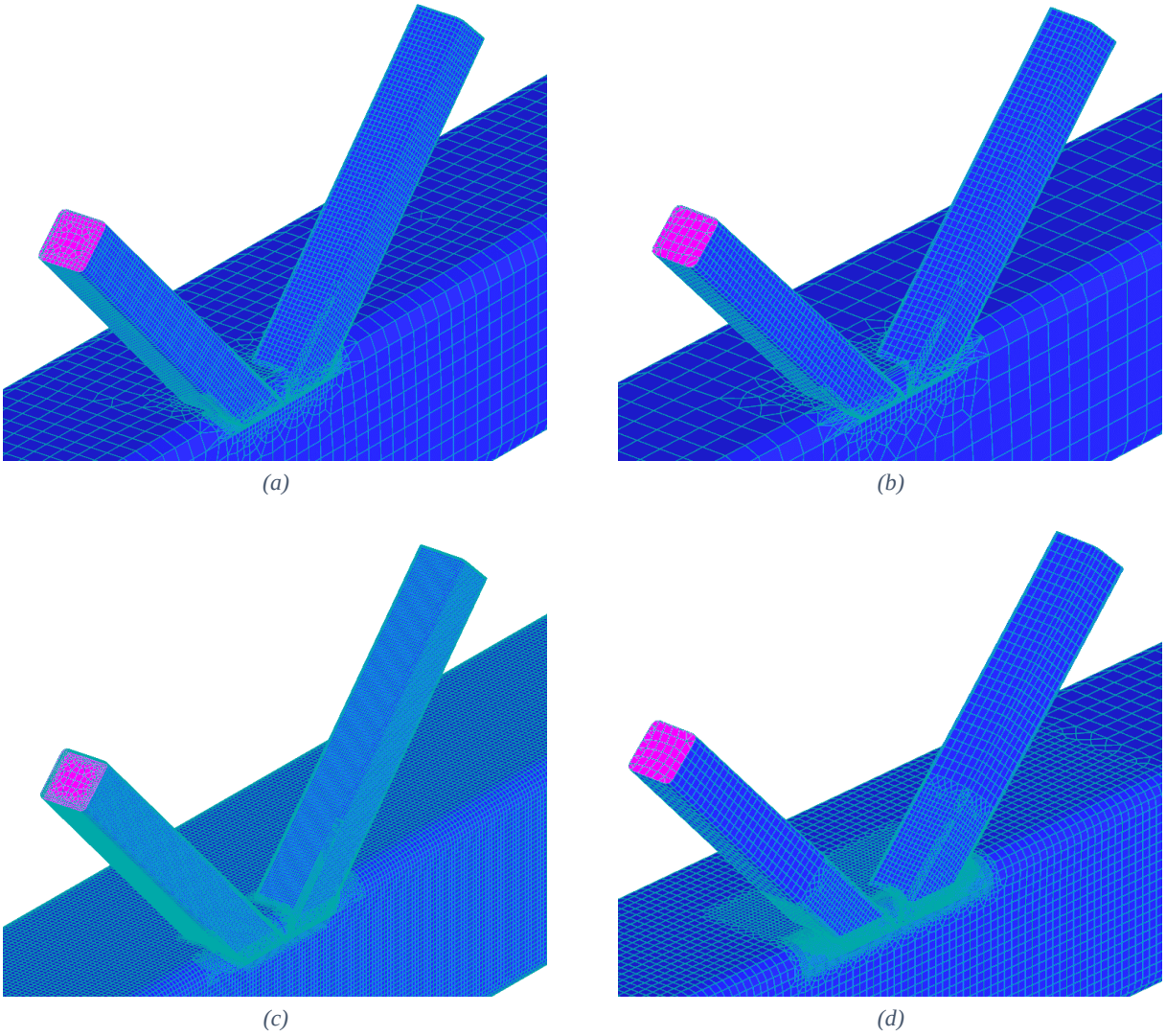

*(a)* *(b)* *(c)* *(d)*

*Figure 141. Details of the eccentric K-joints models used for different target lengths for the elements used. The chord-brace combination presented is SHS 200/16-SHS 50/4. The prescribed target lengths are (a) 1.5t, (b) 1t and (c) 0.5+t, whilst in (d) the proposed final meshing is visualized.*

To conclude, the proposed meshing is compared to the densest mesh used in each case. The results are presented in Table 38. From the comparison with the densest meshes used, the differences appear to be small, and the proposed mesh is suitable for use in the investigations performed in Chapters 3 and 4.

Table 38. Buckling loads of the eccentric K-joint models for the densest and the proposed meshing used.

| Chord | Brace | 1st Eigenvalue | | | 2nd Eigenvalue | | |
|---|---|---|---|---|---|---|---|
| | | Densest mesh | Proposed meshing | Diff. | Densest mesh | Proposed meshing | Diff. |
| 200-6.3 | 50-4 | 292.7 | 291.6 | -0.4% | 309.1 | 307.5 | -0.5% |
| | 150-8 | 3384.7 | 3382.5 | -0.1% | 3941.1 | 3950.8 | 0.2% |
| 200-16 | 50-4 | 100.8 | 101.3 | 0.5% | 168.5 | 168.3 | -0.1% |
| | 150-8 | 1303.0 | 1312.1 | 0.7% | 1417.7 | 1448.5 | 2.2% |

# APPENDIX B EFFECT OF BRACE THICKNESS ON STIFFNESS

In the literature study performed, in all cases examined, it has been assumed that thickness of the brace has little or no effect. This is counterintuitive, as the thickness would be expected to play a role, especially in the way that the brace's cross section distorts on the chord's face (Figure 142). The brace's thickness should be expected to play a stiffening effect on the connection's stiffness. From this observation, it would be logical to conclude that thicker braces have also higher stiffness. When using mid-surface modelling this is not something that is observed. By using the method described in section 3.2 to calculate the stiffness for a K-joint comprised of chord SHS 50/2.6 and braces with a width of 40mm, the stiffness against the thickness of the braces can be plotted. It can be observed in Figure 143 that for increasing thickness the calculated stiffness decreases.

*(a)* *(b)*

*Figure 142. Chord face deformations for (a) a normal thickness brace and (b) a very thick brace*

This can be explained by the fact that, by using mid-surface modelling and changing the thickness of the brace, the actual modelled geometry changes. As such the modelled gap, but also the β parameter changes and specifically increase and decrease respectively for an increase in thickness (Figure 144). It is noted that the effects of this is primarily due to the change of β, as the gap has a relatively small impact on the stiffness compared to the effect of β, especially for large β values which is used in this case (β=0.80)(Figure 145, Figure 146).

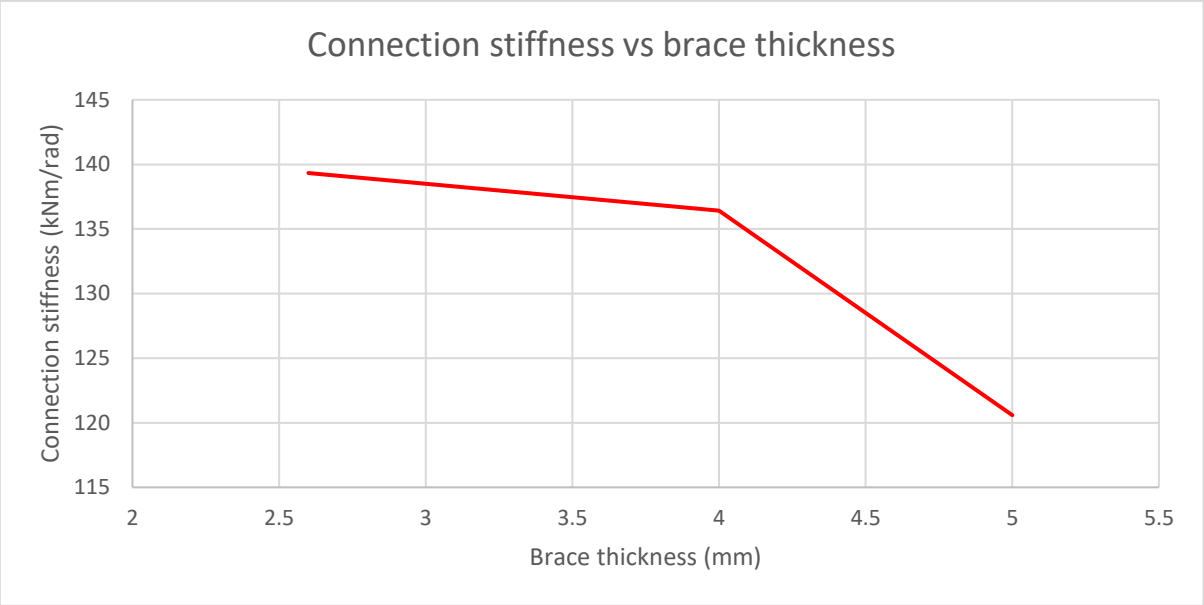


*Figure 143. Stiffness of connection against the thickness of the brace for chord SHS 50/2.6 and brace 40*

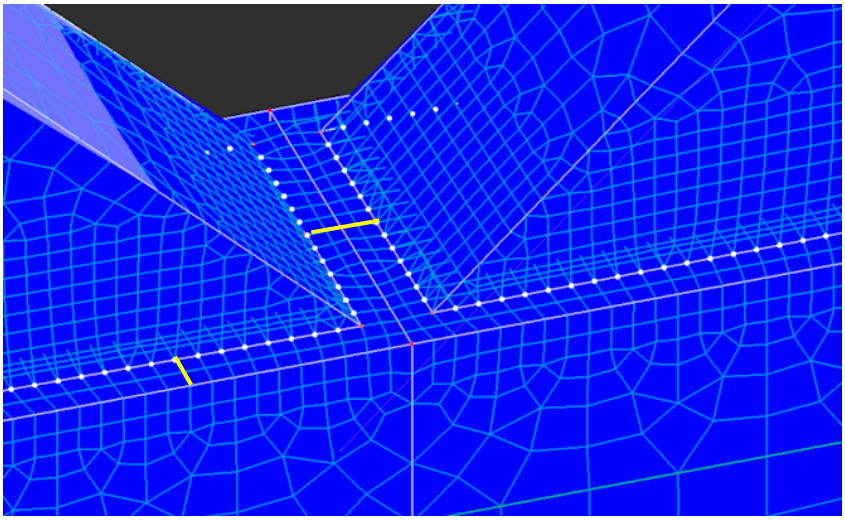

*Figure 144. Relevant distances that change when modelling by changing the thickness of the brace, while using mid-surface modelling*

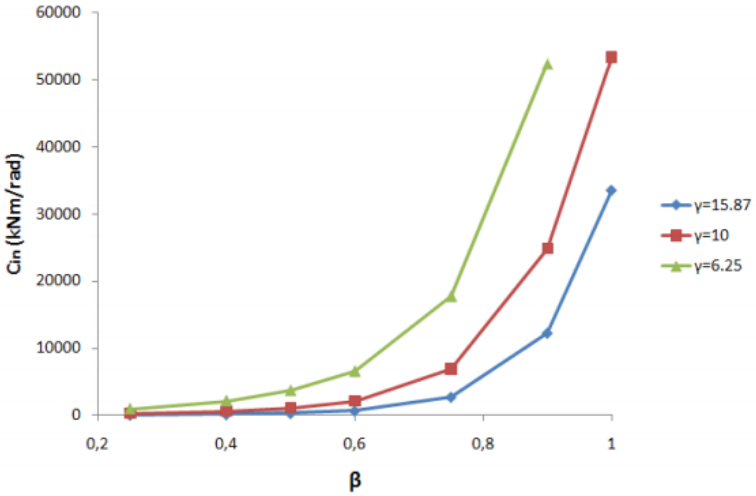


*Figure 145. Stiffnesses of connections depending on their β factors (Boel, 2010)*

| Gap (mm) | Load cases (LC) | | |
|---|---|---|---|
| | LCin1 | LCin2 | LCin3 |
| 15 | 287 | 434 | 214 |
| 50 | 285 | 416 | 217 |
| 100 | 269 | 322 | 231 |
| 135.3 | 262 | 290 | 239 |
| 150 | 262 | 285 | 243 |
| 200 | 260 | 270 | 251 |
| 250 | 259 | 263 | 255 |
| ∞ | 250[8] | - | - |

*Figure 146. Stiffnesses of connections against the connection's gap (Boel, 2010)*

To investigate further, the stiffness of connections having the same geometry (meaning modelled geometric dimensions) but changing the thickness of the brace was calculated. Chords of SHS 50/2.6 and SHS 120/5 were used. For the geometry of the brace the mid-surface of the brace SHS 40/5 was used. It can be observed that for both configurations the stiffness increases with the increase of the brace's thickness (Figure 147), something that is expected.

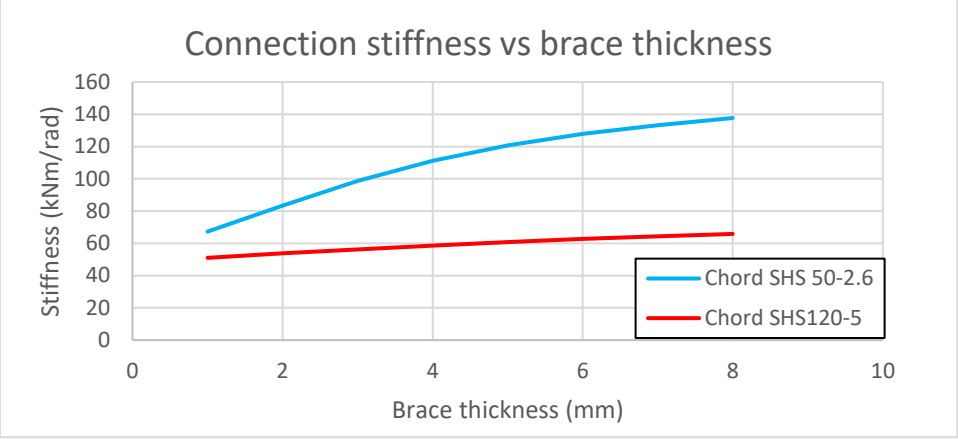


*Figure 147. Stiffness of connection for SHS 40 braces. Geometry given by SHS 40/5 mid surface*

To get a more realistic prediction of the connection's stiffness, a single sided joint was modelled using 3D elements. The configuration consisted of a chord of SHS 50/2.6 and braces of SHS 40-2.6/4/5. Initially the mesh size of the model was investigated to make sure that the results are going to be adequately accurate. The mesh refinement zones were placed all around the connection on the top and bottom of the chord face, as well as around area of interest (Figure 148). Since the results did not change by more than 2% from going from 0.7 mm to 0.35 mm (Figure 149) and to save substantial computational time, an element size of 0.7 was chosen.

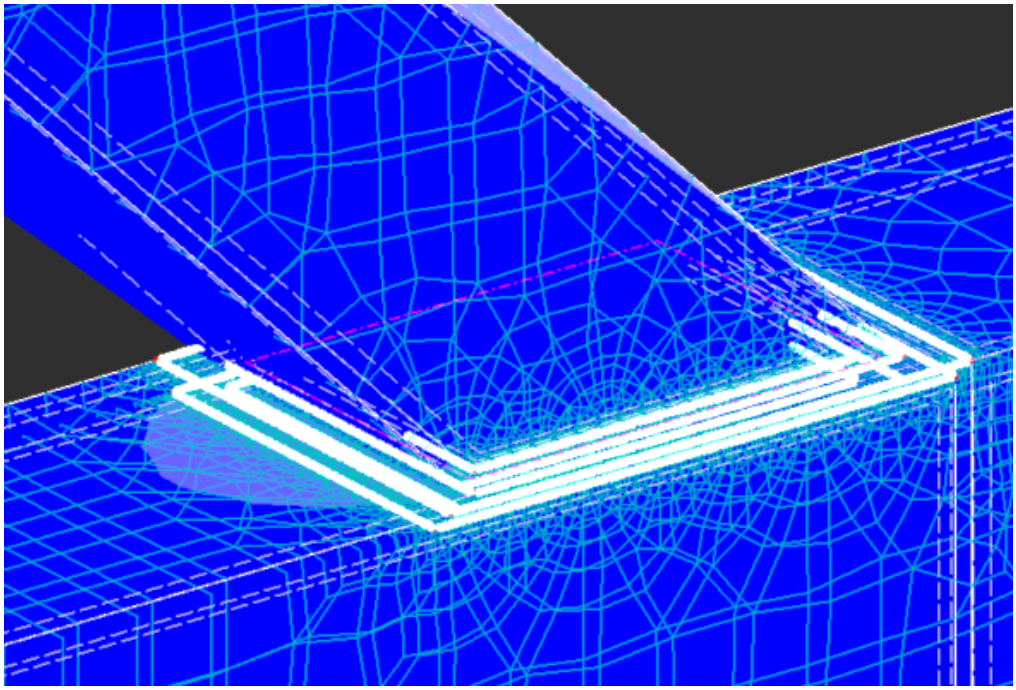

*Figure 148. Example of mesh refinement areas of 3D solid element modelling of connections. Areas of refinement are defined in all lines in the immediate vicinity of the connection.*

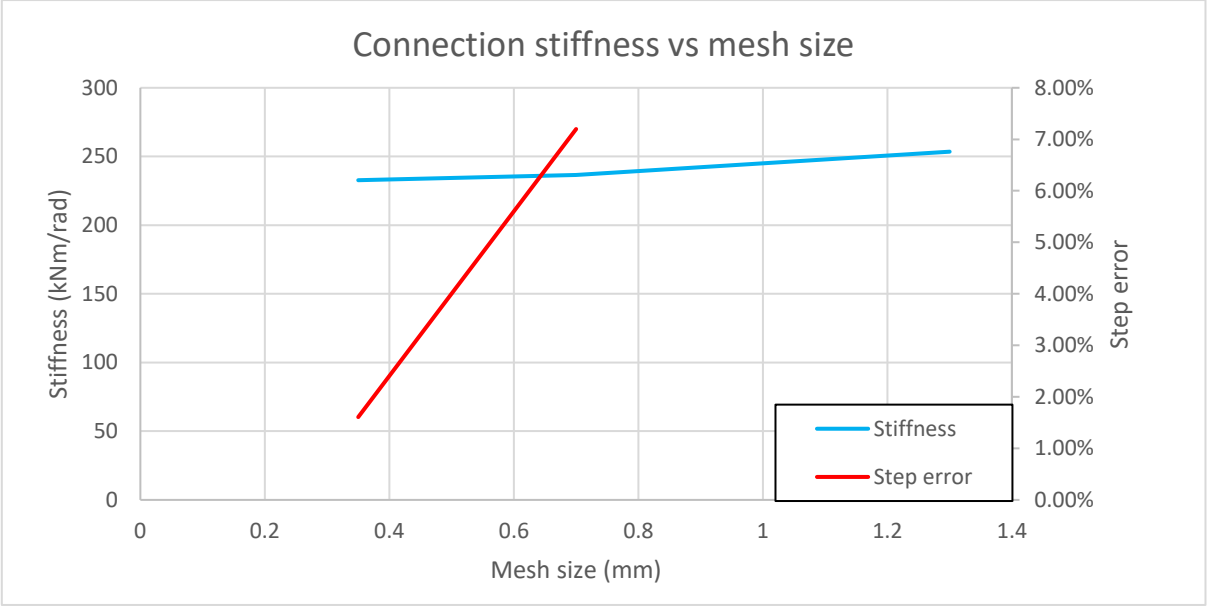


*Figure 149. Stiffness for sequential refinement of the mesh density and step error. The step error is calculated as the relative difference between sequential refinements.*

From the results (Figure 150) it can be observed that with the increase of brace thickness there is an increase in stiffness of the connection for the 3D element model. Also, comparing with the results obtained by the previous analysis, the results of the 2D elements models with changing only the brace thickness follow a similar trend (Figure 150).

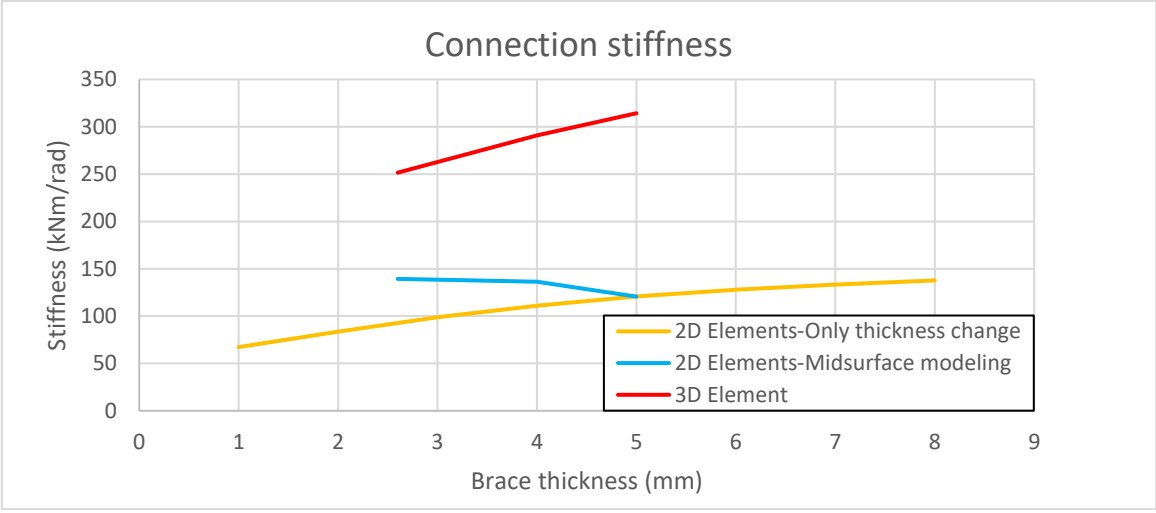


*Figure 150. Stiffness against brace thickness for different modelling technique. The graphs are for a chord SHS 50/2.6 and braces with width 40 mm.*

It can be concluded that modelling connections by using their mid-surface geometry can give some issues with accurately determining the stiffness of the connections. First off, the stiffness decreases instead of increasing with the increase of brace thickness. Secondly, the geometry generation is quite more complicated, and each paring of chord and brace cross sections would require the generation of different model. It should also be noted, as Boel mentions in his work, that some geometries might be non sensical to model as they would not capture reality, such as the case of having small gaps and large chord thicknesses (Figure 151).

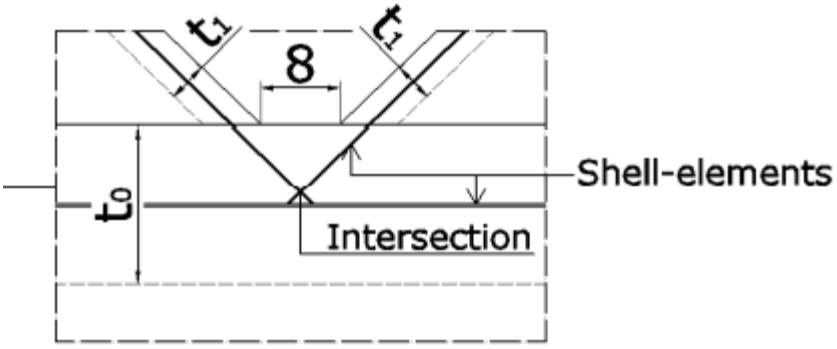


*Figure 151. Potential issues with modelling the connection using the mid-surface geometry of the cross sections (Boel, 2010).*

To address these issues, a new way of modelling the connection, to calculate the stiffness of it, is proposed. In this new proposal, the geometry of the cross sections is defined by the external perimeter of the cross sections. On these surfaces the 2D element mesh is generated but is offset by the half of the thickness inwardly (Figure 153, Figure 152 (c)). This has the effect of overestimating the cross section of the members, but it is assumed that will capture the connection's behaviour more accurately. To deal with this an additional modelling method was also checked, in which the internal and external perimeter of the brace were used, and the surfaces were defined with half the thickness of the brace and offset by a quarter of the thickness to the relevant side (Figure 152 (d)). The surface offset is easily introduced in the finite element program used, RFEM 5 (Figure 154). For the investigations chords SHS 50/2.6 and SHS 120/10 along with braces with widths of 40 mm and 100 mm respectively.

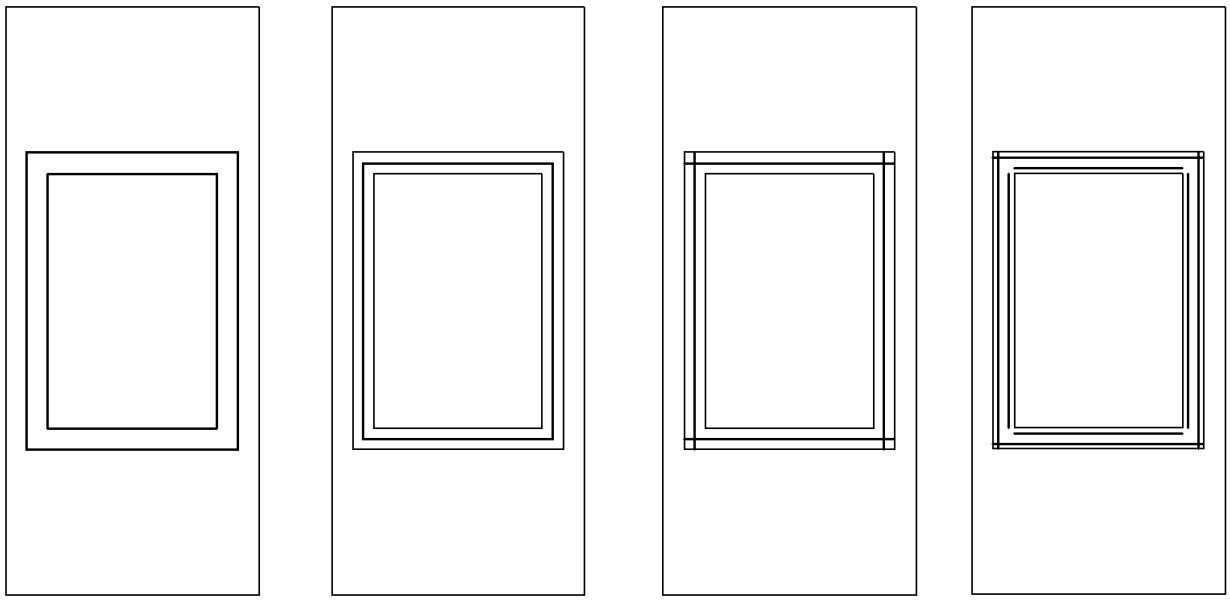

(a) (b) (c) (d)

*Figure 152. Intersection points of braces with chords for (a) 3D elements, (b) mid-surface modelling, (c) offset modelling and (d) double offset modelling.*

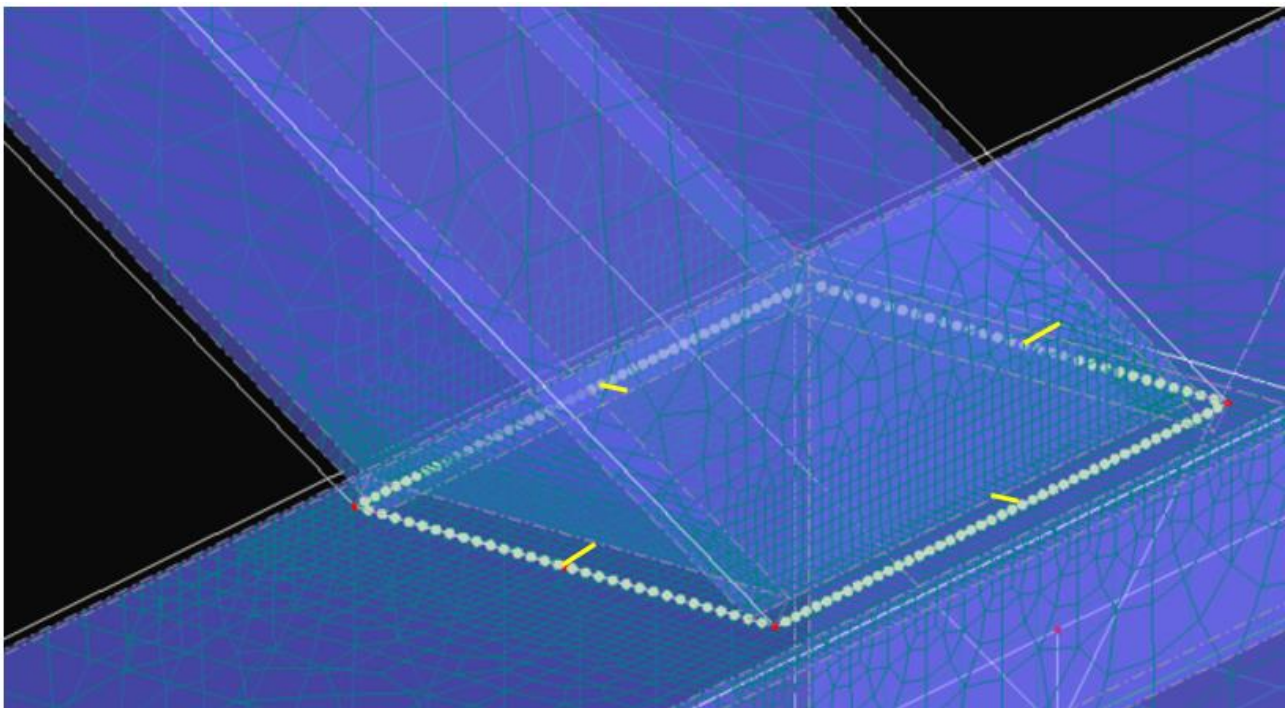

*Figure 153. Offsetting of brace wall in shell element model.*

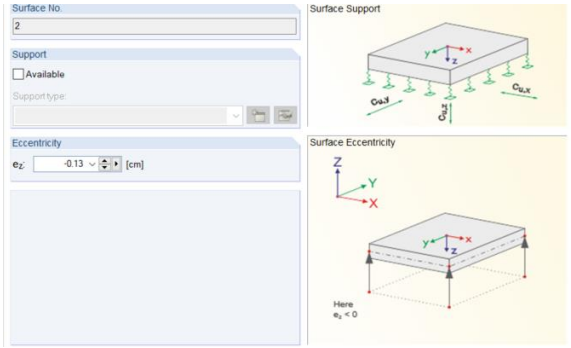


*Figure 154. Definition of offset surface in the RFEM 5 environment.*

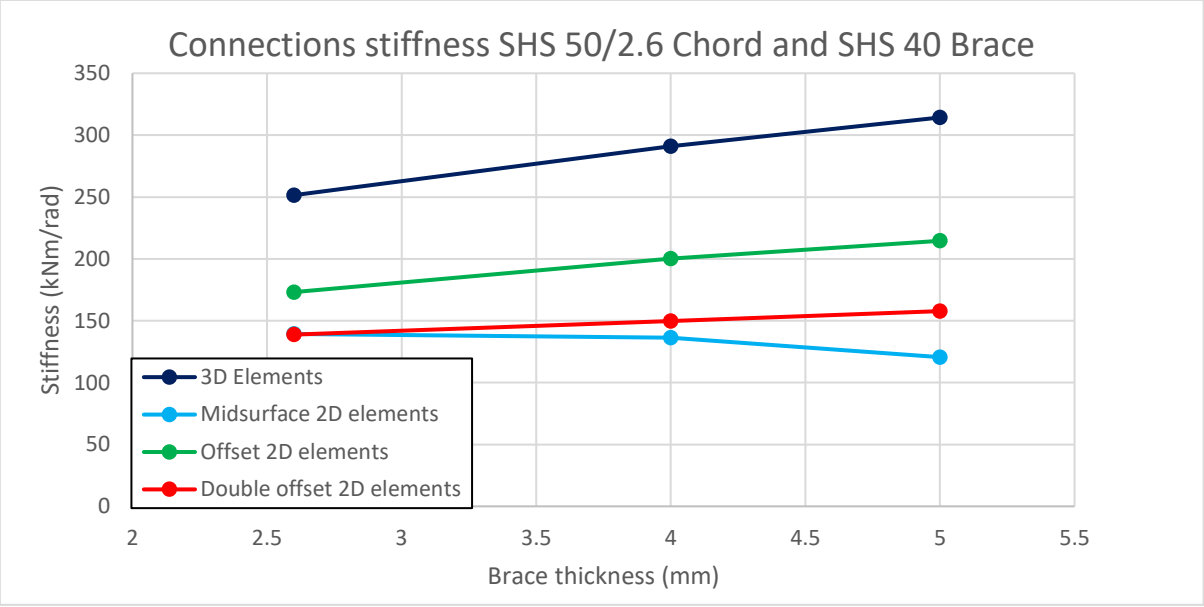


*Figure 155. Stiffness connection of SHS 50/2.6 chord and SHS 40 brace for various modelling techniques*

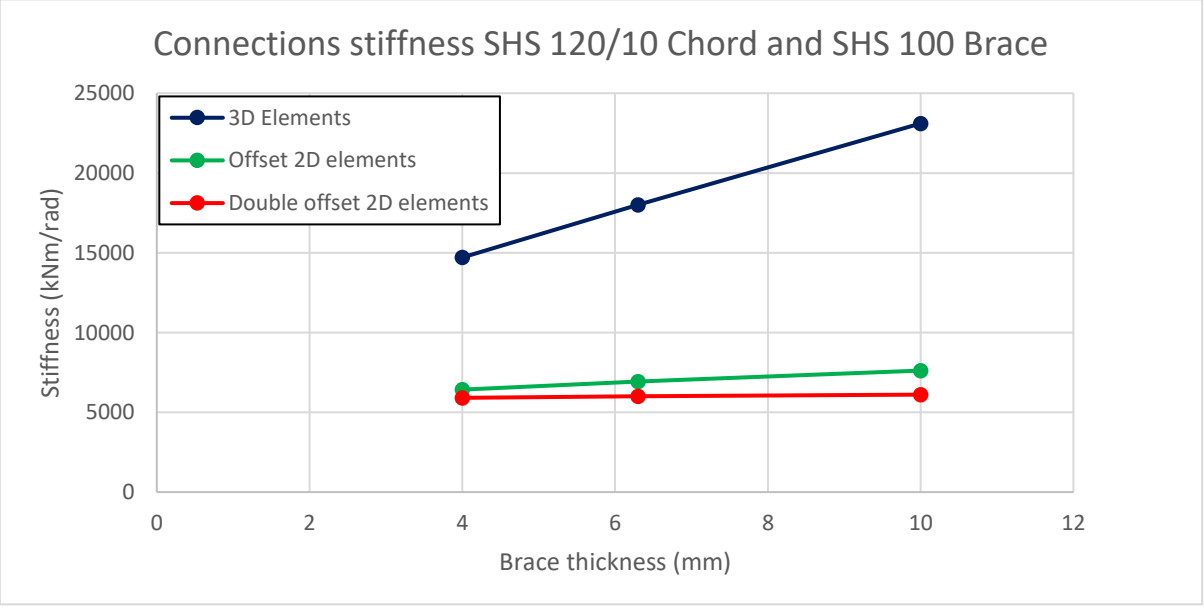


*Figure 156. Stiffness connection of SHS 120/10 chord and SHS 100 brace for various modelling techniques*

It can be seen from the results (Figure 155,Figure 156) the new proposed offset modelling technique captures the stiffness trend of the 3D element model much better, although it still is quite less stiff. Additionally, the

connections modelled with double offset surfaces, also captures the trend of the stiffness from the 3D elements. For this investigation the chord was modelled with its external perimeter and offset inwardly. For practical reasons, though, the double offset technique cannot be applied to the chord, as the two cross surfaces defining the chord face will not be connected and will present problems with force introduction in the whole chord.

Form this is concluded that offset modelling may be the better way of modelling connections, at least for the calculation of their stiffness. The problem arises from the increased cross-sectional area they present due to the way they are modelled. Because of this, the buckling load calculated by using this technique will be an overestimation of the actual value. From results done on fixed cantilevered braces of length 1 m and with cross sections of 40-2.6/4/5, the error reaches 25% (Table 39). The technique doubles the area in the corners of the cross sections and thus the effect is greater the thicker the cross section used.

*Table 39. Load factors of elastic buckling for various cross sections*

| | **SHS 40-2.6** | **SHS 40-4** | **SHS 40-5** |
|---|---|---|---|
| **Offset model** | 5.276 | 7.697 | 9.262 |
| **Mid surface model** | 4.693 | 6.554 | 7.411 |
| **Difference** | 12.4% | 17.4% | 25.0% |

# APPENDIX C NEW METHOD FOR BUCKLING LOAD CALCULATION OF CONTINUOUS COLUMNS

## C.1 Stiffness of members loaded with an axial load

The first step for developing the new method is to account for the loss of stiffness a member experiences under compressive loading. To calculate this, two similar members are assumed (Figure 157). Both have a rotational spring of stiffness $K_{spring}$ on one end and are loaded by an equal moment $M_1$ in the other. Additionally, member 2 is loaded by an axially compressive force $N_{ed}$.

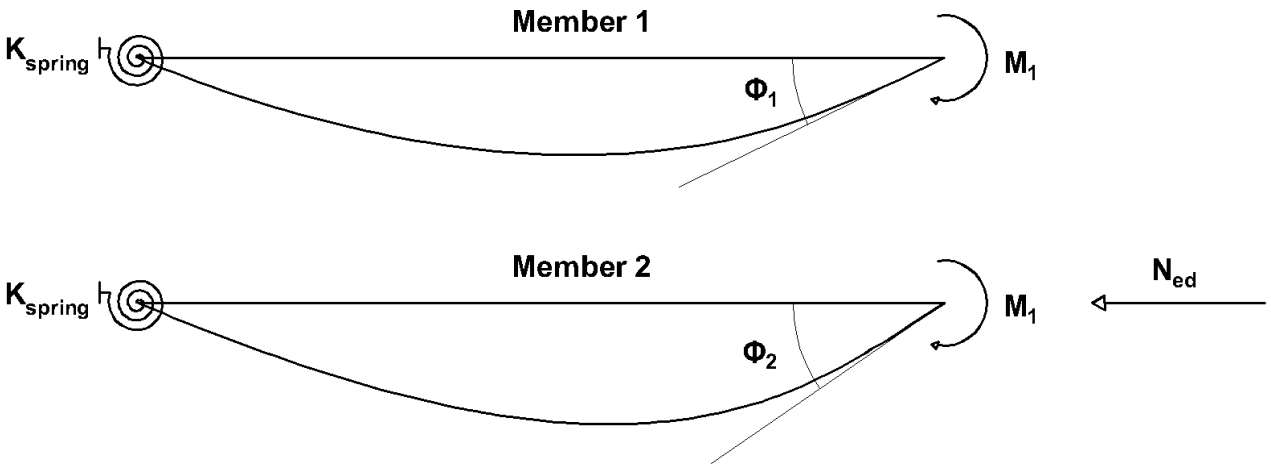


*Figure 157. Displacement field of members subjected to bending and bending/axial load*

By accounting for the spring's stiffness, the stiffness of member 1 at its loaded end is given by Equation 30.. For member 2, as the member is loaded by a compressive load, its displacement field will increase according to the 2nd order theory and will be described by the Equation 31.. By accounting for this increase in the displacement field, a relative decrease of its stiffness compared to member 1 is expected. This given by Equation 32. and is expressed as function of the stiffness of member 1. This can be more generally described as the equivalent stiffness of the axially loaded member as a function of the initial stiffness of the unloaded member (Equation 33.). The produced equation makes intuitive sense as if the axial loading is zero the member has the initial unloaded stiffness, whilst for an axial load equal to its critical buckling load, its bending stiffness becomes zero as it is unable to provide any stiffness anymore.

$$K_1 = \frac{M_1}{\varphi_1} = 4\frac{(3+\alpha)}{(4+\alpha)}K_{member} \quad 30.$$

Where:

$$K_{member} = \frac{EI}{L}$$

$$\alpha = \frac{K_{spring}}{K_{member}}$$

$$\varphi_2 = \varphi_1 \frac{1}{1-\frac{N_{ed}}{N_{cr}}} \quad 31.$$

$$K_2 = \frac{M_1}{\varphi_2} = \frac{M_1}{\varphi_1 \frac{1}{1-\frac{N_{ed}}{N_{cr}}}} = \left(1-\frac{N_{ed}}{N_{cr}}\right)\frac{M_1}{\varphi_1} = \left(1-\frac{N_{ed}}{N_{cr}}\right)K_1 \quad 32.$$

$$K_{eq} = \left(1-\frac{N_{ed}}{N_{cr}}\right)K_{initial} \quad 33.$$

## C.2 Calculation of the equivalent spring in the case of a continuous column

Assuming two members that are rigidly connected between them and supported against out of plane deformations at their intersection. Rotational springs as supports are also assumed at their ends, as the most general boundary conditions (Figure 158). Each member is loaded by a compressive load. Without loss of generality, it is assumed that member 2 buckles first (Equation 34.). As such the Load Ratio (LR) is defined as the ration of the compressive load of member 1 (supporting member) over the compressive load of member 2 (buckled member) (Equation35.). Since member 2 is assumed buckled, according to Equation 33. it has no stiffness remaining. The equivalent supporting spring provided by member 1 is given by Equation 36..

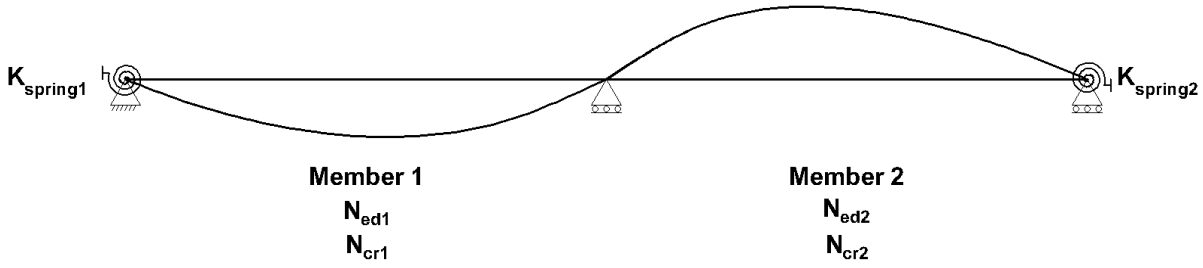


*Figure 158. General problem for the case of a continuous column.*

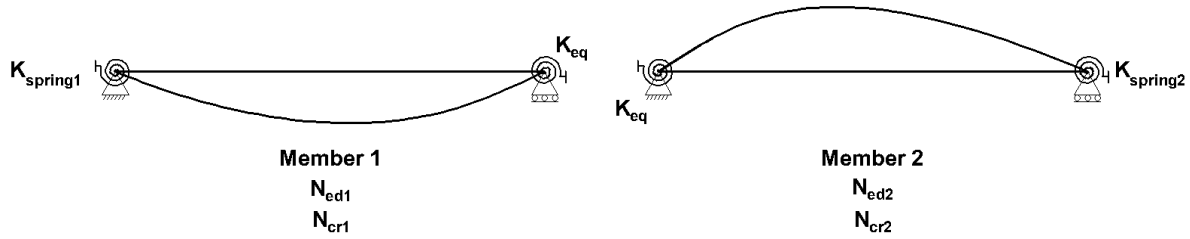


*Figure 159. Equivalent problem for the case of the continuous column.*

$$N_{ed,2} = N_{cr,2} \quad 34.$$

$$LR = \frac{N_{ed,1}}{N_{ed,2}} \quad 35.$$

$$K_{eq} = \left(1 - \frac{N_{ed,1}}{N_{cr,1}}\right) K_{initial} \quad 36.$$

By substituting Equation 34. Into Equation 35., and then Equation 35. Into Equation 36., Equation 37. is created. This equation gives the equivalent stiffness of the supporting member in the buckling problem. If the value of the stiffness becomes negative, then the assumption that member 2 has buckled does not hold and member 1 buckles first. The formulas for this case are the same and only switching the indices is required.

$$K_{eq} = K_{in} * \left(1 - LR \frac{N_{cr,2}}{N_{cr,1}}\right) \quad 37.$$

Even though it has been stated that the buckled member can provide no stiffness, in Figure 159 the supporting member is assumed to be also supported by the equivalent supporting spring. This is due to the continuity of moments, which means that whatever supporting moment can develop at the buckled member's end, the same moment will be developed at the supporting member's end. At a later stage the comparison between assuming a rotation spring equal to the equivalent spring and no rotational support will be performed to judge the validity of each assumption.

## C.3 Solution process

The solution process to be followed has the main goal of calculating the buckling load of the most critical member. This is done by calculating the equivalent problem of the continuous problem as presented in Figure 159, by using Equation 37. to determine the equivalent supporting spring of each member. From Equation 37. it is obvious that the critical buckling loads of both members are needed to calculate the equivalent spring. For this reason, an iterative process is required. By assuming initial buckling loads for each member, the equivalent spring can be calculated, and in turn a new buckling load for each member can be calculated by accounting for their boundary conditions. In this work the buckling load for the simply supported member were used as initial values. The iterative process converges to a reasonable solution by the third iteration, but due to the low computational cost, 15 iterations were performed for all results.

To calculate the buckling load of the members the solution process described in the book of "Exact solutions for buckling of structural members" (C. M. Wang et al., 2004) was used. The specific problem deals with the calculation of the buckling load of a member with elastic restraints on its ends (Figure 160). In this example the ends of the member are considered translationally fixed and thus the stability criteria, as described in the book, is given by Equation 38.. By solving Equation 38. The variable $\alpha$ is caclculated and from Equation 39. the buckling load of each member can be found.

$$[2\xi_0\xi_1 + \alpha(\xi_0 + \xi_1)]\cos\sqrt{\alpha} - \sqrt{\alpha}(\alpha + \xi_0 + \xi_1 - \xi_0\xi_1)\sin\sqrt{\alpha} - 2\xi_0\xi_1 = 0 \quad 38.$$

Where:

$\alpha$ variable to solve the equation for

$\xi_{0,1}$ rotational spring of end 0 and 1. normalized against stiffness of member $\frac{EI}{L}$

$$N_{cr} = \alpha \frac{EI}{L^2} \quad 39.$$

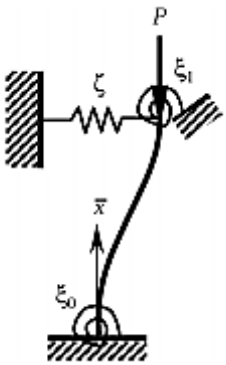


*Figure 160. Buckling problem used to calculate buckling loads in all further investigations* (C. M. Wang et al., 2004).

## C.4 Numerical application

To investigate the validity of the new method, the following investigation is performed (Figure 161):

- Without the loss of generality, member A is defined as the supporting member, meaning it will have a higher buckling load than member B. In all configurations, member A is the first number presented (e.g. configuration 4-6 means that member A is 4 and member B is 6).
- To perform a parametric study, ten different members are defined and presented in Table 40.
- In all configurations supports 2 and 3 prevent all displacements except for axial movement and rotations in the Y axis of the members.
- Support 1 prevents all displacements, with the rotational stiffness of the support in the Y axis being allowed to vary.
- The loading of member A is given as a Load Ratio of the loading on member B.
- Shear deformations are not included in the FEA, as the solution process used does not account for them.

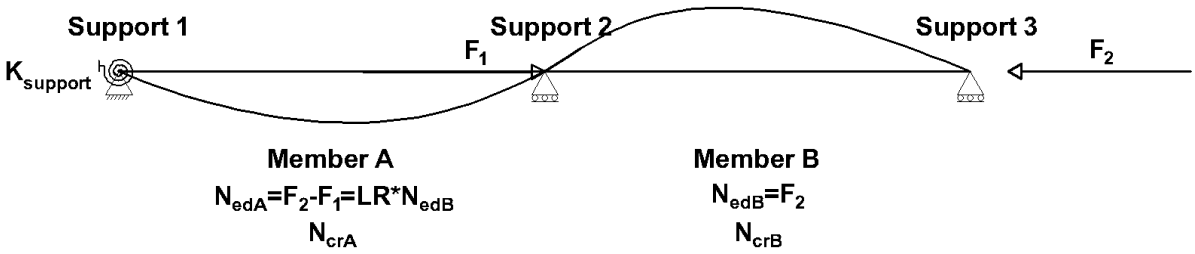


*Figure 161. Set up used for investigation of the proposed new method.*

Table 40. Members used in the parametric study of the new method

| Member | Cross section | Length | I | Ncr/π^2 | EI/L |
|---|---|---|---|---|---|
| | *EN 10210-2:2006* | *[m]* | *[m4]* | *[kN]* | *[kNm/rad]* |
| 1 | SHS 50 /2.6 | 1 | 1.80E-07 | 37.9 | 37.9 |
| 2 | SHS 50 /6.3 | 1 | 3.28E-07 | 68.8 | 68.8 |
| 3 | SHS 100/4 | 2 | 2.32E-06 | 121.7 | 243.4 |
| 4 | SHS 100/10 | 2 | 4.62E-06 | 242.6 | 485.2 |
| 5 | SHS 150/5 | 3 | 1.00E-05 | 233.8 | 701.4 |
| 6 | SHS 150/16 | 3 | 2.43E-05 | 567.0 | 1701.0 |
| 7 | SHS 200/8 | 4 | 3.71E-05 | 486.8 | 1947.2 |
| 8 | SHS 200/16 | 4 | 6.39E-05 | 839.2 | 3356.9 |
| 9 | SHS 200/8 | 8 | 3.71E-05 | 121.7 | 973.6 |
| 10 | SHS 200/16 | 8 | 6.39E-05 | 209.8 | 1678.4 |

## C.4.1 Support 1-Pinned

For the first investigation, the assumption that Support 1 is pinned is adopted. The Load Ratios employed had the values of 0.0, 0.3, 0.7 and 1.0. The results are given as the percentage difference between the calculated buckling value of the new method and the calculated value from the FE analysis (Equation 40.). The results are presented in Figure 162.

$$\Delta_{buckling\ load} = \frac{N_{cr,FEA} - N_{cr,New\ method}}{N_{cr,FEA}} \qquad 40.$$

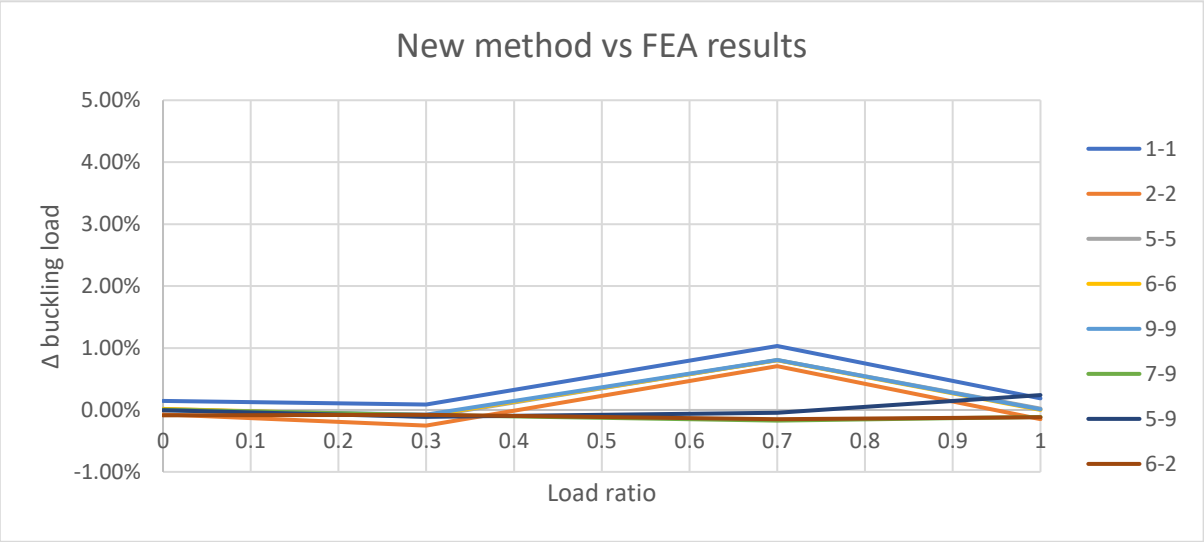


*Figure 162. Initial results for new method. Results given as percentage difference of the new method and values calculated by the FE program*

First, it is observed that the difference between the new method and the FEA results is at the most 1%. It appears that the developed method can predict adequately the buckling, at least for these initial configurations. It is also noted that for the extreme cases of load ratios of 0.0 and 1.0, for the configurations that have the same

members, the new method correctly predicts the buckling load. This makes sense as for a load ratio 0.0, the supporting member is unloaded and thus provides its whole rotational restraint with no interaction from the second member. For load ratio 1.0 the supporting member buckles along with the second member meaning both members act like simply supported members. It is also interesting that all the configurations with the same members the graph follows the same values. For the configurations of 1-1 and 2-2 a small disagreement is observed, and it is attributed to a rounding error as these configurations have small buckling loads. This is also supported by the fact that they appear to not have zero difference for the edge case of load ratios of 0.0 and 1.0.

Another observation that can be made is that, for the configurations that are not composed of the same members, their graphs seem like the configurations that have same members, just extended towards higher values of Load Ratio. This would indicate that the error of the new method increases when the supporting member goes close to buckling but should have a maximum value. This is because, if the supporting member reaches its buckling load, the new method is exact, and the error needs to go to zero. As such the error of the new method should be upper bound.

To further investigate the trend of the error observed, the same set up is used, but this time member A remains the same for all configurations and member B changes from less stiff to most stiff. Again, the same trend is observed (Figure 163). As the second members become less and less stiff and their buckling loads decrease, the graph that is given for symmetric problems (same members) is extended towards the right end of the graph.

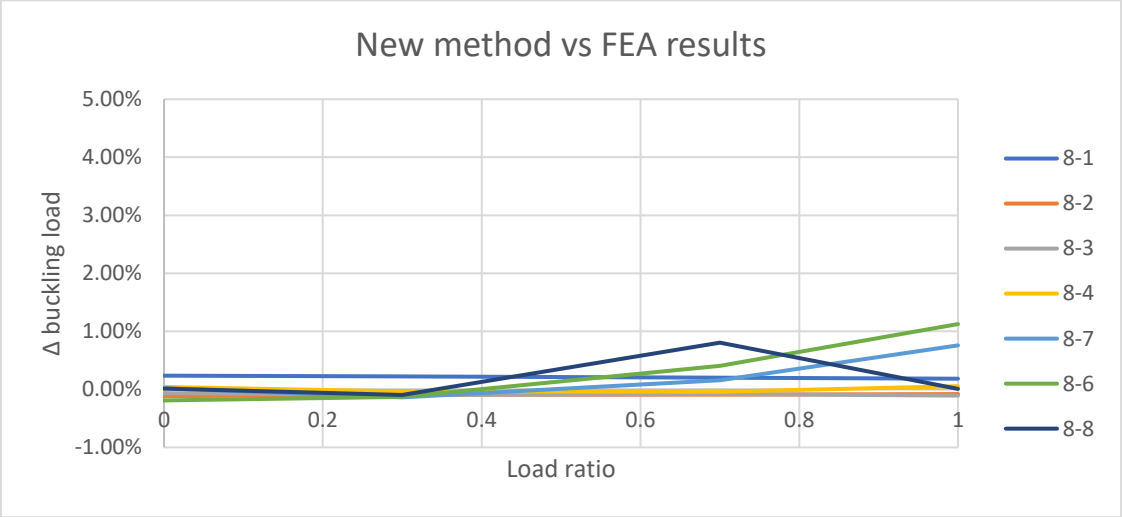


*Figure 163. Results of the new method by keeping the supporting member the same.*

From the results so far, it is certain that the new method has an error, but it appears that it is bounded by a maximum. To further Illustrate this, the differences in buckling load are plotted against the equivalent supporting springs (Figure 164) normalized against the supporting member's stiffness. All the results presented up till now were utilized. A higher rotational spring corresponds to the supporting member being further away from buckling. It can be observed that the higher the value becomes, the lower the expected error becomes. For values of zero the error is also minimized as the supporting member buckles and both members act as simply supported members. Lastly, the closer that both members are to buckling simultaneously, the greater the error appears to become.

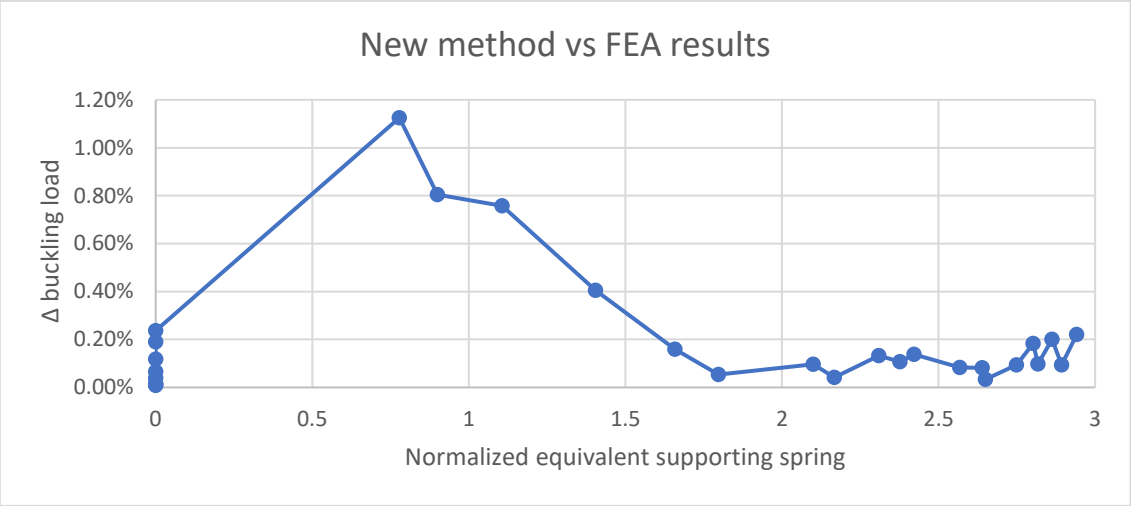


*Figure 164. Percentile difference between new method and FEA results plotted against the equivalent supporting spring normalized against the stiffness of the supporting member. The maximum values of this is three as Support 1 has been assumed pinned.*

## C.4.2 Support 1-Rotationally restrained

Another investigation performed was the increase of the buckling load of the supporting member by increasing the rotational stiffness of Support 1. For this investigation configuration 8-8 was used, to keep members with the same stiffness. The difference is plotted against rotation spring used at the end support (Figure 165). It can be observed that the difference again peaks for the case where the supporting member has a buckling load close to the second member. It is interesting to observe that the error remains the same after a certain rotational stiffness is introduced. This is due to the supporting member reaching fixed boundary conditions and as such the buckling load does not change any more. As such the error converges to the case of a fixed support at Support 1.

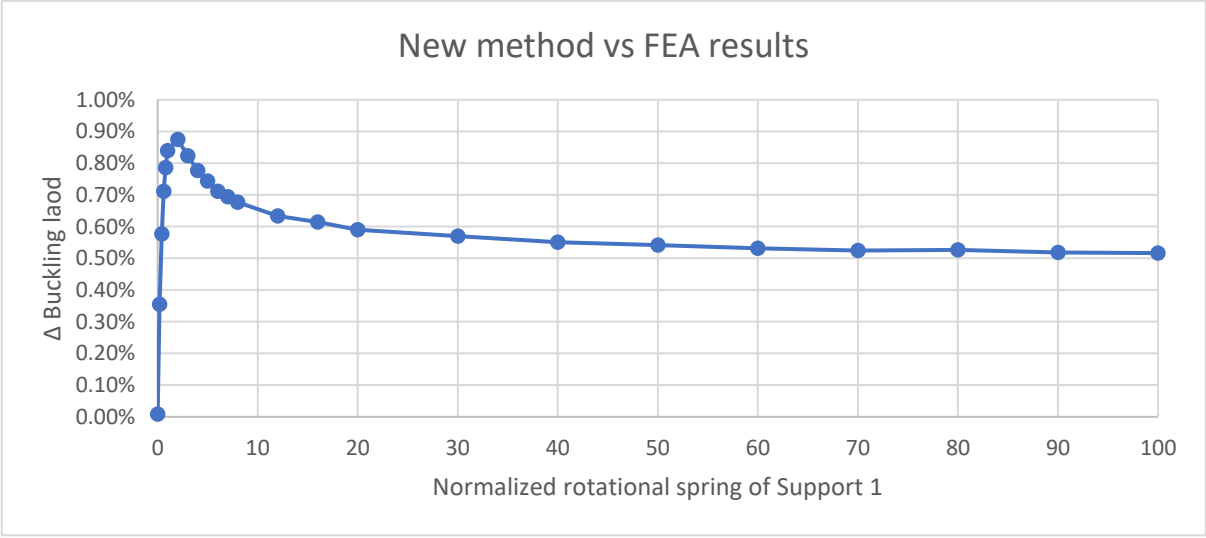


*Figure 165. Percentile difference between new method and FEA results plotted against the rotational spring of Support 1, normalized against the stiffness of the supporting member.*

## C.4.3 Effect of change of Load Ratio

Lastly, the effects of different Load Ratios are investigated by collecting more dense data points for a specific configuration. In this case configuration 6-6 was used and many different Load Ratios were used to create a detailed graph (Figure 166). The boundary condition at Support 1 is assumed pinned. The results are like what has been found up till now, with the additional remark that the error appears to produce a smooth curve. As was already assumed, the more detailed graph gives a maximum error before going to zero in the case where the supporting member buckles simultaneously with the other member.

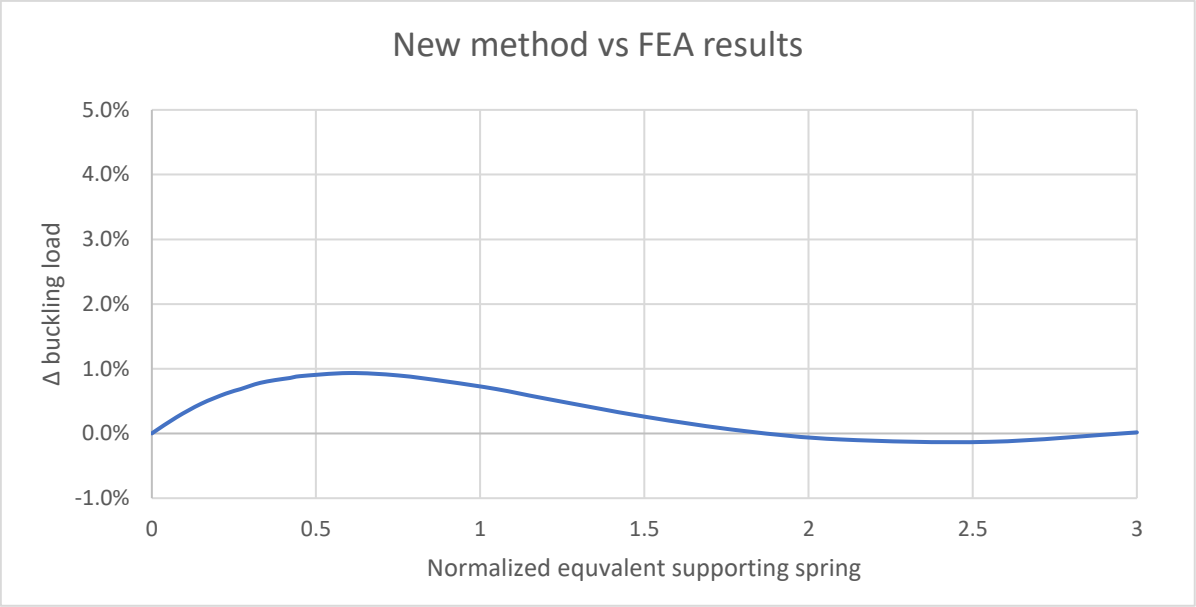


*Figure 166. Percentile difference between new method and FEA results plotted against the equivalent supporting spring, normalized against the buckled member*

### C.4.4 Effects of assuming zero spring for supporting member.

As was mentioned previously in section C.2, one alternative and logical assumption could be to consider that the supporting member is not restrained at all from the buckled member, since the buckled member does not provide any stiffness. To check the effects of such an assumption and to compare it to the assumption adopted by the new method, a similar investigation to the one performed in the previous section (C.4.3) is also done here. The only assumption that changes is that, additionally to the new method results, results produced by assuming that the supporting member has no restraint from the buckled member are also provided.

Additionally, to investigate if the actual effects from the interaction of the two members are significant, two additional graphs are created. The first one is for the case that the buckled member is supported by the complete stiffness of the supporting member, disregarding the effects of the compressive loading (3EI/L). The second one is for the case that the buckled member is not supported at all by the supporting member and is considered pinned.

The four different assumptions that are used can be summed up as follows:

- Supporting member supported by equivalent supporting spring.
- Supporting member with no support from buckled member.
- Assuming no loss of stiffness of supporting member due to the compressive load.
- Assuming no support from supporting member.

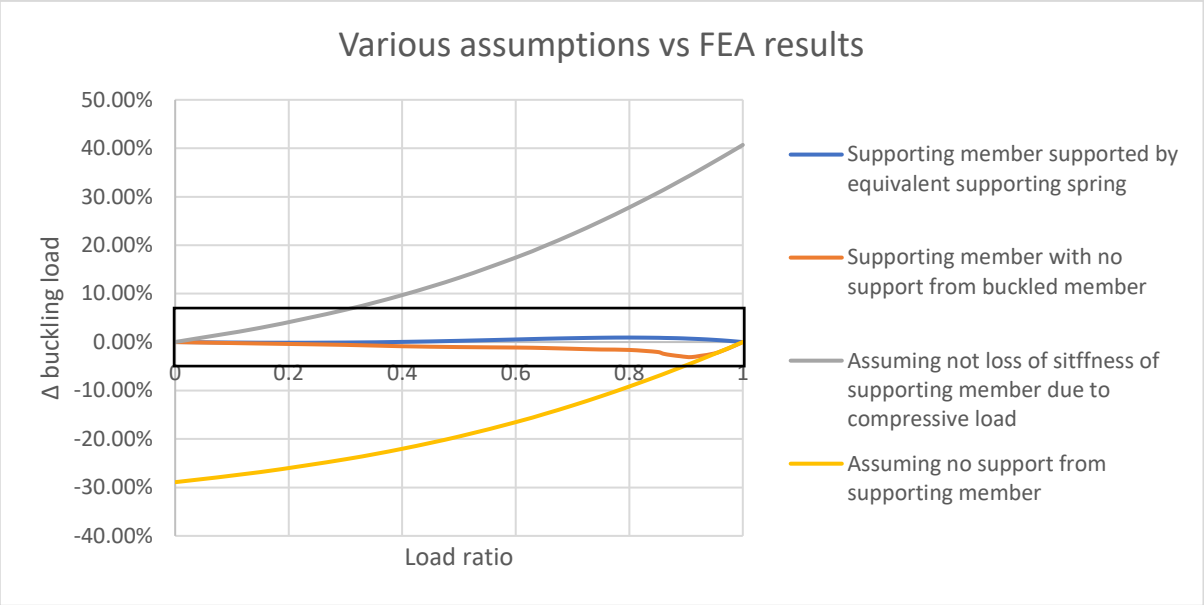


*(a)*

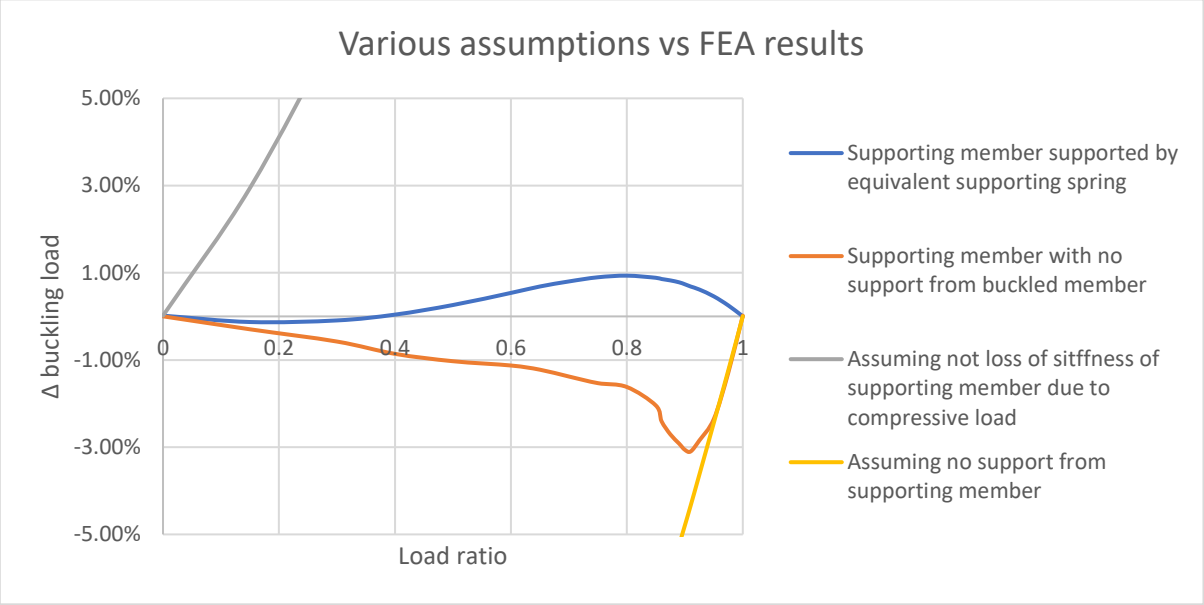


*(b)*

*Figure 167. Comparison of results of using different assumptions for the buckling calculations. On the bottom (b) a zoomed plot of the complete plot (a) is provided, to make details more visible.*

From the results presented in Figure 167 it becomes obvious that the interaction between the members of the continuous needs to be considered. Failing to do so can produce an error of up to 40% which is not acceptable. Regarding the assumptions adopted for the support conditions of the supporting member, it can be observed that the assumption for which the supporting member is not supported by the buckled member provides a worse approximation than the originally stated assumption. The results may be conservative, but the error three times higher (although still only 3%) and additionally the graph appears to have a random form, compared to the smooth form of the original assumption. As such, as is already proposed, for the application of this new method the support of the supporting member by the equivalent supporting spring is prescribed.

## C.5 Conclusions

The main conclusion that can be drawn from the investigations performed, are the following:

- The developed new method can adequately capture and calculate the buckling load of a continuous column. In all investigations performed the error of the new method compared to FEA results remained below 2%.
- The only prescribed limitation for the application of the method is that the three support points of the column are required to be translationally fixed.
- The smooth error graph observed could be due to disregarding certain effects owning to the simplified assumptions adopted for the application of the method. This indicates that the method may be further developed, although the utility of such an endeavour may be questionable as the accuracy achieved is already adequate for engineering practice (below 2%).
- Lastly this method could be generalized, by accounting for the interaction of multiple connected members and potentially be extended to a whole truss structure, making it applicable to this thesis topic.

# APPENDIX D PROPOSAL OF BUCKLING LENGTH CALCULATION APPROACH FOR TRUSS GIRDERS

## D.1 Approach

One of the difficult parts of calculating buckling lengths is to quantify the rotational restraint the truss members provide to other truss members. An attempt was done to investigate this in APPENDIX C by developing a new method but was only developed for a continuous column and not generalized to a truss girder. In this different approach, approximate values of the restraint experienced by an individual truss member are attempted to be quantified. This is done by determining an equivalent supporting spring for the member that the buckling load is required. For this reason, the term "support factor" (SF) is defined. By support factor, the factor by which the stiffness of a member needs to be multiplied by, in order to quantify the bending stiffness it provides to an adjacent member. For example, the SF for an unloaded member connected rigidly to another member with a hinged end is 3, whilst if the member's end is fixed the SF becomes 4. It was shown in APPENDIX C that the presence of a compressive force acting upon a supporting member reduces the SF and it may be difficult to determine it. In this proposed approach these SF are found by fitting the results from a hand calculation to the results produced by the finite element analysis.

To perform the hand calculations simplified assumptions are adopted. Specifically, on both ends of the members investigated, the same spring values is going to be assumed. Also, for the out of plane buckling only the bending stiffness is used, even though the torsional stiffness of the braces and chord may play a role in the behaviour. For the connection stiffness, the results from section 3.2 are used.

For the equivalent supporting spring of the chord the supporting chords stiffness is simply added to the spring value (Equation 41.), whilst the stiffness of the braces must pass through the connection thus Equation 42. is used. The final rotational stiffness of the equivalent supporting spring is given by equation 43.. For the braces, the stiffnesses from the supporting chords and braces are given in the same manor by Equations 44. And 45.. with the additional step of including the effects of the connection at their end. The final rotational stiffness of the equivalent supporting spring is given by Equation 46.. An overview of the process can be seen in Figure 168.

$$K_{chord,buck}^{Chord} = SF_{chord}^{Chord} * K_{chord} \quad 41.$$

$$K_{brace,buck}^{Chord} = \frac{1}{K_{con.}} + \frac{1}{SF_{brace}^{Chord} * K_{brace}} \quad 42.$$

$$K_{spring}^{Chord} = SF_{chord}^{Chord} * K_{chord} + \left(\frac{1}{K_{con.}} + \frac{1}{SF_{brace}^{Chord} * K_{brace}}\right) \quad 43.$$

$$K_{chord,buck}^{Brace} = SF_{chord}^{Brace} * K_{chord} \quad 44.$$

$$K_{brace,buck}^{Brace} = \frac{1}{K_{con.}} + \frac{1}{SF_{brace}^{Brace} * K_{brace}} \quad 45.$$

$$K_{spring}^{Brace} = \frac{1}{K_{con.}} + \frac{1}{SF_{chord}^{Brace} * K_{chord} + \left(\frac{1}{K_{con.}} + \frac{1}{SF_{brace}^{Brace} * K_{brace}}\right)} \quad 46.$$

Where:

| | |
|---|---|
| $K_{chord}$ | The stiffness of the chords, equal to $EI_{chord}/L_{chord}$ |
| $K_{brace}$ | The stiffness of the braces, equal to $EI_{brace}/L_{brace}$ |
| $SF_j^i$ | The supporting factor provided from members $j$ for the buckling of member $i$ |
| $K_{con.}$ | Stiffness of the connections as calculated in section 3.2 |
| $K_{spring}^i$ | Equivalent supporting spring for the buckling of member $i$ |

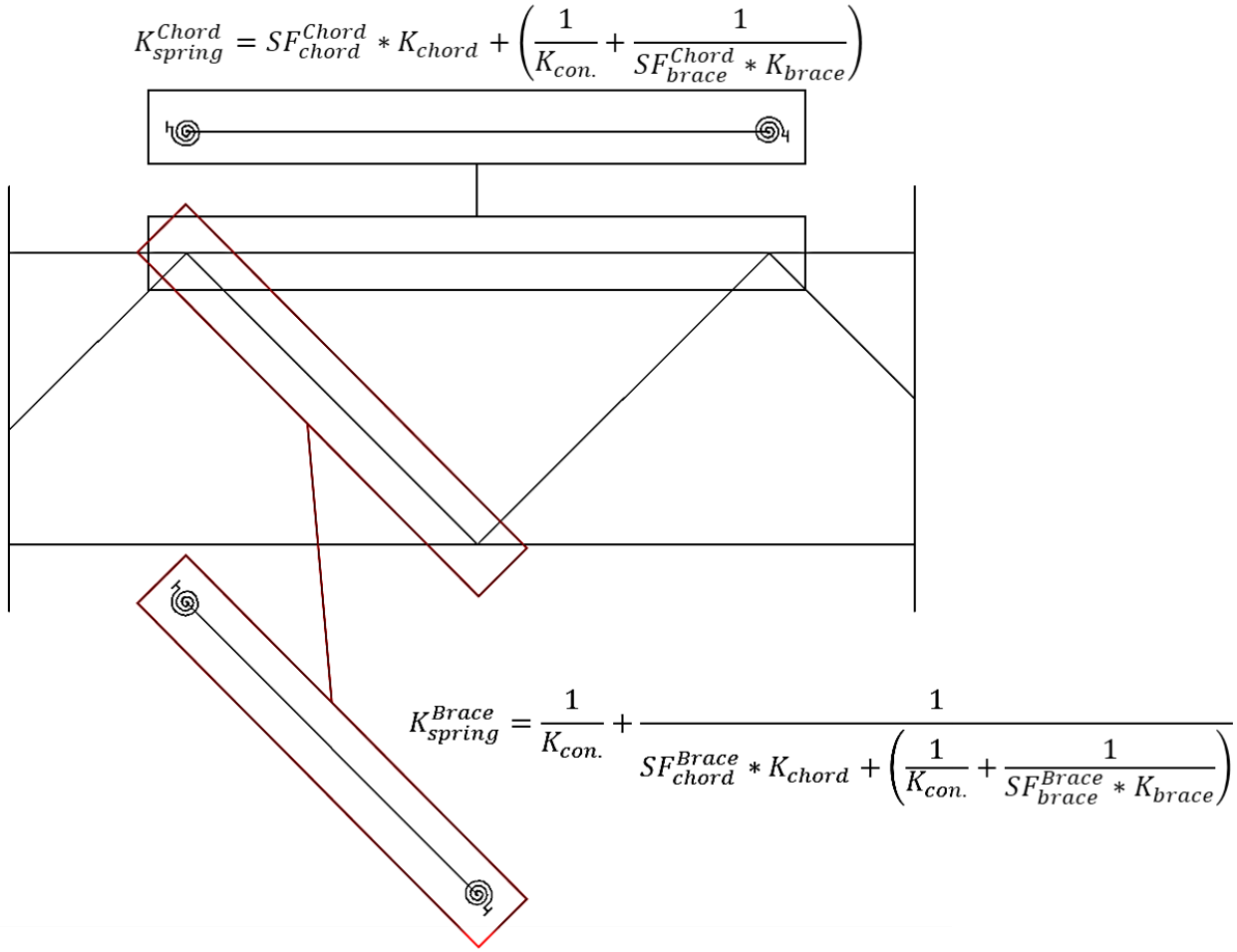


*Figure 168. Overview of the proposed new approach.*

Having formulated the equivalent rotational springs, the buckling solution of the member can be approximated by many different approaches. In this work, the solution process that was described in APPENDIX D was used

(C. M. Wang et al., 2004). For simplicity, the nomograph provided by the Dutch National Annex of Eurocode 3 can also be used (Figure 169), which make the method especially suited for engineering practice. The results obtained from the hand calculation are compared to the results obtained from the investigation into the centric joints from Chapter 3. As only rotational stiffnesses have been accounted for, the buckling lengths refer to the member buckling lengths and the buckling lengths for a restrained tension chord are going to be used.

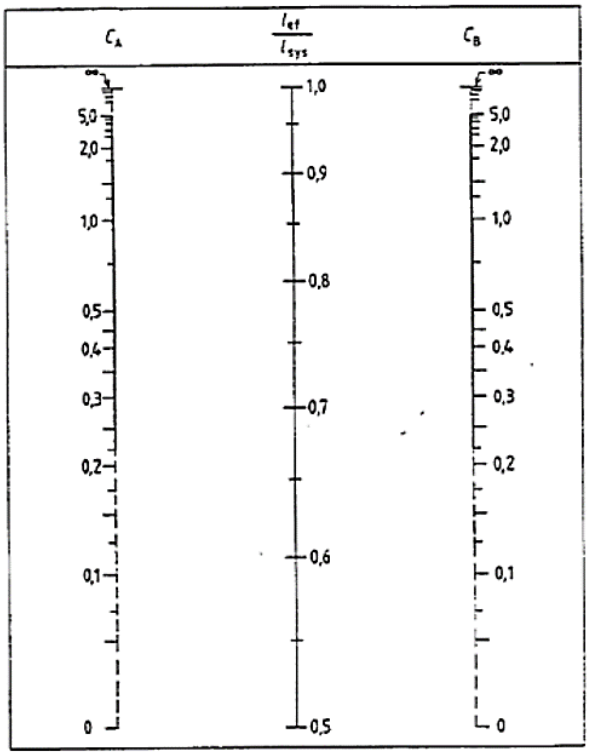


*Figure 169. Nomograph for calculating buckling lengths for a column rotationally restrained on both ends (Dutch National Annex for Eurocode 3).*

## D.2 In-plane buckling

### D.2.1 Chord buckling

For the chord buckling in-plane it was determined that the supporting factors that give the best fit for the proposed approach were $SF_{chord}^{Chord} = 0.6$ and $SF_{brace}^{Chord} = 3$. It is noted that the SF of the brace includes the effects of both braces that support the end of the chord.

Table 41. Chord buckling factor for in plane buckling $K_{ch,in}$

| | | γ = 15.9 | | | γ = 10 | | | γ = 6.25 | | |
|---|---|---|---|---|---|---|---|---|---|---|
| | | Proposal | FEM Results | Diff. | Proposal | FEM Results | Diff. | Proposal | FEM Results | Diff. |
| | 0.25 | 0.90 | 0.88 | 1.8% | 0.90 | 0.88 | 2.5% | 0.90 | 0.89 | 1.4% |
| | 0.40 | 0.88 | 0.85 | 3.3% | 0.89 | 0.86 | 2.5% | 0.89 | 0.90 | -1.0% |
| β | 0.50 | 0.86 | 0.85 | 1.0% | 0.87 | 0.86 | 0.7% | 0.87 | 0.88 | -1.0% |
| | 0.60 | 0.83 | 0.82 | 0.2% | 0.84 | 0.84 | 0.1% | 0.85 | 0.86 | -1.4% |
| | 0.75 | 0.75 | 0.73 | 2.8% | 0.78 | 0.75 | 4.2% | 0.80 | 0.77 | 4.4% |

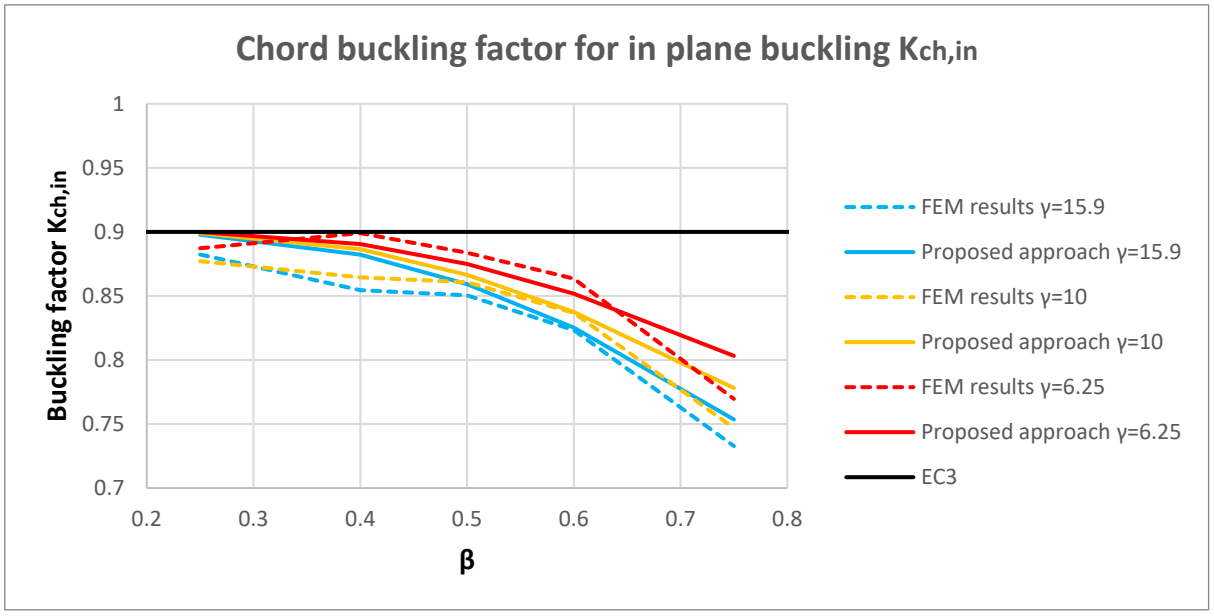


*Figure 170. Chord buckling factor for in plane buckling $K_{ch,in}$.*

## D.2.2 Brace buckling

From the preliminary results it was apparent that the SF that need to be used to capture the buckling of the braces, are different depending on the chord that is used. This also makes sense since the less stiff the chords are, the more interaction would be expected with the buckling of the braces. For this reason, three different SF are defined, each case capturing the behaviour of the finite element results of a chord with a specified γ. In practice, potentially the SF can be given as a function of the chord and brace stiffness.

In the first case, the SF are chosen to match the results of the chord with γ=15.9. The SF chosen are $SF_{chord}^{Brace} = 1.1$ and $SF_{brace}^{Brace} = 1.5$, for the chords and braces respectively.

Table 42. Brace buckling factor for in plane buckling $K_{br,in}$. Results matching chord with γ=15.9.

| | | γ | | | | | | | | |
|---|---|---|---|---|---|---|---|---|---|---|
| | | 15.9 | | | 10 | | | 6.25 | | |
| | | Proposal | FEM Results | Diff. | Proposal | FEM Results | Diff. | Proposal | FEM Results | Diff. |
| β | 0.25 | 0.58 | 0.59 | -0.7% | 0.53 | 0.53 | 0.9% | 0.51 | 0.51 | 1.0% |
| | 0.40 | 0.67 | 0.68 | -1.0% | 0.59 | 0.57 | 2.6% | 0.54 | 0.52 | 3.6% |
| | 0.50 | 0.72 | 0.72 | -0.6% | 0.63 | 0.61 | 4.0% | 0.58 | 0.56 | 4.2% |
| | 0.60 | 0.74 | 0.74 | -0.3% | 0.67 | 0.63 | 5.6% | 0.62 | 0.58 | 7.3% |
| | 0.75 | 0.76 | 0.81 | -5.9% | 0.71 | 0.68 | 4.6% | 0.67 | 0.61 | 10.1% |

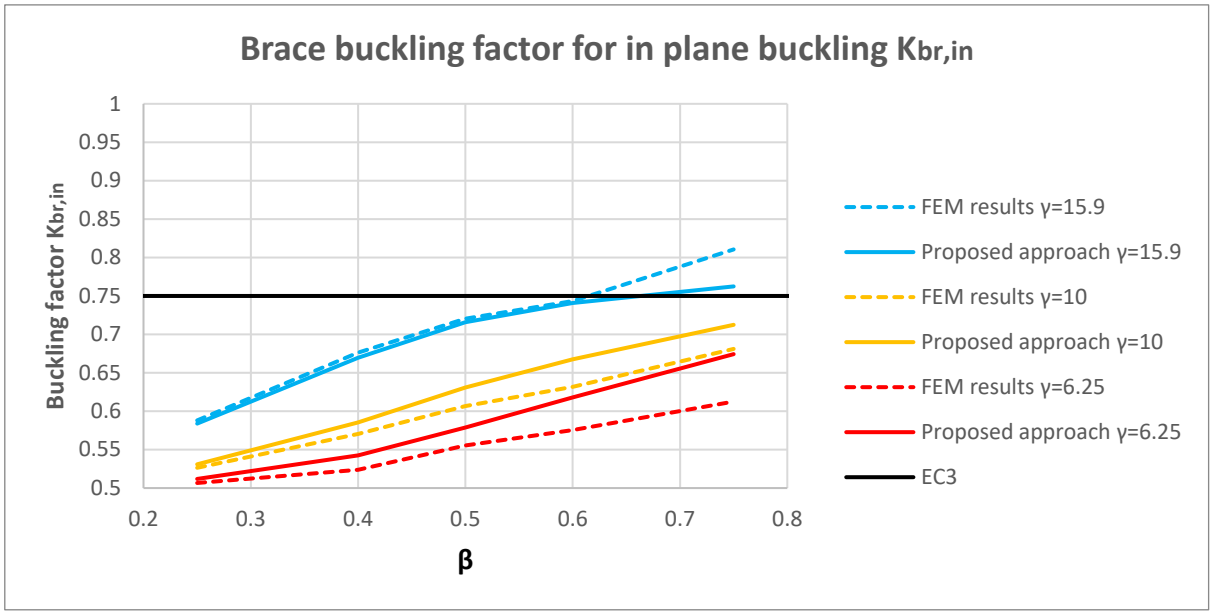


*Figure 171. Brace buckling factor for in plane buckling $K_{br,in}$. Results matching chord with γ=15.9.*

For the second case, the SF are chosen to match the results of the chord with γ=10. The SF chosen are $SF_{chord}^{Brace} = 1.5$ and $SF_{brace}^{Brace} = 2$, for the chords and braces respectively.

Table 43. Brace buckling factor for in plane buckling $K_{br,in}$. Results matching chord with γ=10.

| | | γ | | | | | | | | |
|---|---|---|---|---|---|---|---|---|---|---|
| | | 15.9 | | | 10 | | | 6.25 | | |
| | | Proposal | FEM Results | Diff. | Proposal | FEM Results | Diff. | Proposal | FEM Results | Diff. |
| | 0.25 | 0.56 | 0.59 | -4.2% | 0.52 | 0.53 | -0.7% | 0.51 | 0.51 | 0.4% |
| | 0.40 | 0.64 | 0.68 | -6.0% | 0.56 | 0.57 | -1.0% | 0.53 | 0.52 | 1.5% |
| β | 0.50 | 0.68 | 0.72 | -5.9% | 0.60 | 0.61 | -0.8% | 0.56 | 0.56 | 0.7% |
| | 0.60 | 0.70 | 0.74 | -5.5% | 0.63 | 0.63 | 0.3% | 0.59 | 0.58 | 2.7% |
| | 0.75 | 0.72 | 0.81 | -10.7% | 0.68 | 0.68 | -0.9% | 0.64 | 0.61 | 4.5% |

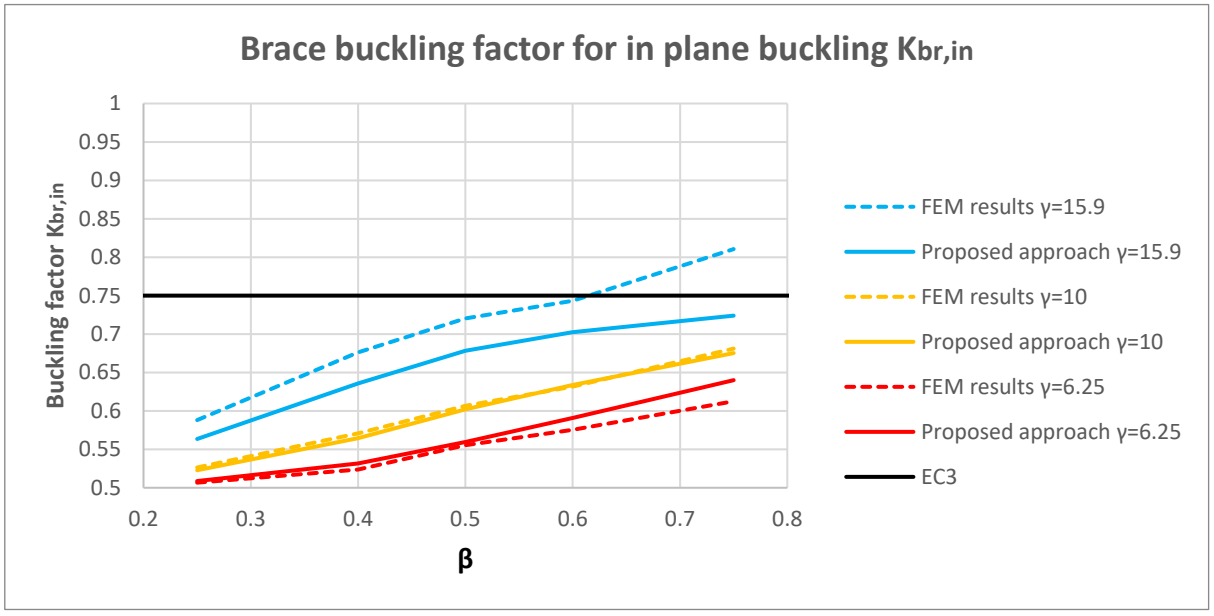


*Figure 172. Brace buckling factor for in plane buckling $K_{br,in}$. Results matching chord with γ=10.*

Lastly, in the third case, the SF are chosen to match the results of the chord with γ=6.25. The SF chosen are $SF_{chord}^{Brace} = 1.9$ and $SF_{brace}^{Brace} = 3$, for the chords and braces respectively.

Table 44. . Brace buckling factor for in plane buckling $K_{br,in}$. Results matching chord with γ=6.25.

| | | γ | | | | | | | | |
|---|---|---|---|---|---|---|---|---|---|---|
| | | 15.9 | | | 10 | | | 6.25 | | |
| | | Proposal | FEM Results | Diff. | Proposal | FEM Results | Diff. | Proposal | FEM Results | Diff. |
| β | 0.25 | 0.55 | 0.59 | -6.5% | 0.52 | 0.53 | -1.6% | 0.51 | 0.51 | 0.0% |
| | 0.40 | 0.61 | 0.68 | -10.0% | 0.55 | 0.57 | -3.5% | 0.52 | 0.52 | 0.2% |
| | 0.50 | 0.65 | 0.72 | -10.4% | 0.58 | 0.61 | -4.3% | 0.55 | 0.56 | -1.6% |
| | 0.60 | 0.67 | 0.74 | -10.4% | 0.61 | 0.63 | -4.0% | 0.57 | 0.58 | -0.7% |
| | 0.75 | 0.68 | 0.81 | -15.6% | 0.64 | 0.68 | -6.0% | 0.61 | 0.61 | -0.3% |

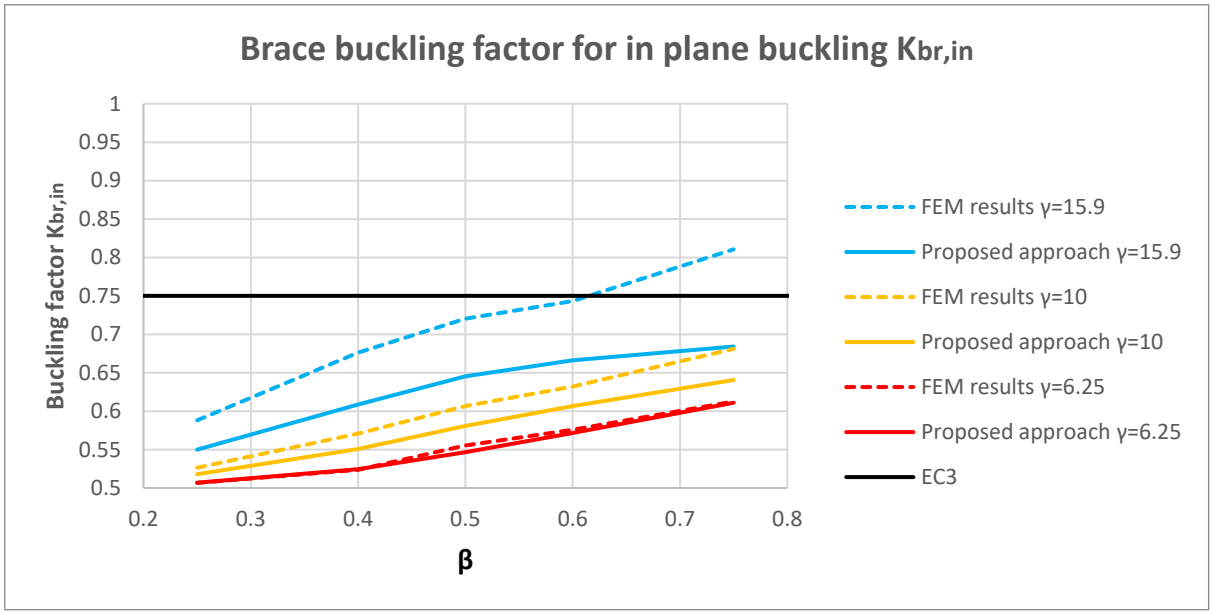


*Figure 173. Brace buckling factor for in plane buckling $K_{br,in}$. Results matching chord with γ=6.25.*

## D.3 Out of plane buckling

### D.3.1 Chord buckling

For the chord buckling out of plane it was determined that the supporting factors that give the best fit for the proposed approach were $SF_{chord}^{Chord} = 0.75$ and $SF_{brace}^{Chord} = 1.5$. It is noted that the SF of the brace includes the effects of both braces that support the end of the chord.

Table 45. Chord buckling factor for out of plane buckling $K_{ch,out}$.

| | | γ = 15.9 | | | γ = 10 | | | γ = 6.25 | | |
|---|---|---|---|---|---|---|---|---|---|---|
| | | Proposal | FEM Results | Diff. | Proposal | FEM Results | Diff. | Proposal | FEM Results | Diff. |
| | 0.25 | 0.88 | 0.88 | 0.5% | 0.88 | 0.88 | 0.5% | 0.88 | 0.88 | 0.6% |
| | 0.40 | 0.87 | 0.85 | 2.2% | 0.88 | 0.87 | 0.2% | 0.88 | 0.92 | -4.5% |
| β | 0.50 | 0.86 | 0.85 | 0.7% | 0.87 | 0.88 | -1.3% | 0.87 | 0.91 | -4.7% |
| | 0.60 | 0.84 | 0.84 | 0.1% | 0.85 | 0.87 | -1.8% | 0.86 | 0.85 | 1.3% |
| | 0.75 | 0.80 | 0.78 | 2.5% | 0.82 | 0.80 | 1.4% | 0.83 | 0.82 | 0.9% |

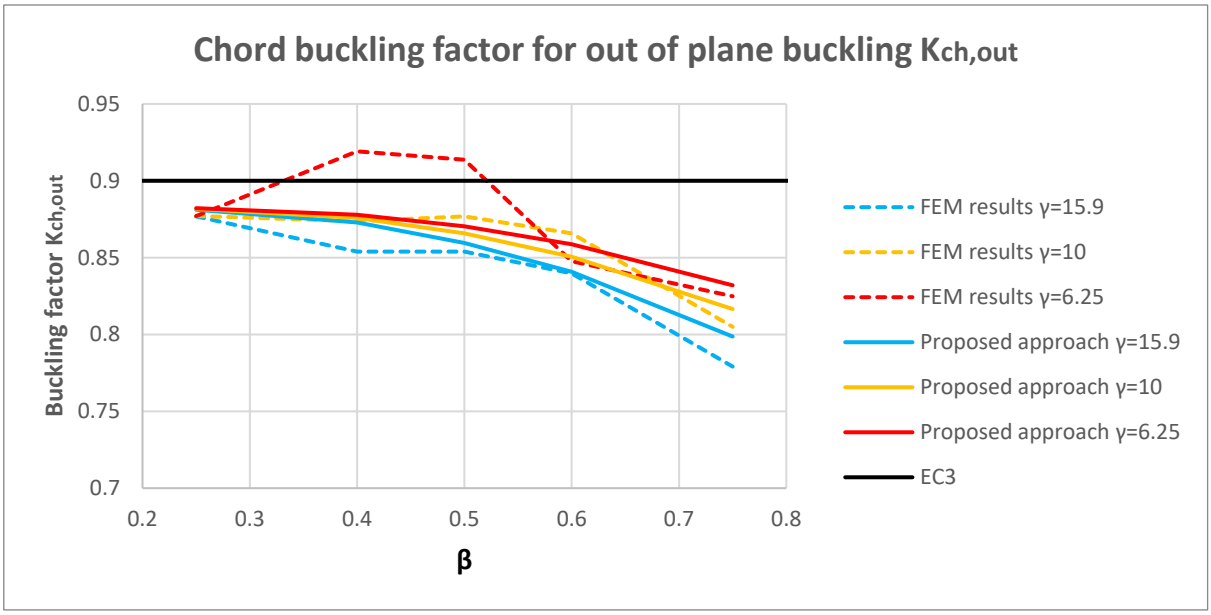


*Figure 174. Chord buckling factor for out of plane buckling $K_{ch,out}$.*

## D.3.2 Brace buckling

For the brace buckling out of plane it was determined that the supporting factors that give the best fit for the proposed approach were $SF_{chord}^{Brace} = 0.65$ and $SF_{brace}^{Brace} = 3$.

Table 46. Brace buckling factor for out of plane buckling $K_{br,out}$.

| | | γ = 15.9 | | | γ = 10 | | | γ = 6.25 | | |
|---|---|---|---|---|---|---|---|---|---|---|
| | | Proposal | FEM Results | Diff. | Proposal | FEM Results | Diff. | Proposal | FEM Results | Diff. |
| | 0.25 | 0.57 | 0.57 | -0.7% | 0.53 | 0.54 | -2.1% | 0.52 | 0.53 | -2.1% |
| | 0.40 | 0.63 | 0.63 | 0.5% | 0.59 | 0.59 | 0.5% | 0.56 | 0.56 | -0.3% |
| β | 0.50 | 0.67 | 0.68 | -0.7% | 0.63 | 0.63 | 1.3% | 0.60 | 0.59 | 1.5% |
| | 0.60 | 0.71 | 0.71 | 0.2% | 0.67 | 0.66 | 0.7% | 0.63 | 0.63 | 1.2% |
| | 0.75 | 0.73 | 0.75 | -3.2% | 0.74 | 0.74 | 0.3% | 0.67 | 0.67 | -0.2% |

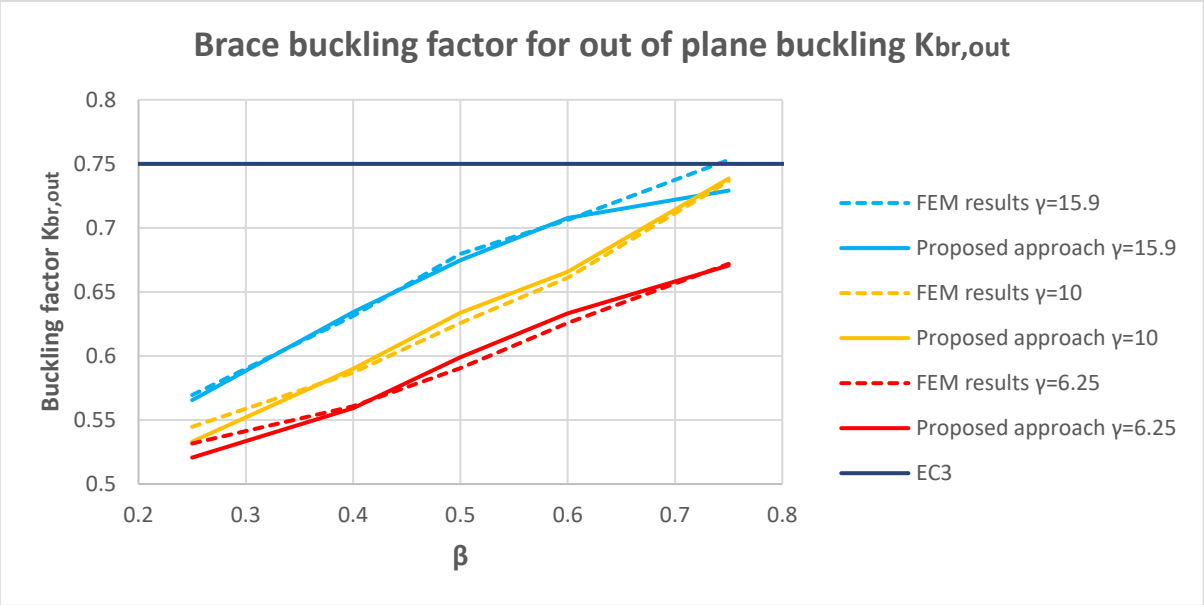


*Figure 175. Brace buckling factor for out of plane buckling $K_{br,out}$.*

## D.4 Conclusions

From comparing the results obtain from the proposed approach and the finite element model of the main investigation, it can be concluded that the proposed approach has potential. Firstly, the results matched quite well between them. Secondly, as the buckling problem required to be solved at the final steps is quite simple, it is suited for everyday engineering practice. Thirdly, only simplified assumptions were used in this investigation as it was outside the scope of the main investigation. The approach can be further improved by accounting for different stiffnesses on the tension and compression side, or by including the torsional behaviour for the out of plane buckling. Lastly, it may have a wider application scope than conventional buckling length formulas, as the calculations are based on the stiffnesses of the members and the connections instead of parameters that account for these indirectly, such as β and γ.

# APPENDIX E NUMERICAL RESULTS

## E.1 Stiffness calculations

In-plane stiffness (kNm/rad)

| | | γ = 15.9 | | | γ = 10 | | | γ = 6.25 | | |
|---|---|---|---|---|---|---|---|---|---|---|
| | | Rounded corners | No radius | Diff. | Rounded corners | No radius | Diff. | Rounded corners | No radius | Diff. |
| | 0.25 | 78.8 | 81.0 | -2.7% | 279.0 | 283.1 | -1.4% | 1025.4 | 1021.9 | 0.3% |
| | 0.40 | 179.5 | 183.8 | -2.3% | 615.7 | 615.1 | 0.1% | 2189.6 | 2156.6 | 1.5% |
| β | 0.50 | 326.8 | 342.7 | -4.6% | 1076.0 | 1097.2 | -1.9% | 3734.5 | 3637.9 | 2.7% |
| | 0.60 | 639.9 | 678.0 | -5.6% | 2021.1 | 2060.2 | -1.9% | 6643.8 | 6423.8 | 3.4% |
| | 0.75 | 2160.1 | 2303.2 | -6.2% | 6005.2 | 6165.8 | -2.6% | 16826.1 | 16585.7 | 1.4% |

Out of plane stiffness (kNm/rad)

| | | γ = 15.9 | | | γ = 10 | | | γ = 6.25 | | |
|---|---|---|---|---|---|---|---|---|---|---|
| | | Rounded corners | No radius | Diff. | Rounded corners | No radius | Diff. | Rounded corners | No radius | Diff. |
| | 0.25 | 203.8 | 216.6 | -5.9% | 606.1 | 630.8 | -3.9% | 1948.4 | 2031.5 | -4.1% |
| | 0.40 | 442.1 | 469.1 | -5.8% | 1296.1 | 1349.9 | -4.0% | 4159.2 | 4229.4 | -1.7% |
| β | 0.50 | 758.3 | 806.6 | -6.0% | 2074.0 | 2148.5 | -3.5% | 6463.9 | 6598.2 | -2.0% |
| | 0.60 | 1231.8 | 1256.9 | -2.0% | 3362.2 | 3384.9 | -0.7% | 10538.9 | 10047.7 | 4.9% |
| | 0.75 | 2930.7 | 3242.6 | -9.6% | 7685.7 | 7883.1 | -2.5% | 22063.7 | 21474.8 | 2.7% |

## E.2 Buckling lengths

### E.2.1 Centric joints

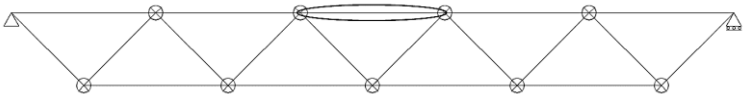

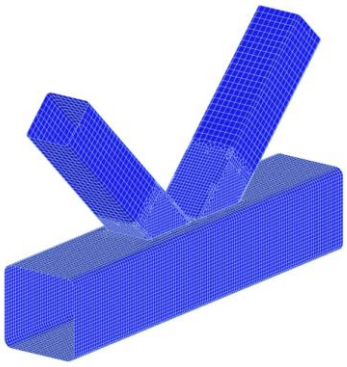

Chord buckling in-plane

| | | β | | | | |
|---|---|---|---|---|---|---|
| | | 0.25 | 0.4 | 0.5 | 0.6 | 0.75 |
| γ | 15.9 | 0.882 | 0.854 | 0.850 | 0.823 | 0.733 |
| | 10 | 0.877 | 0.864 | 0.861 | 0.837 | 0.747 |
| | 8 | 0.910 | 0.878 | 0.871 | 0.849 | 0.759 |
| | 7.04 | 0.911 | 0.889 | 0.878 | 0.857 | 0.765 |
| | 6.25 | 0.887 | 0.899 | 0.884 | 0.864 | 0.770 |

Chord buckling out of plane

| | | β | | | | |
|---|---|---|---|---|---|---|
| | | 0.25 | 0.4 | 0.5 | 0.6 | 0.75 |
| γ | 15.9 | 0.877 | 0.854 | 0.854 | 0.840 | 0.779 |
| | 10 | 0.877 | 0.874 | 0.877 | 0.866 | 0.805 |
| | 8 | 0.890 | 0.888 | 0.894 | 0.829 | 0.810 |
| | 7.04 | 0.878 | 0.903 | 0.906 | 0.842 | 0.821 |
| | 6.25 | 0.877 | 0.919 | 0.914 | 0.848 | 0.825 |

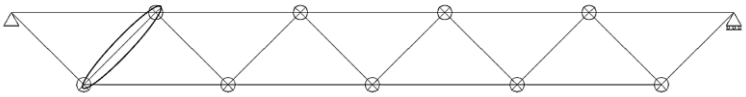

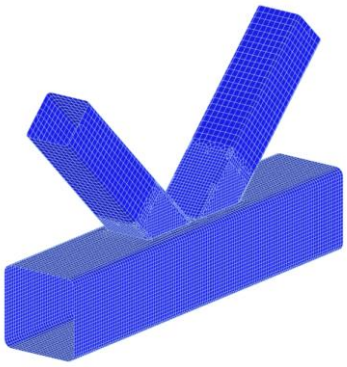

Brace buckling in-plane

| | | β | | | | |
|---|---|---|---|---|---|---|
| | | 0.25 | 0.4 | 0.5 | 0.6 | 0.75 |
| | 15.9 | 0.588 | 0.676 | 0.720 | 0.743 | 0.811 |
| | 10 | 0.526 | 0.571 | 0.606 | 0.632 | 0.681 |
| γ | 8 | 0.514 | 0.543 | 0.571 | 0.590 | 0.633 |
| | 7.04 | 0.511 | 0.532 | 0.555 | 0.576 | 0.613 |
| | 6.25 | 0.507 | 0.524 | 0.542 | 0.560 | 0.594 |

Brace buckling in plane

| | | β | | | | |
|---|---|---|---|---|---|---|
| | | 0.25 | 0.4 | 0.5 | 0.6 | 0.75 |
| | 15.9 | 0.570 | 0.631 | 0.680 | 0.706 | 0.753 |
| | 10 | 0.545 | 0.587 | 0.626 | 0.661 | 0.737 |
| γ | 8 | 0.539 | 0.576 | 0.611 | 0.655 | 0.702 |
| | 7.04 | 0.537 | 0.571 | 0.603 | 0.643 | 0.689 |
| | 6.25 | 0.532 | 0.561 | 0.590 | 0.626 | 0.672 |

## E.2.2 Eccentric joints

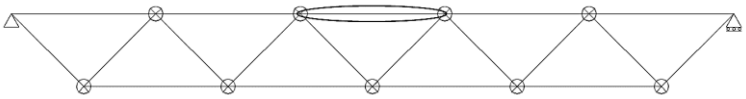

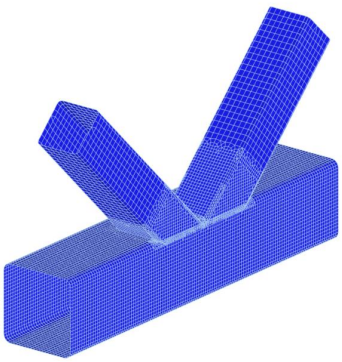

Chord buckling in-plane

| | | β | | | | |
|---|---|---|---|---|---|---|
| | | 0.25 | 0.4 | 0.5 | 0.6 | 0.75 |
| | 15.9 | 0.870 | 0.802 | 0.790 | 0.788 | 0.711 |
| | 10 | 0.874 | 0.856 | 0.845 | 0.819 | 0.741 |
| γ | 8 | 0.897 | 0.873 | 0.861 | 0.841 | 0.755 |
| | 7.04 | 0.902 | 0.883 | 0.870 | 0.846 | 0.763 |
| | 6.25 | 0.884 | 0.893 | 0.884 | 0.856 | 0.769 |

Chord out of plane Chord face to chord face

| | β | | | | |
|---|---|---|---|---|---|
| | 0.25 | 0.4 | 0.5 | 0.6 | 0.75 |
| 15.9 | 0.877 | 0.854 | 0.855 | 0.843 | 0.784 |
| 10 | 0.878 | 0.874 | 0.880 | 0.871 | 0.805 |
| γ 8 | 0.892 | 0.890 | 0.897 | 0.833 | 0.815 |
| 7.04 | 0.878 | 0.906 | 0.910 | 0.844 | 0.822 |
| 6.25 | 0.882 | 0.925 | 0.925 | 0.851 | 0.826 |

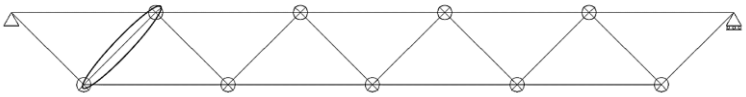

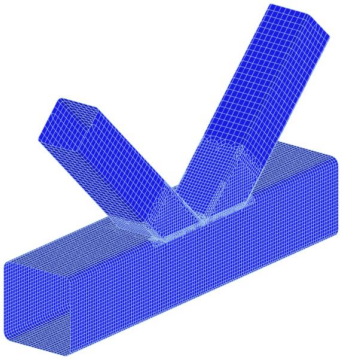

Brace in plane Chord face to chord face

| | β | | | | |
|---|---|---|---|---|---|
| | 0.25 | 0.4 | 0.5 | 0.6 | 0.75 |
| 15.9 | 0.515 | 0.544 | 0.600 | 0.658 | 0.792 |
| 10 | 0.507 | 0.527 | 0.554 | 0.589 | 0.672 |
| γ 8 | 0.505 | 0.520 | 0.542 | 0.566 | 0.628 |
| 7.04 | 0.504 | 0.517 | 0.536 | 0.559 | 0.609 |
| 6.25 | 0.501 | 0.513 | 0.529 | 0.551 | 0.592 |

Brace out of plane Chord face to chord face

| | β | | | | |
|---|---|---|---|---|---|
| | 0.25 | 0.4 | 0.5 | 0.6 | 0.75 |
| 15.9 | 0.579 | 0.641 | 0.688 | 0.713 | 0.759 |
| 10 | 0.549 | 0.597 | 0.636 | 0.670 | 0.741 |
| γ 8 | 0.541 | 0.583 | 0.618 | 0.660 | 0.705 |
| 7.04 | 0.539 | 0.576 | 0.609 | 0.648 | 0.692 |
| 6.25 | 0.533 | 0.570 | 0.599 | 0.637 | 0.678 |

## E.2.3 Change of support conditions

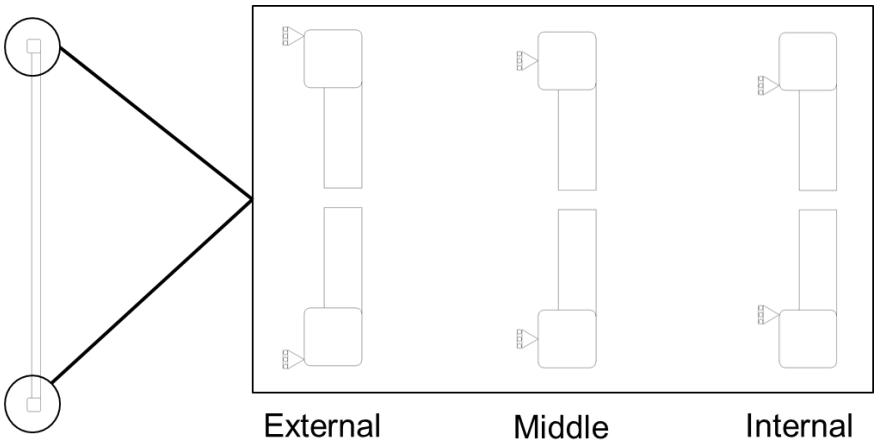


Brace buckling factor for in plane buckling $K_{br,in}$

| | | γ = 10 | | |
|---|---|---|---|---|
| | | **External support** | **Middle support** | **Internal support** |
| β | 0.25 | 0.874 | 0.874 | 0.874 |
| | 0.40 | 0.856 | 0.856 | 0.856 |
| | 0.50 | 0.845 | 0.845 | 0.845 |
| | 0.60 | 0.819 | 0.819 | 0.819 |
| | 0.75 | 0.741 | 0.741 | 0.741 |

Chord buckling factor for out of plane buckling $K_{ch,out}$

| | | γ = 10 | | |
|---|---|---|---|---|
| | | **External support** | **Middle support** | **Internal support** |
| β | 0.25 | 0.507 | 0.507 | 0.507 |
| | 0.40 | 0.527 | 0.527 | 0.527 |
| | 0.50 | 0.554 | 0.554 | 0.554 |
| | 0.60 | 0.589 | 0.589 | 0.589 |
| | 0.75 | 0.672 | 0.672 | 0.672 |

Brace buckling factor for out of plane buckling $K_{br,out}$

| | | γ = 10 | | |
|---|---|---|---|---|
| | | **External support** | **Middle support** | **Internal support** |
| β | 0.25 | 0.877 | 0.878 | 0.878 |
| | 0.40 | 0.874 | 0.874 | 0.874 |
| | 0.50 | 0.880 | 0.880 | 0.880 |
| | 0.60 | 0.869 | 0.871 | 0.872 |
| | 0.75 | 0.805 | 0.805 | 0.805 |

Brace buckling factor for out of plane buckling $K_{br,out}$

| | | γ = 10 | | |
|---|---|---|---|---|
| | | **External support** | **Middle support** | **Internal support** |
| **β** | 0.25 | 0.570 | 0.549 | 0.551 |
| | 0.40 | 0.631 | 0.597 | 0.598 |
| | 0.50 | 0.680 | 0.636 | 0.637 |
| | 0.60 | 0.706 | 0.670 | 0.672 |
| | 0.75 | 0.753 | 0.741 | 0.742 |

## E.2.4 Beam element model with rigid connections

Chord buckling in-plane

| | | β = 0.25 | 0.4 | 0.5 | 0.6 | 0.75 |
|---|---|---|---|---|---|---|
| | 15.9 | 0.865 | 0.775 | 0.746 | 0.764 | 0.678 |
| | 10 | 0.873 | 0.851 | 0.833 | 0.804 | 0.721 |
| **γ** | 8 | 0.899 | 0.869 | 0.853 | 0.822 | 0.740 |
| | 7.04 | 0.897 | 0.879 | 0.863 | 0.833 | 0.750 |
| | 6.25 | 0.880 | 0.891 | 0.873 | 0.845 | 0.759 |

Chord buckling out of plane

| | | β = 0.25 | 0.4 | 0.5 | 0.6 | 0.75 |
|---|---|---|---|---|---|---|
| | 15.9 | 0.873 | 0.834 | 0.826 | 0.818 | 0.756 |
| | 10 | 0.878 | 0.872 | 0.866 | 0.846 | 0.788 |
| **γ** | 8 | 0.887 | 0.885 | 0.879 | 0.803 | 0.802 |
| | 7.04 | 0.875 | 0.896 | 0.888 | 0.825 | 0.809 |
| | 6.25 | 0.885 | 0.913 | 0.899 | 0.838 | 0.814 |

Brace buckling in-plane

| | | β = 0.25 | 0.4 | 0.5 | 0.6 | 0.75 |
|---|---|---|---|---|---|---|
| | 15.9 | 0.502 | 0.514 | 0.536 | 0.566 | 0.765 |
| | 10 | 0.501 | 0.509 | 0.528 | 0.559 | 0.651 |
| **γ** | 8 | 0.501 | 0.508 | 0.521 | 0.543 | 0.610 |
| | 7.04 | 0.501 | 0.507 | 0.518 | 0.537 | 0.591 |
| | 6.25 | 0.501 | 0.506 | 0.517 | 0.533 | 0.576 |

Brace buckling out of plane

| | | ν | | | | |
|---|---|---|---|---|---|---|
| | | 0.25 | 0.4 | 0.5 | 0.6 | 0.75 |
| γ | 15.9 | 0.531 | 0.562 | 0.612 | 0.679 | 0.716 |
| | 10 | 0.528 | 0.552 | 0.580 | 0.616 | 0.708 |
| | 8 | 0.528 | 0.548 | 0.573 | 0.632 | 0.674 |
| | 7.04 | 0.526 | 0.546 | 0.569 | 0.613 | 0.659 |
| | 6.25 | 0.526 | 0.544 | 0.566 | 0.602 | 0.647 |